Energy Management and Power System Operation Vol 5

Jan von Appen

Sizing and operation of residential photovoltaic systems in combination with battery storage systems and heat pumps

Energiemanagement und Betrieb elektrischer Netze

Fraunhofer IEE

KDEE Kompetenzzentrum für Dezentrale Elektrische Energieversorgungstechnik

Energy Management and Power System Operation

Vol. 5

Edited by
Prof. Dr.-Ing. Martin Braun
University of Kassel

Jan von Appen

Sizing and operation of residential photovoltaic systems in combination with battery storage systems and heat pumps

Multi-actor optimization models and case studies

kassel university press

This work has been accepted by the Faculty of Electrical Engineering / Computer Sciences of the University of Kassel as a thesis for acquiring the academic degree of Doktor der Ingenieurwissenschaften (Dr.-Ing.).

Supervisor: Prof. Dr.-Ing. Martin Braun (Universität Kassel)
Co-Supervisor: Prof. Dr.-Ing. Bernd Engel (Technische Universität Braunschweig)

Defense day: 21st July 2018

Bibliographic information published by Deutsche Nationalbibliothek
The Deutsche Nationalbibliothek lists this publication in the Deutsche Nationalbibliografie; detailed bibliographic data is available in the Internet at http://dnb.dnb.de.

Zugl.: Kassel, Univ., Diss. 2018
ISBN 978-3-7376-0554-0 (print)
ISBN 978-3-7376-0555-7 (e-book)
DOI: http://dx.medra.org/10.19211/KUP9783737605557
URN: http://nbn-resolving.de/urn:nbn:de:0002-405559

Printing Shop: Print Management Logistics Solutions, Kassel
Printed in Germany

Abstract

The business case for residential photovoltaic (PV) systems in combination with battery storage systems (BSSs) is thriving in Germany. Consumer preferences for self-sufficiency, investment incentives and new flexibility options, such as heat pumps, increase the complexity of planning processes for all involved stakeholders. Households (HHs) face rising uncertainty for refinancing a system based on varying electricity prices and changing operational incentives for network integration. Distribution network operators (DNOs) have to consider differently sized PV systems in their mid-term network planning to avoid unnecessary network reinforcement and have to cope with losing network charge (NC) revenue from PV BSSs as a result of increased self-supply. Together, residential investors, DNOs and policy makers require a profound understanding of the newly evolving interdependencies for robust decisions on optimal sizing and operation of decentralized heat-power-storage systems (here: PV systems with BSSs and heat pumps) and smart incentive setting for improved PV network integration as well as sector coupling.

Thus, in this thesis different optimization models are developed for evaluating the interdependencies between drivers of PV BSS sizing and operation from a HH investor's as well as a DNO's perspective. A case study-based approach allows assessing implications for additional stakeholders, such as policy makers. In three different parts the optimization model is adapted to analyze how different incentives and drivers impact decision making on the residential PV BSS investor level and on the DNO side. The approach uses mixed integer linear programming and bilevel optimization to derive techno-economic optimal solutions and to model strategic decision making of the involved stakeholders in an open- and closed-loop way. Different case studies are used to analyze how incentives impact sizing and operation of PV BSSs, their network integration and their complementarity towards other flexibility options (here: heat pumps) for improved sector coupling.

From a short-term perspective, self-sufficiency preferences and the BSS investment incentive program (as currently in place in Germany) encourage BSS adoption and larger sized PV systems. The network-supporting BSS operation as a result of a lower feed-in limit through the investment incentive program can be partially offset by the increased PV system sizes. Here, a mixture of tariff setting and new regulatory requirements can provide an opportunity for enabling network-beneficial PV network integration.

Using a bilevel programming approach, the main DNO's decision challenges in the context of an increasing number of PV BSSs are modeled: raising NCs, reinforcing the network, curtailing PV feed-in and choosing the appropriate NC tariff while also increasing the incentive for investing in a PV BSS. The importance of appropriate tariff setting is underlined to

mitigate the danger of a self-reinforcing process between higher NCs, increased PV BSS sizes and raised peaks of PV network feed-in. Yet, disconnecting from the network - so called network defection - is not a realistic scenario as the benefit of further self-supply decreases with higher NCs. Compared to PV curtailment by the DNO or network reinforcements, fixed feed-in limits and power-based NCs reduce the investor's incentive to oversize PV BSSs and provide an operational incentive for peak-oriented BSS operation.

To avoid drastically decreased PV system sizes, once the feed-in tariff drops significantly, a policy framework for enhanced sector coupling through heat pumps is required. The analysis shows that BSSs and heat pumps complement each other. Their combination provides the opportunity to achieve adequately sized PV systems and ensures that the PV rooftop potential can be activated. As heat pumps largely rely on network consumption even with local energy supply, self-sufficiency induced problems, such as a reduced NC revenue for the DNO, can be mitigated while providing an attractive business case for residential PV systems. Establishing a tariff or investment incentive-based framework that allows heat pumps to be an attractive economic alternative to conventional heating systems is crucial, not only for sector coupling, but also for future residential PV systems.

The analyses show that the developed models in combination with the case study framework compose an efficient approach for different actors to anticipate strategic stakeholder behavior and adjust sizing, operation, tariff and policy setting for a changing electric supply and consumption system with higher amounts of decentralized power-heat-storage systems.

Acknowledgments

I feel deep gratitude for my supervisor Martin Braun, who not only guided me through this thesis, but also enabled me to pursue my academic career. I candidly thank Martin and Bernd Engel as my co-supervisor for the valuable remarks and the often not enough appreciated long hours that went into the supervision. Furthermore, I would like to thank Clemens Hoffmann and Andreas Bley for agreeing to participate in the examination committee.

A big thank you also goes out to all my current and former Fraunhofer IEE and academic colleagues and students for the support, fruitful scientific and non-scientific discussions, remarks and laughs, especially to Thomas, Fabian, Markus, Alex, Konrad, Jonas, Haonan, Lyle and Gonçalo. Moreover, I owe sincere gratitude to Ilan, for the critical discussions, the constant challenges, the inspirational remarks, the tough review of this manuscript and his friendship.

A majority of the research has been conducted within public funded projects.[1] Hence, the funding bodies and agencies and the project partners deserve a special thank you as well.

Besides scientific discussions, a productive working environment and adequate funding, true friendship is a corner stone of successful thesis. I have been blessed to find a few around the world, especially Johannes, Nils, Dima, Patrick, Ouss, Wolf, Nate, Cam and Marius.

My parents, Steffi and Michael, deserve my deepest gratitude for their never-ending encouragement and pragmatic advise. Meike and Marc, thank you for the endless joys and the unconditional support despite me being an annoying brother from time to time.

Christina, without you this thesis would have not been possible. Thank you for everything; words cannot express the thank I owe you for the smiles, for the giggles, for building me up when I was down, for your review of this manuscript, for being my partner in crime - at home and traveling the world - and most importantly for your love.

1 The research leading to this thesis has received funding from the German Federal Ministry for Economic Affairs and Energy through the projects INE-VES (FKZ: 0325561A) and 'EMBS' (FKZ: 0350019) as well as from the German Federal Ministry of Education and Research through the project ENavi (FKZ: 03SFK4N0).

Contents

1

Introduction

1.1 *Motivation*

The global energy system is changing. A record setting 138.5 gigawatt (GW) of newly installed renewable energy resources (RESs) in 2016 accounted for 55 % of globally added power plant capacity and two thirds of the related investment costs [1]. Especially Germany has seen a rapid growth of RES, since its parliament introduced its first large-scale support legislation in 2000, the so called German Renewable Energy Act (EEG), to mitigate consequences of climate change. Overall, 54.4 GW of wind and 42.5 gigawatt peak (GWp)[1] of photovoltaic (PV) generation capacity were installed by mid 2017 in Germany, which exceed the conventional based generation capacity [2]. As a result of moving from a feed-in tariff (FIT) based system to an auction mechanism with fixed allowed quota per year, the installation rate of large-scale PV systems has slowed down over the last couple of years. Residential PV systems, however, enjoy a high popularity among house owners. Nowadays, around 1.6 million PV systems are installed in Germany [3]. The growth has been driven by the economic attractiveness of the business case for rooftop PV systems as guaranteed FITs provide a reliable and low-risk source of income to finance the systems. Since the FIT has dropped below the electricity price for households (HHs) in 2012, an additional value stream has emerged: the direct consumption of locally produced PV energy, so called PV self-consumption. Decreasing FITs and PV system costs and increasing electricity prices have led to a shift in focus when planning PV systems. Nowadays, investors in residential PV systems are also focusing on PV self-consumption and self-sufficiency, which describes the independence from network consumption, next to classical cost-benefit drivers [4–7].

Especially battery storage systems (BSSs) are being installed in larger numbers as BSSs help bridge the natural offset of PV generation and consumption in HHs. In Germany, around 80,000 PV BSSs were installed by the beginning of 2018 [7, 8]. The majority of these PV BSSs is installed in the residential sector together with PV systems smaller than 10 kilowatt peak (kWp); meaning that almost every second PV system in Germany is nowadays installed together with a BSS. PV BSS growth has additionally been fostered by an investment incentive program aiming at facilitating PV network integration [9].

1 In this thesis the expression watt peak is used as an abbreviation for the installed PV power in watt under standard testing conditions.

Self-sufficiency and PV BSSs impact distribution network operators (DNOs) in a twofold way. DNOs have to reconsider their network planning premises taking into account that BSSs influence PV system sizing as well as PV network feed-in and can also lead to different PV installation rates. Furthermore, the economics of PV BSSs thrive on the avoidance of paying network charges (NCs), taxes and other surcharges. PV BSSs allow HHs to easily reduce their corresponding NC payments by 60 % [5, 10, 11]. As distribution networks are already partially experiencing higher costs with higher levels of PV penetration [12–14], rising NCs resulting from higher self-sufficiency increase the complexity of network planning and refinancing and can trigger an additional wave of PV BSS investments. DNOs have to be aware of the danger of starting a self-reinforcing process that might end in HHs with PV BSSs leaving the network - so called network defection [15–18] - and the implications of cost redistribution between HHs with and without PV BSSs. On the other hand, DNOs might improve PV network integration through smart incentive setting to exploit the newly available flexibility of BSSs, either through a new NC tariff structure or measures such as PV curtailment.

While BSSs are currently the preferred coupling technology of residential investors for combination with PV systems, new electric loads, such as heat pumps or electric vehicles, are predestined for providing flexibility for RES integration [19, 20]. On the one hand, properly sizing and operating such decentralized power-heat-storage systems becomes even more complex for investors. On the other hand, such systems might help securing the value of local generation in a post EEG world, ensure that the PV rooftop potential of the residential housing sector is activated [21] and might contribute to PV network integration [20].

The new regime of self-supply and additional flexibility to foster self-consumption change the economics of PV systems. Such developments entail far reaching implications for system planning and operation for all involved actors. Residential investors need to account for higher degrees of complexity and uncertainty when investing in PV systems and choosing an appropriate resource for increasing PV self-consumption. DNOs require a better understanding of how investors choose system sizes and decide on flexibility operation with regard to new incentives. In consequence, DNOs can accordingly adjust their network planning and set NCs appropriately. Policy makers require a profound understanding of possible interdependencies between PV BSS sizing and operation and system integration when shaping new investment incentive programs or imposing operational technical limits or tariff structures. To develop suitable recommendations for policy shaping around decentralized PV systems, models are required that allow analyzing sizing and operation of residential PV systems as well as interdependencies between flexibility options, network requirements and policy incentives.

1.2 *Scientific contributions and approach*

A threefold approach is developed to analyze the current and future interdependencies of investment, sizing and operation decisions in PV BSSs with regard to implications for PV network integration, NC setting and appropriate policy shaping for decentralized power-heat-storage systems. The following summary highlights the contributions of this thesis. The derivation of such contributions and the necessity of the work are outlined in detail in the different parts of the thesis.

- First, a single-level optimization model is developed for evaluating investment, sizing and operation decisions into PV systems and BSSs. It allows quantifying the impact of current drivers for PV BSS installations from a residential investor's perspective, but also analyzing key performance indicators (KPIs) for other stakeholders such as DNOs or policy markers. The dynamics between the desire to increase self-sufficiency, the investment incentive program for BSSs, new regulations concerning the smart meter rollout and PV BSS sizing and operation are reflected on PV network integration. Here, the focus lies on the change in peak active power flows at the point of common coupling. Including such new drivers in modeling and performing corresponding case studies has previously not been done, but is necessary to retrieve a clearer picture to adjust network and policy planning premises for such systems.

- PV BSSs also influence NCs as the described above. Understanding the interdependencies between PV BSS sizing and operation, network integration and NCs become crucial factors for DNOs when deciding between different measures to facilitate PV network integration and choosing an appropriate NC tariff for PV BSSs. Current analyses focus on individual aspects within this context and fail to model the underlying dynamics. The above described optimization model is transformed into a new integrated, closed-loop model for a DNO and multiple PV BSSs using bilevel programming to evaluate strategic decision making on the DNO and the PV BSS side when these actors anticipate the reaction of each other. The model allows DNOs to choose an appropriate NC tariff structure for PV BSSs, compare network reinforcement to PV curtailment for PV network integration and mitigate welfare redistribution from HHs with PV BSSs to HHs without PV BSSs, while simultaneously analyzing adapted sizes and operation schedules of PV BSSs. Additionally, the case studies benchmark different NC tariff systems to mitigate undesired effects of self-sufficiency systems and assess the threat of a self-reinforcing process ending in network defection of PV BSSs.

- To evaluate further decentralized power-heat-storage systems and flexibility options, the single-level, open-loop optimization model is ex-

panded by introducing thermal demand related components and constraints, such as unit commitment for heat pumps. Introducing such constraints allows deriving a better understanding of the flexibility offered by the BSS towards the heat pump and the impact of non-flexible power-to-heat applications for increasing PV self-consumption and improving network integration. In combination with the case studies, the developed model allows assessing whether different flexibilities, here BSS and heat pump, compete over local PV generation or complement each other. It allows evaluating how flexibilities influence PV systems sizing and what incentives foster sector coupling and network integration of decentralized power-heat storage systems. Furthermore, the model is used to evaluate the mid-term perspective for residential PV systems when no or only a marginal FIT is available and investors have to rely nearly solely on PV self-consumption.

Fig. 1.1 summarizes the approach, the developed optimization models and the underlying assumptions.

1.3 *Organization*

Naturally, the organization of this work evolves around the three variations of the proposed optimization model. Part I focuses on the current business case for PV systems from a residential investor's perspective. Part II analyzes interactions between DNOs and HHs in the context of PV BSSs with a two to three years future scenario and focuses on interdependencies of NCs and system sizing. Part III is based on a mid-term future scenario and analyzes sizing and operation of decentralized power-heat-storage systems in a post FIT era in Germany. For each part, one chapter summarizes the motivation, provides a literature review on the specific subject and details scientific contributions as well as research questions. The following chapter presents the mathematical formulation of the corresponding optimization problem and highlights differences compared to the model of the previous parts. For each part, a different case study set-up is described, different case studies are performed and a conclusion is derived in the last chapter of each part. The thesis ends with an outlook and summarizing conclusion.

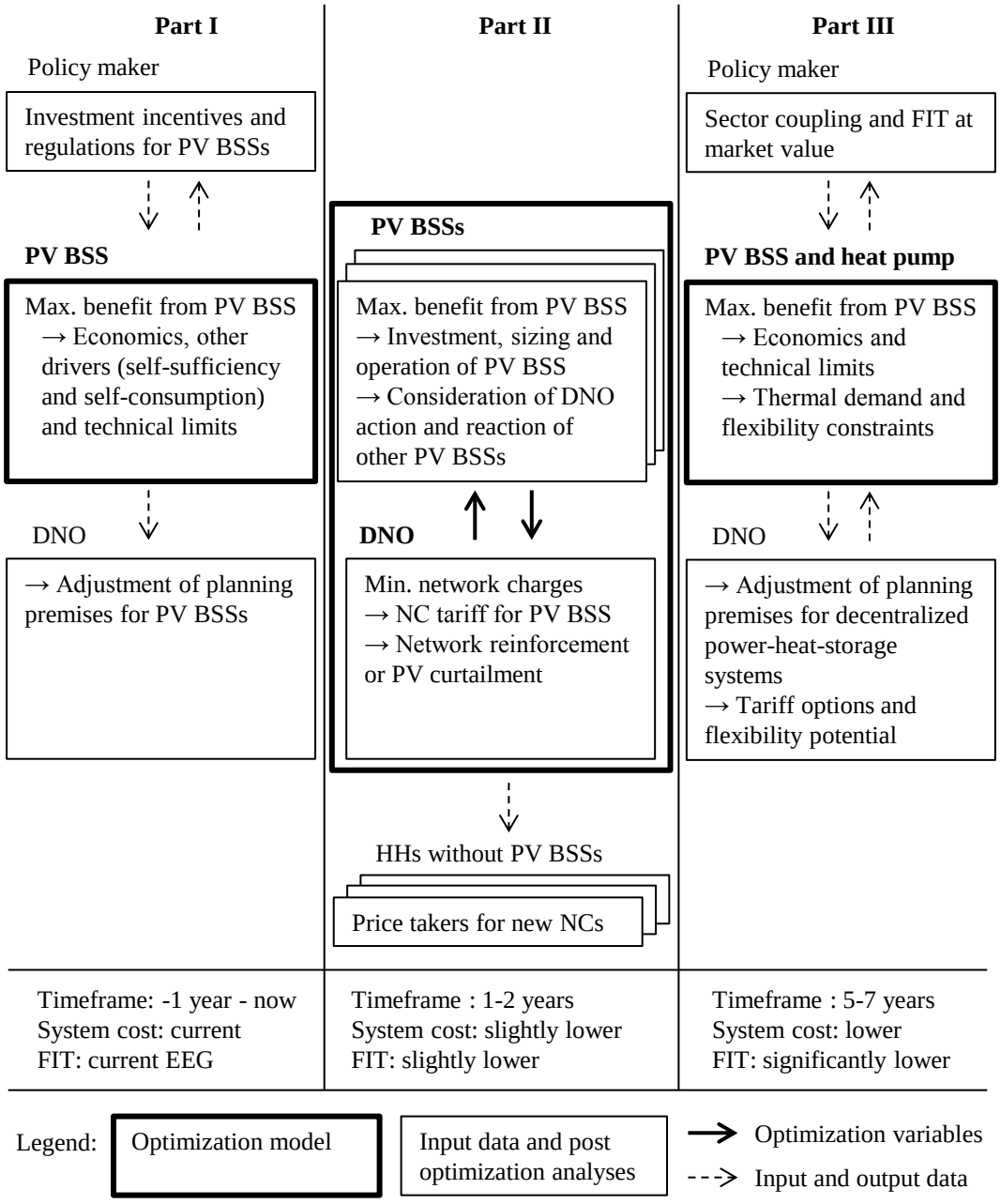

Figure 1.1: Optimization models, relevant actors and scenario for each part of the thesis

Part I

SIZING OF PV AND BATTERY STORAGE SYSTEMS

The business case for residential PV systems in combination with BSSs is thriving in Germany. Next to an increasing spread between electricity prices and FITs, the adoption of PV BSSs is fostered by a preference for higher self-sufficiency and a federal investment incentive for PV BSSs. Such an incentive subsidizes BSSs on the promise of facilitating PV network integration. However, so far a comprehensive analysis of implications of self-sufficiency desire, investment incentive and regulations concerning the smart meter rollout in Germany for PV BSS sizing, the respective PV feed-in peak and PV BSS operation is missing.
To enable the key stakeholders - PV BSS investors, DNOs and policy makers - to derive a better understanding of the underlying interdependencies between these drivers and the corresponding sizing and operation of PV BSSs, a new optimization model is developed. The model includes all relevant cash flows for the business case of PV BSSs, e.g. surcharges on PV self-consumption and the investment incentive, and an approach for adopting preferences for self-sufficiency and new regulatory requirements.
A case study-based analysis shows that BSSs allow for larger sized PV systems in certain cases and the investment incentive program facilitates their adoption. From a network integration perspective, the adoption of a BSS itself does not result in lower peak feed-ins compared to a PV system without a BSS. Imposing a lower feed-in limit through the investment incentive program helps mitigating such peaks in most cases. Once such a program runs out, the operational incentive to limit PV network feed-in disappears, leaving potential for network-supporting BSS operation untapped.

2

Introduction, review and contribution

The shift from refinancing small-scale, rooftop PV systems through FITs towards relying also on local PV self-consumption influences the investment decisions into such systems and their operation [4, 5, 22]. A rapid decline in prices for BSSs, the reliance of this business case on future developments of the electricity price and its tariff structure as well as a changing regulatory framework regarding PV feed-in behavior increase the complexity of planning such systems from a PV system owner's point of view as well as from the DNO's point of view. Potential PV system owners strive to find the optimal balance between PV and BSS size depending on their personal preference (economics vs. self-sufficiency desire) [7]. DNOs require an understanding whether such preferences and different system configurations lead to adapted PV system sizes, which result in different network planning assumptions, and whether BSSs provide an additional benefit for PV network integration [11, 21, 23]. Additionally, taxation of PV self-consumption, PV sizing limits related to regulations and an investment program for BSSs impact the investment decision in PV systems and BSSs, possibly PV system sizing and PV network integration. This section provides an overview on research performed on modeling the increased complexity of investment and operation decisions of PV BSSs as well as their network integration. Based on a literature review, research gaps for the German business case are identified. Additionally, objectives for modeling and analyses of this case are outlined.[1]

2.1 *Literature review*

The business case for PV self-consumption and self-sufficiency of HHs and PV network integration have emerged as significant research topics over the last couple of years. Scientific papers in this context can be distinguished in two categories: papers focusing on modeling PV systems and BSSs to derive optimal sizing decisions and those focusing on optimizing the operational performance for the applicable business case. Papers are selected that either contributed through interesting models in the PV BSS context, discussed the potential of BSSs to facilitate PV integration on the low voltage (LV) level or evaluated the business case for PV self-consumption.

Techno-economic sizes of PV systems and BSSs for a given scenario are mainly determined by using three different approaches (mixed integer linear programming (MILP), heuristic optimization or variation of fixed system sizes):

1 Parts of this chapter are presented in [11, 22, 24, 25].

- Mixed integer linear programs: Most authors model sizing problems by formulating a MILP and use a commercial or non-commercial solver to find the optimal solution. Typically, the objective function consists out of sizing variables for the PV system and the BSS, maintenance costs depending on system sizes, cash flow relevant operational variables, such as network procurement of load or revenue from PV network feed-in. Typical constraints are energy balances ensuring that demand is met or equalities to model the state of charge of the BSS [11, 24, 26, 27]. Certain papers introduce additional costs, such as one-time installation costs through binary variables [28], others adapt additional flexibilities, such as electric vehicles [29] or only focus on storage sizing while PV system sizes are assumed constant [30].

- Heuristic optimization programs: Heuristic optimization techniques largely rely on establishing a constraint set similar to the one described in the previous section, choosing an initial solution, varying the solution according to different heuristic optimization techniques and limiting the amount of variations by implementing an iteration limit. E.g. a tabu search for PV BSS sizing is applied in [31]. Other authors implement additional distributed energy resourcess (DERs), such as wind turbines or diesel generators, as additional investment options and solve the optimization problem by using a discrete harmony search [32], a simulated annealing algorithm [33], genetic algorithms [34] or other iterative heuristics [35].

- Variation of fixed system sizes: In a large portion of PV BSS related research papers, the authors implement a simple rule-based operation strategy for BSS operation that only requires load and PV generation of the current time step and the BSS state-of-charge of the previous time step to derive whether the BSS is charged with PV energy or discharged to cover load [4]. The best-fit PV BSS size is then determined by simulating different PV and BSS sizes and calculating the system value afterwards. Thus, sizes are not decision variables like in the previous two approaches, but fixed parameters that are varied according to a predefined solution space. In several papers such an approach has been applied with various cost assumptions, load profiles and scenarios to assess the validity of the business case over time. Analyses of the German business case for PV BSSs in HHs or commercial buildings have been performed in [5, 10, 11, 24, 36–39].[2] Further publications discuss PV self-consumption and net metering approaches using PV BSSs in country-specific contexts by comparing the case for different European countries using different system sizes and load profiles [40], assessing the case for different Australian states [41, 42], building-specific analyses for Spain [43], Italy [44, 45], Portugal [46],

2 While earlier publications suggest a lack of economic viability of PV BSSs, more recent publications state that at least break-even scenarios are possible and even an economic advantage over stand-alone PV systems are seen depending on the used assumptions.

Sweden [47] or Belgium [48]. Additional reviews are provided in [49, 50].

Approaches used in these models often resemble approaches used for investment and dispatch decisions in bulk power markets, models for community energy systems or microgrid applications, such as MARKAL/ TIMES [51], DER-CAM [52, 53] or Homer [54]. Broader summaries of similar methods for finding optimal investment and operation decisions have been discussed in the literature [55–59]. One of the main differences is that models focusing on PV BSSs often introduce further constraints related to specifics of the business case, e.g. a feed-in limit for PV or BSS aging. Additionally, the simulation time step is often much smaller with less than 15 minutes and entire year time series are used instead of representative hourly day profiles. However, especially tools for microgrid sizing and operation are based on similar bottom-up approaches used for PV BSS problems.

Sizing related literature tends to neglect the impact on PV network integration and solely focuses on the PV BSS owner's perspective from an economic point of view. Yet, in some papers implications and potential benefits of using BSSs to implement peak shaving or voltage control for improved PV network integration are addressed. Typically, a case study is designed with exemplary LV network data to assess trade-offs between DNO and PV BSS owner through an improved operation strategy. Several authors propose peak shaving by implementing PV feed-in limits or other incentives, such as time-of-use tariffs or market prices [60–66]. Others discuss the benefits of reactive power provision and subsequent active power curtailment [4, 67, 68] or using a central instead of a decentral control approach for BSSs [69–71]. Most authors use a fixed system size, optimize storage operation depending on load and PV fluctuations and discuss operational benefits for network integration. A few authors implement sizing approaches that aim at peak shaving [72, 73], but fix PV system sizes and focus on grid-scale applications that are not related for PV self-consumption and its business case. In general, the authors fail to address implications of changing economic conditions for sizing and operation of PV BSSs and the resulting feed-in behavior. However, overall system sizes in combination with operational incentives are relevant for DNOs for network planning. DNOs need to adapt mid- to long-term network expansion strategies according to most likely system sizes.

This work aims at analyzing interdependencies between PV BSS sizing and PV network integration from a HH's as well as a DNO's perspective. Thus, a method that allows solving sizing and operation decision at once is mandatory. A MILP approach seems to be most suitable as it guarantees finding the global optimum and allows adapting new case study-specific constraints for the German business case for PV BSSs. While this specific business case has been discussed in the literature, MILP modeling and analyses have focused on the implications of the used simulation time step [28] or the used load profiles [27]. Other authors have discussed potential

drivers for PV BSS sizing based on sensitivity analyses of different cost or revenue parameters, but do not model interdependencies between sizes and network integration and only use fixed system sizes [5, 37, 74].

With regard to the modeling, these authors tend to neglect specifics related to sizing, such as FIT and taxes, which are crucial for the business case. For example, PV self-consumption is taxed with 40 % of the EEG surcharge if the PV system is larger than 10 kWp. Additionally, preferences of PV BSS owners, such as self-sufficiency and contribution to the German energy transition, are not modeled, but are a common marketing element and investment drivers. They rank equal to economic aspects, such as hedging against increasing electricity prices, in the investment decision [7].

To ease PV network integration using BSSs, the German government provides an investment incentive for BSSs when agreeing to curtail PV network feed-in to 50 % rather than the usual 70 % of the installed PV capacity. The interactions between PV and BSS sizing as well as the investment incentive have not been modeled so far. Additionally, the impact of such a program and the desire to increase self-sufficiency on network integration has not been discussed.

Another impact factor on the business case of PV BSSs are regulatory changes. In 2016, the German parliament passed a law that specifies the smart meter rollout in Germany. The law also requires small-scale PV systems to install a smart meter and states related costs that utilities can charge for the smart meter. The costs depend on the installed PV system size and thus impact the sizing decision. Just like the investment incentive program, implications of the smart meter rollout have not been modeled and potential interactions between sizing decision and network integration have not been analyzed.

2.2 *Main contributions*

In this part, a new optimization model is developed that enables PV BSS investors, DNOs and policy makers to derive a better understanding of complex interdependencies between drivers and robust decisions for optimal system sizing and operation. A case study-based approach is proposed to efficiently evaluate implications of BSS investment incentives, self-sufficiency desires and new regulatory requirements.

Based on the identified gaps for modeling the German business case of PV BSSs, this work additionally contributes as follows.

- Modeling: Three currently missing key aspects are modeled in this work. Implementations of the BSS investment incentive program and of requirements related to the smart meter rollout in Germany are introduced. FIT and other cash flows, such as taxes and surcharges on PV self-consumption, are modeled accordingly. Different modeling approaches are implemented to account for the self-sufficiency desire that partially drives current investments into PV BSSs.

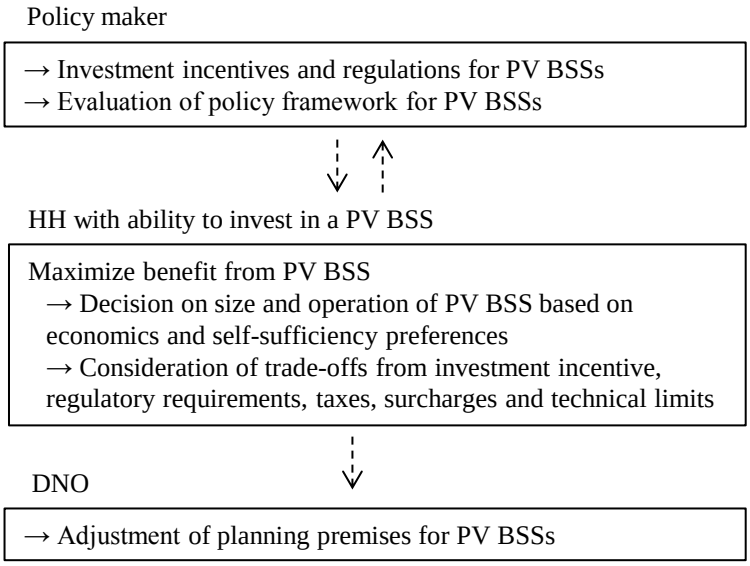

Figure 2.1: Framework and optimization approach for PV BSSs

The new model allows evaluating several key questions that have not been addressed in the context of PV BSSs and PV network integration through exemplary case studies:

- How do different investment drivers of PV systems and BSSs impact sizing and operation with regard to PV network integration (here: peak PV network feed-in), especially when systems are designed to deliver higher rates of self-sufficiency?
- Does the investment incentive program facilitate PV network integration by connecting subsidies to the installed PV system size or does it allow for larger sized PV systems and potentially counteract peak reductions through the lower feed-in limit?
- How do changing regulations that impose artificial limits on PV system sizes, such as a feed-in limit or costs related to the smart meter rollout, impact sizing and operation of PV BSSs and their network integration?

A thorough scenario development for different input parameters and a sensitivity analysis help identifying main drivers of investment decisions in PV and BSSs and their impact on PV network integration. The presented case studies allow investors to derive robust sizing decisions for PV BSSs and DNOs a better understanding of appropriate sizes for network planning. Furthermore, the effectiveness of the current investment incentive program with regard to fostering improved PV network integration by the means of BSSs is assessed for policy makers.

The proposed approach is summarized in Fig. 2.1.

2.3 *Organization of the section*

The section is organized as follows. First, the optimization model for sizing and operation of PV BSSs from a HH's perspective is described. Afterwards, KPIs for case study-based analyses are described as not all KPIs are endogenous to the model. The following section provides an overview of the case study setup and used input data. Subsequently, the aforementioned case studies are detailed before ending this section with a conclusion.

3

Model for investment and operation decisions for PV BSSs

This chapter presents the developed optimization model for investment and operation decisions of PV BSSs.[1,2]

3.1 *Objective function*

Potential owners j of PV BSSs try maximizing their individual economic benefit through a two-fold approach. First, an investment into PV systems enables them to create a steady income based on the remuneration of PV network feed-in with a FIT in Germany. Second, the consumption of locally generated PV energy is favorable over PV network feed-in, since electricity prices are higher than the FIT. Investing into a BSS together with a PV system provides a possibility to further increase the amount of local self-supply. Such systems allow bridging the gap between peak PV generation times, where PV production often exceeds demand and demand in non-solar times. Thus, the HH's objective function comprises all electricity related cash flows:

- for investment costs $I^{PV}, I^{BSSkWh}, I^{BSSkW}$ depending on the system size of PV s_j^{PV}, BSS capacity s_j^{BSSkWh} and BSS inverter s_j^{BSSkW},
- for one-time installation costs for PV In^{PV} and BSS In^{BSS} depending on a binary installation variable b_j^{PV} for PV and b_j^{BSS} for BSS,
- for yearly costs $M^{PV}, M^{BSSkWh}, M^{BSSkW}$, such as maintenance costs or insurance costs, depending on the size of the component,
- and energy flow related cash flows, such as FIT C^{Fit1} depending on the sum of PV network feed-in $e_{j,t}^{PVN}$ and electricity procurement costs C^E depending on the sum of energy consumed from the network $e_{j,t}^{NL}$ over all time steps t in the time set $\mathcal{T}$.

To appropriately model the German business case, further cost and revenue components that are related to the value of FIT rate, taxes, surcharges, the smart meter rollout and the BSS investment incentive program need to be included:

- FIT: The EEG sets the FIT depending on PV system sizes. Thus, once a certain size threshold is surpassed the FIT for PV network feed-in

1 All presented models are implemented in Python using the algebraic modeling language Pyomo [75, 76].

2 Parts of this chapter are presented in [11, 22, 24, 25].

is reduced by C^{Fit2}. The activation of this threshold is modeled via a binary variable b_j^{SkWp}.

- Taxes: Sales tax C^{Sc1} is to be paid on PV energy used for direct self-supply $e_{j,t}^{PVL}$ and indirect self-supply through BSS $e_{j,t}^{BSSL}$, if PV BSS owners want to be able to deduct paid sales tax on investment costs, which is usually beneficial. Income taxes are to be paid on earnings of the PV BSS; costs can be deducted as well. Income taxes on earnings depend on PV network feed-in TE^{Fit}, PV self-supply TE^{Sc} and the investment incentive for the BSS TE^{BSS}. Tax reductions depend on the PV depreciation TE^{Dep}, which is only allowed for the PV system and not the BSS [77].

- Surcharges on self-supply: The EEG states that once a certain threshold in PV system size is surpassed, a surcharge C^{Sc2} has to be paid on PV self-supply.

- Smart meter related costs for PV systems: Three artificial thresholds for PV system sizing are imposed once the smart meter rollout starts in Germany. Thus, two binary variables (b_j^{S1} and b_j^{S2}) and the related yearly costs (C_j^{S1} and C_j^{S2}) are introduced.

- BSS investment incentive: If investors agree to the terms of the investment incentive, they receive a percentage Sub^{BSS} of the eligible costs r_j^{BSSInc} as a BSS grant. Sub^{BSS} varies depending on the installation date, r_j^{BSSInc} depends on BSS costs, but is limited by several constraints.

Economic considerations only partially influence investors when considering investing into a PV system. Another driving force is the desire to reach higher levels of self-sufficiency and autarky [7]. Meeting such objectives requires a minimization of electricity consumption from the network $e_{j,t}^{NL}$. Here, two approaches are implemented to realize higher self-sufficiency. First, weights are included in the objective function to balance the trade-off between financial benefit W^{Npv} and self-sufficiency maximization W^{Self}. If W^{Npv} is set to one and W^{Self} is set to zero, the investor bases its investment decision purely on financial benefits. Vice versa, financial considerations do not play a role and the entire objective is to reduce consumption from the network. Secondly, a higher self-sufficiency can also be reached by including an additional constraint that requires a certain minimum self-sufficiency as described in Eq. 3.14.

Taking all cost and revenue streams and weights into account results in the following objective function z_j for HHs with the ability to invest into a PV BSS:

$$
\begin{aligned}
max\, z_j \;=\;& W^{Npv} \cdot (((C^{Fit1} - C^{Fit2} \cdot b_j^{SkWp}) - TE^{Fit}) \cdot PF^{HH} \sum_{t \in \mathcal{T}} e_{j,t}^{PVN} \\
-\;& (I^{PV} + M^{PV} \cdot PF^{HH} - TE^{Dep} \cdot PF^{HH}) \cdot s_j^{PV} - In^{PV} \cdot b_j^{PV} \\
-\;& (I^{BSSkWh} + M^{BSSkWh} \cdot PF^{HH}) \cdot s_j^{BSSkWh} \\
-\;& (I^{BSSkW} + M^{BSSkW} \cdot PF^{HH}) \cdot s_j^{BSSkW} \\
-\;& In^{BSS} \cdot b_j^{BSS} + (Sub^{BSS} - TE^{BSS}) \cdot r_j^{BSSInc} \\
-\;& (C^{Sc1} + C^{Sc2} \cdot b_j^{SkWp} + TE^{Sc}) \cdot PF^{HH} \sum_{t \in \mathcal{T}} (e_{j,t}^{PVL} + e_{j,t}^{BSSL}) \\
-\;& C^{E} \cdot PF^{HH} \sum_{t \in \mathcal{T}} e_{j,t}^{NL} - (C^{S1} \cdot b_j^{S1} + C^{S2} \cdot b_j^{S2}) \cdot PF^{HH}) \\
-\;& W^{Self} \cdot PF^{HH} \sum_{t \in \mathcal{T}} e_{j,t}^{NL}
\end{aligned} \tag{3.1}
$$

Here, all reoccurring cash flows need to be adjusted through a present value factor PF^{HH} (see Eq. B.46).

3.2 *Constraints*

The investment problem is mainly influenced by several energy constraints. These constraints ensure that PV energy is used properly, load is served and the state-of-charge of the BSS is tracked properly. Furthermore, sizing constraints are required to account for space limitations.

3.2.1 *Energy balances and sizing constraints*

The following equality ensures that demand $E_{j,t}^{L}$ is met during all time steps:

$$
\forall t: \quad e_{j,t}^{NL} + e_{j,t}^{PVL} + e_{j,t}^{BSSL} = \quad E_{j,t}^{L} \tag{3.2}
$$

Depending on the system configuration, load can be served through network supply $e_{j,t}^{NL}$, direct PV supply $e_{j,t}^{PVL}$ or BSS discharging $e_{j,t}^{BSSL}$.

An additional equality guarantees that PV power can only be used according to a given normalized PV profile for the different locations $E_{j,t}^{PV}$ and the installed PV capacity s_j^{PV}:

$$
\forall t: \quad e_{j,t}^{PVL} + e_{j,t}^{PVBSS} + e_{j,t}^{PVN} + e_{j,t}^{PVC} = \quad s_j^{PV} \cdot E_{j,t}^{PV} \tag{3.3}
$$

Next to $e_{j,t}^{PVL}$, PV network feed-in $e_{j,t}^{PVN}$, PV BSS charging $e_{j,t}^{PVBSS}$ and PV curtailment $e_{j,t}^{PVC}$ comprise all PV related energy flows. $e_{j,t}^{PVC}$ can be a result of a fixed feed-in limit, which is introduced in Eq. 3.15.

The current state of charge $soc_{j,t}$ of the BSS is determined through the self-discharge η^{BSSSd} of the previous $soc_{j,t-1}$, charging efficiency η^{BSSCh} and discharging efficiency η^{BSSDis} for BSS related energy flows.

$$\begin{aligned} \forall t: \quad soc_{j,t} = \quad & \eta^{BSSSd} \cdot soc_{j,t-1} + \eta^{BSSCh} \cdot e_{j,t}^{PVBSS} \\ & -(\eta^{BSSDis})^{-1} \cdot e_{j,t}^{BSSL} \end{aligned} \tag{3.4}$$

Additionally, $soc_{j,t}$ is limited by the multiplication of the usable BSS capacity κ^{BSSUc} and s_j^{BSSkWh}:

$$\forall t: \quad soc_{j,t} \leq \quad \kappa^{BSSUc} \cdot s_j^{BSSkWh} \tag{3.5}$$

Next to the usable capacity, BSS cycling is limited to ensure a proper battery lifetime and introduce an additional constraint to address battery aging. As aging processes are usually non-linear [78], here only a simplification of cycling aging is implemented. The overall number of available BSS full cycles is limited by ensuring that the sum of the stored energy in one year is less or equal to maximum allowed yearly cycles κ^{BSSCyc} multiplied by usable BSS capacity:

$$\sum_{t \in \mathcal{T}} \eta^{BSSCh} \cdot e_{j,t}^{PVBSS} \quad \leq \quad \kappa^{BSSCyc} \cdot \kappa^{BSSUc} \cdot s_j^{BSSkWh} \tag{3.6}$$

Furthermore, all energy flows are bounded by the corresponding profile and chosen size, if applicable:

$$\forall k \in [^{NL}, ^{PVL}, ^{BSSL}], t: \quad e_{j,t}^{k} \leq \quad E_{j,t}^{L} \tag{3.7}$$

$$\forall k \in [^{PVL}, ^{PVBSS}, ^{PVN}, ^{PVC}], t: \quad e_{j,t}^{k} \leq \quad s_j^{PV} \cdot E_{j,t}^{PV} \tag{3.8}$$

$$\forall k \in [^{PVBSS}, ^{BSSL}], t: \quad e_{j,t}^{k} \leq \quad s_j^{BSSkW} \cdot \tau \tag{3.9}$$

Here, the rated power of the BSS inverter needs to be adjusted to the time step of the simulation through τ, as rated power is always fixed while the simulation time step and thus energy flows can be adapted.

An additional binary variable $b_{j,t}^{BSSChdis}$ is introduced to avoid simultaneous BSS charging and discharging, which might occur in cases of low PV feed-in limits. Two constraints ensure that only one state (charging or discharging) is active during one time step:

$$\forall t: \quad e_{j,t}^{PVBSS} \leq \quad b_{j,t}^{BSSChdis} \cdot BigM \tag{3.10}$$

$$\forall t: \quad e_{j,t}^{BSSL} \leq \quad (1 - b_{j,t}^{BSSChdis}) \cdot BigM \tag{3.11}$$

Here, $BigM$ is chosen to be a large enough constant that does not enforce further restrictions on energy flow variables than already in place through the constraints stated above.

One-time installation costs for PV and BSS are included to account for economies of scale when choosing system sizes. Two binary variables (b_j^{PV} and b_j^{BSS}) are multiplied by max. system sizes (S^{PV} for PV, S^{BSSkWh} for BSS capacity and S^{BSSkW} for BSS inverter). Max. system sizes implement spacing limits, e.g. available rooftop area for PV systems.

$$s_j^{PV} \quad \leq \quad b_j^{PV} \cdot S^{PV} \tag{3.12}$$

$$\forall k \in [^{BSSkWh}, ^{BSSkW}]: \quad s_j^k \leq \quad b_j^{BSS} \cdot S^k \tag{3.13}$$

Moreover, energy flow and size variables are non-negative real numbers.

As outlined in the previous sections, investments into PV BSSs are currently also driven by self-sufficiency desires. A certain degree of self-sufficiency κ^{Self} can be ensured through the following constraint:

$$\sum_{t \in \mathcal{T}} e_{j,t}^{NL} \quad \leq \quad (1 - \kappa^{Self}) \cdot \sum_{t \in \mathcal{T}} E_{j,t}^{L} \tag{3.14}$$

If a PV BSS investor requires a system that is able to deliver a self-sufficiency of 60 %, the constraint enforces that maximally 40 % of the overall demand is supplied through the network. While increasing self-sufficiency is equal to higher amounts of self-supply through direct PV load supply or indirect PV load supply via BSS, it might not result in higher self-consumption of local PV generation. Thus, while the desire for higher self-sufficiency might result in larger sized systems, installed systems still rely on the ability to feed excess PV energy into the network.

3.2.2 *Self-consumption taxes and other sizing constraints*

To cope with current network integration requirements that only allow a max. PV network feed-in $e_{j,t}^{PVN}$ depending on a certain percentage κ^{PVLim} of the installed PV capacity, the following constraint is introduced:

$$\forall t: \quad e_{j,t}^{PVN} \leq \kappa^{PVLim} \cdot \tau \cdot s_j^{PV} \tag{3.15}$$

The feed-in limit is currently set to 70 % of the installed PV capacity for PV systems under 30 kWp. However, investors can also opt for a full feed-in option, if they install a remote control device. Such control devices might become mandatory with the smart meter rollout in Germany. As the metering infrastructure entails additional costs for PV system owners, the current law introduces three artificial sizing restrictions and related costs. If PV system sizes remain under 1 kWp, no additional meter is necessary and thus no additional costs are imposed. Between 1 and 7 kWp, additional costs of C^{S1} are activated through b_j^{S1}. 15 kWp pose as the next threshold that leads to further costs. The different thresholds are modeled through the following constraint:

$$s_j^{PV} \leq 1 + 6 \cdot b_j^{S1} + 14 \cdot b_j^{S2} \tag{3.16}$$

As only one of the two states can be active at once, the following constraint is introduced:

$$b_j^{S1} + b_j^{S2} \leq 1 \tag{3.17}$$

Additionally, the EEG introduces further thresholds for PV system sizing to differentiate the FIT rate and the surcharge on self-supplied PV energy. The thresholds for the FIT rate are 10 kWp, 40 kWp and 750 kWp. However, for HHs only the 10 kWp threshold is relevant, since rooftop areas allowing for PV system sizes above 40 kWp are unusual for HHs. Additionally, 10 kWp is also the relevant threshold for the surcharge on self-supplied PV energy. Thus, an additional binary b_j^{SkWp} is introduced that enforces the 10 kWp threshold. Again, $BigM$ is chosen to be a large constant that does not interfere with the sizing constraint introduced in Eq. 3.12:

$$s_j^{PV} \leq 10 + b_j^{SkWp} \cdot BigM \tag{3.18}$$

If b_j^{SkWp} is equal to one, the FIT rate is reduced by C^{Fit2} for the sum of the PV network feed-in $e_{j,t}^{PVN}$ and the self-supply surcharge C^{Sc2} has to be paid for the sum of direct PV load supply $e_{j,t}^{PVL}$ and BSS load supply $e_{j,t}^{BSSL}$, as displayed in the objective function (see Eq.3.1). As such a measure results in products of linear and binary variables ($b_j^{SkWp} \cdot \sum_{t \in \mathcal{T}} (e_{j,t}^{PVL} + e_{j,t}^{BSSL})$ and $b_j^{SkWp} \cdot \sum_{t \in \mathcal{T}} e_{j,t}^{PVN}$), linearization techniques have to be applied to enable the

utilization of standard solvers [79]. Two linear variables (eb_j^{ScLin} and eb_j^{FitLin}) are introduced that replace the bi-linear product in the objective function:

$$eb_j^{ScLin} = b_j^{SkWp} \cdot \sum_{t \in \mathcal{T}} (e_{j,t}^{PVL} + e_{j,t}^{BSSL}) \tag{3.19}$$

$$eb_j^{FitLin} = b_j^{SkWp} \cdot \sum_{t \in \mathcal{T}} e_{j,t}^{PVN} \tag{3.20}$$

As eb_j^{ScLin} and eb_j^{FitLin} are non-negative real numbers, three additional constraints allow linearizing each product of variables. Here, only the inequalities for eb_j^{ScLin} are displayed. The same principle is applied to eb_j^{FitLin}.

$$eb_j^{ScLin} \leq BigM \cdot b_j^{SkWp} \tag{3.21}$$

$$eb_j^{ScLin} \leq \sum_{t \in \mathcal{T}} (e_{j,t}^{PVL} + e_{j,t}^{BSSL}) \tag{3.22}$$

$$\sum_{t \in \mathcal{T}} (e_{j,t}^{PVL} + e_{j,t}^{BSSL}) - (1 - b_j^{SkWp}) \cdot BigM \leq eb_j^{ScLin} \tag{3.23}$$

If it is unattractive to surpass the threshold of 10 kWp and b_j^{SkWp} is equal to zero, Eq. 3.21 ensures that the linearization variable eb_j^{ScLin} is also zero and thus the fee on self-supply is set to zero in the objective function. If paying an additional fee on self supply and taking a reduced FIT into account are economically attractive and b_j^{SkWp} is equal to one, Eq. 3.22 ensures that eb_j^{ScLin} is less or equal to $\sum_{t \in \mathcal{T}} (e_{j,t}^{PVL} + e_{j,t}^{BSSL})$. While Eq. 3.23 forces eb_j^{ScLin} to be bigger or equal than $\sum_{t \in \mathcal{T}} (e_{j,t}^{PVL} + e_{j,t}^{BSSL})$. eb_j^{ScLin} has to be equal to $\sum_{t \in \mathcal{T}} (e_{j,t}^{PVL} + e_{j,t}^{BSSL})$. Thus, the self-supply fee has to be paid on the entire self-supply and the FIT rate is reduced for the entire PV network feed-in.

3.2.3 *Investment incentive for BSS*

As stated above, the German government currently provides an investment incentive for BSSs to improve PV network integration with a lower PV feed-in limit to reduce the max. PV network feed-in. Instead of a feed-in limit κ^{PVLim} of 70 % of the installed PV capacity, the max. PV network feed-in is not allowed to be higher than 50 % of s_j^{PV}. Such a measure is expected to lower the overall PV peak and reduce the need for network reinforcements. Here, a trade-off for the owner of a PV BSS becomes visible; in order to

receive the investment bonus the investor faces higher PV losses due to the lower feed-in limit unless the BSS can be operated in a way to avoid such losses. To model this decision appropriately, a binary variable b_j^{BSSInc} is introduced to reflect the PV BSS owner's choice for taking the investment incentive and agreeing to lower the feed-in limit κ^{IncLim} to 50 %. By agreeing to the terms of the investment incentive, b_j^{BSSInc} is set to one. The following inequality ensures that the network feed-in does not surpass the new feed-in limit. Otherwise, Eq. 3.15 still imposes a limit the network feed-in.

$$\begin{aligned} \forall t: \quad e_{j,t}^{PVN} \leq \quad & (\kappa^{IncLim} \cdot s_j^{PV} \\ & + (1 - \kappa^{IncLim}) \cdot (1 - b_j^{BSSInc}) \cdot BigM) \cdot \tau \end{aligned} \tag{3.24}$$

Additional constraints imposed by the investment incentive are that PV systems larger than 30 kWp are not eligible to receive the bonus. In other words, if b_j^{BSSInc} is equal to one and the investment incentive is received, s_j^{PV} is limited to 30 kWp:

$$s_j^{PV} \leq 30 + (1 - b_j^{BSSInc}) \cdot BigM \tag{3.25}$$

The amount of the receivable investment incentive r_j^{BSSInc} is bounded by several aspects. r_j^{BSSInc} is a non-negative real number and is not allowed to exceed 2,000 € per installed kWp, which results in the following inequality:

$$r_j^{BSSInc} \leq 2000 \cdot s_j^{PV} \tag{3.26}$$

Furthermore, r_j^{BSSInc} is limited by the actual installation costs of the PV BSS, which include the one-time installation and the size depending costs for both PV and BSS:

$$\begin{aligned} r_j^{BSSInc} \leq \quad & I^{PV} \cdot s_j^{PV} + In^{PV} \cdot b_j^{PV} + I^{BSSkWh} \cdot s_j^{BSSkWh} \\ & + I^{BSSkW} \cdot s_j^{BSSkW} + In^{BSS} \cdot b_j^{BSS} \end{aligned} \tag{3.27}$$

The decision to agree to the terms of the investment incentive program and the receivable amount are linked through the following inequality:

$$r_j^{BSSInc} \leq BigM \cdot b_j^{BSSInc} \tag{3.28}$$

If b_j^{BSSInc} equals one, r_j^{BSSInc} is limited by Eq. 3.26 and 3.27. If b_j^{BSSInc} equals zero and the terms of the investment incentive program are not accepted, r_j^{BSSInc} is also zero.

4

Case studies and conclusions

From the previously presented model, case studies are derived to answer the questions posed in section 2.2. An analysis is performed to evaluate the viability and key drivers for the current business case for PV BSSs for different locations as well as different HH customers in Germany. The main focus lies on evaluating interdependencies between PV system sizing and BSS installation with regard to the potential impact on PV network integration. Especially, as self-sufficiency becomes a major driver for BSSs and is supported through an investment incentive program in Germany, it needs to be analyzed if the current program fulfills one of its core objectives, the improvement of PV network integration, how self-sufficiency desire and additional regulatory changes impact PV system sizing and individual peak PV feed-in. The derived conclusions provide DNOs and policy makers with an indication whether PV BSSs stimulate the growth of decentral PV systems and if such systems facilitate PV network integration at the same time.

The first case studies focus on the economics for the individual HH and the current policy implications for investment decisions in PV BSSs by deriving typical PV BSS sizes and evaluating the system's individual PV peak feed-in power. An subsequent analysis concentrates on the aggregated peak PV feed-in and peak demand depending on the penetration rate of installed PV BSSs and introduces a DNO perspective. Typical system sizes in combination with the likelihood of higher penetration levels impact strategic mid- and long-term network reinforcement and expansion planning of DNOs [21, 23, 80]. Thus, besides PV system sizes, changes of peak feed-in and demand simultaneity due to BSS operation are of high interest for DNOs and are presented in the last case study.[1,2]

4.1 *Key performance indicators*

To evaluate the case studies, the following KPIs are used:

- System sizes:

  The installed PV capacity s_j^{PV} and the BSS capacity s_j^{BSSkWh} are direct result of the optimization model.

- Peak PV feed-in and peak demand per HH and installed PV BSS:

1 PV BSSs also impact procurement processes for utilities. Usually, utilities contract and operate their balancing areas according to standard load profiles (SLPs) for HHs. While stand-alone PV systems are easily integrated into operation, BSS provide an additional flexibility. Thus, an additional case study discusses the impact of PV BSS investment and their operation strategy on SLP (see A.3).

2 Parts of this chapter are presented in [11, 22, 24, 25].

The peak PV feed-in per installed system and HH P_t^{PVN} is the max. PV network feed-in from the PV system $e_{j,t}^{PVN}$ adjusted by τ:

$$P_j^{PVN} = max_{t\in\mathcal{T}}(e_{j,t}^{PVN}) \cdot \tau \tag{4.1}$$

The peak demand from the network per HH P_j^{NL} is the max. network load consumption $e_{j,t}^{NL}$ adjusted by τ:

$$P_j^{NL} = max_{t\in\mathcal{T}}(e_{j,t}^{NL}) \cdot \tau \tag{4.2}$$

- Aggregated peak feed-in and peak demand:

  DNOs usually design networks according to peak loads and their simultaneity SF^{NL}, which is described as the max. demand of the aggregated demand P^{NLagg} divided by the sum of all individual peaks P_j^{NL} depending on the number of HHs $\mathcal{J}$ taken into account:

$$SF^{NL} = \frac{P^{NLagg}}{\sum_{j\in\mathcal{J}} P_j^{NL}} = \frac{max_{t\in\mathcal{T}}(\sum_{j\in\mathcal{J}} e_{j,t}^{NL}) \cdot \tau}{\sum_{j\in\mathcal{J}} max_{t\in\mathcal{T}}(e_{j,t}^{NL}) \cdot \tau} \tag{4.3}$$

  The simultaneity decreases with an increasing number of HHs as the individual HH's contribution to the overall peak decreases.
  However, with an increasing number of installed PV systems, peak PV feed-in becomes of high relevance for network planning. Feed-in peaks tend to have a higher simultaneity than peak loads as most PV systems in Germany face south. The peak feed-in varies nonetheless from HH to HH because the individual demand varies during PV peak hours. Thus, for network planning purposes worst-case scenarios usually take residual network peaks, which are defined through P_j^{PVN} and low load situations during transition or summer days [80, 81]. A residual energy flow profile E_t^{Res} is necessary to determine whether load or PV are the driving factor for network expansion:

$$E_t^{Res} = \sum_{j\in\mathcal{J}} e_{j,t}^{PVN} - \sum_{j\in\mathcal{J}} e_{j,t}^{NL} \tag{4.4}$$

  Here, the minimum P^{Resmin} describes the aggregated peak load over all HHs, which can be influenced by the HH's individual PV feed-in:

$$P^{Resmin} = min(E_t^{Res}) \cdot \tau \tag{4.5}$$

  The maximum P^{Resmax} describes the overall peak PV feed-in, if it surpasses the network demand of all HHs (if not, it is set to zero):

$$P^{Resmax} = max(0, E_t^{Res}) \cdot \tau \tag{4.6}$$

Whether peak demand or peak PV feed-in are the relevant parameters for network planning can be determined by comparing P^{Resmin} and P^{Resmax}. Depending on the PV penetration (the number of HHs with a PV systems compared to all HHs), the likelihood of network reinforcements rises, especially if P^{Resmax} is larger than $|P_j^{Resmin}|$.
BSS operation might impact peak feed-in, low load situations and peak demand. Previous studies have indicated that the peak demand is usually not or only minimally impacted through BSS operation, since the typical German HH's peak demand occurs during the evening in winter. During such days not enough surplus PV energy is produced to charge the BSS sufficiently to later discharge it during peak hours.[3] However, as PV and PV BSS penetration rates highly vary from network to network and highly depend on the underlying PV penetration scenario, the peak impact varies. To present DNOs with a KPI that allows for a suitable comparison of the peak change depending on the penetration level, residual peak profiles $E_{i,t}^{Res}$ depending on the number of HHs with a PV system i are calculated:

$$\forall i \in 0..\mathcal{J}: \quad E_{i,t}^{Res} = \sum_{j \in i} e_{j,t}^{PVN} - \sum_{j \in \mathcal{J}} e_{j,t}^{NL} \tag{4.7}$$

P_i^{Resmin} and P_i^{Resmax} are determined following the logic presented in Eq. 4.5 and Eq. 4.6. As the number of HHs is not ordered and depends on the amount of installed PV systems or PV BSSs i, HH_i combinations are possible for the different penetration rates:

$$HH_i = \frac{\mathcal{J}!}{i!(\mathcal{J} - i!)} \tag{4.8}$$

Here, only 500 randomized HH combinations are selected for each PV penetration rate i to reduce the calculation time. For the graphical representation, the spread in results is displayed by only indicating minimum and maximum values for peak feed-in ($P_i^{Resmaxmin}$ and $P_i^{Resmaxmax}$) and peak demand ($P_i^{Resminmin}$ and $P_i^{Resminmax}$) for the different penetration rates for the average HH:

$$\forall i \in 0..\mathcal{J}: \quad P_i^{Resmaxmin} = min(P_{i,0}^{Resmax}..P_{i,500}^{Resmax}) \cdot \mathcal{J}^{-1} \tag{4.9}$$

$$\forall i \in 0..\mathcal{J}: \quad P_i^{Resmaxmax} = max(P_{i,0}^{Resmax}..P_{i,500}^{Resmax}) \cdot \mathcal{J}^{-1} \tag{4.10}$$

$$\forall i \in 0..\mathcal{J}: \quad P_i^{Resminmin} = |\, min(P_{i,0}^{Resmin}..P_{i,500}^{Resmin}) \cdot \mathcal{J}^{-1} \,| \tag{4.11}$$

3 Yet, this might not hold for all HHs and highly depends on operational incentives [11].

$$\forall i \in 0..\mathcal{J}: \quad P_i^{Resminmax} = \quad | \, max(P_{i,0}^{Resmin}..P_{i,500}^{Resmin}) \cdot \mathcal{J}^{-1} \, | \tag{4.12}$$

4.2 *Scenario data*

Based on a literature review and an analysis of historical data, a parameter set to assess the described case studies is derived. Next to system costs, such as investment costs, reoccurring costs for PV systems and BSSs, and finance costs, especially the development of the electricity price and the FIT development are of high importance. While the FIT is currently fixed through the EEG in Germany over the next 20 years once the system is installed, the electricity price changes constantly and thus poses a source of high uncertainty. As the focus lies on analyzing the impact of the BSS investment incentive program, scenario data for 2017 and 2018 is developed, since the subsidy program is currently foreseen to end in 2018. Such data includes a forecast on the electricity price development; further details on how the input parameters are derived are described in Appendix A.1.

The general simulation setup can be summarized as follows: 48 HH profiles with a yearly demand ranging from 3.25 megawatt hour (MWh) to 5.75 MWh are simulated together with normalized PV profiles for four different locations in Germany with each three different PV system orientations (south, south-east and south-west).

4.3 *PV BSSs, self-sufficiency and PV network integration*

In this section, different case studies are conducted to analyze the business case for PV systems and BSSs, to evaluate whether the investment incentive program facilitates PV network integration and to deduct what kind of role self-sufficiency plays in the investment decision.

4.3.1 *Sensitivity and driver analysis for PV BSSs*

An in-depth analysis for the developed reference scenarios shows that an investment into a PV BSS is currently not economically efficient for the majority of analyzed HHs (see Appendix A.2.1). However, for locations with a good solar resource and HHs with a high yearly demand, it might already be a valid option today and is likely to become even more attractive in the years ahead, since increasing self-supply becomes even more beneficial.

To derive conclusions regarding the interdependencies of PV system sizes and different drivers, a sensitivity analysis is performed, where only one input parameter is varied and simulation results are compared to the ref. scenario. Next to economic parameters, a preference for higher self-sufficiency is included. Here, only results for the modeling approach implementing a weighted objective function (W^{Npv}) are displayed. The appropriate weight and modeling approach are chosen based on an in-depth analysis representing the current ratio of PV only vs. PV BSS installations (see Appendix

A.2.5). Resulting changes are ordered from the max. to the min. change in median PV system size and displayed in Fig. 4.1 (top) for 2017 and 2018. Additionally, the median change in BSS capacity is displayed in Fig. 4.1 (bottom) for 2017 and 2018. The analysis focuses on south-facing PV systems (SOs) as such systems are more likely to adopt BSSs and have a higher impact PV network integration than south-east-facing PV systems (SEs) and south-west-facing PV systems (SWs).

In 2017, a change of the expected rate of return (ERR) has the highest impact on PV system sizing for the used parameters. A higher profit orientation results in a smaller sized PV system as value of network feed-in and of self-consumption drop over time. The median PV system size decreases to 3.5 kWp from the ref. median of 5.3 kWp. A lower profit expectation leads to a significant rise in PV system size and the 10 kWp threshold is reached. A change in mean electricity price, in PV system costs and in inflation impact PV system sizing similarly for 2017 in this example. For all cases, the absolute change for parameters that have a decreasing effect on sizes is less significant than the potential increase in size. Thus, a slight oversizing of PV systems might be an option for investors to hedge against such developments. Additionally, lower variable BSS costs also result in larger PV systems, while changes in one-time BSS or PV costs and a higher BSS subsidy have no impact on the median PV system size in 2017.

Only four parameter changes lead to a median BSS capacity above zero in 2017: a higher mean electricity price, a lower FIT, a lower BSS price and a higher self-sufficiency preference. For example, expecting a higher electricity price results in a median BSS capacity of 5.3 kilowatt hour (kWh) and an increase in PV system size to 8.4 kWp. Here, higher electricity prices provide the best economic leverage for PV system sizes. For one additional 1 kWh of BSS capacity 0.6 kWp of PV power is installed (compared to only 0.2 kWp for lower BSS prices), despite the fact that the BSS price changes by 25 % compared to an electricity price change of 21 %. A higher self-sufficiency preference leads to similar BSS sizes than lower BSS costs, but goes along with increased PV system sizes.

In 2018, parameter changes tend to have a more significant impact on PV and BSS sizing. Again, an increase in ERR leads to the highest reduction in median PV system size. The 10 kWp threshold is now reached in several cases: a lower ERR, a higher electricity price, lower variable PV system costs, a lower expected inflation, a higher FIT and a higher self-sufficiency preference. BSS related parameters, such as variable and one-time BSS costs or higher subsidies, also result in larger PV system sizes, going along with a boarder adoption of BSSs. Again, as the installed number and size of BSSs increase, median PV system sizes also increase. Like in 2017, a higher expected electricity price has the most significant impact on BSS sizes followed by a higher preference for self-sufficiency. Furthermore, compared to 2017, additional parameter changes also trigger a median BSS size larger than zero. As the levelized costs of PV energy production decrease (either through lower investment costs or lower expectations on return from ev-

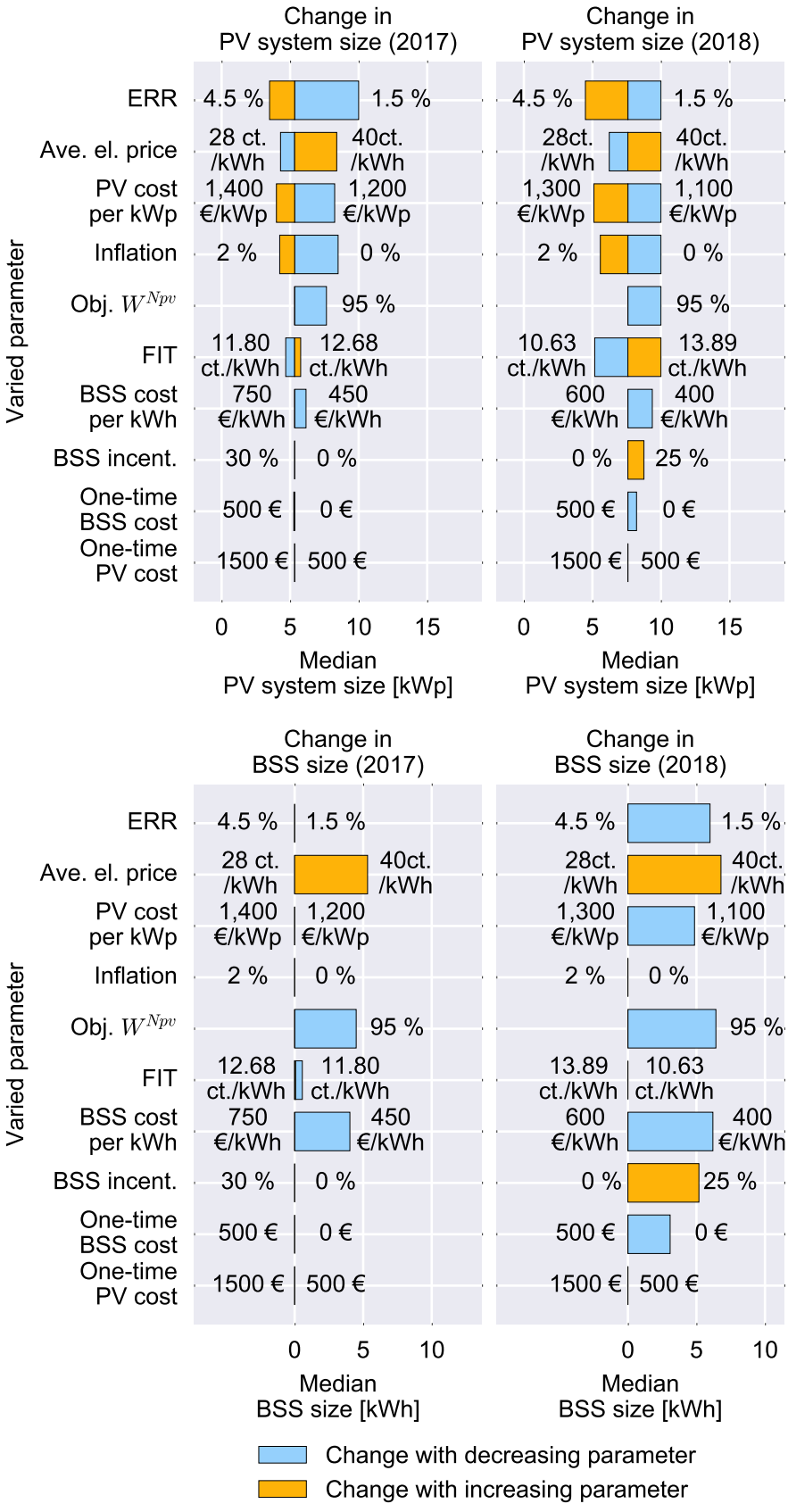

Figure 4.1: Sensitivity analysis for PV system size (top) and BSS size (bottom) for 2017 (left) and 2018 (right) for south-facing PV systems

ery produced kWh) or self-sufficiency desire increases, the attractiveness of storing energy instead to feeding it into the network also increases.[4]

The sensitivity analysis highlights the potential drivers behind sizing of PV BSS. It indicates an increasing likelihood of a continuous surge of BSS investments. As a further price drop in BSS and PV system prices as well as a reduction of value of PV network feed-in are likely to be seen in the near future, self-supply becomes even more attractive. Having a higher self-sufficiency preference and lower profit expectations or assuming a higher increase in electricity price accelerate such developments. Investor expectations on rising electricity prices and higher self-sufficiency desire the main reasons for BSS investment according to a recent survey [7] and explain partially why more PV systems are installed together with a BSS than economically reasonable according to the derived scenario data. Here, the presented model and the corresponding results are in line with the seen adoption rates. In general, the value of BSS unfolds in three-ways: Next to allowing for increased self-sufficiency, it helps hedging against higher electricity supply costs through additional self-supply and reduces losses on PV network feed-in through PV self-consumption. In consequence, a positive correlation between a more frequent adoption of BSSs and larger PV systems becomes visible. PV system sizes surpass in no case the above described 10 kWp threshold, since additional taxes on self-consumption impose a strong limit.

4.3.2 *PV network integration and investment incentive program for PV BSSs*

Changing PV system sizes in combination with BSS investments need to be analyzed from a PV network integration perspective. It has often been argued that a higher penetration of BSSs mitigates PV network integration problems and facilitates the accommodation of higher PV penetration in LV networks [63, 82]. Yet, previous analyses have also shown that a potential benefit resulting from a BSS is strongly related to the operational incentives for the BSS [4, 23, 24, 83]. The operational incentive can either be price related, e.g. lower PV FITs during peak generation hours, or peak oriented, e.g. a fixed feed-in limit for PV feed-in or a dynamic feed-in limit. Currently, the focus for residential PV systems in Germany lies on fixed feed-in limits. Usually, DNOs rely on static rather than dynamic peak PV values

4 It has to be pointed out that the magnitude of system size changes has to be seen in context of the chosen scenarios that aim at providing a realistic range of parameter changes rather than assessing the interdependencies based on varying input parameters with similar percentages (e.g. the ERR varies by 50 %, while PV system costs only vary by 7.7 %). A more detailed analysis based on nominated parameter changes is presented in Appendix A.2.4 The presented analysis so far leaves out an additional parameter, which might impact the sizing decision: the simulation time resolution. A case study regarding its impact is also conducted (see Appendix A.2.8). This analysis shows that a 15 min. simulation time step provides a good estimate for accurate sizing and peak results. Slight overestimation of PV system sizes and peaks are possible once BSS are economically attractive. Size variations lie within an acceptable margin of error (3-4s % for PV sizes when a BSS is installed). BSS capacities are minimally underestimate. Thus, one can conclude that the general conclusions drawn above remain viable and are merely influenced by the simulation time step.

for mid-term network planning, which are often described as a percentage value of installed system sizes. The height of the limit depends on whether an investor agrees to the terms of the investment incentive program and limits max. PV feed-in to 50 % of the installed PV system size instead of the usual 70 % (see Section 3.2.3). Yet, the analysis above indicates that BSSs can enable larger sized PV systems for certain HHs. Thus, a potential benefit from a lower feed-in limit might be offset by larger PV systems as a result of the increasing attractiveness to invest into BSSs with the incentive.

The following analysis evaluates the impact of the investment incentive program on PV and BSS sizing as well as on peak PV feed-in for selected case studies. Especially, SOs are of high interest as they are more likely to cause PV induced network peaks. In Fig. 4.2 a box plot is used to capture the variety of load profile and location induced effects. The box plots are paired according to results with (left) and without (right) investment incentive for different parameter variations. Besides results for lower BSS prices, only results for parameters that are subject to the investor's expectation or preference are included: the ERR, the expected mean electricity price and the self-sufficiency desire. Additional optimizations are performed for PV systems without BSSs to enable a comparison of BSS induced impact on sizing and peak feed-in.

PV system sizes are similarly high when comparing the ref. case in both years to the 'No BSS' case. The ability to invest into BSSs does not increase PV system sizes for the ref. case. However, the location depending attractiveness of the BSS investment and the influence of the 10 kWp threshold become visible. For 2017, the majority of HHs at the location 1 have already reached the threshold, thus oversizing the PV system to produce more PV energy for self-supply is not economically efficient. For 2018, even more HHs reach the 10 kWp threshold. One can see that BSS system sizes vary depending on the availability of the investment incentive for the ref. case, as displayed through the higher whisker in 2017 and the larger 75 % quantile for 2018. The median remains at zero for both cases, underlining that the economic attractiveness of BSSs investment is not given in the ref. case. However, the investment incentive program slightly fosters the adoption of additional BSSs, especially for locations with a higher solar resource.

With regard to network integration, the adoption of a BSS leads to a median peak PV feed-in that is slightly lower for the ref. case compared to 'No BSS' and PV BSS without the incentive. Thus, a marginal benefit is seen for the ref. case in 2017, which is a result of the lower feed-in limit enforced by the investment incentive program. While the median peak is also only slightly lower with the incentive in 2018 (0.4 kW), the 75 % quantile decreases compared to the case without an incentive. As more HHs opt for BSSs with the incentive, more HHs are required to curtail their peak PV feed-in while having a similar sized PV system like in the ref. case.

The impact of the investment incentive program on peak PV feed-in is increasing with a higher attractiveness of the business case. With a higher BSS penetration, the difference between median peak with and without the

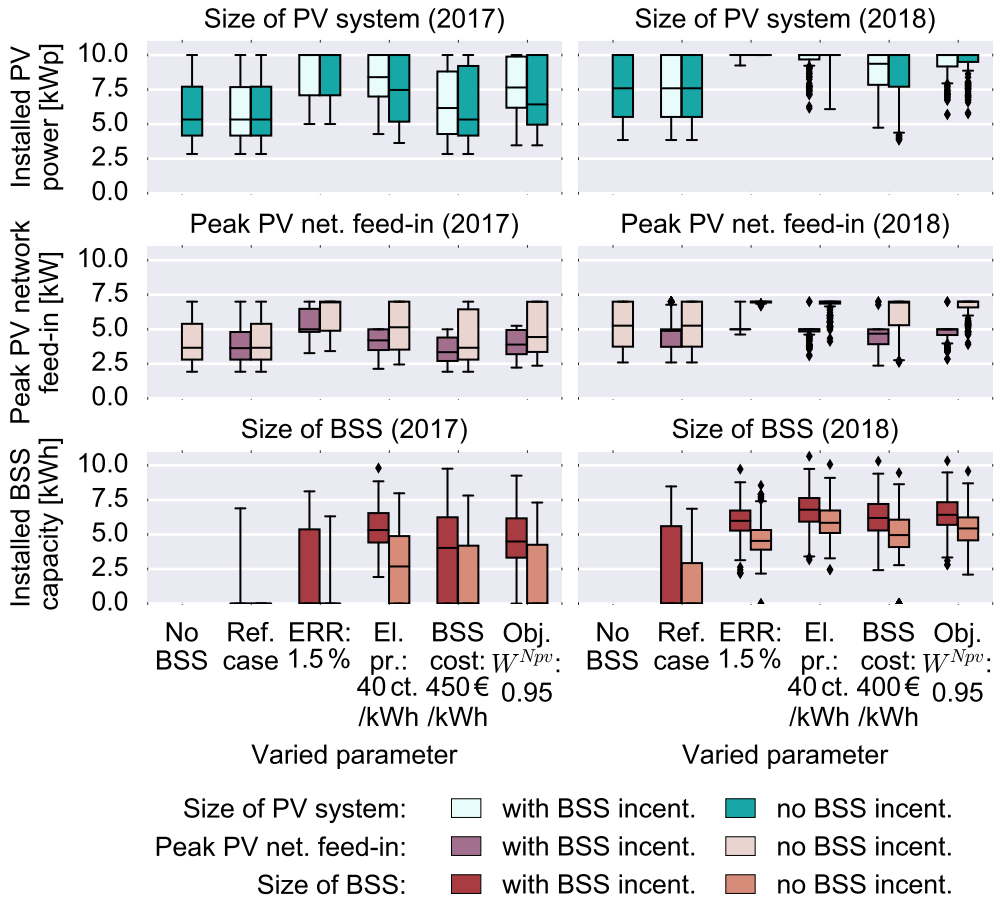

Figure 4.2: Size of PV system (top), peak PV feed-in (middle) and size of BSS (bottom) for selected case studies for 2017 (left) and 2018 (right) for south-facing PV systems

incentive increases. For a lower ERR, larger sized PV systems go along with larger sized BSSs with the incentive and a median decline in peak feed-in of nearly 2 kilowatt (kW) for both years. Depending on whether a HH installs a BSS or not lowers the peak from 7 kW to 5 kW for maximally sized PV system of 10 kWp.

For higher electricity prices, the incentive leads to increase in median PV system size by 3.1 kWp in 2017 (2.4 kWp in 2018) compared to only 2.2 kWp (2.4 kWp) without the incentive. While the median peak PV feed-in lies at 3.7 kW (5.3 kW) for the ref. case without BSSs, it increases to 4.2 kW (5.0 kW) with and to 5.3 kW (7.0 kW) without incentive. Thus, the increase in PV system size can only partially be compensated by a lower feed-in limit in 2017. In 2018, the incentive program fully fulfills its purpose.

Potential contradicting effects resulting from adoption of BSSs based on the investment incentive become visible when analyzing the change in PV system size and peak PV feed-in for a higher self-sufficiency preference (lower BSS prices) in 2017. Here, a purely induced increase of PV system size is noticeable as a result of the BSS investment incentive. The median

PV system size rises by 1.3 kWp (0.9 kWp) compared to the size without the investment incentive program. For a higher self-sufficiency preference, the effect of this increase on peak PV feed-in cannot be compensated by the lower feed-in limit; the median peak feed-in lies 0.3 kW above the ref. case without investment incentive in 2017. For lower BSS costs, the size increase is offset by the feed-in limit as the peak feed-in lies 0.4 kW under the ref. case. However, this does not capture the full potential of the expected reduction. Without the increase in PV system size, a peak PV feed-in of only 2.6 kW would have been expected with the lower network feed-in limit of 50 %. Instead, the median peak PV feed-in only decreases to 3.3 kW, falling short of 0.7 kW reduction potential. For these cases, one can conclude that the investment incentive program only partially fulfills its purpose of lowering peak PV feed-in as the adoption of BSSs also incentivizes HHs to oversize their PV systems.

In 2018, the effects are not seen anymore. The median PV system size is 0.6 kWp lower with the investment incentive compared to without the incentive (but still 1.8 kWp larger than the ref. case) for lower BSS prices. The incentive increases the attractiveness of adopting a higher ratio of installed BSS capacity vs. installed PV power to avoid PV curtailment and to increase self-sufficiency. In other words, the value of storing excess PV generation over a longer period becomes economically more attractive than producing more PV power, storing it over shorter time periods and risking higher amounts of PV curtailment. Here, the BSS investment incentive program manages to have a two-fold positive impact on network integration as also median peak PV feed-in is lower than expected.

While the BSS penetration rate significantly increases for all SOs from 2017 to 2018 with and without the investment incentive program, the adoption of such systems follows a less steep path for SEs and SWs. Here, the incentive fosters their adoption notably. PV system sizes also experience a large increase. E.g. in 2018 for lower BSS costs, median PV system sizes are around 6.2 kWp with and 5.3 kWp without the incentive (compared to 4.5 kWp for the ref. case in 2018). Peak PV feed-in is - as expected - lower than for SOs. For SEs and SWs the above described effect of not capturing the full peak reduction potential as a result of the incentive program becomes more visible than for SOs. Again, the incentive fulfills its purpose only partially. However, as the peak PV feed-in is usually set by SOs, not capturing the full benefit here should not be an issue for the overall PV integration (compare Appendix A.2.6). On a positive note, the incentive program actually fosters adoption of larger sized PV systems for such unfavorable orientations and allows capturing the full rooftop potential here.

In summary, it can be concluded that the investment incentive program limits the peak feed-in. However, in certain cases adopting BSSs allows larger PV systems. While the impact of this increase on peak PV feed-in is more noticeable when no incentive program is in place, it sometimes is also seen with the program. The increase in PV system size partially offsets the lower feed-in limit. In some cases, such as a higher self-sufficiency desire,

the adoption of BSSs - as a result of the investment incentive program - does not result in the full expected peak reduction. However in other cases, the increase in PV system size is slightly slowed down with the investment incentive. Here, storing PV energy is traded for producing additional energy.

The adoption of a BSS itself does not result in a lower peak compared to a PV system without a BSS for the majority of cases in this example; only imposing a lower feed-in limit results in a lower PV feed-in. Achieving higher degrees of self-sufficiency (either through endogenous modeling or assumptions such as higher electricity prices) is facilitated through the investment incentive program. While BSS adoption and the program itself might also lead to larger sized PV systems, only a lower feed-in limit mitigates potential increases in peak PV feed-in. Yet, once such a program runs out, this advantage disappears and increasing attractiveness of the business case for self-supply using BSSs will lead to larger sized PV systems without an additional peak reduction (if PV network feed-in remains partially attractive).

4.3.3 *Aggregated peak analysis for PV BSSs in a new regulatory environment*

Previous analyses have focused on the change of the individual HH's system sizing and its peak PV feed-in. The assessment provides estimation for DNOs on how PV BSSs evolve depending on different factors and what median sizes to expect for their mid-term network planning. Yet, from those results no conclusions can be drawn at which point networks are likely to reach critical PV penetration levels. As pointed out above, current networks are often still dimensioned according to the simultaneity of demand peaks. Aggregated feed-in peaks become dominating planning factors for DNOs with an increasing PV penetration. Thus, the following analysis describes at what penetration rate the aggregated peak PV feed-in surpasses the aggregated demand peak. As such analyses are always network specific, the analysis focuses on one location to highlight some trends.[5] Next to a 'PV only' case study (no BSS), only scenarios are analyzed that result in every HH being equipped with a BSS (with and without the BSS investment incentive program). Here, a high electricity price is chosen. Furthermore, scenario 'Smart meter, no incentive' displays the impact of changing regulatory requirements for small-scale PV systems with the currently planned, but still uncertain smart meter rollout in Germany. Such requirements impose additional economic thresholds at 1 kWp, 7 kWp and 10 kWp. On the other hand, the smart meter infrastructure is supposed to enable more dynamic active power management and thus fixed feed-in limits are not required anymore.

Fig. 4.3 shows the range of peak PV feed-in ($P_i^{Resmaxmin}$ and $P_i^{Resmaxmax}$) and the range of peak demand ($P_i^{Resminmin}$ and $P_i^{Resminmax}$) per HH depend-

5 Results for other locations can be found in the appendix.

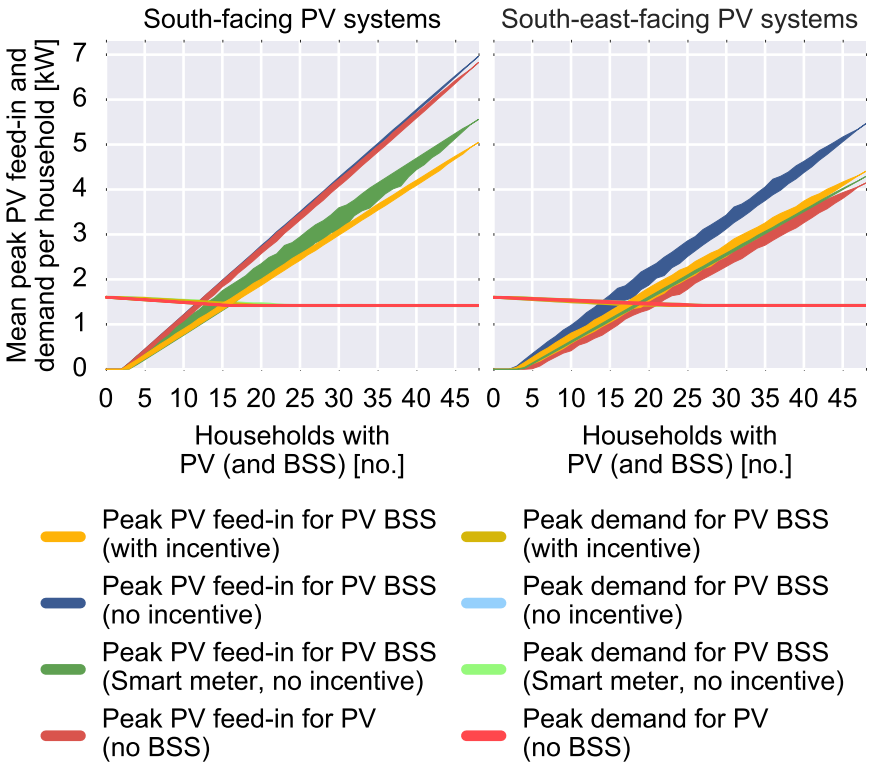

Figure 4.3: Comparison of mean peak PV feed-in and peak demand per HH depending on the amount of HHs with a PV system for different scenarios: PV only (no BSS), PV BSS with and without BSS investment incentive as well as PV BSS subject to regulator requirements of the German smart meter rollout for high mean electricity prices for south-facing systems (left) and south-east-facing systems (right) for location 4 for 2018.

ing on the total number of HHs with a PV system and on different case studies for SOs and SEs. Mean peak values per HH are calculated as described in Section 4.1 and thus include peak simultaneity. They depend on the number of HHs equipped with a PV system or PV BSSs. For example, if 20 HHs invest in a PV BSS, 28 HHs have no PV BSS in this example.

When evaluating the development of the mean peak demand per HH, one notices a slight reduction in peak demand with an increasing number of PV systems or PV BSSs being installed for all presented cases. As no difference in the reduction between just PV systems or PV BSSs can be observed, one can conclude that there is a small overlap between the aggregated peak demand and PV energy production for the used data. However, even if all HHs have a PV system installed the peak change remains negligible (with less than 0.2 kW per HH). This impact highlights that results highly depend on the underlying profiles. Other analyses performed by the author have shown that there might be no impact on the aggregated peak load or is only observed with new operational incentives [11, 24].

For SOs, a main conclusion of the previous analysis is still valid. BSSs do not improve peak PV feed-in without an additional operational or investment incentive. When comparing the aggregated peak feed-in for PV

systems and PV BSSs without the investment incentive, PV systems are minimally larger with BSSs. With the incentive, the feed-in limit drops to 50 % compared to 70 % for cases 'no BSS' and 'no incentive'. While the median PV system size remains at the 10 kWp threshold, this operational incentive results in a lower peak feed-in due to the lower feed-in limit. When the incentive program runs out and additional regulatory requirements related to the smart meter rollout kick in, PV system sizes are reduced to 7 kWp. Such a reduction can partially compensate the omission of feed-in limits; the aggregated peak PV feed-in is slightly higher than with the incentive program. Additionally, the spread between min. and max. peaks widens depending on the penetration rate as PV system sizes are not sized according to the 10 kWp threshold and no feed-in limit in relation to PV system size exists anymore.

For SEs, PV BSSs without the investment incentive lead again to the highest mean peak. Compared to SOs, undesired effects of the incentive program become visible. The mean peak feed-in with an incentive exceeds the peak of the case without BSS. The spread between min. and max. peak feed-ins is wider in this case because PV system sizes vary more depending on the underlying HH. With new investment restrictions related to the smart meter roll-out, PV system sizes are again reduced (by 2.1 kWp in median). Such undersizing leads to a lower mean peak per HH of 0.1 kW compared to the incentive program.

When comparing case studies, it also becomes visible that - as expected - SEs pose a lower threat to potential network reinforcement needs than SOs. For case 'no BSS' and 'Smart meter', the peak PV feed-in per HH is higher than the peak demand per HH once more than 19 HHs or 40 % of HHs are equipped with a SE. With SOs, this percentage decreases to 25 % (or 12 HHs) for 'no BSS' and to 29 % (or 14 HHs) for 'Smart meter'. In case PV BSSs are installed without the incentive, the peak feed-in exceeds the peak demand at the same number of installed PV systems (25 % or 12 HHs for SOs) and is lower for SEs (31 % or 15 HHs). With the investment incentive and a lower feed-in limit in place, the PV penetration rate can rise to 33 % or 16 HHs for SOs and 35 % or 17 HHs for SEs in this example.

Several key findings can be pointed out. The peak feed-in becomes the relevant network planning factor for an increasing amount of PV systems or PV BSSs. In the presented example, a penetration rate as low as 25 % of HHs being equipped with PV systems leads to a peak feed-in that exceeds the peak demand. A general conclusion that BSSs lower the PV peak cannot be drawn. The peak feed-in is more determined by operational incentives, such as the feed-in limit, or investment restrictions, such as constraints related to the smart meter rollout. Previous results from the individual HH analysis are supported by the aggregated analysis. The incentive program successfully limits peak feed-ins for SOs. For SEs, the program enables larger sized PV systems that partially compensate the expected reduction in peaks. If no further restrictions are in place, BSSs can even lead to higher aggregated peaks, since they do not impact feed-in simultaneity in the presented case

studies. New regulatory requirements might mitigate peak PV feed-in, but come at the price of reducing PV system sizes and not making use of the available rooftop area.[6]

4.4 *Conclusion*

Since network parity has been reached, the economics of residential PV systems have changed and BSSs are becoming a favorable option for investors to increase PV self-consumption and self-sufficiency. To address the changing complexity of sizing and operating a PV BSS, an optimization model is developed. By modeling the current BSS incentive program, preferences for self-sufficiency, new regulatory requirements and taxes, PV BSS investors are enabled to derive a better understanding of complex interdependencies between sizing drivers and robust decisions for optimal system sizing and operation. Using the developed model and the proposed case study-based approach, other stakeholders such as DNOs and policy makers are empowered to efficiently evaluate implications of this dynamically evolving business case.

The analyses show that the current uptake of BSS investments is mainly supported by the following drivers: a higher expected electricity price, lower expected return and higher preference for self-sufficiency in combination with the investment incentive program. A BSS helps hedging against higher electricity supply costs through additional self-supply and reduces losses on PV network feed-in through PV self-consumption. With decreasing system costs and a declining value of PV network feed-in, a more frequent adoption of BSS is likely. BSSs allow for larger sized PV systems in some cases. Yet, PV system sizes do not surpass the 10 kWp threshold, where additional taxes on self-consumption impose a strong limit.

From a network integration perspective, the adoption of a BSS itself does not result in lower peak feed-ins compared to a PV system without a BSS in the presented examples. Imposing a lower feed-in limit through the investment incentive program helps mitigating PV network feed-in in most cases. However, in some cases the peak reduction does not translate into the expected decline in peak feed-in as larger sized PV systems partially compensate the potential peak decrease and limit the effectiveness of the investment incentive program. Once such a program runs out, the operational incentive to limit PV network feed-in disappears. The increasing attractiveness of self-supply and desire for self-sufficiency (in combination with fairly moderate FIT) might lead to larger PV systems resulting in a higher peak feed-in again. BSSs help accelerating such tendencies without providing an imminent benefit for PV network integration.

New regulatory requirements that influence the sizing decision might reduce expected PV systems sizes again and thus mitigate peak PV feed-in. In general, the results support the conclusion that has been drawn before:

6 Similar conclusions can be drawn for other locations (see A.11).

Operational incentives determine whether a BSS mitigates PV induced network integration challenges, e.g. feed-in limits or price-based incentives [11, 24]. However, when imposing an operational incentive, such as a lower feed-in limit, e.g. through an investment incentive program, its effects on the sizing decision cannot be neglected and need to be taken into account when evaluating and designing such incentives as they can lead to counter-intuitive results.

Since a further drop in BSS and PV system prices as well as a FIT reduction are likely in the near future, the business case for self-supply and PV self-consumption becomes even more attractive. Next to PV network integration challenges, an additional challenge arises for DNOs. The trend towards higher amounts of self-sufficiency leads to a declining revenue in NCs. Less electricity is procured from networks, while network costs potentially rise as a result of higher PV penetration. Challenges and implications for the business case for PV systems as well as DNO network planning and pricing are discussed in the next part.

Part II

AN INTEGRATED APPROACH FOR EVALUATING INTERACTIONS BETWEEN DNO AND HOUSEHOLDS WITH A PV BSS

As BSSs are more frequently installed together with PV systems at residential buildings in countries like Germany, additional questions for DNOs arise. Part of the investment incentive for such systems stems from avoiding paying NCs while still relying on the network for peak loads and PV feed-in. On the one hand, DNOs face a reduced NC revenue as a result of increased self-sufficiency. On the other hand, PV network integration is impacted.

In this part a bilevel optimization model is developed to evaluate the resulting dynamics and interdependencies between two core PV BSS stakeholders: DNOs and investors of PV BSSs. Using an integrated, closed-loop approach, the main DNO's decision problems are modeled: raising NCs, reinforcing the network, curtailing PV feed-in and choosing the appropriate NC tariff while also increasing the incentive for investing in a PV BSS. It allows DNOs to test what kind of tariff structures provoke which PV BSS sizing and operation decisions and how such decisions impact HHs without PV BSSs. DNOs are enabled to trade-off the effectiveness of different measures to foster PV network integration and the danger of starting a self-reinforcing process, potentially leading to network defection. PV BSS investors are empowered to include strategic decision making with respect to the DNO's and other investors' reactions in their sizing and operation decisions.

Two case studies show that the reached equilibrium between DNO and PV BSSs comes at a price of raised NCs, which fosters the incentive to increase PV BSS sizes, but also augments the peak of PV network feed-in. Yet, total network defection is not a realistic scenario as the marginal value of additional self-supply decreases with higher NCs. Compared to PV curtailment by the DNO or network reinforcements, fixed feed-in limits and power-based NCs reduce oversizing of PV BSSs and provide an operational incentive for peak-oriented BSS operation.

5

Introduction

Since FITs for rooftop PV systems have dropped below end customer electricity prices in countries like Germany or Australia, the demand for BSSs has risen tremendously [11, 84]. The business case for such PV BSSs relies on replacing network electricity consumption with self-generated PV energy, while still relying on the network connection for peak load supply and excess PV feed-in. As outlined in the previous part, current PV BSSs are sized according to attractiveness of additional self-supply. That can easily lead to self-sufficiency rates of over 60 %, while more than 50 % of the generated PV energy is still fed into the network. Avoiding paying NCs is part of the self-sufficiency incentive in Germany, since such charges are mainly collected based on energy procured from networks at HH level.

HH customers saw a 3 % increase of NCs in 2016. The rise is partially linked to an increasing amount of installed RESs in Germany as network reinforcements have been implemented and larger volumes of RES curtailment are currently seen to preserve system stability (see § 14 EEG in combination with § 13 German Energy Industry Act (EnWG)) and have to be compensated [14]. For example, costs related to RES curtailment have amounted to 373 mio. € in 2016 [85]. Curtailment costs can directly impact redistribution effects within HH electricity prices, e.g. when RES curtailment is used to avoid network reinforcement (see EnWG § 11 (2) with German Incentive Regulation Ordinance (ARegV)). Curtailed RESs are reimbursed according to the individual FIT of each RES plant (see § 15 EEG). The resulting costs are recollected via NCs, leading to NC rises in areas of high RES penetration. With no curtailment, RES plants would have been reimbursed with the FIT, which is collected nationwide via the EEG surcharge. Thus, an additional self-supply incentive is created through higher NCs. Besides additional network costs and higher NCs, an increasing amount of self-supply leads to a redistribution of network costs among customers. However, DNOs already start adjusting NC structures, as an analysis of the development of NC for the biggest 30 DNOs serving rural and suburban areas, where PV is typically installed, shows (see Fig. 5.1).

While the overall median compound annual growth rate (CAGR) is at 5.7 % for the analyzed years, the CAGR for fixed yearly fees lies at 25.2 % compared to only 3.4 % for energy-based components. Such a development indicates a shift towards yearly fixed fees, which used to account for 13 % of the total paid NCs in 2014 and have nearly doubled to 22 % in 2017 for the analyzed DNOs. Yet, such adjustments do not address structural flaws of pricing NCs according to peak usage and do not incentivize a network-supporting PV BSS operation. The urgency of understanding dynamics between NCs and self-supply systems is underlined by forecasts for

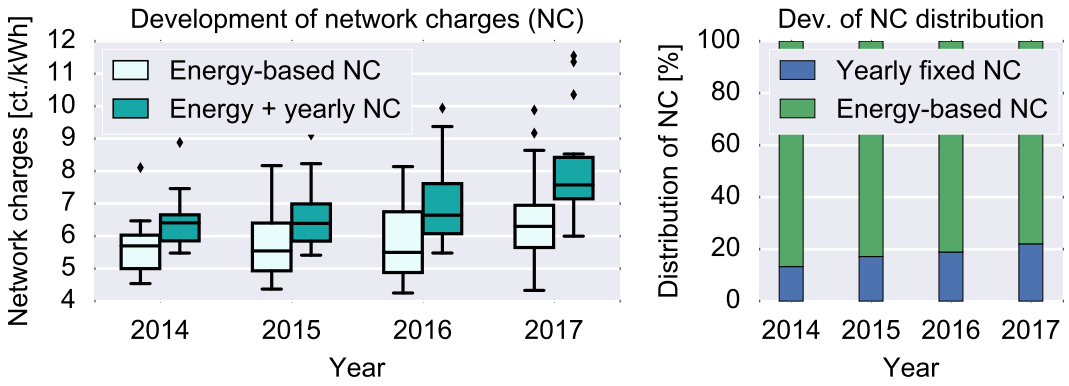

Figure 5.1: Historical development of network charges (NCs) (left) and development of percentage of yearly fixed vs. energy-based NCs (right) for 30 regional DNOs in Germany

the development of HHs' NCs that suggest an increase by up to 25 % until 2022 [86].

Hence, this part presents an analysis of the dynamics of NC pricing and the business case for PV BSSs. A literature review is performed on PV BSS sizing with regard to interdependencies with NC setting, their impact on network integration and operational incentives for PV BSSs to avoid an additional increase in network costs. Based on the review, this work's analytical and modeling contributions are specified.[1]

5.1 *Literature review*

As outlined in the previous part, several authors propose models to analyze the business case for PV BSSs and self-sufficiency. In the German context, most authors evaluate PV BSS sizing from a HH's perspective under the self-supply theme using different approaches ranging from iterative case study-based analysis to MILP (such as the one presented in the previous chapter) [5, 11, 27, 28, 40, 50]. International analyses focus more on use cases related to hedging against price differences, storage sizing for energy communities or peak shaving [30, 64, 72, 88]. While these business cases partially depend on NCs, since they are part of self-supply or price hedging incentives, the analyses do not address possible implications for DNOs, NC pricing and PV BSS sizing resulting from increased NCs due to self-supply.

Other authors discuss how BSSs can ease PV network integration by addressing voltage problems or line overloading [10, 41, 67, 69]. However, the previous part and the literature review show that PV BSSs only provide a relief for networks if operational incentives are set accordingly [62, 65, 68, 83]. If such systems are operated under the current self-supply strategy, it is likely that no reduction of peak PV feed-in is achieved [11, 83] and other measures, such as reactive power provision, are more effective to improve

1 Parts of this chapter are presented in [87].

PV network integration [12, 68]. Yet, current studies do not investigate latest regulatory developments in Germany, which allow DNOs to curtail PV network feed-in to extenuate need for network expansion. So far, it has not been investigated whether such measures incentivize a different, more network-beneficial BSS operation and result in a different PV BSS sizing.

Several authors address potential issues and negative side-effects of higher PV BSS penetration. In worst-case scenarios a contentious adoption of PV BSSs creates an additional self-supply incentive, since network costs have to be redistributed among lower volumes of energy procured from networks. Thus, even more HHs opt for a PV BSS investment; a self-reinforcing process is started. A spiral of death is initiated where each self-supply system increases the incentive for additional HHs to follow, which ultimately leads to complete network defection of HHs [15]. The assessment of this thread varies depending on the case study. While some authors see a real case for network defection within the near future in the US [18], others conclude that costs are too high for leaving the network all over the US [89, 90]. Differences may stem from used assumptions and most significantly from used modeling approaches. Some authors base their assessment on yearly energy values and do not include any optimization approach [18, 90]. Other authors go into more detail by modeling time-dependent energy flows using a simple heuristic for BSS operation and a brute force approach for simulating different system sizes [89]. Optimization approaches are also implemented, but focus more on optimal PV BSS sizing under varying assumptions [17]. The approaches fall short of modeling interactions between NC setting and PV BSSs and discussing implications for sizing. Dynamics between tariff options and PV BSS adoption using fixed PV BSS sizes and yearly energy balances are modeled in [91]. Here, conclusions regarding implications of PV BSS sizing considering rising NC on optimal system sizing as well as network integration are not drawn. Other authors develop a framework that integrates a network and customer adoption model, but uses fixed PV and BSS sizes for simulations and thus dynamics of sizing and network integration are not assessed [16]. A bilevel approach for modeling PV sizing and increasing electricity prices is proposed in [92]. Here, PV system sizing and electricity prices are decision variables in one integrated problem. However, the focus is on PV systems, which are limited in increasing self-supply due to temporal differences between PV and load. Additionally, implications for PV network integration are not analyzed.

The analysis shows that different aspects of PV network integration, PV BSS sizing as well as implications for tariff systems have been discussed in the literature. However, an integrated model and a corresponding approach for understanding proper NC setting and trading-off network reinforcement measures by DNOs and the resulting reaction from potential PV BSS investors with regard to optimal system sizing and operation is missing. Such a model needs to reflect strategic decision making of these stakeholders dynamically to address the danger of a self-reinforcing process. Furthermore, tariff options are not discussed with regard to PV BSS

sizing, welfare distribution among HHs and network-supporting BSS operation.

5.2 *Main contributions*

This part presents presents a new optimization model to evaluate the dynamics and interdependencies between two core PV BSS stakeholders: DNOs and investors of PV BSSs. The closed-loop model allows DNOs to assess trade-offs of increasing NCs and thus fostering the incentive to defect from networks while simultaneously solving the sizing and operation problem of PV BSS investors. The following additional contributions are made by this work:

- Modeling: A bilevel optimization model is developed to integrate the DNO's decision of increasing NCs, choosing a different tariff structure and reinforcing the network as well as the PV BSS investors' reactions to such actions. On the DNO level, the model furthermore allows determining whether it is more cost-efficient to reinforce the network or to curtail PV energy with regard to the network integration of PV BSSs. On the PV BSS level, the approach integrates strategic decisions on PV BSS sizing and operation to incorporate closed-loop interdependencies of the PV BSS business case, NC structure and decision making of other PV BSS investors.

Case studies are designed to address specific questions related to dynamics of NC setting and PV BSS sizing and operation in the German context:

- A main question that arises is whether an equilibrium between rising NCs and increasing PV BSS sizes can be reached or whether a self-reinforcing process is started, which eventually leads to total defection from the distribution network?
- What NC tariff system fosters PV adoption, eases PV network integration and minimizes welfare redistribution of network costs from HHs with PV BSSs to HHs without PV BSSs?
- How do DNO options for addressing higher PV penetration rates, such as network reinforcements or PV curtailment, reflect on proper NC setting, PV BSS sizing and policy setting?

5.3 *Organization of the section*

Section 6 describes the problem formulation, which is divided into the DNO's optimization, the upper level (UL), PV BSSs' problems, the lower level (LL), and a section on integrating the two problems by adopting a mathematical problem with primal and dual constraints. Section 7 provides two main case studies. The first case study analyzes the impact of tariff

structures on PV self-supply and quantifies economic changes for HHs with and without PV BSSs. The second case study focuses on a network reinforcement theme and discusses the trade-offs described above. The part ends with a conclusion.

6

Bilevel optimization for strategic DNO and PV BSS decision making

With more PV BSSs being connected to the network, DNOs face the challenge of reinforcing networks and coping with reduced NC revenues, while keeping their costs at a minimum [24, 82, 93, 94]. Besides a preference for higher self-sufficiency, HHs invest in PV BSSs to maximize their individual profit (see Part I). By investing in PV BSSs, HHs are influencing the NC value by not paying NCs for self-supplied energy and relying on feeding PV into the network. Thus, conflicting optimization objectives between the DNO (minimizing NCs while coping with higher network integration costs and lower demand) and HHs with the ability to invest in PV BSSs (maximizing profit from PV network feed-in and increased self-supply) have to be modeled to derive a better understanding of strategic decision making of these players (see Fig. 6.1).[1]

6.1 *Modeling approach*

Optimization problems that are impacted by other optimization problems are referred to as bilevel problems. Typically, conflicting optimization objectives of different actors lead to a hierarchical problem structure. Such closed-loop problems are connected through an equilibrium that describes the clearing price and volume. The equilibrium is of high relevance for any market participant because it influences decision making with regard to

1 Parts of this chapter are presented in [87].

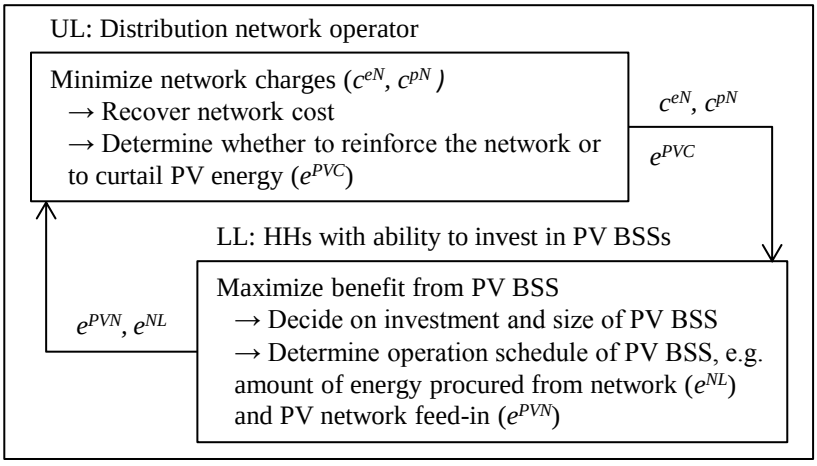

Figure 6.1: Strategic decision making of DNO (UL) and HHs with PV BSSs (LL)

anticipated prices and volumes. If an actor is able to anticipate the equilibrium, the actor can chose its strategy accordingly [95]. These so called Stackelberg games typically comprise a leader, the DNO on the UL, and followers, HHs with the ability to invest in PV BSSs on the LL, and result in a new equilibrium between leader and followers [96]. Here, the DNO anticipates electricity procured from the network and peak PV feed-in, which are impacted by PV BSS sizing and operation decisions, and chooses NCs and network reinforcement accordingly. Thus, the DNO's optimization problem is constrained by HHs' optimization problems. On the LL, HHs strategically optimize PV BSS investments according to their own benefit, but take into account other HHs' reactions and DNO NC setting. Interdependencies of such problems are similar to Nash problems.[2] In such games, every player (HH on the LL) chooses a strategy (optimization of PV BSS sizing and operation) that implies that all players stick to their chosen strategy. If all players are satisfied with their strategy, a Nash equilibrium is reached [95, 98].[3]

In power systems research, bilevel approaches are usually used for strategic pricing decisions in wholesale markets or for transmission network expansion problems as well as storage sizing for price hedging or market integration of RESs [95, 99–102]. While the literature suggests that such an approach is fitting for the described problem, it has not been applied to analyze the dynamics of NC setting, network expansion and PV curtailment with regard to PV BSS sizing and operations.

6.2 *DNO optimization problem*

DNOs are incentivized to provide secure and stable network operation at regulated revenues and costs. Usually, NCs are billed per kWh on a LV level in Germany. However, networks are dimensioned according to the aggregated peak load and not consumed energy. Under current incentives, PV BSS operation does not lower or only marginally lower peak demand when operated under a standard self-consumption strategy in Germany. With higher PV penetration, peak PV feed-in becomes the driver of network reinforcements [12]. BSSs can even enable larger sized PV systems and partially base their business case on avoiding paying NCs. Thus, DNOs have to integrate more PV systems while coping with a reduction in revenue.

6.2.1 *UL objective function*

Usually, DNOs are supervised by the regulators to ensure that they provision distribution networks at minimum cost. If no network reinforcements are necessary, it is assumed that the total costs remain nearly unchanged

2 HHs without the ability to invest in PV BSSs are additional stakeholders, which are pure price takers in this problem. It is assumed that they cannot change their behavior by replacing or consuming less electricity as electricity is a fairly inelastic product [97].

3 Details on the mathematical theory can be found in Appendix B.1.

with and without PV BSSs and self-supply leads only to a redistribution of NCs among HHs. If network reinforcements are required, additional costs need to be recovered by increasing NCs. It is assumed that the DNO's objective z_{UL} is to minimize the NC increase while achieving full cost recovery. DNOs usually distinguish between NC paid per consumed energy c^{eN} or per peak demand or peak feed-in c^{pN}.[4]

$$min\ z_{UL} = W^e \cdot c^{eN} + W^p \cdot c^{pN} \tag{6.1}$$

Currently, HH customers are billed according to consumed energy and have to pay a fixed yearly fee. Adopting peak demand pricing requires a new metering infrastructure at HH level, which is likely to be installed within the next few years. A NC tariff system that would not distinguish between peak demand and peak feed-in would be a major adjustment to the current tariff structure; currently only loads bear network costs and generators do not pay for feed-in. Such changes might not be in compliance with providing a non-discriminatory network connection for generators.

6.2.2 *UL constraints*

Since network costs remain unchanged in case of no network reinforcements, NCs have to account for the original NCs (C^{eNorg} and C^{pNorg}) over all HHs (with PV $\mathcal{J}^{PV}$ and without PV . A decrease in network consumption $e^{NL}_{j,t}$ or peak demand p^{NL}_{j} compared to the original demand $E_{j,t}$ or original peak P_j resulting from investments in PV BSSs has to be retrieved through a rise in energy-based NCs c^{eN} or power-based NCs c^{pN}.

Network reinforcements are necessary if a certain network capacity is exceeded. Corresponding costs are included via C^{NR}_r and binary variables n^{bi}_r, where r is a measure in the corresponding set $\mathcal{R}$. Previous studies show that no linear relationship between reinforcements and higher PV penetration exists in LV networks [12, 83]. As underlying research questions focus on dynamics of reinforcement, NC setting and PV BSS sizing, here only a methodological approach for network refinance and reinforcement is implemented and the reinforcement problem is simplified via binary variables.

Instead of reinforcing the network, DNOs can also curtail PV energy $e^{PVC}_{j,t}$. Then, the DNO has to reimburse PV system owners for $e^{PVC}_{j,t}$. Currently, such compensation payments C^{Cur} are equal to the PV FIT (see § 15 EEG) and are retrieved by adjusting NCs (see ARegV § 11 (2) 17).

Overall, three cost components (original costs, costs related to network reinforcements and costs related to PV curtailment) have to be recovered by increasing NCs, as Eq. 6.2 shows:

4 Weights for energy-based NCs W^e or power-based NCs W^p serve nominating purposes.

$$
\begin{aligned}
&(C^{eNorg} + c^{eN}) \sum_{t \in \mathcal{T}} \Big(\sum_{j \in \mathcal{J}^{PV}} e_{j,t}^{NL} + \sum_{j \in \mathcal{J}^{L}} E_{j,t}^{L} \Big) \\
&- C^{eNorg} \sum_{t \in \mathcal{T}} \Big(\sum_{j \in \mathcal{J}^{PV}} E_{j,t}^{L} + \sum_{j \in \mathcal{J}^{L}} E_{j,t}^{L} \Big) \\
&+ (C^{pNorg} + c^{pN}) \Big(\sum_{j \in \mathcal{J}^{PV}} p_{j}^{NL} + \sum_{j \in \mathcal{J}^{L}} P_{j}^{L} \Big) \\
&- C^{pNorg} \Big(\sum_{j \in \mathcal{J}^{PV}} P_{j}^{L} + \sum_{j \in \mathcal{J}^{L}} P_{j}^{L} \Big) \\
&- C^{Cur} \sum_{t \in \mathcal{T}} \sum_{j \in \mathcal{J}^{PV}} e_{j,t}^{PVC} \\
&- \sum_{r \in \mathcal{R}} (PF^{DNO})^{-1} \cdot C_{r}^{NR} \cdot n_{r}^{bi} \quad \geq \quad 0
\end{aligned} \tag{6.2}
$$

DNOs are now allowed to curtail up to 3 % of the yearly produced PV energy per system to avoid network reinforcements in Germany (see § 11 (2) EnWG (2016)). The curtailed energy $e_{j,t}^{PVC}$ depends on the chosen PV system size s_{j}^{PV} per HH and the given nominated PV profile $E_{j,t}^{PV}$ per HH.

$$
\forall j \in \mathcal{J}^{PV} : \sum_{t \in \mathcal{T}} e_{j,t}^{PVC} - 0.03 \cdot s_{j}^{PV} \cdot \sum_{t \in \mathcal{T}} E_{j,t}^{PV} \leq 0 \tag{6.3}
$$

If the given network capacity P_{r}^{Lim} is exceeded as a result of peak PV feed-in p^{PV}, a network reinforcement measure P^{NR} is enabled through the activation of a binary variable. In LV networks, such a measure is usually a discrete decision, e.g. upgrading a transformer or investing into a parallel line to address hosting capacity issues.

$$
\forall r \in \mathcal{R} \colon p^{PV} - P_{r}^{Lim} - n_{r}^{bi} \cdot P^{NR} \leq 0 \tag{6.4}
$$

p^{PV} is determined by aggregating PV feed-in $e_{j,t}^{PVN}$ over all HHs with PV system and time-adjusting it via τ:

$$
\forall t \colon \sum_{j \in \mathcal{J}^{PV}} e_{j,t}^{PVN} - \tau \cdot p^{PV} \leq 0 \tag{6.5}
$$

6.3 *Investment and operation decision problem for HHs*

HHs attempt maximizing their benefit by investing in a PV system and possibly a BSS to reduce energy procurement and receive a FIT for PV feed-in. As the previous part detailed the investment and operation decisions on the LL, this section summarizes the main aspects and additionally introduces dual variables necessary for merging the UL and LL optimization problem.

6.3.1 *LL objective function*

The main cost drivers and revenues remain as proposed in the previous part. For the sake of linearity, one-time investment costs for the PV system I^{PV}, the storage inverter I^{BSSkW} and the storage capacity of the BSS I^{BSSkWh} and corresponding yearly maintenance costs M^{PV}, M^{BSSkW} and M^{BSSkWh} depend on sizing decision variables for the different components s_j^{PV}, s_j^{BSSkW} and s_j^{BSSkWh}. Fixed investment costs independent of sizing are neglected. Direct revenues result from $e_{j,t}^{PVN}$ and $e_{j,t}^{PVC}$, direct costs occur from network consumption $e_{j,t}^{NL}$. Indirect costs are related to German tax law. As PV system owners operate such a system commercially, which is required to receive FIT, they have to pay sales taxes C^{Sc1} on PV self-consumption (direct PV self-consumption $e_{j,t}^{PVL}$ and indirect via the BSS $e_{j,t}^{BSSL}$). Additionally, taxes on earnings have to be paid based on the difference of revenues from network feed-in TE^{Fit}, curtailment TE^{Cur}, self-consumption TE^{Sc} and a deduction of investment and yearly operational costs TE^{Dep}. Eq. 6.6 sums up the LL objective function.

$$
\begin{aligned}
max\ z_{LL} \;=\;& (C^{Fit1} - TE^{Fit}) \cdot PF^{HH} \sum_{t \in \mathcal{T}} \sum_{j \in \mathcal{J}^{PV}} e_{j,t}^{PVN} \\
+\;& (C^{Cur} - TE^{Cur}) \cdot PF^{HH} \sum_{t \in \mathcal{T}} \sum_{j \in \mathcal{J}^{PV}} e_{j,t}^{PVC} \\
-\;& (I^{PV} + M^{PV} \cdot PF^{HH} - TE^{Dep} \cdot PF^{HH}) \sum_{j \in \mathcal{J}^{PV}} s_j^{PV} \\
-\;& (I^{BSSkWh} + M^{BSSkWh} \cdot PF^{HH}) \sum_{j \in \mathcal{J}^{PV}} s_j^{BSSkWh} \\
-\;& (I^{BSSkW} + M^{BSSkW} \cdot PF^{HH}) \sum_{j \in \mathcal{J}^{PV}} s_j^{BSSkW} \\
-\;& (C^{En} + C^{eNorg} + c^{eN}) \cdot PF^{HH} \sum_{t \in \mathcal{T}} \sum_{j \in \mathcal{J}^{PV}} e_{j,t}^{NL} \\
-\;& (C^{pNorg} + c^{pN}) \cdot PF^{HH} \sum_{j \in \mathcal{J}^{PV}} p_j^{NL} \\
-\;& (C^{Sc1} + TE^{Sc}) \cdot PF^{HH} \sum_{t \in \mathcal{T}} \sum_{j \in \mathcal{J}^{PV}} (e_{j,t}^{PVL} + e_{j,t}^{BSSL}) \qquad (6.6)
\end{aligned}
$$

6.3.2 *LL constraints*

While most of LL constraints are similar to the model presented in Section 3.2.1, a summary of selected constraints is provided in this section to map primal and dual variables. Again, the focus lies on keeping energy balances for demand and available supply as well as modeling the BSS.

6.3.2.1 *LL equalities*

Eq. 6.7 ensures that $E^{L}_{j,t}$ is met during each time step (either by procuring $e^{NL}_{j,t}$, consuming PV $e^{PVL}_{j,t}$ directly or indirectly via the BSS $e^{BSSL}_{j,t}$).

$$\forall j \in \mathcal{J}^{PV}, t: h^1 \quad = e^{NL}_{j,t} + e^{PVL}_{j,t} + e^{BSSL}_{j,t} - E^{L}_{j,t} \quad = 0 : \mu^{h^1}_{j,t} \tag{6.7}$$

Eq. 6.8 couples the sizing variable s^{PV}_{j} with PV energy flows. Only PV energy can be used to charge the BSS $e^{PVBSS}_{j,t}$ as BSS charging from the network is not economically favorable.

$$\begin{aligned} \forall j \in \mathcal{J}^{PV}, t: h^2 \quad &= e^{PVN}_{j,t} + e^{PVL}_{j,t} + e^{PVBSS}_{j,t} \\ &\quad + e^{PVC}_{j,t} - E^{PV}_{j,t} \cdot s^{PV}_{j} \qquad = 0 : \mu^{h^2}_{j,t} \end{aligned} \tag{6.8}$$

The BSS's $soc_{j,t}$ is modeled via an intertemporal relationship including charging η^{BSSCh}, discharging η^{BSSDis} and self-discharging efficiencies η^{BSSSd}.

$$\begin{aligned} \forall j \in \mathcal{J}^{PV}, t: h^3 \quad &= soc_{j,t} - \eta^{BSSSd} \cdot soc_{j,t-1} - \eta^{BSSCh} \\ &\quad \cdot e^{PVBSS}_{j,t} + (\eta^{BSSDis})^{-1} \cdot e^{BSSL}_{j,t} \qquad = 0 : \mu^{h^3}_{j,t} \end{aligned} \tag{6.9}$$

6.3.2.2 *LL inequalities*

System sizes are limited by individual maxima, e.g. as displayed for the PV system with S^{PV}:

$$\forall j \in \mathcal{J}^{PV}: g^1 = s^{PV}_{j} \; - \; S^{PV} \; \leq \; 0 : \theta^{g^1}_{j} \tag{6.10}$$

All energy flows are limited by the given profiles. Here, only exemplary constraints for PV and demand are displayed (for others, see B.2):

$$\forall j \in \mathcal{J}^{PV}, t: g^4 = e^{PVN}_{j,t} - S^{PV} \cdot E^{PV}_{j,t} \leq 0 : \theta^{g^4}_{j,t} \tag{6.11}$$

$$\forall j \in \mathcal{J}^{PV}, t: g^8 = e^{NL}_{j,t} - E^{L}_{j,t} \leq 0 : \theta^{g^8}_{j,t} \tag{6.12}$$

Next to dynamic PV curtailment by the DNO, PV system owners might be required to permanently limit their feed-in κ^{PVLim} relative to the installed PV capacity, e.g. if they opt for the 70 % threshold instead of dynamic curtailment capabilities or if they have received an investment subsidy for their BSS. In that case, curtailment losses are not reimbursed ($C^{Cur} = 0$).

$$\forall j \in \mathcal{J}^{PV}, t: g^{11} = e^{PVN}_{j,t} - \kappa^{PVLim} \cdot \tau \cdot s^{PV}_{j} \leq 0 : \theta^{g^{11}}_{j,t} \tag{6.13}$$

For power-based NCs, Eq. 6.14 allows determining the HH's yearly peak demand from the network or peak PV network feed-in. The latter is only

relevant if NCs have to be paid equally for peak demand and peak feed-in. Otherwise, it is set to zero.

$$\forall j \in \mathcal{J}^{PV}, t\colon g^{12} = e_{j,t}^{NL} + e_{j,t}^{PVN} - \tau \cdot p_j^{NL} \leq 0 : \theta_{j,t}^{g^{12}} \tag{6.14}$$

BSS charging is limited by the sizing of the BSS inverter, as Eq. 6.15 displays. Same applies to discharging.

$$\forall j \in \mathcal{J}^{PV}, t\colon g^{13} = e_{j,t}^{PVBSS} - \tau \cdot s_j^{BSSkW} \leq 0 : \theta_{j,t}^{g^{13}} \tag{6.15}$$

BSS capacity is adjusted to a usable BSS capacity κ^{BSSUc}:

$$\begin{aligned} \forall j \in \mathcal{J}^{PV}, t\colon g^{15} \quad &= soc_{j,t} \\ &-\kappa^{BSSUc} \cdot s_j^{BSSkWh} \leq 0 : \theta_{j,t}^{g^{15}} \end{aligned} \tag{6.16}$$

Furthermore, all variables have to be greater than or equal to zero (see B.2).

6.4 *Method for solving bilevel optimization problems*

The investment decision in PV BSSs depends on the new NC that the DNO sets by anticipating the LL reaction. This interaction provides an opportunity to integrate the two optimization problems into one joined problem. Hence, the HH optimization problem needs to be recast and integrated into the DNO problem. One way to guarantee an optimal solution of the LL problem while solving the UL objective is to exploit advantages of strong duality in linear programming. Thus, one can replace the LL problem with its primal constraints, dual constraints and the strong duality theorem equality. The strong duality theorem states that optimality is preserved when the primal objective function $(f(x) = c^T x)$ is equal to dual objective function $(\mu^T b + \theta^T e)$, as shown in Eq. 6.17:

$$c^T x = (\mu^T b + \theta^T e) \tag{6.17}$$

x are the LL variables, μ are the dual variables related to LL equality constraints and θ are the dual variables related to LL inequality constraints. b, c and e are cost and constraint vectors of the LL problem.

Such a problem is called a mathematical program with primal and dual constraints (MPPDC) [95]. Primal constraints are those of the LL problem. Dual constraints are derived using the Lagrangian function:

$$\nabla \mathcal{L} = \nabla_x f(x) + (\mu^h)^T \nabla_x h(x) + (\theta^g)^T \nabla_x g(x) = 0 \tag{6.18}$$

$h(x)$ and $g(x)$ describe LL equality and LL inequality constraints. Partial derivatives with respect to all LL decision variables lead to the corresponding dual constraints that contain related dual variables (see Appendix B.3).

6.4.1 *Advantages of MPPDC formulation*

Compared to other reformulations, such as a mathematical program with equilibrium constraints, a MPPDC formulation does not require complementarity conditions to guarantee optimality as the strong duality theorem ensures optimality. Thus, the problem is easier to solve with commercial grade solvers and no binary variables are needed for the reformulation.

6.4.2 *Strong duality theorem*

Following Eq. 6.17 the LL objective function is set equal to the objective function of the dual problem, which is derived using LL constraints (e.g. $\mu^T b$ is based on Eq. 6.7 with μ^T equal to $\sum_{t\in\mathcal{T}}\sum_{j\in\mathcal{J}^{PV}}\mu^{h^1}_{j,t}$ and b equal to $\sum_{t\in\mathcal{T}}\sum_{j\in\mathcal{J}^{PV}}E^{L}_{j,t}$):

$$\begin{aligned} z_{LL} &= \sum_{t\in\mathcal{T}}\sum_{j\in\mathcal{J}^{PV}}(\mu^{h^1}_{j,t}\cdot E^{L}_{j,t}) + \sum_{j\in\mathcal{J}^{PV}}(\theta^{g^1}_{j}\cdot S^{PV}) \\ &+ \sum_{j\in\mathcal{J}^{PV}}(\theta^{g^2}_{j}\cdot S^{BSSkWh}) + \sum_{j\in\mathcal{J}^{PV}}(\theta^{g^3}_{j}\cdot S^{BSSkW}) \\ &+ \sum_{t\in\mathcal{T}}\sum_{j\in\mathcal{J}^{PV}}(\theta^{g^4}_{j,t}\cdot S^{PV}\cdot E^{L}_{j,t}) + \sum_{t\in\mathcal{T}}\sum_{j\in\mathcal{J}^{PV}}(\theta^{g^5}_{j,t}\cdot S^{PV}\cdot E^{PV}_{j,t}) \\ &+ \sum_{t\in\mathcal{T}}\sum_{j\in\mathcal{J}^{PV}}(\theta^{g^6}_{j,t}\cdot S^{PV}\cdot E^{PV}_{j,t}) + \sum_{t\in\mathcal{T}}\sum_{j\in\mathcal{J}^{PV}}(\theta^{g^7}_{j,t}\cdot S^{PV}\cdot E^{PV}_{j,t}) \\ &+ \sum_{t\in\mathcal{T}}\sum_{j\in\mathcal{J}^{PV}}(\theta^{g^8}_{j,t}\cdot E^{L}_{j,t}) + \sum_{t\in\mathcal{T}}\sum_{j\in\mathcal{J}^{PV}}(\theta^{h^9}_{j,t}\cdot E^{L}_{j,t}) \\ &+ \sum_{t\in\mathcal{T}}\sum_{j\in\mathcal{J}^{PV}}(\theta^{g^{10}}_{j,t}\cdot E^{L}_{j,t}) \end{aligned} \tag{6.19}$$

With the LL problem reformulated, the UL-LL problem is successfully transformed into a single-level optimization problem.

6.4.3 *Linearization*

However, the problem contains bi-linear terms: the multiplication of the NC increase and the energy or power demand from the network. As such problems are hard to solve for most solvers, linearization techniques are applied to formulate a MILP. Here, only the linearization of the product for the energy-based NCs eN_{lin} is displayed.

$$eN_{lin} = c^{eN}\sum_{t\in\mathcal{T}}\Big(\sum_{j\in\mathcal{J}^{PV}}e^{NL}_{j,t}\Big) \tag{6.20}$$

To separate NC increase from energy demand, binary variables eN_{be}^{bi}[5] and incremental cost increase parameters Δc^{eN} are introduced:

$$c^{eN} = \Delta c^{eN} \sum_{be \in \mathcal{B}} 2^{be-1} \cdot eN_{be}^{bi} \tag{6.21}$$

eN_{lin} is replaced with a product of a linear and a binary variable ce_{be}, which allows an easy separation using a standard linearization technique as follows:

$$\forall be \in \mathcal{B}\colon ce_{be} \leq BigM \cdot eN_{be}^{bi} \tag{6.22}$$

$$\forall be \in \mathcal{B}\colon ce_{be} \leq \sum_{t \in \mathcal{T}} \sum_{j \in \mathcal{J}^{PV}} e_{j,t}^{NL} \tag{6.23}$$

$$\forall be \in \mathcal{B}\colon \sum_{t \in \mathcal{T}} \sum_{j \in \mathcal{J}^{PV}} e_{j,t}^{NL} - ce_{be} \leq BigM \cdot (1 - eN_{be}^{bi}) \tag{6.24}$$

5 *be* describes the binary in the corresponding set $\mathcal{B}$.

7

Case studies and conclusions

Two case studies are conducted to assess the bilevel approach. The first case study focuses on interdependencies between strategic NC tariff setting and the LL's response to reach an equilibrium. Moreover, it addresses how overall network costs are distributed among HHs with and without PV BSSs. The second case study concentrates on trade-offs between network reinforcement and PV feed-in curtailment with regard to PV BSS sizing and operation.[1]

7.1 *Key performance indicators*

Several KPIs are used to evaluate the bilevel approach.

- NC setting:

  Different tariff options are assessed with regard to the following criteria in the context of PV BSS investment:

  1. Distribution and welfare effects between HHs with and without the ability to invest in a PV BSS. Here, the focus lies on the overall NC development and how the NC contribution changes with the investment in PV BSSs under different tariff options.
  2. Incitement of a market and network-supporting control of loads and RESs. Here, network-support via BSS operation and NC impact on peak PV feed-in and peak demand are of special interest.
  3. Avoidance of undesired arbitrage effects. Here, especially self-reinforcing processes with regard to PV BSS oversizing, network defection and network reinforcement are addressed.

  Additional less measurable aspects concern transaction costs related to the tariff system and the facilitation of energy efficient behavior. While the latter is out of scope here, transaction costs are related to metering infrastructure and billing processes. Both are assumed to be not an issue once smart meters are rolled out in Germany.

- PV system size, BSS size and net present value of PV BSSs:

  PV systems size, BSS size and NPV are KPIs for HHs with the ability to invest in PV BSSs. While PV and BSS size are decision variables, NPVs are calculated according to Eq. 7.1.

1 Parts of this chapter are presented in [87].

$$\forall k^S \in \mathcal{K}, \forall j \in \mathcal{J}^{PV} : NPV_{j,k^S} = (C^{En} + C^{eNorg}) \cdot PF^{HH} \sum_{t \in \mathcal{T}} E^L_{t,j} - z_{LL,j,k^S} \quad (7.1)$$

HH-specific NPVs are compared to costs without PV BSSs and thus without any increase in NCs for each chosen PV penetration scenario k^S, which is part of the scenario set $\mathcal{K}$. Furthermore, changes of these KPIs are compared to original sizing decisions in a single-level optimization. Changes in NPVs are determined by evaluating what advantage each HH gains from adjusting PV BSS sizing according to the new NC equilibrium instead of sticking to original sizing. The NPV for original PV BSS sizing and corresponding energy flows (here displayed by setting scenario index k^S to zero) $NPVo_{j,k^S}$ is calculated for new NCs depending on k:

$$\begin{aligned}
\forall k^S \in \mathcal{K}, \forall j \in \mathcal{J}^{PV} : NPVo_{j,k^S} &= (C^{En} + C^{eNorg}) \cdot PF^{HH} \sum_{t \in \mathcal{T}} E^L_{t,j} \\
&- ((C^{Fit1} \cdot PF^{HH} - TE^{Fit}) \sum_{t \in \mathcal{T}} e^{PVN}_{j,t,0} \\
&+ (C^{Cur} \cdot PF^{HH} - TE^{Cur}) \sum_{t \in \mathcal{T}} e^{PVC}_{j,t,0} \\
&- (I^{PV} + M^{PV} \cdot PF^{HH} - TE^{Dep}) \cdot s^{PV}_{j,0} \\
&- (I^{BSSkWh} + M^{BSSkWh} \cdot PF^{HH}) \\
&\cdot s^{BSSkWh}_{j,0} \\
&- (I^{BSSkW} + M^{BSSkW} \cdot PF^{HH}) \\
&\cdot s^{BSSkWh}_{j,0} \\
&- (C^{En} + C^{eNorg} + c^{eN}_{k^S}) \\
&\cdot PF^{HH} \sum_{t \in \mathcal{T}} e^{NL}_{j,t,0} \\
&- (C^{pNorg} + c^{pN}_{k^S}) \cdot PF^{HH} \cdot p^{NL}_{j,0} \\
&- (C^{Sc} \cdot PF^{HH} + TE^{Sc}) \\
&\cdot \sum_{t \in \mathcal{T}} (e^{PVL}_{j,t,0} + e^{BSSL}_{j,t,0}))
\end{aligned} \quad (7.2)$$

The change in NPV per HH and scenario $\Delta NPV_{j,k^S}$ is determined as follows:

$$\forall k^S \in \mathcal{K}, \forall j \in \mathcal{J}^{PV} : \Delta NPV_{j,k^S} = \frac{(NPV_{j,k^S} - NPVo_{j,k^S}) \cdot 100}{NPVo_{j,k^S}} \quad (7.3)$$

7.2 *Input data*

To parameterize the case studies, a scenario is chosen that resembles the scenario used in the previous part (see A.1). Electricity prices are assumed to remain at same average, while the FIT drops further as the PV installation rate starts increasing again. Additionally, PV system prices and BSS prices continue to decrease slightly compared to previously assumed prices. No binary variables are required with the proposed approach, one-time installation costs for PV and BSS are included in kWh and kWp prices. PV system sizes are limited to 10 kWp. While the HH profiles from the previous part are used, only the PV profile from location 1 for SOs is used. All relevant case study data can be found in B.4.

7.3 *Case studies for interactions between DNOs and PV BSSs*

7.3.1 *Energy- vs. power-based network charges*

The first case study assesses the impact of the energy- and power-based NCs on PV BSS sizing. The analysis investigates if energy- or power-based NCs provide a fairer distribution of additional costs related to the NC increase among HHs with and without PV BSSs. Scenario 'Power-based NC 'Load'' is billed according to the yearly peak demand. Scenario 'Power-based NC 'Load+PV'' describes the scenario where the peak charge is paid on the yearly max. network exchange, which can either be a result of demand or of PV network feed-in. As highlighted above, such a power-based tariff would be a renunciation of demand-based billing of network usage and equally charge generators, which is not common as of today. For this case study, it is assumed that the example network has sufficient capacity to cope with additional PV systems, and that network costs remain constant.[2] Three scenarios with different PV penetration rates are investigated. For scenario 'low PV', 'med. PV' and 'high PV', 12, 24 and 38 HHs have the ability to invest in a PV BSS, which amounts to 25 %, 50 %, or 75 % of all HHs with the ability to invest in PV BSSs.

Table 7.1 displays the results of the DNO's optimization problem: the relative increase in energy- and power-based NCs.

As the DNO anticipates that the business case for PV BSSs is attractive, it continuously raises NCs to recover its costs. While power-based NCs rise by 8.7 % for 12 systems for both power-based tariffs, energy-based NCs increase by 12.1 % for the same amount of systems. The difference between energy- and power-based NCs steadily grows as more HHs have the ability to adopt PV BSSs. For scenario 'med. PV', energy-based NCs augment by 27.3 %, while a slight difference between the two power-based NCs becomes visible. The power-based NC 'Load' case leads to an increase by

2 Recent studies have shown that specific type of LV networks, e.g. in cities, in Germany do not require network reinforcements with a higher PV penetration in the near future [86].

Table 7.1: Increase in network charges for different PV scenarios and tariff structures (assumption: constant network cost)

Scenario	Increase in network charges (NC)					
	Energy-based NC		Power-based NC 'Load'		Power-based NC 'Load+PV'	
low PV	0.8 ct/kWh	12.1 %	3.9 €/kW	8.7 %	3.9 €/kW	8.7 %
med. PV	1.8 ct/kWh	27.3 %	8.8 €/kW	19.7 %	8.7 €/kW	19.5 %
high PV	3.2 ct/kWh	48.5 %	15.1 €/kW	33.8 %	14.5 €/kW	32.7 %

19.7 % and the 'Load+PV' rises by 19.5 %. The difference between energy- and power-based NCs grows to more than 10 % for 36 systems as energy-based NCs increase by 48.5 %, compared to 33.8 % ('Load') and to 32.7 % ('Load+PV') for power-based NCs. Additionally, higher self-reinforcing tendencies are observed for energy-based NCs because the NC increase with each additional 12 systems grows from 12.1 % for 0 to 12 systems to 16.7 % for 24 to 36 systems. Growth rates are lower for power-based NCs; an adoption of 12 additional systems results in NC increases of 11.8 % ('Load') and 10.8 % ('Load+PV') for 24 to 36 systems. It becomes visible that the business case for PV self-supply prospers more with energy-based NCs as BSS operation is easier adaptable to energy than peak demand differences. Additionally, self-supply benefits increase with larger differences in energy network procurement costs and energy generation costs. When comparing both power-based approaches, nearly no difference in mitigating NC rise is observed, indicating no clear benefit from pricing network feed-in. In general, from a DNO's perspective power-based NCs slow down the potential self-reinforcing growth process for PV BSSs.

HHs with the ability to invest in PV BSSs anticipate the increase in NCs and react accordingly when optimizing size and operation of PV BSSs. Fig. 7.1 displays the LL results for the three tariffs. Three subplots show PV system sizes, BSS sizes and NPVs of each system on the left-hand side.

The LL reacts to the NC rise by increasing PV BSS sizes to enable more self-supply or limit the exposure to load or feed-in peaks. The median PV system size increases from 6.77 kWp to 7.51 kWp for energy-based NCs, from 5.00 kWp to 5.44 kWp for power-based NCs 'Load' and from 4.66 kWp to 4.74 kWp for power-based NCs 'Load+PV' between 12 and 36 systems. For energy-based NCs, some HHs already reach the 10 kWp limit for scenario 'high PV'. Despite such a limit, energy-based NCs result in faster growing PV system sizes; the incremental increase changes from an additional 0.34 kWp to 0.40 kWp between scenarios 'low PV' and 'med. PV' and scenarios 'med. PV' and 'high PV'. For power-based NCs 'Load', median PV system sizes rise first by 0.31 kWp and then only by 0.13 kWp between scenarios. For power-based NCs 'Load+PV', the complex nature of peak load and feed-in pricing becomes visible. PV system sizes of the lower quantile remain similar for all scenarios, while median, upper quantile and whisker steadily increase. This indicates that some HHs are able to cope better with

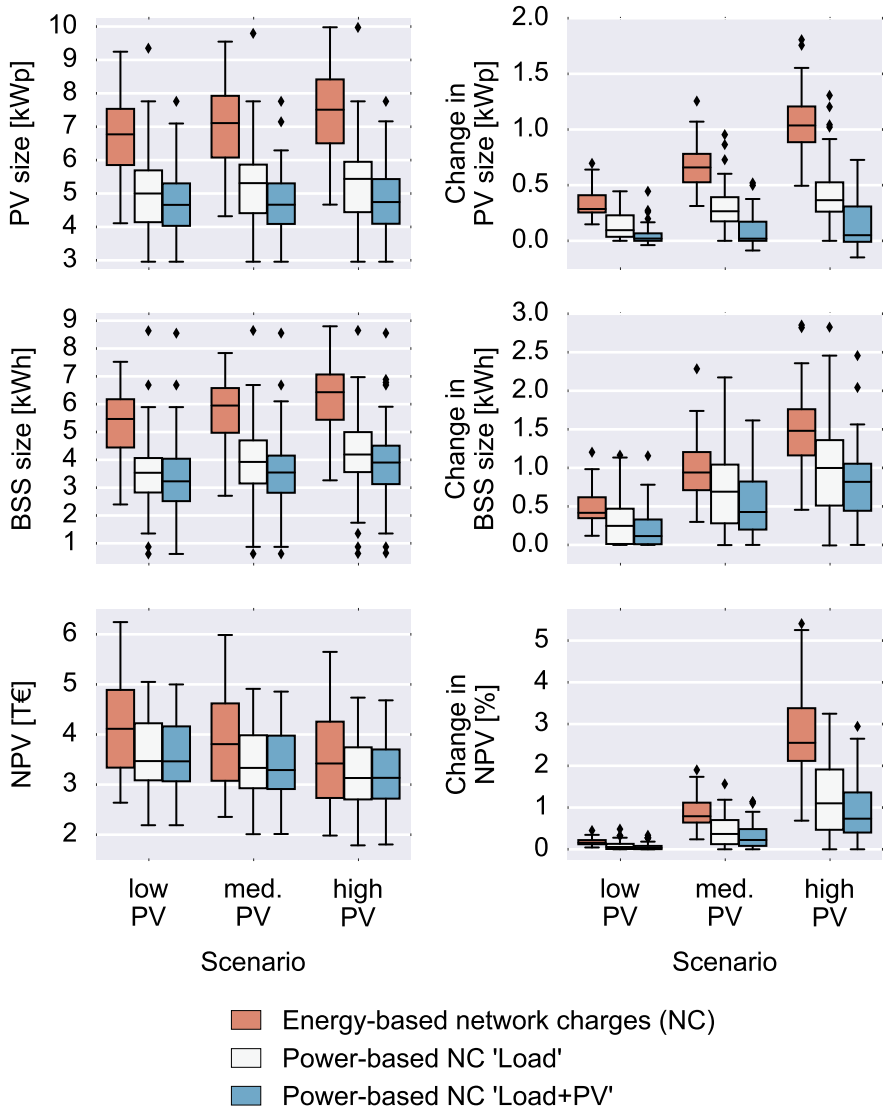

Figure 7.1: Results for PV sizes, BSS sizes and NPVs (left) as well as change in sizing and NPV for single vs. bilevel optimization (right) for different PV penetration scenarios and tariff structures (assumption: constant network cost)

peak-oriented NCs than others and the BSS provides the necessary flexibility to avoid peaks.

BSS capacities also change at different rates for each tariff. For energy-based NCs, median BSS capacity starts at 4.9 kWh for a single-level optimization, jumps to 5.5 kWh for scenario 'low PV' and continues to steadily increase to 6.0 kWh for 'med. PV' and to 6.4 kWh for 'high PV'. Yet, the increase in kWh slightly decreases between scenarios as the value added from additional self-supply comes at higher costs. For power-based NCs 'Load', median BSS capacity rises from 3.2 kWh to 4.2 kWh from single optimization to 'high PV'. Here, capacities first increase at larger rates (with 0.4 kWh between 'low PV' and 'med. PV') and then the rise slows down (with 0.3 kWh between 'med. PV' and 'high PV'). With power-based

NCs 'Load+PV', BSS capacities augment from 2.9 kWh to 3.9 kWh. 1 kWh is added between the reference scenario and 'high PV', like 'Load', which is a higher growth rate compared to PV system sizing.

NPVs decrease with an increasing number of systems as NCs rise. Despite a larger incentive to increase self-supply, larger system sizes cannot compensate additional costs of the remaining network consumption and higher investment costs. Median self-supply can only be increased by up to 15.3 % from 61.2 % for a single level optimization to 70.6 % for 'high PV'. At the same time, the median NPV decreases by 21.6 %, overall supply cost increase by 5.3 % and energy-based NCs rise by 48.5 %. Similar effects are seen for power-based NCs. Here, self-supply only increases from 52.7 % to 58.5 % for 'Load' (from 51.1 % to 55.3 % for 'Load+PV'), while median NPVs only decline by 13.2 % for 'Load' and by 13.1 % for 'Load+PV'. While the DNO increases NCs, the self-supply business case remains still attractive but additional costs and technical limits, such as intertemporal differences between load and PV, reduce the marginal value added of additional self-supply per additionally installed kWp and kWh.

The simultaneous reaction of all LL players forces them to consider their impact on NCs and adapt their system to the new equilibrium. Despite a lower absolute NPV of the system, HHs push for larger systems to cope with increasing NCs as their original system size would have not been an optimal solution to the higher NCs. Here, the non-cooperative game aspect becomes visible. While it would be in everyone's interest to stick to the original sizing decision to increase their own benefit, relying on all HHs to act similar is risky as one player could increase sizes to its personal advantages. To derive a better understanding of such behavior, changes compared to a single-level optimization are displayed on the right-hand side in Fig. 7.1. Relative NPV changes indicate potential losses HHs would have incurred, if they had stuck to results of their single level optimizations. Compared to such results, system sizing highly varies. For energy-based NCs, PV and BSS size increase by up to 1.04 kWp and 1.48 kWh for scenario 'high PV'. For power-based NCs 'Load' ('Load+'PV'), the rise is not so significant with 0.37 kWp and 1.00 kWh (0.05 kWp and 0.82 kWh). While NCs increase significantly, the median change in NPV is quite low when comparing $NPVo_{j,k}$ and $NPV_{j,k}$. Increasing sizing and thus contributing to an additional increase in NCs only provides an advantage of 2.6 % for scenario 'high PV' for energy-based NCs. For power-based NCs 'Load' ('Load+PV'), the advantage is even smaller with 1.1 % (0.7 %).

Despite the negative impact on the HH's NPV, increasing NCs provide an additional incentive for further self-supply and securing the own benefit by oversizing PV BSSs. While higher NCs are partially incorporated by the responsible actors, they mainly have to be borne by HHs without PV BSSs. Fig. 7.2 displays the contribution of HHs with PV BSSs to the overall paid NCs before they invested in a PV BSS and afterwards compared to HHs without PV BSSs for scenario 'high PV'.

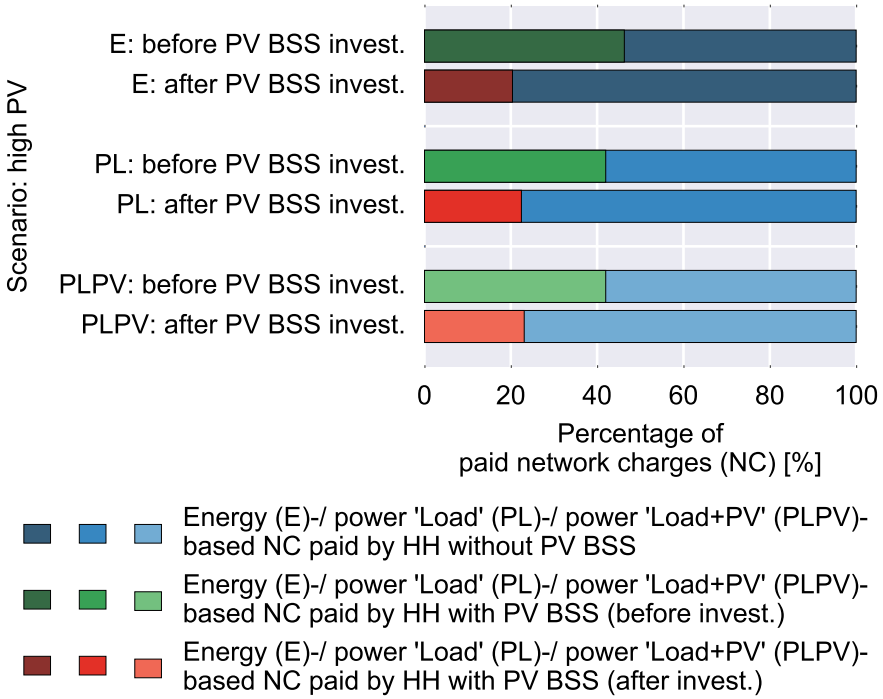

Figure 7.2: Comparison of distribution of network charges among HHs with and without PV BSSs for different tariff structures for scenario 'high PV' (assumption: constant network cost)

The total contribution is reduced from originally 46.3 % to only 20.4 % for energy-based NCs and from 42.0 % to 22.5 % for power-based NCs 'Load' and to 23.1 % for 'Load+PV'. HHs with PV BSSs are able to reduce their individual contribution to overall NCs by 57 % with energy-based NC. The individual share per HH without a PV BSS tremendously increases depending on the number of installed systems. While 12 systems only increase this share by 18.4 %, 36 systems lead to a rise of 105.4 % per HH without a PV BSS. Both power-based NCs absorb rising inequality to a certain degree. With only a few additional PV BSSs, such HHs are able to lower their individual contribution to the overall share by 53.5 % for 'Load' and by 52.6 % for 'PV+Load'. The reduction decreases to 46.5 % and 45.0 % with 36 systems. All HHs without PV BSSs experience an individual increase from 12.4 % to 59.5 % for 'Load' and from 12.2 % to 58.1 % for 'Load+PV'. Again, a clear advantage from introducing generator-oriented peak pricing is not observed as such NCs do not significantly improve inequality effects.

Power-based NCs seem to be favorable for HHs without PV BSSs. Such NCs lower the investment incentive for self-supply systems and buffer distribution effects among LL players slightly. For DNOs, peak-oriented NCs might bear the advantage of incentivizing network-supporting BSS operation. Fig. 7.3 shows the mean peak PV feed-in and peak demand per HH and the relative NC increase depending on the number of HHs with a PV BSSs for all three tariff options. Next to peak PV feed-in per HH with systems sized according to the new NC equilibrium, peaks for single-level optimization sizes with original NCs are displayed.

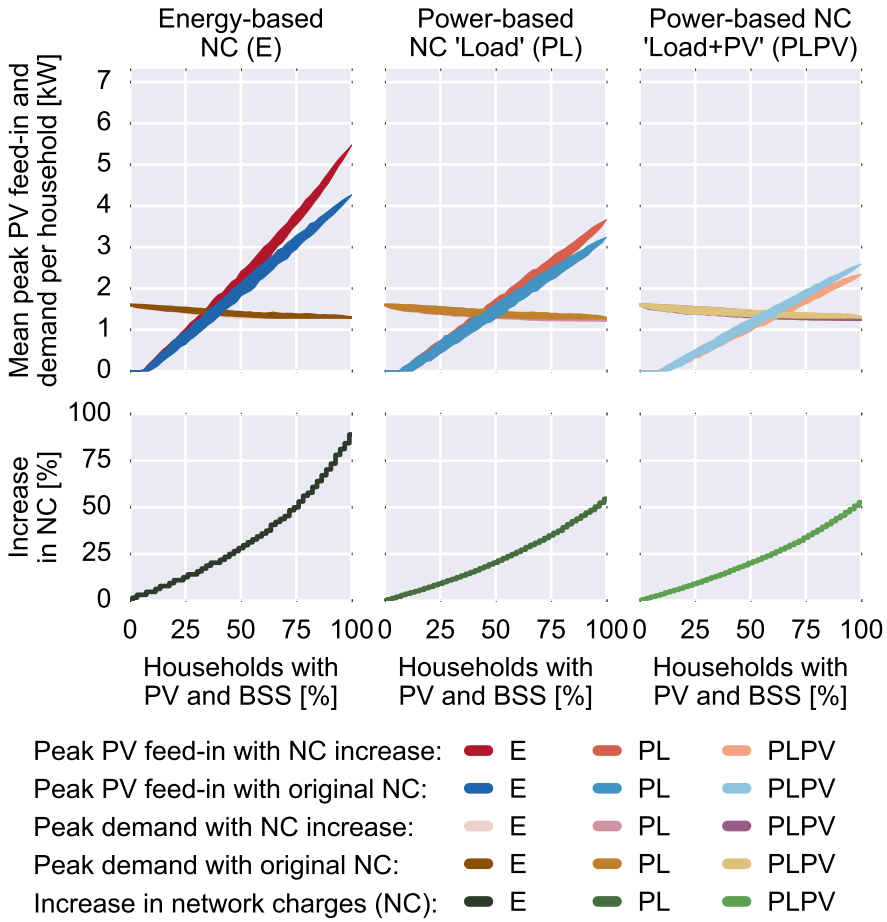

Figure 7.3: Comparison of mean peak PV feed-in and peak demand per HH depending on the amount of HHs with a PV BSS (top) and relative increase in network charges (NC) for different NC tariffs

For energy-based NCs, tendencies for a self-accelerating PV peak with the bilevel approach are underlined. While single-level optimization results in a max. mean peak PV feed-in of 4.3 kW and follows a linear path with higher PV penetration, simultaneous, bilevel sizing leads to a max. mean peak of 5.5 kW and follows a more quadratic growth. In both cases, peak PV feed-in exceeds the peak demand once 35 % of HHs are equipped with a PV BSS. Power-based NCs 'Load' lead to smaller sized PV systems (see above), which reflects on the aggregated peak, and lead to a max. of 3.7 kW. As the NC increase is also lower than with energy-based NCs, peak differences between single and bilevel approach only amount to 0.4 kW. The intersection of PV and demand peak rises to 46 % of HHs being equipped with a PV BSS. Power-based NCs 'Load+PV' impact peak PV feed-in in two ways. First, again PV system sizes are significantly smaller than for the other two tariff options. Second, a peak PV-oriented BSS operation is incentivized, resulting in a lower max. mean peak PV feed-in per HH with bilevel optimization (2.3 kW) than with single level optimization (2.6 kW). The higher the NCs, the higher is the incentive to adjust BSS operation.

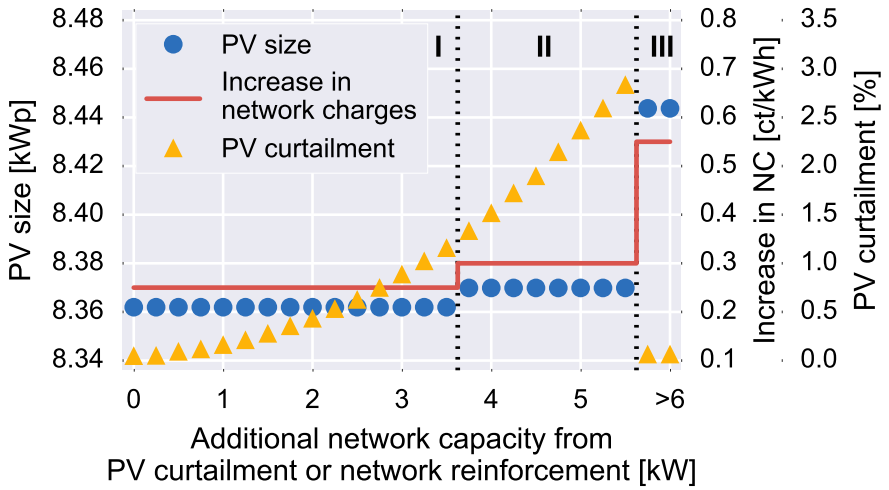

Figure 7.4: Network charges (NC), PV size and PV curtailment depending on additional network capacity with minor PV curtailment (I), PV curtailment leading to an increase in NC (II) and network reinforcement (III)

Here, 58 % of HHs can be equipped with a PV BSS before peak PV feed-in surpasses peak demand. However, as pointed out above, such NCs result in smaller PV system sizes, even without the bilevel approach, and thus leave large amounts of the available rooftop potential untapped, while leading to similar unequal distribution effects like load-oriented NCs.

In summary, one can highlight that HHs tend to oversize PV BSSs, once they take their and other HHs impact on NCs into account. While all NC options lead to an accelerated growth in system sizes and increase in distribution inequalities, they do not result in complete network defection due to economic and technical limits.

7.3.2 *Network reinforcement vs. PV curtailment*

The trade-off between increasing NCs and providing an additional self-supply incentive becomes visible for the current energy-based NCs in the first case study. The LL responds to higher NCs with larger systems, which result in an augmented PV peak. To address this problem, an additional case study is performed that includes a network reinforcement decision for the DNO. Additionally, the DNO is allowed to curtail PV feed-in, but needs to reimburse such curtailment with the FIT. Here, four additional systems are installed and NCs are energy-based. The network capacity is varied to analyze when a reinforcement measure is triggered or when curtailment is sufficient. Fig. 7.4 shows how much additional network capacity is provided depending on curtailment or reinforcement and how NCs, median PV size and median curtailment losses change accordingly.

The results indicate the impact of reaching the limit of the network capacity for system sizing on the LL. Minor PV curtailment allows for an additional hosting capacity of 3.5 kW in this example. Compensation costs related to PV curtailment do not require an additional NC increase compared

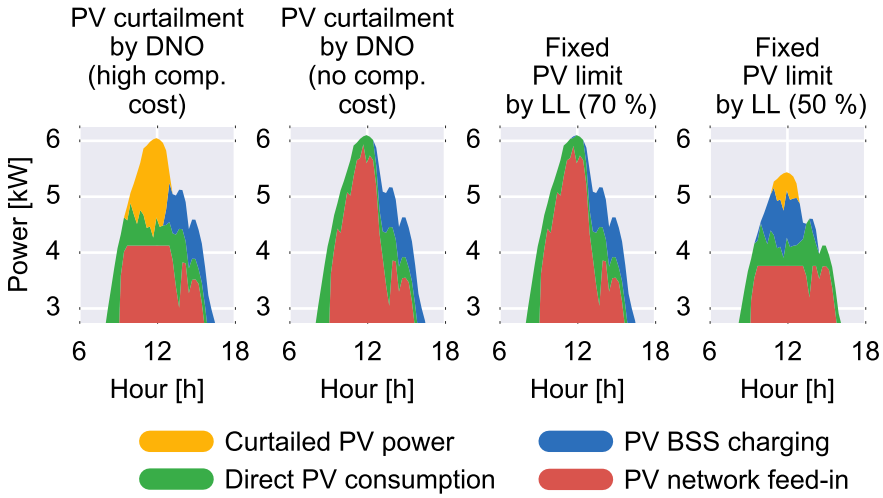

Figure 7.5: PV related energy flows for one HH for four different operational incentives for the PV peak day

to the case without curtailment (see (I) in Fig. 7.4). Increased PV curtailment by the DNO allows delaying a network reinforcement measure by a couple of kW. As a result of higher PV curtailment, NCs also increase once a certain threshold is surpassed (between 3.5 kWp and 3.75 kWp), which leads to an increase of PV size (see (II) in Fig. 7.4). The effectiveness of PV curtailment is limited as DNOs are only allowed to curtail up to 3 % of the produced yearly PV energy. Once, another threshold (between 5.5 kWp and 5.75 kWp) is exceeded, a network reinforcement measure is required in this example. Such a measure results in further costs for the DNO, thus it raises NCs. These higher NCs trigger a LL reaction to adapt system sizes. PV systems are 0.08 kWp larger than for the same amount of systems without network reinforcement and minor PV curtailment (compare (I) and (III) in Fig. 7.4). Overall, the dynamic between UL and LL reduces the hosting capacity as the combination of self-supply and reimbursement of curtailment or costs of reinforcement measures result in larger PV systems.

To analyze the impact of network limits - peak feed-in restrictions - on BSS operation, Fig. 7.5 displays all PV related energy flows for the peak day for one HH for four scenarios. The general assumption is again that the same number of additional systems is being installed in each scenario. Depending on the scenario and the corresponding network integration measures, the potential NC increase and thus PV system sizing might differ with such an assumption.

The first subplot shows results of a scenario with PV curtailment. The DNO tries to maintain the hosting capacity within allowed limits by curtailing PV (yellow area) and reducing network feed-in (red area). As dynamic PV curtailment by the DNO is currently reimbursed with the same tariff as network feed-in, the LL sees no benefit in shifting BSS operation (blue area) towards peak-oriented charging during mid-day.

The second subplot alters the first scenario by decreasing the compensation costs of curtailed PV energy to zero to analyze the LL reaction as PV BSSs are now not indifferent between network feed-in and curtailment. PV BSSs would lose revenue by allowing DNO curtailment, thus PV is fed into the network instead and BSS operation is not adapted. As the hosting capacity is exceeded, the DNO is forced to reinforce the network. That results in higher NCs compared to curtailment and slightly larger PV BSSs.

The third subplot describes a scenario where the LL opts out of the dynamic curtailment option and agrees to a fixed PV feed-in limit at 70 % of the installed PV capacity. Curtailment losses are not reimbursed in this scenario [11]. No additional devices are needed to receive DNO curtailment signals and transaction costs for the reimbursement process are avoided. The PV curtailment variable is now a decision variable of the LL and not enforced by the DNO anymore. The fixed limit leads to a similar high PV feed-in peak as the previous example with a reinforced network. Thus, a network reinforcement measure is necessary to increase the hosting capacity. No different BSS operation is incentivized for the peak day as the limit is too high. With a simulation time step of 15 min., the 70 % limit leads to nearly no PV losses as direct PV consumption (green area) is high enough and the system is sized accordingly.

To analyze the impact of a lower fixed feed-in limit, the fourth subplot displays results for a limit at 50 % of the installed PV power. Such a %-limit is comparable to the limit seen with dynamic PV curtailment by the DNO with a full compensation payment. BSS operation is now peak-oriented and charging happens during peak generation hours. Furthermore, the lower fixed limit impacts the sizing decision and results in a smaller sized PV system, but a larger BSS. Thus, the overall peak is lower for the same number of systems and the hosting capacity is increased.

In summary, one can conclude that the current regulatory framework increases the flexibility for DNOs and allows them to trade-off network reinforcement measures and PV curtailment. Yet, it sets no incentive for a peak-oriented BSS operation. In fact, NCs actually rise leading to an oversizing of PV BSSs. Fixed feed-in limits without reimbursement incentivize such peak-oriented BSS operation, if the limit is set low enough. Additionally, they decrease the overall system size, increase the hosting capacity and lower transaction costs as DNOs and HHs do not have to engage in the reimbursement process for PV curtailment. Nevertheless, the NPV of the PV BSSs is minimally reduced.

7.4 *Conclusion*

The business case for PV BSS thrives on decreasing network demand while being able to feed PV into the distribution network. For DNOs, this results in a reduction of paid NCs, since such charges are part of the self-supply

incentive for PV BSSs. Moreover, DNOs face additional costs from PV network integration, which need to be refinanced through less billable kWh.

A bilevel optimization model is developed to describe dynamics between strategic decision making on the DNO and the PV BSS level in the context of creating additional self-supply incentives for PV BSSs. By modeling interdependencies between tariff setting, network integration measures and PV BSS sizing and operation as a closed-loop system, the analytic capabilities of the involved stakeholders are enhanced. MPPDC is used to integrate the DNO's cost minimization problem and HHs' profit maximization problems of deciding on optimal PV BSS sizing and operation. Such an integrated model allows qualifying the danger of starting a self-reinforcing process of higher NCs and larger PV BSSs as well as mitigating undesired redistribution between HHs with and without a PV BSS.

The analysis shows that interdependencies between higher NCs and larger system sizes start a slow, self-reinforcing process that can lead to a high decrease of network consumption with self-supply systems until technical and economical limits are reached. Yet, total network defection is not a realistic scenario as the marginal value of additional self-supply decreases with higher NCs. It becomes visible that the described problem requires new tariff structures to address how benefits from decentral PV energy supply and an opting out of NC payment can be balanced. Power-based NCs are favorable as they decrease the investment incentive in self-supply systems and mitigate inequality effects among HHs with and without PV BSSs. Yet, they also lead to lower PV system sizes. That might hinder energy transition goals and decrease the attractiveness of investments in PV BSSs.

The trade-off between raising NCs and fostering the investment incentive becomes clearly visible as the LL responds to higher NCs with larger systems, which in the end increase the aggregated peak of PV network feed-in. Higher NCs are also fostered by network reinforcement measures or dynamic curtailment under the current regulatory framework in Germany. However, no incentive for a revised BSS operation is provided if DNOs reimburse curtailment. Compared to DNO curtailment, a fixed feed-in limit provides an operational incentive to adopt a peak-oriented PV BSS operation and reduces transaction costs between DNOs and HHs. Peak-oriented NCs that equally price peak demand and peak feed-in offer an incentive for network-supporting BSS operation at the cost of an additional decrease in overall PV system sizes, while not solving unwanted distribution effects among HHs. To foster decentral PV system growth, tackle NC redistribution and incentivize network-supporting BSS operation, it is worth considering raising FIT while introducing a peak-dependent price component.

Besides NCs, taxes and surcharges are also reduced in a self-supply environment. Nevertheless, decentral PV systems provide an opportunity to foster the spread of RESs and are far easier to adopt than larger scale systems. Thus, further analyses on regulations and tariff structures, which foster PV growth, but guarantee a network-beneficial integration of PV BSSs, are required.

Part III

FUTURE RESIDENTIAL PV SYSTEMS AND FLEXIBILITY OPTIONS

Previous analyses show that PV system sizes are heavily influenced by the value of the PV network feed-in. In the future, the remuneration of PV network feed-in might significantly drop and questions arise about realistic sizes for future residential PV systems in a post FIT era. In consequence, the full PV rooftop potential might not be tapped. However, BSSs and sector coupling by using power to heat applications, such as heat pumps, as additional electric loads might provide a promising opportunity to increase PV self-consumption and value of local energy generation.

In this part the optimization model is extended to evaluate how the business case for future residential PV systems is shaped by different flexibility options to consume excess PV energy. The introduction of new component-specific constraints in combination with a case study-based approach allow an efficient evaluation of a potential competition among such flexibilities, the impact of such decentralized power-heat-storage systems on appropriate assumptions for network integration as well as the proper tariff and incentive setting for sector coupling.

The analysis shows that future PV systems require such shifting technologies to avoid undersizing PV systems. In general, a complementarity between BSS and heat pump is observed, but BSSs are rarely used for heat pump operation. BSSs only provide a benefit for the adoption of inflexible heat pumps, which is not preferable from a network integration point of view. As heat pumps largely rely on network supply even with local energy supply, self-sufficiency induced problems can be mitigated while providing an attractive business case for residential PV systems. Establishing a tariff or investment incentive-based framework that allows heat pumps to be an attractive economic alternative to conventional heating systems is not only crucial for sector coupling, but especially for adequate sizing of future PV systems.

8

Introduction, review and contribution

The business case for decentralized self-supply systems is becoming more and more attractive as PV system and BSS prices drop while electricity prices rise and remuneration of PV network feed-in steadily decreases in Germany. Previous analyses show that PV system sizes still heavily rely on the value of the PV network feed-in. In the future, this remuneration might significantly decline as the current version of the EEG foresees a phase-out of FIT based funding once a cap of 52 GWp of installed PV capacity is reached. Currently, approx. 42 GWp of PV capacity are already installed [103] and the German government aims at a yearly installation rate of 2.5 GWp (compare § 4 EEG), which implies that 52 GWp would be reached within 4 years. Even if the yearly PV installation rate remains at last year's level of 1.5 GWp, the goal would be reached within 7 years. Thus, questions arise about realistic sizes for future residential PV systems in a post FIT world, where the value of PV network feed-in approaches the PV market value or even zero and PV self-consumption is the only source for refinancing the system.

The complexity of the business case for such PV systems and their planning further rises as new options emerge, such as BSSs, that allow increasing PV self-consumption. Yet, the analysis of the previous parts indicates that focusing on PV self-consumption with BSSs can lead to smaller sized systems. In consequence, the full PV rooftop potential might not be tapped. However, additional loads provide promising alternatives to BSSs to increase PV self-consumption. New loads, such as electric vehicles and heat pumps, expand PV usage possibilities by fostering electricity consumption in the mobility and heating sector. Especially residential heat pumps play a key role for moving towards higher RES penetration levels in future energy scenarios [19, 104] and are frequently discussed as flexibility options to enhance smart grid and demand response capabilities [20]. Hence, an understanding how such systems integrate together with PV systems and BSSs is necessary. It allows determining how future rooftop PV systems are sized and what kind of flexibility serves best to capture the full rooftop potential while also addressing network integration aspects.

This chapter discusses modeling approaches for optimal PV system sizing when BSSs and heat pumps provide additional energy shifting flexibility and demand. Based on a literature review, research gaps are identified when combining such flexibility options with analyses regarding typical PV system sizes in a post FIT world, their impact on network planning from a DNO's perspective and sector coupling requirements.[1]

1 Parts of this chapter are presented in [21, 105, 106].

8.1 *Literature review*

Heat pumps provide a promising option to foster RES growth, since they offer additional flexibility to the system. The integration of PV systems and heat pumps has already been discussed from a technological point of view, e.g. in review papers [107, 108], and demonstrated successfully in different countries, e.g. in Austria [109] and in Italy [110]. The focus of these papers lies on describing implications of different heat sources for heat pumps and heating alternatives, such as solar thermal systems, technical constraints, typical system configurations (heat pump plus electric heater) and rule-of-thumb methods for sizing heating systems. Abstract modeling of interactions between input parameters, PV sizing and heat pumps is not discussed. An addition of a BSS and its impact on sizing and operation are not analyzed.

Planning tools that allow optimizing joint power and heat systems for district and microgrid applications are well described and reviewed in the literature. Commonly, MILP approaches are used to formulate the investment problem for different decentralized heat and electricity generation technologies as well as thermal and electrical storage devices to serve electric and thermal load [111–113]. The main focus of these analyses lies on planning integrated power-heat systems using district-scale combined heat and power systems (CHPs) from a utility's point of view rather than from a HH's perspective. Other authors using MILP approaches for power-heat planning optimize investment according to specific customer needs, e.g. residential customer [114], residential vs. district heating [115] or commercial buildings [53]. Other approaches used for solving the investment problem in residential power-heat applications involve using dual programming [116] or an iterative analysis for different power-heat-storage applications [117]. While heat pumps are often discussed as a potential source for heating in these papers, the focus does not lie on residential PV heat pump systems for increasing PV self-consumption, but on CHPs.

The German business case for PV heat pumps in residential buildings is only analyzed and modeled in a few papers. In [118], the authors focus on the thermal system and a MILP approach is implemented for solving the sizing and operation problem of a heat pump and a hot water storage system (HWS). Here, time-variable tariffs are analyzed for different one- and multifamily buildings. The results indicate that neither heat pump nor HWS size vary significantly depending on the chosen price scenario or the installed PV capacity. Implications for the electric side regarding PV system and BSS sizes as well as network integration aspects are neglected. A genetic algorithm is used in [119] to model the current and future business case for PV self-consumption. While storage system sizes are decision variables here, PV system size and heat pump size are fixed. The results indicate that there might be a competition over excess PV generation and that BSSs provide a better solution. However, as interactions between PV system and BSS sizing are neglected, the conclusion lacks generalizability. Interde-

pendencies between PV system, heat pump and BSS are analyzed for the German business case using a MILP approach in [120]. The paper follows the standard modeling approach by including investment and operational costs for each DER in the objective function and constraints that enforce energy balances for thermal and electrical energy flows. Space heating demand only needs to be met over a larger time interval rather than during each time step. Such a measure decouples heat supply from immediately following heating demand, but does not automatically implement a discrete operation of heat pumps, which is currently immanent for certain systems and leads to inflexible operation. Such unit commitment constraints have an impact on system sizing and operation that has been shown for bulk power investment decisions [121]. For different economic scenarios, sizing results are presented indicating that electrical component sizes vary significantly higher than thermal competent sizes, which are rather constant. Sensitivity analyses are performed that evaluate sizing impact of investment costs, feed-in limitation and variable electricity prices [120]. The paper does not include tax related effects for the business case (see previous sections) and does not address the impact of PV or heat pump network integration, especially with regard to flexibility offered by the BSS to cope with non-flexible heat pumps.

Network integration aspects of PV BSSs and heat pumps are addressed in several papers for the German business case [122–125]. Typically, fixed system sizes are simulated and interdependencies of incentive system, system sizing and operational constraints are neglected. A general conclusion on how future residential PV systems are sized and how that impacts network integration cannot be drawn. More in-depth network integration analyses can be found for just PV and heat pump systems. The authors of such papers focus on introducing new control strategies through optimized peak shaving through tariffs [126] or fixed curtailment limits for PV [127], voltage control through set-points depending on PV output [128] or droop-voltage control for heat pumps with PV [129]. The value added of introducing a BSS to improve demand response capabilities of heat pumps with unit commitment constraints and enhance network integration of heat pumps is discussed in [130]. Overall, only operational implications of different control strategies are highlighted in these papers and interactions with regard to sizing of PV BSSs are neglected. While most authors focus on PV network integration aspects, other authors highlight that heat pumps might be the driver for network reinforcement depending on the penetration level [131]. Again, a combination with BSSs and introduction of optimal PV and BSS sizing for power-heat applications are not included in the analysis.

In summary, one can conclude that a comprehensive analysis that evaluates complementary of BSSs and heat pumps for future residential PV systems and interdependencies between sizing, tariff system, operational constraints as well as network integration is missing so far.

8.2 *Main contributions*

In this part, the single-investor, open-loop optimization model is extended to enable investors, DNOs and policy makers to derive a better understanding of interdependencies between different flexibility options, especially decentralized power-heat-storage systems. Here, the focus lies on sector coupling through heat pumps, which bring an additional load and flexibility that might allow for larger sized PV systems. As BSSs are currently emerging as the preferred coupling technology to increase self-consumption of PV systems, this part provides an in-depth analysis of the complementarity of BSSs and heat pumps for PV systems, their impact on PV network integration as well as the corresponding tariff and policy setting for sector coupling.

Additionally, the adapted model for sizing and operating of PV BSSs in combination with heat pumps offers following contributions:

- Modeling: A unit commitment formulation is introduced for heat pump operation that allows a better understanding of the flexibility offered by the BSS towards the heat pump and the impact of non-flexible power-to-heat applications for increasing PV self-consumption and improving network integration. Additionally, relevant cash flows, such as taxes on PV self-consumption, are also included for heat related energy flows.

Based on the adapted model, several case studies are performed to answer the following questions:

- Do BSSs and heat pumps compete for excess PV generation or do they complement each other?
- Does an additional load, such as a heat pump, allow capturing the full rooftop potential in a post FIT world and are such systems an economically viable alternative to conventional heating systems?
- Do heat pumps have a positive impact on PV network integration and what tariff ensures a proper network integration of heat pumps?
- Can a BSS offer additional flexibility for non-flexible heat pumps?

The assessment is based on using different electrical and thermal HH profiles for different building types for several locations in Germany. A sensitivity analysis varying different economical, electric component and thermal component related parameters highlights their impact on overall energy supply costs, PV self-consumption and self-sufficiency with regard to future PV business case and their network integration.

The proposed approach is summarized in Fig. 8.1.

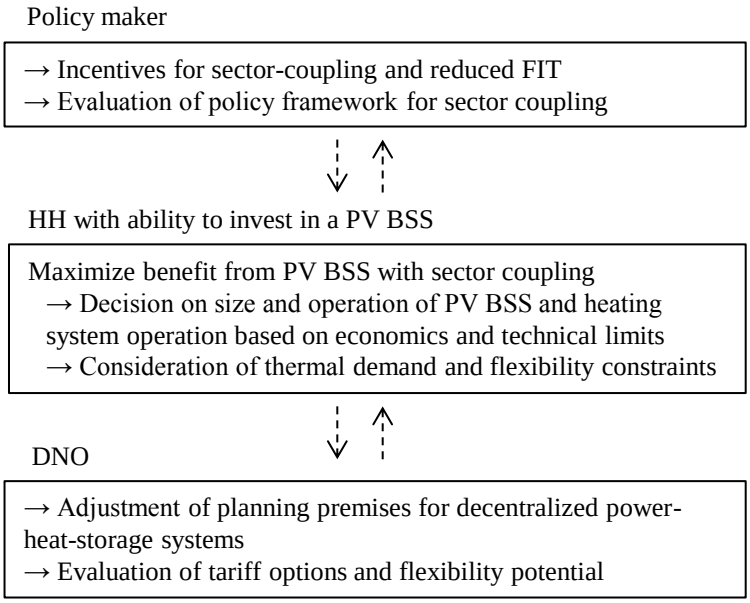

Figure 8.1: Framework and optimization approach for decentralized power-heat-storage systems

8.3 *Organization of the section*

The section is organized similarly as the previous parts. First, the optimization model is adapted to include thermal energy flows and corresponding cash flows. Case studies are presented to address the key aspects of future PV system sizing, the influence of different incentive systems on their network integration as well as the complementarity of BSSs and heat pumps. The part ends with a conclusion.

9

Model for PV BSS and heat pump

To evaluate whether BSS and heat pump compete over excess PV energy or complement each other, an adaption of the previously presented open-loop model is necessary. To model the thermal demand side, next to a thermal demand profile, a heat supply system is implemented. Usually a heat pump is additionally equipped with an electric heating element. Such a heating element has a lower power to heat conversion factor, but provides additional peak power capability, e.g. to cover instant peak demand from hot water. The heat pump and the electric heating element are connected to a HWS, which allows decoupling heat generation and serving heat demand. Furthermore, a condensing natural gas boiler is modeled as a conventional heating system. This section describes the new optimization model and highlights heat-specific adjustments.[1]

9.1 *Objective*

Here, it is assumed that HHs have already made an investment decision into a heating system: a heat pump or a condensing boiler plus an electric heating element and HWS. As outlined, such HHs are inclined to explore whether locally generated PV energy can be used to operate the heat pump efficiently and if there is a value added by investing in a BSS to not only cover standard electric demand but also to support heat pump operation. HHs j again try to maximize their economic benefit by deciding on the optimal balance of investing in additional PV capacity and/or a BSS and procuring energy from the network (electricity or natural gas). Thus, the HH's objective function comprises all electricity and thermal related cash flows as well as fictional costs related to heat pump operation:

- Investment costs $I^{PV}, I^{BSSkWh}, I^{BSSkW}$ depend on PV system size s_j^{PV}, BSS capacity s_j^{BSSkWh} and BSS inverter size s_j^{BSSkW}; investment costs for the heat pump or the condensing gas boiler plus electric heater and HWS are neglected.
- One-time installation costs for PV In^{PV} and BSS In^{BSS} depend on the discrete decision to install the technology (b_j^{PV} for PV and b_j^{BSS} for BSS) and are included to ensure that their impact is not neglected, which is highly relevant for small-scale systems. Again, heating related costs are disregarded.

1 Parts of this chapter are presented in [21, 105, 106].

- Yearly costs $M^{PV}, M^{BSSkWh}, M^{BSSkW}$, such as maintenance costs or insurance costs, depending on component sizes are included as well.
- Revenues resulting from PV network feed-in $e_{j,t}^{PVN}$ reimbursed per fed-in kWh at the price C^{Fit1} lead to a positive cash flow.
- Energy procurement costs C^{E} related to electricity consumption per kWh from the network for standard demand $e_{j,t}^{NL}$ are included. Additionally, electricity for heating purposes currently enjoys privileges that can lead to reduced costs C^{Eh} for demand for heat pump operation $e_{j,t}^{NHP}$ and for operation of the electric heater $e_{j,t}^{NEH}$. Additional energy procurement costs C^{Ng} for natural gas demand $q_{j,t}^{CB}$ from the condensing boiler are included, if such a heating device is installed.
- Power procurement costs C^{P} related to the yearly peak demand from network p_{j}^{NL} are additional costs. The addition of a peak charge follows the assumption that in future the likelihood of peak pricing on a HH level steadily increases as electricity networks are designed according to power demand or feed-in and not energy demand.

Furthermore, cost and revenue components related to taxes and surcharges are included:

- Taxes: Currently sales tax C^{Sc1} has to be paid on PV self-supply. Compared to the previous model, an additional sales tax component for self-consumption related to heating C^{Sch1} is introduced for direct supply to the heat pump $e_{j,t}^{PVHP}$ and the heating element $e_{j,t}^{PVEH}$ as well as indirect self-supply through the BSS ($e_{j,t}^{BSSHP}$ and $e_{j,t}^{BSSEH}$). Additionally, income taxes have to be paid on earnings of PV BSSs; vice versa, related costs can be deducted. Income taxes on earnings depend on PV network feed-in TE^{Fit}, PV self-supply for standard demand TE^{Sc} and for heat related demand TE^{Sch}. Possible tax reductions are based on the depreciation of the PV BSS TE^{Dep}.
- Surcharges on self-supply: Once a threshold of 10 kWp as installed PV capacity is surpassed, surcharges C^{Sc2} for standard demand and C^{Sch2} for heat related demand on PV self-consumption have to be paid. Resulting bi-linear products are linearized following the approach presented in Section 3.2.2.

A heat pump specific-cost parameter C^{HPs} is added to influence the number of starts $o_{j,t}^{HP}$ of the device and to avoid to frequent start-stop operation. Such costs are not included for the electric heating element; operation is presumed to be continuous and not discrete as heat pump operation. This helps to reduce the complexity of the optimization problem as less binary variables are required. A preferred heat pump operation over the operation of the electric heater is modeled endogenously through different conversion efficiencies of heat pump and electric heater.

In summary, the following objective function z_j for a HH with the ability to invest into a PV BSS is derived:

$$
\begin{aligned}
max\, z_j \;=\;& (C^{Fit1} - TE^{Fit}) \cdot PF^{HH} \sum_{t \in \mathcal{T}} e_{j,t}^{PVN} \\
-\;& (I^{PV} + M^{PV} \cdot PF^{HH} - TE^{Dep} \cdot PF^{HH}) \cdot s_j^{PV} - In^{PV} \cdot b_j^{PV} \\
-\;& (I^{BSSkWh} + M^{BSSkWh} \cdot PF^{HH}) \cdot s_j^{BSSkWh} \\
-\;& (I^{BSSkW} + M^{BSSkW} \cdot PF^{HH}) \cdot s_j^{BSSkW} \\
-\;& In^{BSS} \cdot b_j^{BSS} \\
-\;& (C^{Sc1} + C^{Sc2} \cdot b_h^{SkWp} + TE^{Sc}) \cdot PF^{HH} \\
\cdot\;& \sum_{t \in \mathcal{T}} (e_{j,t}^{PVL} + e_{j,t}^{BSSL}) \\
-\;& (C^{Sch1} + C^{Sch2} \cdot b_j^{SkWp} + TE^{Sch}) \cdot PF^{HH} \\
\cdot\;& \sum_{t \in \mathcal{T}} (e_{j,t}^{PVHP} + e_{j,t}^{PVEH} + e_{j,t}^{BSSHP} + e_{j,t}^{BSSEH}) \\
-\;& C^{E} \cdot PF^{HH} \sum_{t \in \mathcal{T}} e_{j,t}^{NL} - C^{Eh} \cdot PF^{HH} \sum_{t \in \mathcal{T}} (e_{j,t}^{NHP} + e_{j,t}^{NEH}) \\
-\;& C^{Ng} \cdot PF^{HH} \sum_{t \in \mathcal{T}} q_{j,t}^{CB} - C^{P} \cdot p_j^{NL} \cdot PF^{HH} \\
-\;& C^{HPs} \cdot \sum_{t \in \mathcal{T}} o_{j,t}^{HP}
\end{aligned}
\tag{9.1}
$$

9.2 *Constraints*

Next to investment and energy balance constraints on the electrical side, additional constraints to meet thermal demand are required and to model heat pump or condensing boiler, electric heater as well as the HWS.

9.2.1 *Component-specific energy balances and sizing constraints*

Three equalities are set up to guarantee that standard demand $E_{j,t}^{L}$ plus heat pump and heating element related demand are met during all time steps. The equality for standard electric demand remains as previously presented in Eq. 3.2. The heat pump can be served using the same sources as standard demand: network supply $e_{j,t}^{NHP}$, direct PV supply $e_{j,t}^{PVHP}$ or through BSS discharging $e_{j,t}^{BSSHP}$. The three energy flows comprise the time-dependent electricity demand of the heat pump. Depending on the operational states u, the overall heat pump energy needs to be disaggregated into different heat pump related electricity flows $e_{j,t,u}^{HP}$. The total number of different states $\mathcal{U}$ depends on whether the heat pump is fully modulating, only operates in an on-off fashion or is capable to operate at certain partial-load areas u, e.g. 33 % of the max. load:

$$\forall t: \quad e_{j,t}^{NHP} + e_{j,t}^{PVHP} + e_{j,t}^{BSSHP} = \sum_{u \in \mathcal{U}} e_{j,t,u}^{HP} \tag{9.2}$$

The overall demand from the electric heating element $e_{j,t}^{EH}$ is also supplied through the same energy sources: direct PV supply $e_{j,t}^{PVEH}$, indirect PV supply through BSS $e_{j,t}^{BSSEH}$ and the network $e_{j,t}^{NEH}$.

$$\forall t: \quad e_{j,t}^{NEH} + e_{j,t}^{PVEH} + e_{j,t}^{BSSEH} = e_{j,t}^{EH} \tag{9.3}$$

An additional equality guarantees that PV power can only be used according to the given normalized PV profile for the different locations $E_{j,t}^{PV}$ and the installed PV capacity $s^P V_j$:

$$\begin{aligned} \forall t: \quad & e_{j,t}^{PVL} + e_{j,t}^{PVBSS} + e_{j,t}^{PVN} + e_{j,t}^{PVHP} + e_{j,t}^{PVEH} + e_{j,t}^{PVC} \\ & = s_j^{PV} \cdot E_{j,t}^{PV} \end{aligned} \tag{9.4}$$

The current state of charge $soc_{j,t}$ of the BSS is determined through the self-discharge η^{BSSSd} of the previous $soc_{j,t-1}$, the charging efficiency η^{BSSCh} and discharging efficiency η^{BSSDis} for BSS related energy flows. In this case, BSS discharging can also be used to supply the heat pump $e_{j,t}^{BSSHP}$ or the heating element $e_{j,t}^{BSSEH}$:

$$\begin{aligned} \forall t: \quad soc_{j,t} = \; & \eta^{BSSSd} \cdot soc_{j,t-1} + \eta^{BSSCh} \cdot e_{j,t}^{PVBSS} \\ & - (\eta^{BSSDis})^{-1} \cdot (e_{j,t}^{BSSL} + e_{j,t}^{BSSHP} + e_{j,t}^{BSSEH}) \end{aligned} \tag{9.5}$$

BSS constraints to avoid aging are implemented as before (see Eq. 3.5 and Eq. 3.6) and energy flows are again bounded by their sizing variable:

$$\forall k \in [PVL, PVBSS, PVN, PVHP, PVEH, PVC],\ t: \quad e_{j,t}^{k} \leq s_j^{PV} \cdot E_{j,t}^{PV} \tag{9.6}$$

$$\forall k \in [PVBSS, BSSL, BSSHP, BSSEH],\ t: \quad e_{j,t}^{k} \leq s_j^{BSSkW} \cdot \tau \tag{9.7}$$

Demand related variables remain bounded as described in Eq. 3.7. One-time investment costs as well as PV curtailment to facilitate network integration persist as displayed in Eq. 3.15, Eq. 3.12 and Eq. 3.13.

Additionally, the following constraint determines the peak demand:

$$\forall t: \quad e_{j,t}^{NL} + e_{j,t}^{NHP} + e_{j,t}^{NEH} \leq \quad p_j^{NL} \cdot \tau \tag{9.8}$$

Here, network demand to cover standard loads as well as heating related network demand are accumulated for each time step. The inequality ensures that only the yearly peak is set equal to the decision variable p_j^{NL}.

9.2.2 *Constraints for thermal energy flows and components*

The heat pump, the condensing boiler and the electric heater indirectly serve space heating $Q_{j,t}^{SH}$ and drinking hot water demand $Q_{j,t}^{DHW}$ by charging the HWS. As thermal demand is more open to individual perception and small-scale temperature variations are not immediately felt in the room temperature, two inequalities allow for flexibility in meeting thermal demand (instead of an equality such as for electricity demand). A reduction of κ^{Qmin} or an increase of κ^{Qmax} of the overall thermal demand are allowed per time step, which has to be met by discharging the HWS $q_{j,t}^{HWSL}$:

$$\forall t: \quad q_{j,t}^{HWSL} \leq \quad \kappa^{Qmax}(Q_{j,t}^{SH} + Q_{j,t}^{DHW}) \tag{9.9}$$

$$\forall t: \quad \kappa^{Qmin}(Q_{j,t}^{SH} + Q_{j,t}^{DHW}) \leq \quad q_{j,t}^{HWSL} \tag{9.10}$$

To ensure that the overall comfort is not reduced, thermal demand can only be advanced or delayed over a certain time period. Here, an additional constraint guarantees that the adjusted demand over one day is equal to the original demand over the same 24 hours. Two additional time subsets are introduced: $\mathcal{T}^S$ contains all time steps over one day, while $t^D \in \mathcal{T}^D$ describes a set of all days of one year.

$$\forall d: \quad \sum_{t \in \mathcal{T}^S} q_{j,(t+T^D \cdot t^D)}^{HWSL} \quad = \sum_{t \in \mathcal{T}^S} (Q_{j,(t+T^D \cdot t^D)}^{SH} + Q_{j,(t+T^D \cdot t^D)}^{DHW}) \tag{9.11}$$

T^D is the length of a day period, which depends on the chosen simulation time step.

The HWS is modeled similar to the BSS. It is described through its current state of charge $qsoc_{j,t}$, which is a reflection of the temperature level inside the HWS. Next to discharging (with efficiency η^{HWSDis}), self-discharging η^{HWSSd} depending on the storage level $qsoc_{j,t-1}$ of the previous time step and energy flows related to charging the HWS (here: thermal energy produced by the heat pump $q_{j,t}^{HP}$, by the electric heating element $q_{j,t}^{EH}$ or by a

condensing boiler $q_{j,t}^{CB}$, which is adjusted according to its efficiency COP^{CB}) with a charging efficiency of η^{HWSCh} impact $qsoc_{j,t}$:

$$\begin{aligned} \forall t: \quad qsoc_{j,t} = \quad & \eta^{HWSSd} \cdot qsoc_{j,t-1} \\ & + \eta^{HWSCh} \cdot (q_{j,t}^{HP} + q_{j,t}^{EH} + COP^{CB} \cdot q_{j,t}^{CB}) \\ & - (\eta^{HWSDis})^{-1} \cdot q_{j,t}^{HWSL} \end{aligned} \tag{9.12}$$

HWS usage is bounded by the lower κ^{HWSmin} and the upper limit κ^{HWSmax} of storage capacity S^{HWS}:

$$\forall t: \quad qsoc_{j,t} \leq \quad \kappa^{HWSmax} \cdot S^{HWS} \tag{9.13}$$

$$\forall t: \quad \kappa^{HWSmin} \cdot S^{HWS} \leq \quad qsoc_{j,t} \tag{9.14}$$

S^{HWS} can be described as the product of water volume, the assumed temperature delta between lower and upper water temperature, the corresponding water density and specific heat capacity.[2]

The available thermal energy from the heat pump depends on the heat pump's coefficient of performance (COP). The COP varies depending on the temperature difference between the heat source (air, soil) and the heat sink (HWS). To account for temperature differences, the COP is described as a function, which varies depending on the temperature l of the heat source (here, the ambient temperature of the used location). The COP for a given temperature can be found in a data sheet of the chosen heat pump.[3] By interpolating given data points, two COP functions are derived depending on whether the ambient temperature is below or above 0 °C:

$$\forall l: \quad COP_l^{HP} = \quad \begin{cases} COP_0^{HP} + 0.07 \cdot l & l \geq 0 \\ COP_0^{HP} + 0.11 \cdot l & l < 0 \end{cases} \tag{9.15}$$

This goes along with a slight temperature-dependent adjustment of the max. available electric power of the heat pump:

$$\forall l: \quad S_l^{HP} = \quad \begin{cases} S_l^{HP} + 0.013 \cdot l & l \geq 0 \\ S_l^{HP} - 0.07 \cdot l & l < 0 \end{cases} \tag{9.16}$$

2 Here, the following values are used: volume: 450 l, temperature delta: 20 K, water density at 50 °C: 988.03 kg/m³ and specific heat capacity at 50 °C: 4.18 kJ/(kg·K)

3 Here, data of the Vaillant heat pump flexotherm VWF 117/4 is used [132].

As time-dependent ambient temperatures are available for each HH's location ($l = t$) , time-dependent COP_t^{HP} and S_t^{HP} can be determined. An electric power-heat conversion equality is established for the heat pump:

$$\forall t: \quad COP_t^{HP} \cdot \sum_{u \in \mathcal{U}} e_{j,t,u}^{HP} = \quad q_{j,t}^{HP} \tag{9.17}$$

The thermal power provided by the heat pump is indirectly limited by available electric power:

$$\forall t: \quad \sum_{u \in \mathcal{U}} e_{j,t,u}^{HP} \leq \quad S_t^{HP} \cdot \tau \tag{9.18}$$

The power-heat conversion of the electric heater is independent of the ambient temperature:

$$\forall t: \quad COP^{EH} \cdot e_{j,t}^{EH} = \quad q_{j,t}^{EH} \tag{9.19}$$

The max. available power of the heating element and of the condensing boiler are limited by the installed rated power of each device:

$$\forall t: \quad e_{j,t}^{EH} \leq \quad S^{EH} \cdot \tau \tag{9.20}$$

$$\forall t: \quad q_{j,t}^{CB} \leq \quad S^{CB} \cdot \tau \tag{9.21}$$

9.2.3 *Unit commitment constraints for heat pump operation*

As stated above, certain heat pumps are not modulating and are only able to operate in an on-off mode or can only be operated at discrete, non-continuous operating points. Binary variables are introduced to model such a discrete operation, which is typically called unit commitment. For each operational state u, one binary variable $b_{j,t,u}^{HP}$ ensures that the corresponding $e_{j,t,u}^{HP}$ is limited to the specific power of each operating state $P_{j,u}^{HP}$:

$$\forall t, i: \quad e_{j,t,u}^{HP} \leq \quad P_{j,u}^{HP} \cdot b_{j,t,u}^{HP} \tag{9.22}$$

$$\forall t, i: \quad P_{j,u}^{HP} \cdot b_{j,t,u}^{HP} \leq \quad e_{j,t,u}^{HP} \tag{9.23}$$

As $b_{j,t,u}^{HP}$ can only be equal to one or zero during one time step, the constraints ensure that if $b_{j,t,u}^{HP}$ is equal to one, $e_{j,t,u}^{HP}$ is equal to $P_{j,u}^{HP}$ ($P_{j,u}^{HP} \leq$

$e^{HP}_{j,t,u} \leq P^{HP}_{j,u}$). The same logic ensures that if $b^{HP}_{j,t,u}$ is equal to zero, $e^{HP}_{j,t,u}$ is set to zero.

To guarantee that only one operating point can be active during one time step, the following constraints is introduced:

$$\forall t: \ \sum_{u \in \mathcal{U}} b^{HP}_{j,t,u} \leq \ 1 \tag{9.24}$$

Once one $b^{HP}_{j,t,u}$ is active (equal to one), all other operating states need to be zero as the sum cannot exceed one.

Additional technical constraints for heat pump operation are imposed through minimum up and down time requirements. A minimum up time requirement ensures that a heat pump has to stay on for a certain time κ^{HPup} before it can be turned off. If the heat pump is activated during time step t, it has to stay on until a period of $t + \kappa^{HPup} - 1$ is passed:

$$\forall t: \ \sum_{u \in \mathcal{U}} b^{HP}_{j,t,u} - \sum_{u \in \mathcal{U}} b^{HP}_{j,t,u-1} \ \leq o^{HPup}_{j,t} \tag{9.25}$$

Once the heat pump is activated, the start counter variable $o^{HPup}_{j,t}$ is set to one. Now, the heat pump can only be turned off again after κ^{HPup} is reached:

$$\forall t, v \in 1..(\kappa^{HPup} - 1): \ o^{HPup}_{j,t} \leq \sum_{u \in \mathcal{U}} b^{HP}_{j,min(T^Y,t+v),u} \tag{9.26}$$

During the next time step, $o^{HP}_{j,t+1}$ is set to zero again, while Eq. 9.26 requires that the heat pump remains on as $\sum_{u \in \mathcal{U}} b^{HP}_{j,t+1,u}$ needs to be equal to one. The same logic is applied to guarantee a minimum down time. Once the heat pump is turned off, it needs to remain off for κ^{HPdown} as the following two constraints enforce by introducing a turn-off variable $o^{HPdown}_{j,t}$:

$$\forall t: \ \sum_{u \in \mathcal{U}} b^{HP}_{j,t-1,u} - \sum_{u \in \mathcal{U}} b^{HP}_{j,t,u} \ \leq o^{HPdown}_{j,t} \tag{9.27}$$

$$\forall t, v \in 1..(\kappa^{HPdown} - 1): \ o^{HPdown}_{j,t} \ \leq 1 - \sum_{u \in \mathcal{U}} b^{HP}_{j,min(T^Y,t+v),u} \tag{9.28}$$

While $o^{HPup}_{j,t}$ and $o^{HPdown}_{j,t}$ do not necessarily need to be binary, they need to be bounded by zero and one.

10

Case studies and conclusions

The presented model is used to assess the attractiveness of the business case of residential PV systems with new options, such as heat pumps, for additional PV self-consumption. After discussing the relevant KPIs and input data for the case studies, different case studies for future PV self-consumption systems are performed. Specific parameters are varied to highlight key aspects of competition of BSSs and heat pumps for excess PV energy. Implications for PV network integration of future PV self-consumption systems are analyzed by evaluating the impact of different incentive systems on network peaks. The final case study evaluates the impact of flexibility of heat pumps on PV BSS sizing and potential value added of BSSs to compensate inflexibility of the heat pump. The section ends with a conclusion.[1]

10.1 *Key performance indicators*

As additional energy flows are introduced, an adaption of the KPIs with regard to the heat related energy consumption is necessary.

- System sizes:

  For the presented case studies, all heat related components (heat pump, electric heater, HWS or condensing gas boiler) are fixed in size and assumed to be installed.[2] The focus lies on sizing results for the installed PV capacity s_j^{PV} to assess complementarity and competitiveness between PV energy shifting using a BSS and PV energy consumption using additional heat related demand (either through a heat pump or an electric heater). PV system sizes serve as an indicator for the general attractiveness of the business case without a high FIT. Installed BSS capacities s_j^{BSSkWh} are also analyzed, especially with regard to their impact on PV system sizing and their replaceability through heat pumps.

- Overall costs of energy supply:

  The overall costs of energy supply of the chosen system configuration CoS_j are a function of the objective z_j and an addition of fictional cost terms, which are included in the objective function (here: only costs related to heat pump starts):

1 Parts of this chapter are presented in [21, 105, 106].

2 Previous analyses have shown that fixed system sizes for the heating unit as well as TES are valid assumptions as their impact on PV BSS sizing is limited [120]. The claim will be validated by varying system sizes in a sensitivity analysis.

$$CoS_j = (z_j + C^{HPs} \cdot \sum_{t \in \mathcal{T}} o_{j,t}^{HPup}) \tag{10.1}$$

Investment costs for heating related components are not included. Yet, the presented CoS_j allows analyzing max. investment cost differences for various heating technologies, e.g. heat pumps vs. condensing gas boilers, by comparing differences in overall operational costs. The comparison of operational cash flows also allows deriving whether PV self-consumption through heat pumps is competitive enough to substitute natural gas based heating.

- Self-sufficiency of electric and heat demand:

  An understanding of what percentage of electric and heat demand is served using locally generated PV energy is crucial to evaluate the general compatibility of PV generation, heat demand and potential competition among BSSs and heat pumps. Separate self-sufficiency indicators for electric demand SP_j^E and for heat demand SP_j^Q are introduced. Both indicators are calculated using the overall electric or heat demand and subtracting the fraction supplied via electric network or via natural gas supply.

$$\begin{aligned} SP_j^E = & \sum_{t \in \mathcal{T}} (E_{j,t}^L + e_{j,t}^{HP} + e_{j,t}^{EH} \\ & - e_{j,t}^{NL} - e_{j,t}^{NHP} - e_{j,t}^{NEH}) \\ & \cdot 100 \cdot (\sum_{t \in \mathcal{T}} (E_{j,t}^L + e_{j,t}^{HP} + e_{j,t}^{EH}))^{-1} \end{aligned} \tag{10.2}$$

For the thermal self-sufficiency, the temperature dependency of heat pump's COP is included through an element-wise product for the applicable terms.

$$\begin{aligned} SP_j^Q = & \sum_{t \in \mathcal{T}} (Q_{j,t}^{SH} + Q_{j,t}^{DHW} \\ & - COP_t^{HP} \cdot e_{j,t}^{NHP} - COP^{EH} \cdot e_{j,t}^{NEH} \\ & - COP^{CB} \cdot q_{j,t}^{CB}) \cdot 100 \\ & \cdot (\sum_{t \in \mathcal{T}} (Q_{j,t}^{SH} + Q_{j,t}^{DHW}))^{-1} \end{aligned} \tag{10.3}$$

- PV self-consumption:

  PV self-consumption SC_h describes the percentage of locally generated PV energy that is used for direct load consumption via standard demand, heat related consumption by the heat pump or the electric

heater or indirectly via BSS charging. While self-sufficiency indicators display the necessity of network for load supply, PV self-consumption measures the attractiveness of PV network feed-in and the means necessary to avoid it:

$$SC_j = \frac{\sum_{t \in \mathcal{T}} (e_{j,t}^{PVL} + e_{j,t}^{PVHP} + e_{t,j,t}^{PVEH} + e_{j,t}^{PVBSS}) \cdot 100}{s_j^{PV} \cdot \sum_{t \in \mathcal{T}} E_{j,t}^{PV}} \quad (10.4)$$

- Peak PV feed-in and peak demand per HH:

  Peak PV feed-in per installed system and HH might be impacted by additional load flexibilities and thus remains an important aspect for PV network integration of future PV systems. It is determined through Eq. 4.1. The peak demand p_j^N is described by also considering heat related electricity demand from the network and is endogenously modeled through the demand charge (see Eq. 9.8).

10.2 *Input data*

A main contribution of the presented work aims at assessing the attractiveness of the business case of residential PV systems in a post FIT world in Germany. The scenario data is chosen according to the potential passing of the cap of 52 GWp installed PV capacity in Germany. Once the cap is reached, it is currently foreseen to switch from a FIT based system to a market price based system. The following sections detail the used parameters for such a scenario.

10.2.1 *Key electric and cost input parameters*

The underlying scenario of the case studies is set in the early 2020s, since around that time the 52 GWp-cap is most likely reached. It is assumed that additional metering requirements related to the smart meter rollout in Germany (see section 2) equally effect load as well as generation, so that no additional costs need to be included and the overall German policy framework is adapted to foster the power-heat coupling technologies.

- Remuneration of PV network feed-in:

  A PV growth rate that is in-line with current policy making would result in yearly installation rates around 1.5 to 2.5 GWp. Thus, in approx. 4-5 years the installed PV capacity would surpass 52 GWp. Afterwards, it is likely that PV network feed-in is reimbursed with the PV market value. While the PV market value experienced a significant drop until 2015, it has stabilized around 3.5 ct/kWh in 2016 [14]. Assuming that the phase out of all nuclear power plants until 2022 will

stabilize electricity spot market prices and certain customers are willing to pay a moderate premium for consuming PV energy[3], a range of 1 to 5 ct/kWh as remuneration for PV network feed-in seems reasonable (see also [21]).

- Electricity procurement price:

  The mean electricity price per kWh is assumed to remain at 33 ct/kWh following the assumption that EEG surcharge will reach its peak in the early 2020s and then slowly decrease. The decrease will be counterbalanced by a rise in NCs (see section A.1.1). To cover the uncertainty entailed in electricity price development, a bandwidth of 28 ct/kWh to 40 ct/kWh is chosen, which accounts for different paths of NC development and an adjustment of other taxes and surcharges.
  If loads are controllable and separately metered, electricity can be sold with discounted NCs according to §14a EnWG. Reduced NCs vary from 20 % to nearly no reduction of the original NCs depending on the DNO and come with the prohibition of operating controllable loads during certain predefined hours, typically during peak load hours. As heat pumps are controllable loads, a price discounted to 75 % of the original price is assumed for the reference case.
  Furthermore, a case study is conducted that analyzes the introduction of power-based NCs. Current peak charges lie between 2.5 and 71 €/kW for the analyzed larger DNOs.[4] Next to peak charges, customers are still required to pay an energy-based NC. Such charges are 9 to 44 % lower than typical HH customer charges. It is assumed that the ratio between energy- and power-based charges remains intact and increases at a similar rate as NCs of HH. This results in a energy-based price of 31 ct/kWh and a peak charge of 25 €/kW.

- Investment costs for PV systems and BSSs:

  For PV system costs, an additional price drop of 20 % of variable investment costs for the next 4-5 years is assumed for small-scale PV systems. Such a price decline is equal to a yearly reduction of approx. 5 % and is based on a literature review [133–135], but also takes into account that small-scale systems do not see the full extent of possible reductions as economies of scale are harder to reach compared to larger systems. While 1,000 €/kWp are assumed as reference case, a variation of ± 100 €/kWp is used for a sensitivity analysis. One-time installation costs remain at 1,000 € per installation.
  For BSS prices, a slight decrease in the yearly price drop to approx. 13 % compared to the currently observed 20 % is assumed. For the next five years, that results in a price reduction by 50 % leading to BSS

3 Such premiums are typically around 1 ct/kWh and can be derived by comparing mean electricity prices of ordinary electricity retailers with ones that only procure from German RES.

4 Currently, such NCs are mandatory for customers that consume over 100 MWh/a.

capacity prices of 250 €/kWh and inverter prices of 150 €/kW. A variation of ± 50 €/kWh, respectively kW, is introduced to cover uncertain price development.

- Other parameters:

  BSS efficiencies for charging and discharging are assumed to increase to 95 % for the reference case and are varied by ± 4 %-points to assess their impact on using PV energy for BSS or heat pump operation. Additionally, the PV curtailment threshold is lowered to 30 % of the installed PV capacity for one case study to test its impact on scheduling BSS and heat pump operation. All other parameters remain within the same range described in Tab. A.3.

10.2.2 *Thermal input parameters*

Besides different fixed installed sizes of HWS and heat pump as well as a variation of the used COP, thermal demand profiles might impact the attractiveness of using PV energy for heat pump operation. Thus, relevant thermal input parameters are outlined in the following sections.

10.2.2.1 *Building type*

Three different types of buildings are used for the simulation. The building selection aims at covering a wider variety of buildings based on the actual German building stock for single family houses. Thus, one building with a high energy demand is included, one building with a moderate heating demand that could reflect a building from the 1990s as well as one building that reflects a relatively new building with a low space heating demand. Next to space heating, heat demand for drinking hot water marks the second necessary heat related energy flow. While the underlying models are described in the following section, Table 10.1 summarizes the most important parameters.

10.2.2.2 *Thermal demand profiles*

Thermal demand profiles are derived as follows.

- VDI 4655 profiles:

  The profiles were originally established to facilitate the planning and efficiency comparison of different CHPs. They are based on yearly measurements of five different single family houses that have been categorized into different day types, weekdays and weekends, for three different seasons, winter, spring and fall as well as summer, just like SLP for electric demand. Furthermore, all winter and transition days are categorized in sunny and cloudy days. Location-specific profiles can be derived by choosing from 15 different climate zones that represent different weather conditions in Germany. An important remark

		Building type		
Parameter	Unit	1	2	3
Construction period		2010 - now	1984 - 1994 (usual refurbishment)	1958 - 1968 (usual refurbishment)
Energy need for heating [kWh/m²a]	kWh/m²	45	94	118
Heated area	m²	155	160	186
Yearly space heating demand	MWh/a	7	15	22
Residents	no.	3	3	3
Yearly hot water demand	MWh/a	2.5	2.5	2.5

Table 10.1: Used building types for the simulation

regarding the usage of these profiles is that they are heat generator oriented and not fully demand oriented [136, 137]. As a result, the profiles have longer periods of continuous heat demand and do not follow an on-off-characteristic.

- IWES profiles:

  The DIN V 4108-6 guideline serves as a baseline for modeling these profiles [138]. Thermal demand is derived by taking into account building geometry, heat transfer coefficients, the proximity to neighboring buildings, the type of heating system, conducted modernization measures and behavior of the inhabitants for a specific building type. Such data is obtained through a survey of the German building stock [139]. By choosing a specific location and selecting one weather year, ambient temperatures for the selection are retrieved from the German weather service [140]. The ambient temperature is then used as input to model the room temperature based on building characteristics and an occupancy model of the building. The occupancy model determines set values for different room temperatures. For the given model, the room temperature is assumed to be 22 °C when the inhabitants are at home and 16 °C when they are not. Typical occupancy is based on the guideline VDI 2067 . A mathematical description of the model can be found in [137].

- Drinking hot water profiles:

  One of the main influences on the overall hot water demand is the number of residents of the simulated building and their bathing habits. Typically, yearly demand ranges from 500 kWh to 1700 kWh [136, 141]. Here, a bottom-up approach based on HH appliances used for con-

suming drinking hot water and their usage is used to generate corresponding load profiles. The guideline VDI 2067 provides the baseline for consumption length as well as frequency of usage per day for each appliance [142]. In combination with an occupancy model, which depends on the characteristics of the HH type, a probability of appliance usage for each simulation time step is determined. Afterwards, the actual appliance demand profiles are subsequently aggregated to the overall profile $Q_{j,t}^{DHW}$. Further details of the model and a mathematical description can be found in [137].

- Case study profiles:

  Thermal demand profiles using the IWES model as well as the VDI 4655 model are generated for each of the four locations described in Tab. A.2 based on weather data for 2009. If the location-specific climate data is not available, data from a location in close proximity is used. Overall, PV generation profile and thermal demand profile match in year, ambient temperature and radiation. Coefficients allowing for a temporary reduction thermal demand κ^{Qmin} and κ^{Qmax} are set to one for most case studies. An additional case study is conducted where κ^{Qmin} and κ^{Qmax} are set to 90 % and 110 % to allow for flexibility during each time step.

10.3 *Case studies for future PV systems*

As outlined above, three case studies are designed to evaluate whether the business case for residential PV systems remains attractive in a post FIT world. First, three different scenarios are analyzed to determine whether BSS, electric heater and heat pump provide a significant value added for PV systems. It is evaluated whether there is a general competition among heat pumps and BSSs over excess PV energy and whether heat pumps and electric heaters are a viable economic option compared to condensing gas boilers. A sensitivity analysis is used to evaluate the robustness of the results. A second case study focuses on network integration aspects and evaluates suitable tariff systems for decentralized power-heat-storage systems. A third case study discusses the implications of non-flexible heat pump operation and a potential value added through flexibility delivered by a BSS.

10.3.1 *Impact of BSSs and thermal demand on PV systems*

Three different scenarios with each two different system configurations are examined in the following case study. Scenario 'Electricity only' displays results for the business case for residential PV systems when home-owned heating systems are out of scope, e.g. when a centralized heating device serves several terraced houses. 'PV only' indicates results for PV system

sizing when neither BSS nor heat pump are an option, e.g. due to space or financial constraints. 'PV+BSS' describes the case when PV and BSS are possible investment options, but using PV energy for heating through a heat pump is not an option. Scenario 'Condensing gas boiler and electric heater' adds a conventional heating system as the main heating source and allows for electric heating through a simple electric heater, which is inserted in the system's TES. Again, two sub-scenarios are distinguished: one with only a PV system and one with the possibility to invest in a PV BSS. Scenario 'Heat pump and electric heater' refers to a fixed heat pump installation while installation and size of PV system as well as BSS are decision variables for each HH. Furthermore, the orientation of the PV system is varied for all scenarios. Next to the PV system size, BSS size, PV self-consumption, electric and thermal self-sufficiency are evaluated to determine what drives future PV investments. Fig. 10.1 summarizes the results by displaying a box plot per scenario and PV system orientation for four different locations and one thermal load profile per location as well as for 48 electric demand profiles for heat demand of 17.5 MWh.

When just PV systems are installed, the median PV system size amounts to 2.3 kWp per HH. While median PV self-consumption is at 53.6 %, median self-sufficiency is only at 23.5 % in this scenario. Compared to current PV system sizing, the median PV system size for SOs drops by over 50 %, indicating that the decline in system prices cannot compensate the decrease in FIT. However, differences between system orientations vanish as median PV system sizes only vary by 0.1 kWp and come close to current sizes. When a BSS is available, PV system sizes increase by over 80 % for the scenario 'PV+BSS'. The median PV system reaches 4.2 kWp with a median BSS capacity of 6.7 kWh and comes close to current median sizes, which lie around 5 kWp. Such larger sizes are possible as BSS allow increasing PV self-consumption to 68.8 %. BSS help avoiding an even bigger portion of locally generated energy from being fed into the network while increasing median self-sufficiency to 53.4 %. Compared to current systems, both PV self-consumption and self-sufficiency rise, while BSS sizes increase by more than 20 %.

When power-heat coupling through a heating element is possible and a condensing gas boiler is available as alternative heat source, PV and BSS sizes remain at the same level of scenario 'Electricity only'. Median PV-self-consumption increases to 74.4 % without and 80.3 % with a BSS, indicating that it is economically attractive to use excess PV energy for heating purposes rather than feeding it into the network. Differences due to PV system orientation become visible; using excess PV energy for heating is more attractive for SOs (with a median PV-self-consumption of up to 95.1 %) than for SWs and SEs (with PV self-consumption of 57.1 to 58.1 %). However, as a result of the low efficiency of the heating element, oversizing PV systems to achieve even higher amounts of local heat supply is not a viable option.

When combining PV systems with heat pumps and not a BSS, the influence of the additional electric load as a result of thermal demand is distin-

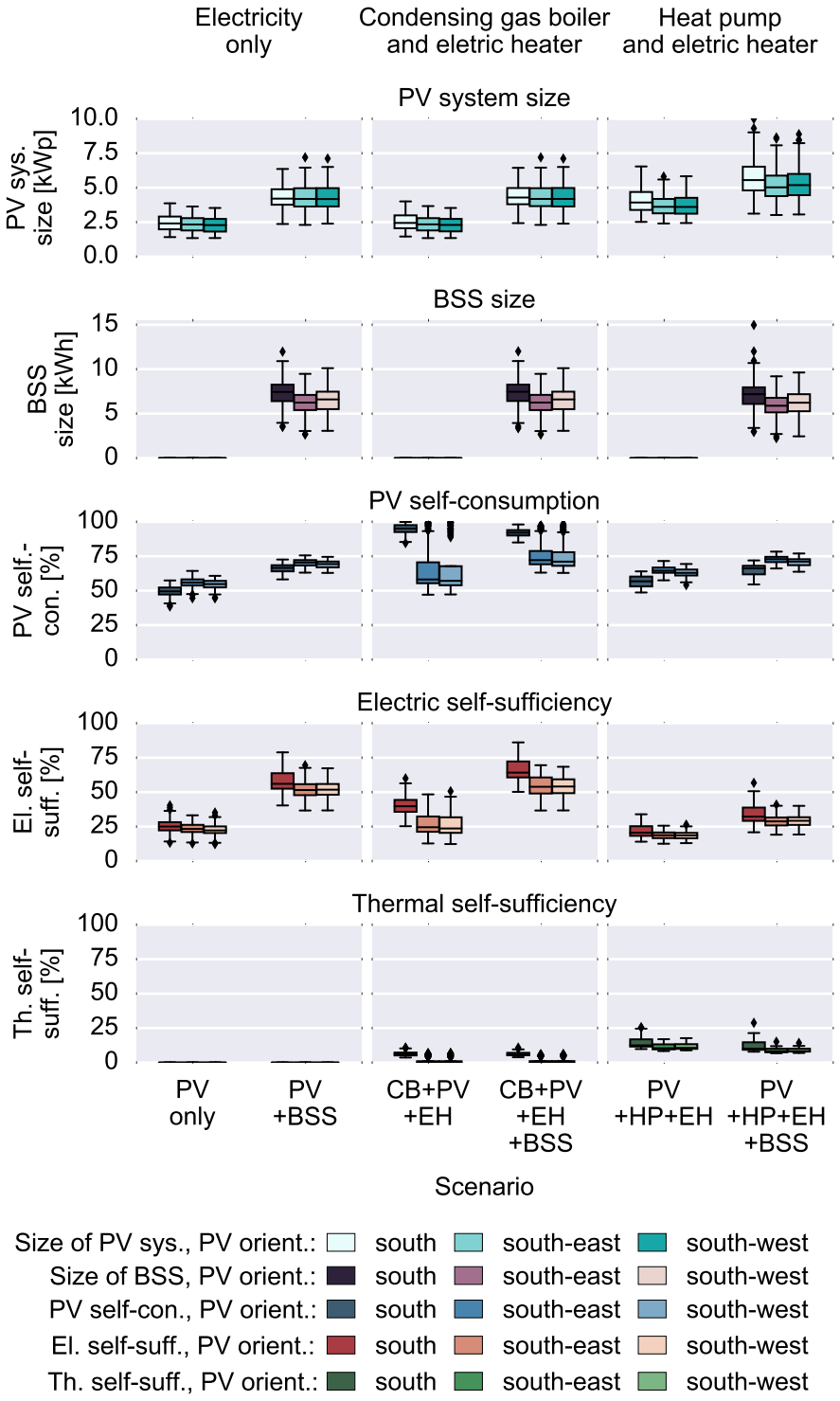

Figure 10.1: Results for PV system size (top), BSS size (top-middle), PV self-consumption (middle), electric self-sufficiency (middle-bottom) and thermal self-sufficiency (bottom) for different scenarios and PV system orientations for a yearly heat demand of 17.5 MWh.

guishable. Median PV system sizes vary from 3.6 kWp to 3.9 kWp without and from 5.0 kWp to 5.6 kWp with BSSs depending on PV system orientation. For the chosen heat demand, BSSs provide a better leverage than heat pumps, if only one additional component next to a PV system is installed. The median PV system size is slightly higher for scenario 'PV+BSS' with 4.2 kWp than for scenario 'PV+HP+EH' with 3.7 kWp. While median PV self-consumption remains at a similar high level with the increasing heat related electric load, self-sufficiency decreases significantly by over 30 %-points to 19.2 % compared to scenario 'PV+BSS'. Thermal self-sufficiency only reaches a median of 11.3 % for 'PV+HP+EH'. The largest PV system sizes are seen when BSS and heat pump are installed together. Here, median PV system sizes are more than twice as large with 5.3 kWp compared to scenario 'PV only'. Median BSS sizes are slightly smaller compared to scenario 'PV+BSS' with 6.4 kWh. The similarity in BSS sizes gives an indication that BSSs usually use PV energy during different seasons than heat pumps. It points towards a complementarity of BSS and heat pump.

Several first conclusions can be drawn. Median PV system sizes are significantly smaller when no BSS or heat pump are installed compared to current system sizes. Thus, the drop in PV system costs and rising electricity prices cannot compensate the significant decrease in remuneration of PV network feed-in. While BSSs as well as heat pumps offer a chance to partially offset this drop in value and stop the decrease in PV system sizes, the combination of both systems allows best capturing the rooftop potential and leads to the largest PV system sizes, which can reach current levels of PV system sizes. Sizing differences between HHs, locations and PV system orientation shrink to a thinner margin compared to today's systems. BSSs and heat pumps pave the way for tapping the potential of not optimally oriented PV systems, such as SEs and SWs. As PV systems combined with heat pump and BSS offer a higher value added than PV systems with just one additional flexibility, a general complementarity seems to be present. Furthermore, it is worth emphasizing that future marketing of PV systems has to focus on PV self-consumption rather than on self-sufficiency, as only BSSs allow for high self-sufficiency rates while the additional electric demand introduced through heat pumps cannot sufficiently be covered by local PV generation.

A sensitivity analysis in combination with an energy flow analysis supports the conclusion of a good complementarity between heat pumps and BSSs, but also indicates a limited coupling potential for direct BSS heat pump operation. While excess PV energy for heat pump operation is especially used in winter and transition days that still require some heat supply, excess PV energy can also be used for load shifting through the BSS during those days. BSS operation is highly beneficial during summer days, when nearly no heat demand is available and network supply can be significantly reduced. The load shifting potential is also not endless here as it is limited by the demand during the night. Overall, BSS operation provides a good alternative for load shifting and mid-to-long-term thermal storage possibil-

ities do not seem to be an attractive alternative. An additional important findings of the sensitivity analysis is that PV BSS sizing can drastically vary depending on the yearly heat demand and the used heat profile. VDI 4655 profiles that attribute less thermal demand to winter than the IWES profiles allow for a higher amount of heat pump operation using PV energy and result in larger sized PV systems. However, cost related parameters tend to have a more significant impact on PV BSS sizing, while overall energy supply costs are driven by thermal demand and prices of served energy (see Appendix C.2.1, C.2.2 and C.2.3).

Additionally, the installation of heat pumps mitigates distribution effects inflicted by current PV BSSs. Investors into such systems benefit from opting out of paying NC, taxes and other surcharges while still feeding large amounts of excess PV energy into the network. With heat pumps, high PV self-consumption is possible, while self-sufficiency remains at a low level. Self-accelerating processes as described in the previous part are likely to be stopped. However, an additional challenge arises. PV systems solely rely on the attractiveness of increasing self-consumption as PV network feed-in is nearly worthless, and benefit from increased self-supply triggered by rising electricity prices. The economic feasibility of heat pumps on the other hand relies on a low electricity price. A cost-benefit analysis of PV BSSs in combination with heat pumps and a comparison to a conventional heating system are necessary. Fig. 10.2 displays the mean discounted yearly costs for three different scenarios ('Condensing gas boiler and electric heater' (left), 'Heat pump and electric heater (Reference case)' (middle) and 'Heat pump and electric heater (full electricity price for heat)') and two different yearly heat demands (Reference case (top) and low heat demand (bottom)). The categorized costs include all operational costs for standard and heat supply as well as investment costs for PV and BSS.[5] Resulting differences can be used to determine max. allowed differences for investment costs of heating systems.

Condensing boilers in combination with PV BSSs lead to the lowest overall supply costs in all scenarios. Given that current investment costs for such systems are at the same level as heat pump systems or even lower (especially compared to heat sources other than air), an investment incentive would need to compensate the difference to foster power-heat coupling technologies. For the medium thermal load case, heat pumps with a reduced electricity price (Ref. case) lead to additional energy supply costs of 11.3 to 19.3 % compared to the equivalent system configuration with a conventional heating system. Overall costs with a PV BSS heat pump combination are actually lower than just a conventional heating system without a PV system, if no differences in investment costs exist between a condensing boiler and a heat pump. When a PV system or a PV BSS is installed, higher costs of approx. 4 k€ are seen. Such a difference could currently be compensated, since investment incentives of up to 4.5 k€ are available from

5 The corresponding KPIs are detailed in C.1.1.

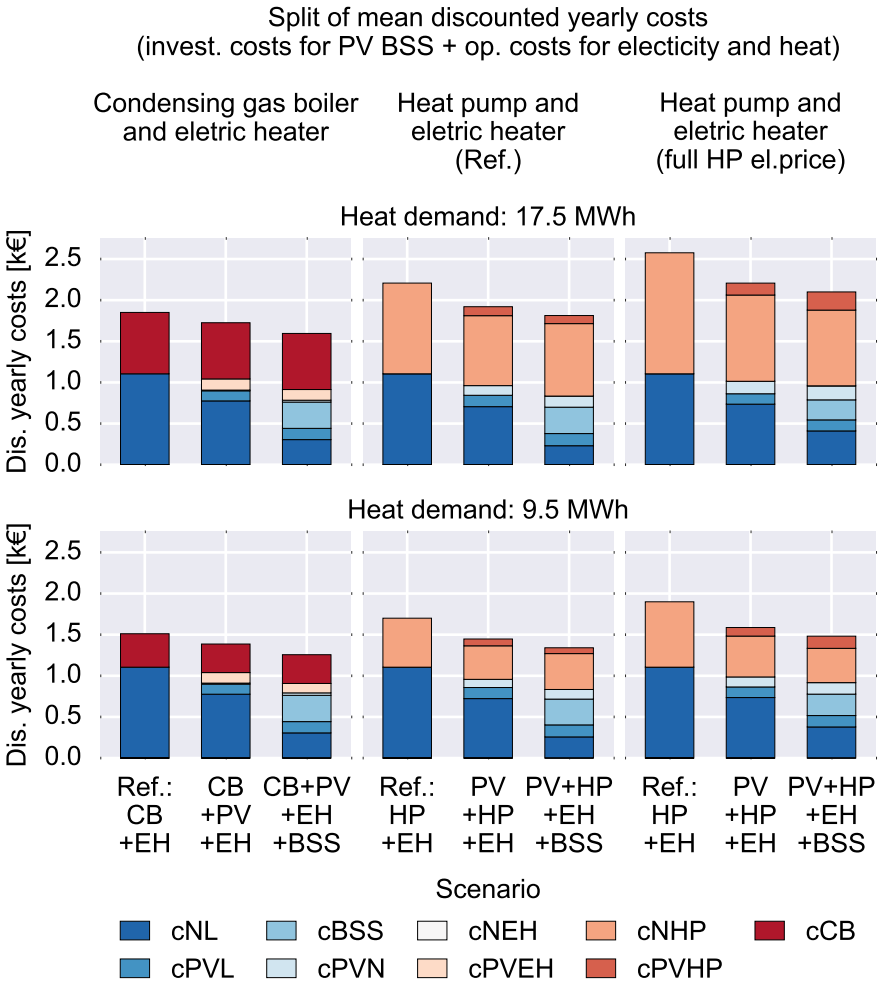

Figure 10.2: Mean yearly discounted costs for different system configurations ('Condensing gas boiler and electric heater' (left), 'Heat pump and electric heater (Ref. case)' (middle) and 'Heat pump and electric heater (full electricity price for heat)' (right)) and heat demand (Ref. case (top) and low heat demand (bottom)) (categorized according to different costs).

the German government for heat pump systems [143]. Yet, the already discounted electricity price for heat in combination with cheap self-supply cannot compete with natural gas prices. However, as natural gas consumption is only taxed with 0.4 ct/kWh, while HH electricity sees taxes of up to 10-12 ct/kWh [144]. A dramatic distortion of competition is observed. When a reduced electricity price for heat pumps is not available, costs increase by 28 to 39 %, with absolute differences of 10-15 k€. Even as PV systems and PV BSSs are able to reduce costs here, overall the costs seem too high for heat pumps to be an attractive alternative. This would require higher subsidies or an adjustment of taxes for natural gas. On the plus side, higher median PV system sizes are observed, leading to a better utilization of residential rooftop potential.

For a low yearly heat demand, a condensing boiler is still the option with the lowest energy supply costs, but its advantage over heat pumps shrinks to 6.7 % with a PV BSS and to 12.5 % for option without a PV BSS (instead of 13.6 to 19.3 % for a yearly heat demand of 17.5 MWh). Compared to just a boiler without PV system, a heat pump with a PV BSS even offers an advantage of 3.5 k€. In the same category, additional costs only amount to 1.2 to 1.7 k€. Even with full electricity prices for heat, mark-up costs remain in range of subsidy with 4 to 4.5 k€. As the pricing of electricity is different, a shift among cost categories is seen again. Costs related to network heat actually decrease when electricity for heating is priced equally to standard demand, since more PV energy is used for heat pump operation (which goes along with higher costs attributed to heat related PV energy). Additionally, higher costs are borne by standard demand as direct PV energy is used for heat pump operation instead of load supply. That can only be partially compensated by decreased costs for direct and indirect PV supply for standard demand. A trade-off between BSS and heat pump becomes visible: Decreased costs attributed to the BSS are outweighed by an increase in costs related to PV heat pump operation resulting from increased investment costs of larger sized PV systems.

In conclusion, it might be worth considering raising investment incentives for PV heat pump coupling and voiding reduced electricity prices instead. Such a measure would allow tapping into the full rooftop potential while shifting subsidies away from NC to taxes. It would partially compensate the inequality in taxation of natural gas and electricity, foster PV adoption and mitigate self-supply induced effects that could still only trigger investments into PV BSSs instead of PV BSSs in combination with heat pumps.

10.3.2 *Network integration of PV systems coupled with heat pumps and BSSs*

Reduced electricity prices are available for heat pumps on the condition that their operation can be blocked during certain hours. Yet, if this privilege is waived or higher amounts of installed heat pumps are seen, DNOs might consider a different tariff structure to ensure smooth network integration. From a DNO's perspective, several aspects need to be evaluated with regard to the impact on network integration when combining PV systems with heat pumps and BSSs. Heat pumps provide an additional flexibility that might assist PV network integration, but can also increase demand peaks. Such feed-in and demand peaks might, however, be mitigated in combination with a BSS. Previous analyses show that current PV BSSs lack an incentive for peak-oriented BSS charging. In the presented future scenario, remuneration of PV network feed-in is significantly lower than in the previous case studies and BSSs provide a leverage to allow for larger PV systems. Thus, the role of BSSs needs to be reassessed to determine if

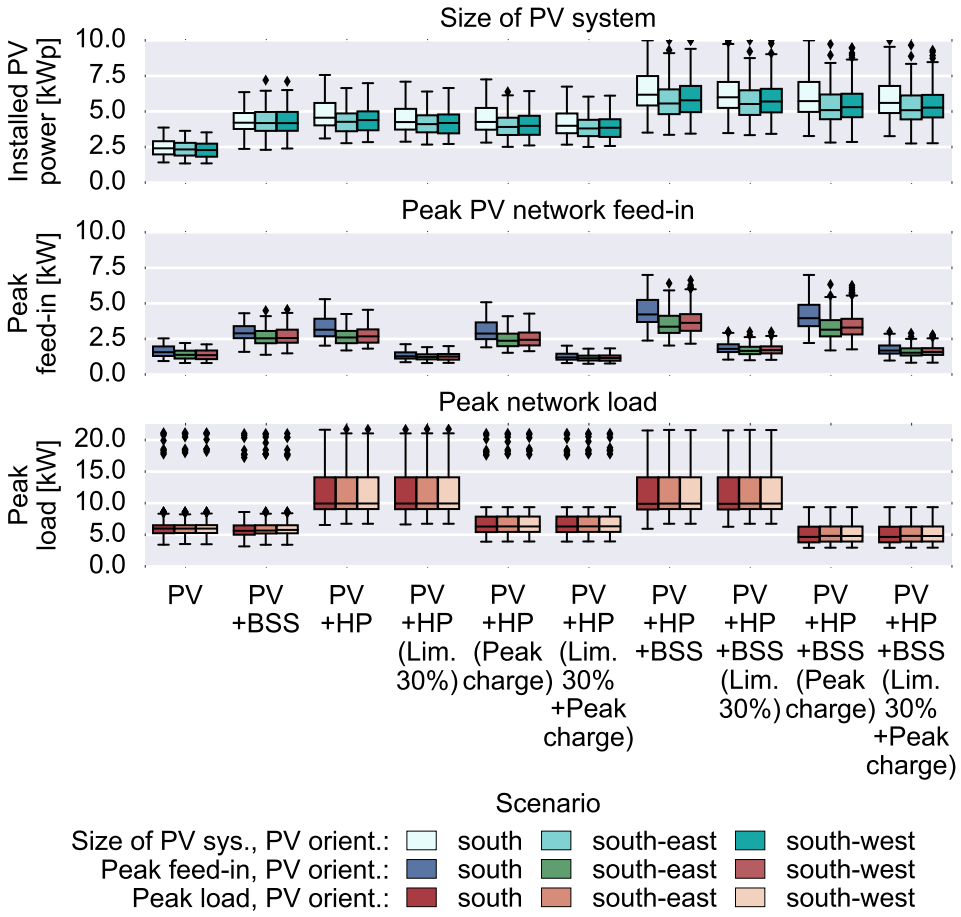

Figure 10.3: Peak integration analysis for different system configurations, PV system orientations and incentive systems (PV system sizes (top), peak PV feed-in (middle) and peak demand (bottom))

future PV BSSs provide a feed-in peak reduction as the dimensioning of PV BSSs changes.

Additionally, two incentives are examined that might provide operational incentives to adapt a peak reducing scheduling of BSS and heat pump. A scenario is simulated where the curtailment limit for PV network feed-in is lowered to 30 % of the installed PV capacity. The scenario is called 'Lim. 30%'. In scenario 'Peak charge', NCs are partially billed according to the yearly peak demand. A combination of both measures is displayed in 'Lim. 30%+Peak charge'.

Additional simulations are conducted for these two parameter variations for all scenarios involving thermal demand, 'PV+HP' and 'PV+HP+BSS'. In the following, only results with a yearly thermal demand of 15 kWh are evaluated. PV system sizes, peak PV network feed-in and peak network demand are displayed in box plot form for these scenarios and three different PV system orientations in Fig. 10.3. As reference scenarios only PV systems (scenario 'PV') and PV BSS (scenario 'PV+BSS') are displayed as well.

As pointed out in the previous analysis, the impact of PV system orientation diminishes when only PV systems are installed. PV system sizes are only slightly smaller for SEs and SWs for scenario 'PV' (with a median of 2.3 kWp) compared to SOs (with a median of 2.4 kWp). Peak PV feed-in shrinks in median to 1.4 to 1.6 kW for this scenario and decreases in importance compared to the yearly peak demand that lies at 6 kW (independent of system orientation). Given a higher PV simultaneity of around 85-90 % and a typical load simultaneity of around 40 % [80], peak loads would remain the relevant planning criteria for DNOs. Thus, PV network integration challenges related to local voltage problems are likely to not pose a high risk in this scenario.

This assessment needs to be reconsidered once BSSs and/or heat pumps are installed. As PV system sizes increase, so does the peak PV network feed-in. For scenario 'PV+BSS', median feed-in peaks rise to 2.5 to 2.9 kW and median demand peaks slightly decrease to 5.6 to 5.8 kW depending on PV system orientation. Furthermore, the impact of the PV curtailment limit at 70 % of the installed PV system size becomes visible again when comparing increase in PV system size (1.7 to 1.8 kWp) and rise peak PV network feed-in (1.1 to 1.3 kW) to scenario 'PV'. Here, the lower increase in peak feed-in is not a result of BSS operation, but of the PV curtailment threshold. Thus, the previous conclusion still stands that BSSs enable larger sized PV systems, but do not necessarily lead to smaller or similar peaks of PV feed-in.

Scenario 'PV+HP' leads to even larger sized PV systems and PV peaks increase to 2.6 to 3.1 kW. The marginal increase of PV feed-in per additional installed kWp remains at the same level as with BSSs. No additional benefit resulting from heat pump operation is observed for PV network integration. However, peak PV feed-in becomes less relevant when analyzing the increase in peak demand to 9.9 kW, which is 3 kW larger than for both previous scenarios. With no additional incentives to operate heat pumps in a network-friendly way, DNOs would have to reconsider current planning premises for peak demand.

Scenario 'PV+HP+BSS' underlines the previous conclusions. PV system sizes increase to a median of 6.2 kWp for SOs and 5.6 to 5.8 kWp for SEs and SWs. While the marginal peak PV feed-in per additional installed kWp slightly decreases to 0.68 kW/kWp compared to 0.72 kW/kWp for the previous scenarios, the peak increase is still significant. The combination of heat pumps and BSSs does not have a positive impact on PV network integration with regard to peak feed-in. A similar conclusion can be drawn for peak load. The peak load remains at the same level as for scenario 'PV+HP'. Thus, adding a BSS without an additional operational incentive does not result in lower peaks in this example.

Operational incentives need to be implemented to capture the given flexibility potential of BSSs and heat pumps in a network-friendly way. Thus, the impact of a further decrease of the PV curtailment threshold to 30 % as

well as the introduction of peak charges are evaluated for scenarios 'PV+HP' and 'PV+HP+BSS'.

A lower curtailment limit only results in a slight decrease in median PV system sizes by 0.0 to 0.3 kWp compared to a higher curtailment limit. PV peaks are successfully lowered to 1.2 to 1.3 kW for scenario 'PV+HP' and 1.7 to 1.8 kW for scenario 'PV+HP+BSS'. The reduction also results in an adjustment of BSS and heat pump operation, which only leads to median PV curtailment losses of 0.1 % and a minimal decrease in efficiency due to storage losses. Overall, the median overall energy costs of SOs only increase by 0.2 %. However, no improvement of peak demand is observed.

Peak charges impact the optimization decision in different ways. The mixture of energy- and power-based charges leads to slightly lower PV system sizes for both scenarios. The median PV system size only decreases up to 0.5 kWp to 5.7 kWp for SOs for scenario 'PV+HP+BSS'. As the energy-based component is 2 ct/kWh lower in these scenarios, the attractiveness of PV self-consumption decreases and load shifting using a BSS becomes less attractive. The incentive for oversizing a PV system to produce more PV energy for load shifting decreases. The reduction in PV system size goes along with a decrease of peak PV feed-in of 0.2 kW for scenario 'PV+HP+BSS'. A significant reduction is seen in peak demand. For scenario 'PV+HP', the median peak demand decreases to 6.3 kW, which is only 0.3 kW above the original peak without heat pumps and 3.6 kW lower compared to standard heat pump operation with no peak charges. Such a reduction is possible as heat pumps are operated more in partial-load mode. In combination with the different pricing system that leads to a median increase of overall energy costs by only 0.3 % for SOs. An even more significant reduction in peak demand is seen when installing a BSS. A median peak demand of 4.7 to 4.8 kW depending on PV system orientation is achieved, which is 1.2 to 1.3 kW below the original peak without heat pumps and 5.2 to 5.3 kW lower compared to the results without peak charges. Here, the BSS value becomes clearly visible as it assists in further reducing the peak.

A combination of both incentives leads only to a minor reduction of median PV system sizes to 4.0 kWp for SOs for scenario 'PV+HP' and to 5.6 kWp for SOs for scenario 'PV+HP+BSS'. Here, the BSS assists in limiting the reduction; the change in size is only 9 % with BSS compared to 12 % without BSS compared to the reference case. In both scenarios, peak PV feed-in and peak demand are successfully reduced to similar levels of each individual scenario. Thus, disadvantages of only addressing PV or heat pump network integration are successfully mitigated. Additionally, the median increase in overall energy costs is comparable to the peak charge scenario. Again, a BSS helps limiting the cost change and has a higher impact on peak demand.

Overall, it can be concluded that a higher penetration of heat pumps can shift the focus from peak PV feed-in back to peak demand. Without additional incentives, no additional benefits for a smoother PV and heat pump network integration are achieved, even when installing a BSS. Thus,

		Scenario					
		PV+HP			PV+HP+BSS		
		Full mod.	Mod. 100 %	Mod. 33 %	Full mod.	Mod. 100 %	Mod. 33 %
PV system size	kWp	4.7	4.7	4.9	6.0	5.8	6.2
BSS size	kWh	-	-	-	6.2	6.6	6.3
El. self-sufficiency	%	24.4	24.1	24.8	35.5	35.0	35.8
Th. self-sufficiency	%	18.5	10.1	16.8	22.4	15.7	19.9
PV self-consumption	%	50.6	52.7	50.1	59.4	62.7	58.8
Change in overall energy costs compared to case without PV	%	-10.6	-6.8	-10.1	-12.6	-10.2	-12.1

Table 10.2: Results for different modulation capabilities for median demand profile for location 4 for scenarios 'PV+HP' and 'PV+HP+BSS'

the flexibility of such systems remains unused. Peak charges and curtailment limits are effective measures that provide an operational incentive to level peaks while only leading to a slight reduction in system value and PV system size in this example. DNOs should adapt their network planning premises and restructure NCs to address increasing load simultaneity resulting from higher heat pump penetration. As ambient temperatures are one of the main drivers for heat pump operation and all HHs within one area see similar temperatures, the derived conclusion provides a good indication of upcoming network challenges.

10.3.3 *Impact of flexibility*

All previously presented case studies assumed a fully modulating heat pump. As current heat pumps are often not fully modulating and can only operate in partial-load mode or even only have an on-off-mode, an additional case study is performed to assess how missing flexibility impacts sizing and operation of future PV self-consumption systems. The case study also evaluates if BSS can be used to provide missing flexibility.

Three operation modes are compared: full modulation with continuous operation (just like in the previous case studies ('Full Mod.')), an on-off-behavior with only two states (0 %, 100 % of the installed heat pump capacity ('Mod. 100 %')) and a partial-load operation that allows four states (0 %, 33 %, 66 %, 100 % of the installed heat pump capacity (Mod. 33 %')). Binary variables are introduced depending on the number of states and following the modeling presented in section 9.2.3. The analysis is conducted using the median load profile with one PV profile at location 4. Tab. 10.2 displays the results for the case study for a case without and with a BSS.

In both cases without and with BSSs, PV system sizes are only minimally impacted as a result of missing flexibility. For 'PV+HP', no change in size is observed for 'Mod. 100 %', while partial-load capability leads to a slight oversizing of 4.4 %. However, missing flexibility results in significantly lower thermal self-sufficiency and increased PV self-consumption caused by increased usage of the flexible, but inefficient electric heater (see change in heat supply (light red area) in combination with PV energy usage (light blue area) in Fig. 10.4). That goes along with a loss of potential savings; energy supply costs are only reduced by 6.8 %-points compared to 10.6 % for 'Full Mod.'.

When a BSS is introduced, PV system sizes vary by ± 3.3 %. For 'Mod. 100 %', an increased BSS capacity helps balancing out missing heat pump flexibility. A higher amount of BSS heat pump operation is observed (compare change in heat supply by BSS energy used for heat pump (pastel area) in combination with increased PV BSS charging (light red area) in Fig. 10.4). Thus, BSS can facilitate inflexible heat pump operation, while ensuring that overall energy costs only change by 2.4 %-points (as the overall energy supply costs can only be reduced by 10.2 % for 'Mod. 100 %' compared to 12.6 % for 'Full Mod.'). If partial-load operation of the heat pump is possible, the benefit of the BSS is again switched to standard load shifting.

From a network integration perspective, inflexible heat pumps put additional stress on the network as they always operate at full power. While BSSs can help mitigating the heat pump induced peak, peaks remain at higher levels than for fully modulating heat pumps, since currently no incentives for peak-oriented operation are provided. If such an incentive is introduced through peak-oriented NCs, a fully modulating heat pump is able to reduce the peak load by 34.9 %. Inflexible heat pumps exceed the peak of the fully modulating heat pumps by up to 5.5 % without a BSS. With a BSS and peak charges, the peak demand is reduced by 36.3 % with a fully modulating heat pump. An inflexible heat pump operation cannot fully be compensated by a BSS; the peak reduction drops to 21.5 % (see C.2.4). Thus, fostering fully modulating heat pumps should be incentivized, possibly through an investment incentive.

10.4 *Conclusion*

Future residential PV systems in Germany face the challenge that the value of their network feed-in will be close to zero. Thus, PV self-consumption and possibilities to further increase it, such as BSSs, are likely to gain additional importance. However, other options for higher PV self-consumption, such as heat pumps, emerge and possibly pose a threat to the attractiveness of BSSs. Changing economic and operational incentives for residential PV systems are likely to impact PV network integration. Especially, since power-heat coupling might solve unwanted distribution effects related to self-supply systems, e.g. rising NCs.

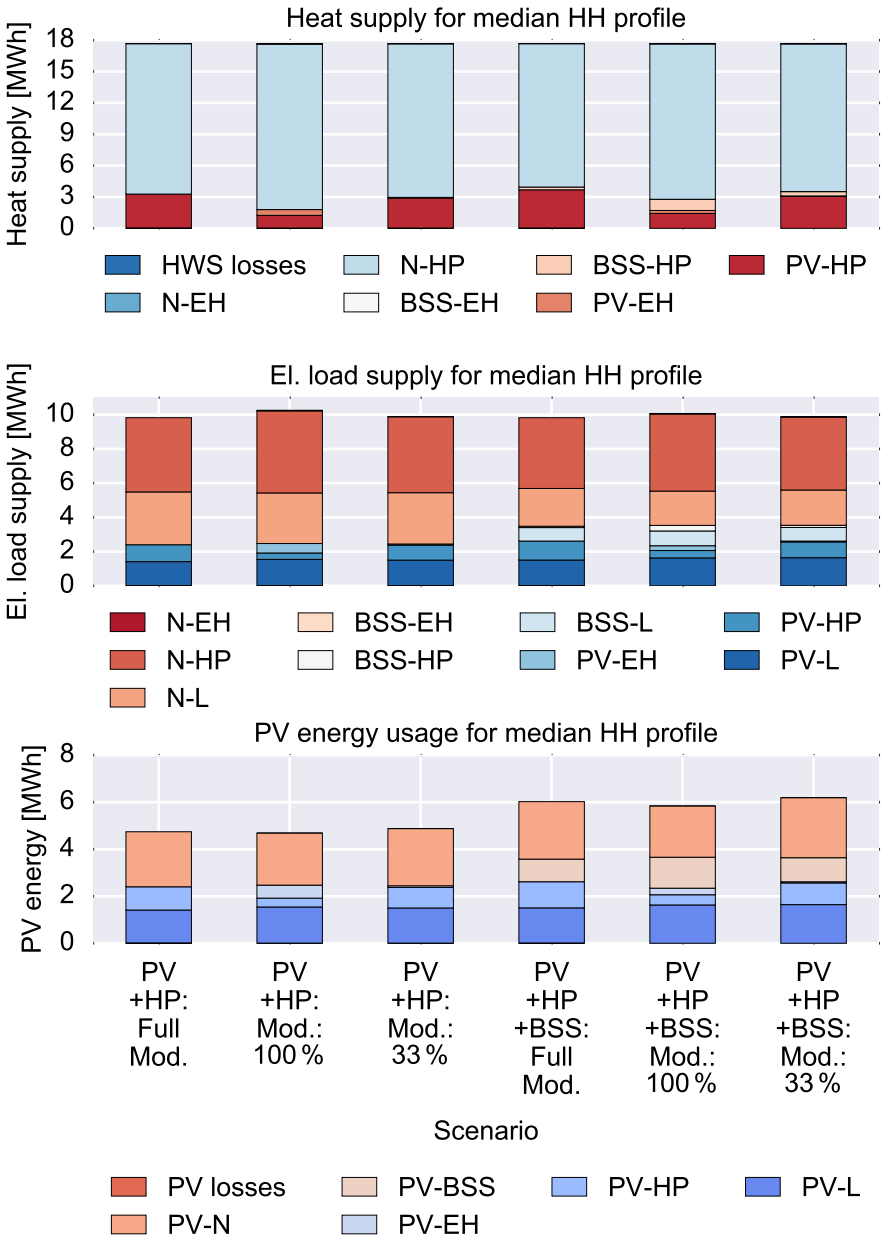

Figure 10.4: Distribution of energy flows to fulfill heat (top) and electric demand (middle) as well as usage of PV energy (bottom) for 'PV+HP' and 'PV+HP+BSS' for median HH profile

The section presents an adapted model that empowers different stakeholders to analyze interdependencies between decentralized power-heat-storage systems and tariff setting for improved sector coupling and network integration. The model is adjusted to efficiently integrate relevant techno-economic constraints, such as unit commitment constraints, to evaluate whether a competition or a complementarity is seen between different flexibility options.

The conducted case studies show that future PV systems require such shifting technologies to avoid leaving PV rooftop potential untapped. Fostering their adoption would be the next consequent step for a local energy transition. Especially, PV system sizes remain sensitive towards changes in cost related parameters, such as electricity price, ERR or FIT, while thermal parameters highly impact the overall cost-competitiveness of such a system. Seasonal differences in heat demand and PV generation drive PV heat pump operation and PV BSS operation. Overall, the analysis shows a good complementarity and only occasional competition between BSSs and heat pumps. However, BSSs are rarely used for heat pump operation, but might provide a benefit for the adoption of non-modulating heat pumps, which are unfavorable from a network integration perspective.

Future marketing of PV systems has to focus on PV self-consumption rather than on self-sufficiency as only BSSs allow for high self-sufficiency rates while additional electric demand introduced through heat pumps cannot sufficiently be covered by local PV generation. Such systems provide a solution for self-supply inflicted challenges, such as rising NCs, as heat pumps still largely rely on network supply. To foster a network-supporting adoption of heat pumps while also providing an incentive for PV systems, power charges should be introduced, feed-in limits could be adjusted, if required by the DNO, and higher investment incentives for heat pumps should be favored over a differentiation between electricity prices for standard and heat demand. The analysis shows that BSS and heat pump offer sufficient flexibility to adjust operation with such incentives without leading to significantly higher energy supply costs. A tariff or investment incentive-based framework that allows heat pumps to be an attractive economic alternative to conventional heating systems is not only crucial for decentralized sector coupling and increased demand flexibility, but also for a promising business case for future residential PV systems.

It has to be kept in mind that the presented analysis focuses on incentive systems that provide planning benefits for owners of decentralized power-heat-storage systems and DNOs. Such incentives do not necessarily foster a market-oriented operation of BSS and heat pump, since the static nature of max. yearly power and max. yearly PV peak depend on individual HH demand and feed-in rather than overall market or network situation. However, from a planning perspective, a framework is set that allows limiting the overall impact on the network by mitigating feed-in peaks and load simultaneity situations.

11

Outlook

Based on the contributions of this thesis, the following leads for further research are identified:

- Modeling and evaluating investor preferences as well as introducing further DERs present promising opportunities to improve outcomes and predictions on how decentralized RESs can contribute in a technically preferable and economically efficient way to create a fossil-fuel-free energy supply system. Next to further sector coupling options, such as e-mobility, additional factors influencing the investment decision, such as income, location, etc., are of high interest.

- While the current work covers uncertain parameter development by using a sensitivity analysis to assess the robustness of the results, stochastic optimization or a real-options approach could be implemented to further analyze the impact of uncertainty on system sizing.

- Model improvements might be possible by adapting the current model structure to reduce simulation times and facilitate even faster analyses. Such measures could be realized by using selected aggregated input data, e.g. type days that represent the entire year based on a limited number of data points, and adjusting the model parameterization accordingly.

- The DNO model could be further integrated in network planning. Rather than relying on abstract modeling of the network reinforcement problem, new interfaces to network planning tools, which are able to solve non-linear network integration problems, could be defined to ensure that the interdependencies between NC setting, network reinforcement, investment and operation decisions of decentralized power-heat-storage systems are properly reflected when choosing the cost-minimal network expansion solution. Further integration of an investor-focused perspective and corresponding bottom-up approaches in current network planning allow identifying potential PV growth areas at an early stage and adjusting network planning strategies accordingly.

- The utility perspective could be integrated into the bilevel model to derive optimal NC setting in combination with market-oriented end customer prices. Such an approach would allow evaluating the trade-offs of operating flexibilities in a market-oriented way and their contribution to local network problems. It would foster finding equilibrium

prices that ensure market- and network-supporting operation of decentralized power-heat-storage systems.

12

Conclusion

Residential PV systems change the electric power system as a whole. The business case of self-supply through PV self-consumption while still receiving FIT remuneration for network feed-in is changing consumption and supply network-wide. In countries such as Germany with high electricity prices for final customers, residential PV systems in combination with BSSs enjoy increasing popularity. Nowadays, nearly every second residential PV system is installed together with a BSS. The surge in investment is not only driven by rising electricity prices or decreasing PV BSS prices, but also fostered by a preference for self-sufficiency and an investment incentive program for PV BSSs. The program aims at addressing PV network integration challenges that are experienced with higher PV penetration rates. However, the business case for PV BSSs thrives on avoiding network consumption and paying NCs as well as other surcharges and taxes, while still feeding into the network and relying on the network for peak demand. Thus, this poses several challenges for DNOs: coping with a reduction of NCs, potentially higher costs as a result of PV network integration and a threat of contributing to a self-reinforcing process by raising NCs and triggering an additional self-sufficiency incentive. Besides BSSs, further flexibility options emerge for integrating PV systems in local energy systems, such as heat pumps.

Overall, the complexity of planning processes for all involved actors in residential PV systems increases. HHs face rising uncertainty for refinancing a system based on varying electricity prices and changing operational incentives for network integration. DNOs have to integrate differently sized PV systems in their mid-term network planning to avoid unnecessary network reinforcement and have to cope with losing NC revenue from PV BSSs as a result of increased self-supply. Regulators and policy makers have to balance out trade-offs between fostering decentralized PV system growth and setting incentives for increased network integration, while keeping electricity prices at low levels to allow for sector coupling and to mitigate unwanted welfare transfer among HHs with and without the ability to invest in residential PV systems with BSSs and heat pumps.

Thus, this thesis provides different optimization models for evaluating the dynamics between different investment, sizing and operation drivers of such systems from a HH investor's as well as a DNO's perspective and a case-study based approach to evaluate implications for other actors, such as policy makers, which in combination are the core contributions of this thesis. In three different parts the approach is adapted to analyze how different incentives and drivers impact decision making on the residential PV BSS investor level and on the DNO side.

- The first part focuses on interdependencies between investment drivers of PV BSSs, the desire to increase self-sufficiency, the investment incentive program for BSSs, new regulations concerning the smart meter rollout and PV BSS sizing and operation. A MILP model is developed and provides a good foundation for investor-focused analyses. Here, especially the adoption of self-sufficiency reflecting objectives, the implementation of the German investment incentives program and additional German regulatory and tax requirements differentiate the developed model from previously used models. It is shown that the chosen approach allows for an efficient integration of such new aspects, such as regulatory requirements. In combination with the developed KPIs and case studies, the approach provides an effective way to perform analyses for the key stakeholders. Optimal sizing and operation decisions that include such self-sufficiency aspects are then reflected on their improvement of PV network integration. Case studies have a short-term focus on analyzing the business case for PV BSSs in a present-day context.

- In the second part the optimization model is transformed from an open-loop to a closed-loop model to evaluate interactions between DNOs and PV BSS investors using a bilevel programming approach. The developed approach has the significant advantage that the DNO's problems, such as setting NCs and deciding on the optimal way to foster PV network integration, and corresponding sizing and operation decisions of PV BSS investors are merged into one optimization problem. The model provides a new characterization of stakeholder behavior and allows foreseeing and evaluating strategic decision making of the considered stakeholders. A MPPDC is formulated to guarantee that a stable equilibrium can be found. Using the optimization model and the case study results, the DNO is enabled to anticipate PV BSS investors' decisions and sets new NCs appropriately. DNOs and policy markers are empowered to choose effective measures to mitigate undesired effects of self-sufficiency systems, such as network defection, in a two-three year perspective and determine trade-offs between network reinforcement and PV curtailment with regard to fostering PV network integration of PV BSSs.

- The third part shifts the underlying scenario to a post fixed FIT era for residential PV systems, which is likely to be set in the early to mid 2020s. Assuming that the PV FIT is close to zero and refinancing a residential PV system heavily relies on self-supply, the investor-focused model is adapted to integrate new emerging flexibility options, here heat pumps, next to BSSs. Next to thermal related sizing and operational constraints, unit commitment constraints for heat pump operation are adopted. The model allows an efficient assessment whether such flexibilities compete over local PV generation, how flexibilities influence PV system sizing and what incentives foster network inte-

gration of such decentralized power-heat storage systems to facilitate sector coupling and network integration at the lowest level.

In summary, the developed models in combination with the case study framework compose an efficient approach for different stakeholders to anticipate strategic stakeholder behavior in a changing electric supply and consumption system with higher amounts of decentralized prosumer systems, such as PV BSSs:

- Investors are enabled to cope with increasing investment complexity decisions and to anticipate system sizes and operation decisions for a changing regulatory framework.
- DNOs are empowered to integrate PV BSSs in decision making on future NC setting and to consider corresponding effects on PV system sizes for their mid-term network planning.
- Policy makers are enabled to determine interdependencies between PV system sizing, sector coupling and PV network integration, when deciding on future incentives and tariff setting for decentralized power-heat-storage systems.

The main conclusions based on the case studies can be summarized as follows:

- BSSs allow for larger sized PV systems in certain cases and the investment incentive program facilitates their adoption. Especially, self-sufficiency desires drive larger PV system sizes. From a network integration perspective, the adoption of a BSS itself does not result in a lower peak feed-in compared to a PV system without a BSS. Imposing a lower feed-in limit through the investment incentive program helps mitigating such peaks in most, but not all cases. However, as the BSS allows for larger PV system sizes, the peak reduction resulting from the feed-in limit is lower than expected. Once such a program runs out, the operational incentive to limit PV network feed-in disappears, leaving potential for network-supporting BSS operation untapped. Yet, several regulatory requirements related to additional surcharges of PV self-consumption or the smart meter rollout in Germany impose sizing limits that could offset gains from self-sufficiency and investment incentive (see Part I of Fig. 12.1).
- The closed-loop dynamics behind self-sufficiency based investments in PV BSSs resulting in decreased NC revenues that can lead to higher NCs and eventually provide an additional incentive for larger sized PV BSSs are displayed in Part II of Fig. 12.1. The process is further reinforced as larger sized PV systems result in a higher peak of PV network feed-in and thus potentially require network reinforcements. Such reinforcements can lead to higher network costs, which contribute to an additional NC rise. Here, the analysis shows that a self-reinforcing tendency with higher NCs and larger PV BSSs is observed,

but DNO and PV BSSs reach a new NC equilibrium. The growth of system sizes is bounded by techno-economic limits as the marginal value of additional self-supply and the benefit resulting from PV BSSs decrease with higher NCs. It is shown that complete network defection is not a realistic scenario despite NC increases. Moreover, compared to PV curtailment by the DNO or network reinforcements, fixed feed-in limits and power-based NCs reduce oversizing of PV BSSs and provide an operational incentive for peak-oriented BSS operation. Additionally, it has to be highlighted that no benefit can be seen from adopting peak-charges that equally price peak feed-in next to load.

- To avoid their undersizing, future PV systems require additional storage and shifting options, once the FIT drops significantly. PV systems without BSSs or heat pumps face the challenge that a decreasing FIT cannot fully be compensated by higher PV self-consumption. In general, a complementarity between BSSs and heat pumps is observed, but BSSs are rarely used for heat pump operation. BSSs only provide a benefit for the adoption of inflexible heat pumps, which is not preferable for network integration. As heat pumps largely rely on network supply even with local PV supply, self-sufficiency induced problems related to a decrease in NC revenue can be mitigated and offset potential negative aspects of a larger PV BSS deployment (see Part III of Fig. 12.1). While both BSS and heat pump allow for larger sized PV systems and thus contribute to an increase of peak PV feed-in, implementing new tariff systems in combination with curtailment limits can efficiently improve network integration without leading to significantly higher energy supply costs. Establishing a tariff or investment incentive-based framework that allows heat pumps to be an attractive economic alternative to conventional heating systems is not important for sector coupling, but also for an attractive business case for residential PV systems.

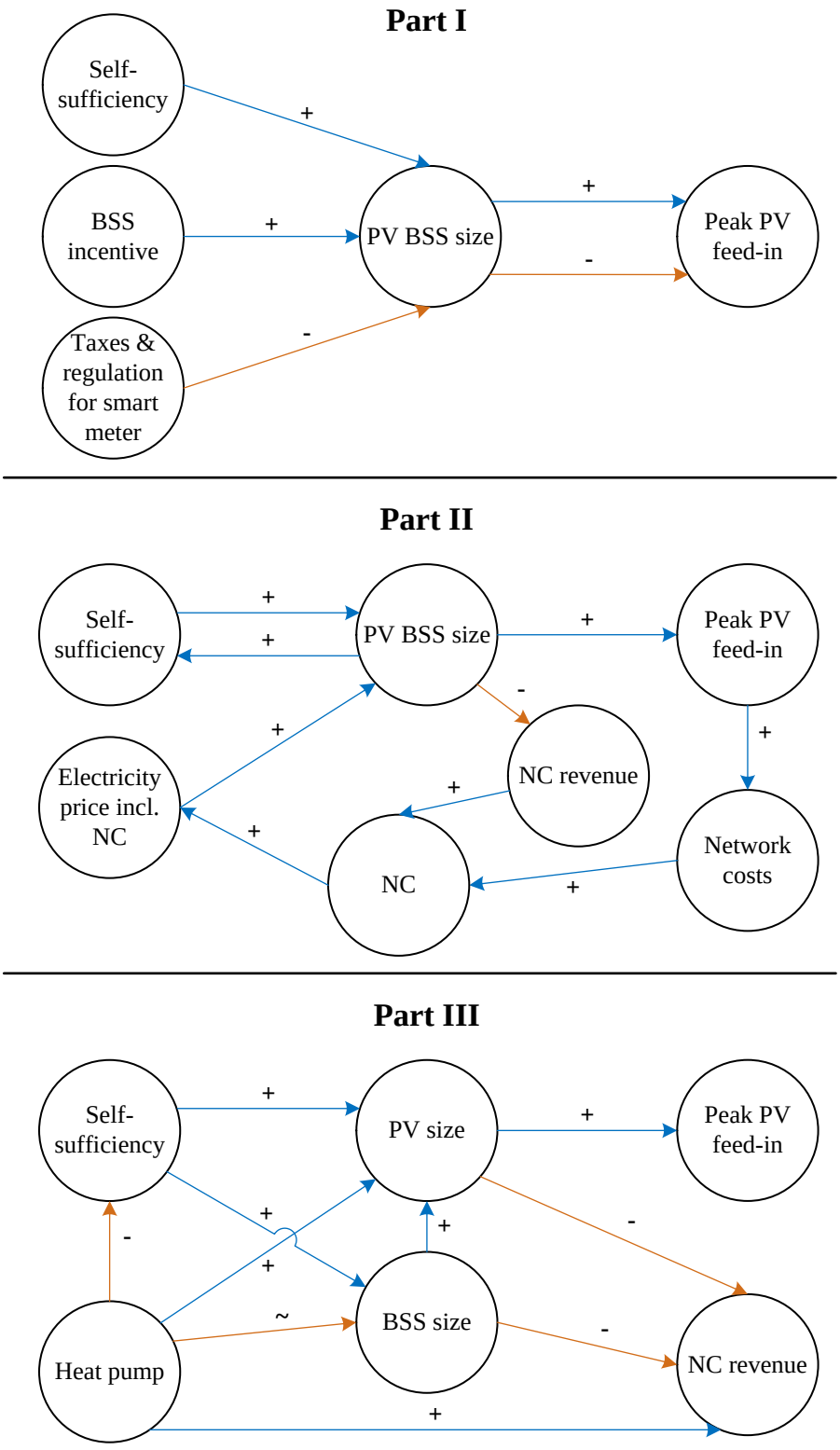

Figure 12.1: Identified dynamics and interdependencies for PV BSSs

Part IV

APPENDIX

A

Appendix for Part I

A.1 *Detailed information on input parameters*

All input parameters are derived based on detailed literature review and data analyses. This section provides the corresponding assumptions.[1]

A.1.1 *Electricity price*

Currently, ten different components constitute the German HH's electricity price, which are all subject to yearly changes. A HH with a yearly consumption of 3,500 kWh spends approx. 34.5 % of the electricity invoice on generation related price components. The average spot market price of 2016 accounts for approx. 10.9 % of the overall payments, the EEG surcharge, which refinances FIT payments for RESs, accounts for 22.1 %. NCs make up 24.3 % of the total costs. Taxes, such as a sales tax, an electricity tax, a concession surcharge and other surcharges and levies account for 30.3 % of the total costs. In average that leaves a 10.9 % margin for the electricity retailer. While uncertain developments as a result of a change in regulation and taxation are hard to predict, all price components related to the RES development are discussed in the following sections.

A.1.1.1 *Spot market price and EEG surcharge*

Over the past years, the increasing share of RESs produced electricity has tremendously impacted the spot market price. As RESs produce at marginal costs close to zero, they have pushed more expensive conventional power plants out of the market due to the merit order effect. A lower average spot market price currently goes along with a lower market value of RESs [145]. As the difference between average FIT and RES market value increases, the EEG surcharge also increases [146]. Additionally, commitments for the FIT payments have increased continuously over the last years, leading to an increase in the EEG surcharge.

A scenario for the development of the spot market price and EEG surcharge as well as RES growth is derived based on a tool developed by Agora Energiewende. Based on several key parameters, such as RES growth per RES type, average RES reimbursement value, spot market price and overall electricity demand, the evolution of the EEG surcharge can be calculated [147]. Additionally, the yearly FIT drop-out rate of RESs is highly relevant for the development of the EEG surcharge (from 2025 to 2035 over 38 GWp

1 Parts of this chapter are presented in [25].

Parameter	Scenario		
	Ref.	Min	Max
Yearly PV growth (from 2020)	2.5 GWp/a	1.5 GWp/a	4.5 GWp/a
PV reimbursement (in 2035)	8.6 ct./kWh	9.9 ct./kWh	7.0 ct./kWh
Spot market price	2.5 ct./kWh	6.0 ct./kWh	1.5 ct./kWh

Table A.1: Main input parameters to calculate EEG surcharge development

of PV systems fall out of high fixed FIT payments). The drop-out of older systems and the reduced FIT for newer PV systems will reduce EEG payments related to PV systems from 9.6 billion € in 2025 over 6.8 billion € in 2030 to 2.6 billion € in 2035 (for the ref. scenario) [147]. Thus, the overall EEG surcharge will also decrease once a peak is surpassed in the mid-2020s.

To derive possible EEG surcharge developments, three scenarios are calculated using the described tool with assumptions presented in Tab. A.1.

RES growth rates are chosen according to the suggested values by the Agora scenarios 'Reference (Ref.)', 'Low' and 'High'. For the 'Ref.' scenario, the yearly PV installation rate reflects the current target corridor of the German government of 2.5 GWp. The 'Max' scenario assumes a persistence of the low PV installation rates seen in 2015 and 2016. The 'Min' scenario marks a return to higher installation rates, which were last seen during the boom years of PV between 2008 and 2013 in Germany. The current EEG foresees an automatic adjustment of PV FITs depending on the installation rate over the past months; a higher PV installation rate results in a faster reduction of FITs. The same logic is applied to set the reimbursement parameter for the 'Min' scenario; a low PV growth rate results in higher reimbursements per kWh. Moreover, higher amounts of installed RESs are likely to reduce spot market prices. For the 'Min' scenario, lower RES installation rates and higher reimbursements are combined with a higher spot market price. The resulting price developments are displayed in Fig. A.1.

For all three scenarios, the combination of spot market prices (here: procurement), sales and EEG surcharge increases until 2022 and then slowly decreases as a result of the effects described above. Overall, higher spot market prices and higher reimbursement rates offset each other. Future price increases are more likely to stem from other components.

A.1.1.2 *Network charges*

The main source of variance between scenarios are NCs. A NC bandwidth is influenced by several factors. Over 800 DNOs serve the German HHs with 800 different NCs. When analyzing the biggest 30 DNOs that serve rural and suburban areas as well as the DNOs that serve the bigger cities, several trends can be distinguished. Bigger German cities and the western German

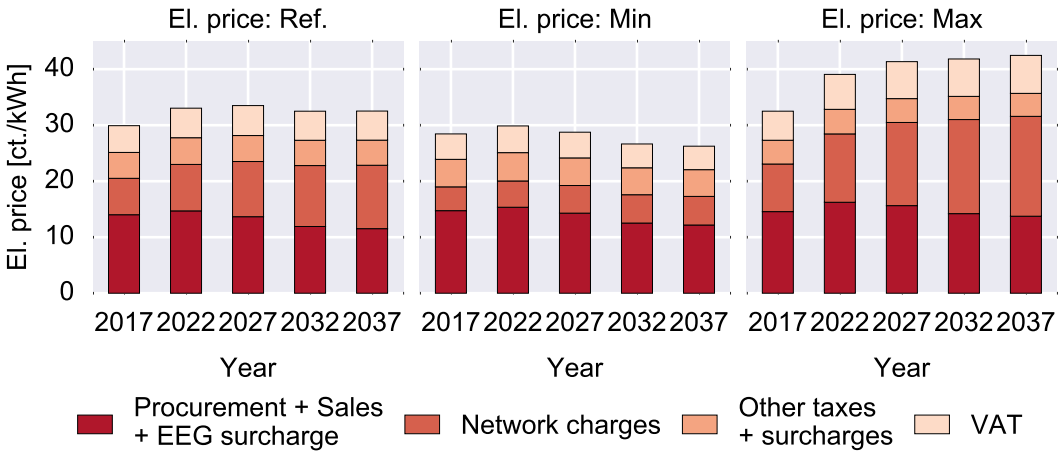

Figure A.1: Electricity price forecast for different scenarios for HHs (inflation-adjusted)

states typically have the lowest NCs, while in rural areas in the northern and eastern parts of Germany the highest NCs occur. This is mainly a result of population density and wind power penetration in the serviced areas. In the southern German parts where typically a high PV penetration is seen, NCs are at a moderate level [148].

Additional trends become visible when analyzing NC development over the last four years for the 30 largest regional DNOs (see Fig. 5.1). While the median overall change was moderate from to 2014 to 2016, an increase by 14 % is observed from 2016 to 2017. Increasing differences between energy-based and total NCs indicate a paradigm shift as more DNOs move towards higher yearly fixed fees. While fixed fees used to account for 13 % of the total paid NCs, they nearly doubled to 22 % in 2017 for the analyzed DNOs.

Forecasts predict that transmission and distribution network investments are likely to result in an increase of NCs by 25 % for HHs until 2022 from 2015 onward [86]. To capture the bandwidth of possible rises and regional differences, it is assumed that NCs increase from 2 to 7.5 %/a for the next five years and then decrease to account for the effect that a majority of network investments happen over the next ten years to adopt higher amounts of RESs (see Fig. A.1). Today's mean NCs in combination with a mean increase of 3.0 %/a are used as a base line. This is lower than the increase seen over the last year, but 0.3 %-points higher than the median increase since 2010 [149]. For the other scenarios, the lower and the upper whisker values are chosen as current NCs. For the 'Max' scenario, a yearly mean rise of 4.0 %/a is chosen, which more than doubles current energy-based NCs from 8.5 to 18.1 ct./kWh over 20 a. For the 'Min' scenario, a yearly rise of 1.0 %/a is chosen, which only leads to an increase of 21 % of energy-based NCs over 20 a. Such a scenario would assume that DNOs only increase energy-based billing moderately and a change in regulation would limit the NC increase. Such changes can result from a unification of NCs across all transmission system operators or a further decrease of the regulated rate of

return for DNOs. The scenario bandwidth depicts the uncertainty of NC development. For example, it is suggested that an overall increase between 4 % and 30 % depending on the region and the RES growth scenario is possible [13]. Yet, recent studies indicate that adopting an appropriate mix of different measures to mitigate or avoid network reinforcements can decrease the RES related costs significantly. Overall network integration costs can only be reduced by 10 % and 20 % when smart grid technologies are used instead of conventional network reinforcements [13]. Other authors suggest a higher cost reduction potential when using a network-by-network analysis approach. Here, only a small fraction of networks need reinforcements and costs can be reduced by 90 % for LV and MV networks when implementing a mix of OLTC transformers and reactive power provision [12, 150].

The resulting NC developments are displayed as pale red areas in Fig. A.1. Overall, the increase in NC surpasses the reduction in EEG surcharge and spot market prices for the 'Ref' and the 'Max' scenario when comparing costs in 2017 to 2036. For the 'Min' scenario, the decline of EEG surcharge and spot market price compensate the NC increase.

A.1.1.3 *Other electricity price components*

Concession surcharges vary depending on the inhabitant size of the end customer's city or village. A higher number of inhabitants leads to a higher concession surcharge. As pointed out above, higher NCs are typically seen in rural areas. Thus, it is assumed that a lower concession scenario goes along with higher NCs in scenario 'Max', and vice versa. For the ref. scenario, the current mean concession surcharge is assumed. As these surcharges have not been adjusted over the last 20 a, it is assumed that they are only adjusted to inflation in the future [149].

The CHP surcharge for scenario 'Max' is assumed to marginally increase until 2030 and decrease afterwards. For the 'Min' scenario, a reduction to zero is assumed until 2025. The 'Ref' scenario uses the mean of both other scenarios [21]. All other components remain at present day level and are only inflation adjusted. The value added tax (VAT) varies with the sum of all other components, since it is calculated as percentage value. The resulting development is displayed in Fig. A.1.

A.1.2 *PV development and feed-in tariff*

For residential PV systems, the current EEG guarantees fixed payments for the next 20 a. Depending on the system size, the current FIT varies depending on the system size, e.g. 12.30 ct./kWh for PV systems smaller or equal to 10 kWp and 11.96 ct./kWh for PV systems smaller or equal to 40 kWp. To react dynamically to PV installation rates, a control mechanism to increase or decrease the FIT has been introduced with the EEG 2014. As a baseline the FIT declines on a monthly basis by 0.5 %. Four times a year, the monthly rate of change is adapted depending on the PV installation rate

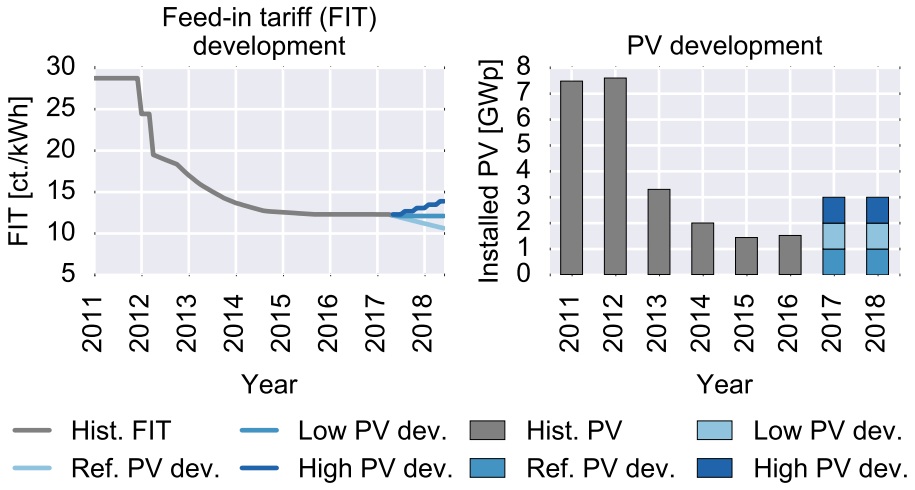

Figure A.2: Historical development and forecast of feed-in tariff for PV systems under 10 kWp (left) and of PV installation rate for three different scenarios in Germany (right)

of the previous six months. For example, if the yearly adjusted installation rate of the past six months drops below 2.1 GWp/a, the monthly reduction is paused for the next three months. If it drops below 1.7 or 1.3 GWp/a, a one-time increase by 1.5 or 3.0 % is implemented. The reduction rate can be increased to 2.8 % per month, if PV installation rates return to historic yearly peak installation rates of 7.5 GWp/a.

For the presented case studies, PV installation rates are predicted to derive a FIT bandwidth for 2017 and 2018. To forecast the PV installation rate over this period, historic PV developments and the current regulation are taken into account. Fig. A.2 displays the historic FIT development (left, grey) and the historic PV installation rates (right, grey).

PV installation rates peaked in Germany in 2012 and have decreased until 2015; since then they have stagnated around 1.5 GWp/a. The driving force behind the decline in PV installation rates has been the FIT reduction. Moreover, new restrictions on large-scale PV parks caused a sharp decline of installation rates of PV systems above 1 MWp. Currently, non-building PV systems are limited to a yearly installation rate of 600 MWp.

While the PV installation rate in 2016 was only slightly above the one in 2015, a surge in installations was observed in Dec. 2016, leading to annualized installation of approx. 2 GWp. For the ref. scenario, it is assumed that such a yearly growth persists and is evenly distributed over all 12 months. In consequence, the FIT is first slightly reduced by 0.5 % for three months. Afterwards, the annualized PV growth drops below 2.1 GWp and the FIT reduction rate is set to zero. For the 'Min' scenario, a low PV installation rate of 1 GWp/a is presumed. Compared to the ref. scenario, the FIT decrease is already set to zero in May 2017 and increases then once a quarter by 3.0 %, since the annualized installation rate is below 1.3 GWp/a. For the 'Max' scenario, a yearly installation rate of 3 GWp is assumed. Such a rate results in

a continuous monthly FIT reduction of 1.0 %. The different developments are displayed in Fig. A.2.

By mid 2018, the FIT reaches 13.89 ct./kWh (10.63 ct./kWh) for scenario 'Min' ('Max'), while the FIT for the ref. scenario only changes by 0.19 ct./kWh to 12.11 ct./kWh compared to its value in Jan. 2017.

A.1.3 *Additional main input parameters*

Next to electricity prices and FIT, PV system and BSS prices, ERR as well as technical parameters are of high importance. Moreover, previous analyses indicate that the HH and the PV profile influence PV BSS sizing [5, 11].

A.1.3.1 *PV system costs and parameters*

PV system costs have dropped over 60 % over the last 10 a [151, 152]. While average prices for small-scale PV systems were around 1,500 €/kWp in 2016, min. and max. prices varied from 1,350 to 1,700 €/kWp for PV systems under 15 kWp. Downwards price pressure continues as further cost reductions are expected with a growing worldwide PV market [133]. For the case studies, mean prices of 1,300 €/kWp for 2017 and 1,200 €/kWp for 2018 are used. One-time fixed costs of 1,000 € are assumed. As yearly costs, e.g. costs for maintenance and insurance, 2 % of variable costs are assumed [22].

A system life time of 20 a is expected. As PV modules typically tend to last longer (approx. 25 a), while the inverter might need to be replaced after 15 a [133], it is assumed that potential positive revenues after 20 a offset replacement costs for the inverter, stand-by losses from the PV systems and dismantling costs at the end of the lifetime.

A yearly PV system degradation η^{PVDeg} of 0.5 % is used. As the optimization is based on a one-year-period simulation, the PV input profile E_t^{PVorg} is reduced by the mean time-adjusted degradation over the system's lifetime (which is equivalent to the calculation period $\mathcal{A}$):

$$\forall t \in \mathcal{T}: \quad E_t^{PV} = E_t^{PVorg} \cdot \frac{\sum\limits_{a \in \mathcal{A}} (1-\eta^{PVDeg})^a \cdot (1+ERR)^{-a}}{\sum\limits_{a \in \mathcal{A}} (1+ERR)^{-a}} \tag{A.1}$$

ERR describes the expected rate of return of the investor.

A.1.3.2 *BSS costs and parameters*

BSS costs have seen yearly price reduction rates of 20 % over the last couple of years [7, 152, 153]. The market entrance of several big players from the automotive industry has driven the prices even further down. Tesla sells its new 13.5 kWh Powerwall battery for 7,000 $, or 519 $/kWh (usable capacity) [154], which is significantly less than the 1,000 to 1,400 €/kWh, which were mean system prices end of 2015 [84]. The prices are hard to compare as

it is often unclear whether costs include all BSS components (cells, battery monitoring system, converters and installation costs). Here, a component-specific differentiation is used that depends on installed component sizes as well as one-time installation costs. For the BSS capacity price ranges of 450 to 750 €/kWh for 2017 and 400 to 600€/kWh for 2018 are chosen. For the BSS inverter, lower end market prices between 250 to 350 €/kW for 2017 and 200 to 300 €/kW for 2018 are used. One-time installation costs range from 0 to 500 €/kW in both years. Depending on configuration and size, average costs lie around 800 €/kWh for 2017 and 675 €/kWh for 2018 (with an inverter to capacity ratio of one-to-two for a 5 kWh system). Such prices are in-line with a continued yearly price decline of approx. 20 % for mean system costs.

To ensure a long BSS lifetime, the depth-of-discharge (DOD) is limited and only the so called usable capacity $\kappa^{BSSUcorg}$ is available for charging and discharging. For Lithium-Ion BSSs, the usable capacity is set to 80 % of the installed capacity [78, 155]. With such a usable BSS capacity, average prices are around 1,000 €/kWh for 2017 and 844 €/kWh for 2018. A cycling constraint ensures a sufficient BSS lifetime. 5,000 to 10,000 cycles are typically promised for systems that last 10 to 20 a [156]. Here, a best-case scenario with a BSS lifetime of 20 a and 7,500 cycles is assumed.

As BSS aging also impacts the BSS capacity, $\kappa^{BSSUcorg}$ is adjusted using the aging factor η^{BSSDeg} to determine a mean usable capacity κ^{BSSUc}:

$$\kappa^{BSSUc} = \kappa^{BSSUcorg} \cdot \frac{\sum_{a \in \mathcal{A}} (1 - \eta^{BSSDeg})^a \cdot (1 + ERR)^{-a}}{\sum_{a \in \mathcal{A}} (1 + ERR)^{-a}} \tag{A.2}$$

The aging factor is chosen so that the BSS capacity is reduced to 80 % of the original BSS capacity by end of lifetime [10].

Charging and discharging efficiencies are set at 92.5 %. A self-discharge of 2 % per month is chosen. These values are lower than the typical values found on data sheets, which range from 95 to 98 % for one-way efficiencies [154, 157]. However, these values assume an optimal point of operation and do not sufficiently account for BSS operation in non-optimal set-points [84, 158]; thus assuming a round-trip of approx. 85 % is justifiable.

The height of the receivable subsidy from the BSS investment incentive program is adjusted twice a year. Overall, the program runs out in mid-2018. The current program started with 25 % in 2016. Over the course of the next 1.5 a it will drop from 19 to 13 % [159]. However, only limited funds are available each half-year. Thus, investors face the thread of receiving no subsidy, which is used as input for the 'Min' scenario.

A.1.3.3 *Expected rate of return and inflation*

The ERR quantifies the investor's desired return on the investment and is used as discount rate in the model. The rate needs to account for debt

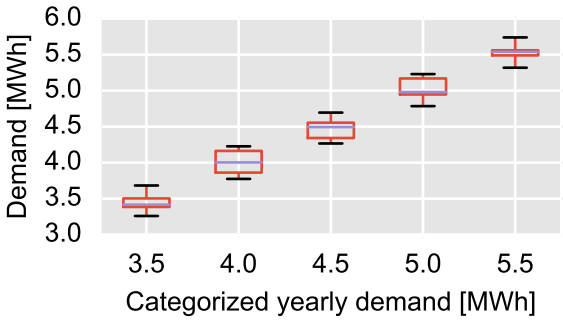

Figure A.3: Yearly demand of the simulated 48 HHs

related costs, e.g. interest, or the expected return on used equity. If debt and equity capital are mixed, usually weighted average capital costs are calculated. This differentiation is neglected here. It is assumed that only equity is used; thus debt-related cash flows are excluded. A mark-up is included to reflect the investment risk. A typical risk-free investment is a German government bond 'Bund', which serves as an orientation for the min. discount rate. Long-running bonds over 20 a, currently offer a rate of return of less than 1 % [160]. To account for the current investor's dilemma that even junk bonds do not offer more than 5-7 %, a mark-up between 0.5 and 3.5 % is sufficient. Hence, an ERR of 3 % is chosen for the ref. scenario, which is varied by ±1.5 %-points for the other scenarios.

While all cost parameters are presented as actual values, the FIT requires inflation-adjustment, since it is locked-in with the investment decision and paid in nominal values. As a reference inflation 1 % is chosen. For the other scenarios, a variation of ±1 %-points is used.

A.1.3.4 *Load profiles*

The business case for PV BSSs is assessed using individual HH profiles and not average SLP. Here, a data set is used that includes over 70 different measured and slightly synthesized HH profiles [161]. As typical HHs with the ability to invest into a PV BSS, profiles with a yearly demand of 3.25 - 5.75 MWh are chosen. Their yearly load consumption is categorized in 0.5 MWh-steps and displayed in Fig. A.3.

A.1.3.5 *PV profiles*

12 different nominated PV time-series with a 15 min time step resolution are used, varying in location (North-, East-, South- and West-Germany) and system orientation (30 ° orientation angle for south, south-east and south-west for each location), as shown in Tab. A.2. The data is based on 2009.

The produced energy varies from 818 to 1,130 kWh/kWp depending on location and orientation (average: 910 kWh/kWp).

To analyze the impact of the simulation time resolution, an additional south-oriented PV time-series from Kassel is used, which is based on 15 sec

Location	State	Orientation	Yearly produced energy [kWh/kWp]
Wolfratshausen (1)	Bavaria	south	1,130
		south-west	843
		south-east	848
Altenburg (2)	Saxony-Anhalt	south	932
		south-west	827
		south-east	840
Leverkusen (3)	North Rhine-Westphalia	south	932
		south-west	818
		south-east	842
Kiel (4)	Schleswig-Holstein	south	1048
		south-west	926
		south-east	936

Table A.2: Nominated PV energy for different locations in Germany

DC power measurements. The time-resolution is adjusted to 1 min, 5 min, 10 min, 15 min and 1 h time steps through averaging and transformed to AC values using an inverter efficiency of 95.6 %, as described in [162–164]. The AC profile results in a yearly produced energy of 940 kWh/kWp.

A.1.3.6 *Summary of input data*

Tab. A.3 summarizes the parameters described in the sections above.

A.2 *Additional case study results*

A.2.1 *Economic assessment of PV BSSs for reference scenario*

The first analysis evaluates the economic attractiveness of PV systems and BSSs for the reference scenario 2017 and 2018. A full cost-benefit focus is assumed (meaning the chosen system delivers the highest net present value (NPV) and the weights in the objective function are chosen accordingly ($W^{Npv} = 1$)). Potential costs and restrictions related to the currently uncertain smart meter rollout in Germany are neglected in this case study. Fig. A.4 displays the results for the ref. scenario according to categorized yearly load consumption and to PV system orientation.

It becomes visible how PV sizing depends on the underlying demand and PV system orientation. In 2017, the median installed PV size varies between 4.1 kWp for HHs with a yearly demand around 3.5 MWh and 6.5 kWp for HHs with a demand around 5.5 MWh for SOs. A higher demand results in an increased self-sufficiency, which ranges from 31.7 % to 35.8 %, and justifies larger PV sizes. The benefits are two-fold: a reduction of network

Parameter		Unit	Year					
			2017			2018		
			Scenario					
			Min	Ref.	Max	Min	Ref.	Max
System	S^{PV}	kWp	16.7					
	$A^{[PV,BSS]}$	a	20					
	η^{PVDeg}	%/a	0.5					
	κ^{PVLim}	%	70					
	S^{BSSkW}	kW	16.7					
	S^{BSSkWh}	kWh	25					
	$\eta^{[BSSCh,BSSDis]}$	%	92.5					
	η^{BSSSd}	%/mo.	2					
	$\kappa^{BSSUcorg}$	%	80					
	η^{BSSDeg}	%/a	1.1					
	κ^{BSSCyc}	no.	7,500					
	κ^{IncLim}	%	50					
Cost & revenue	I^{PV}	€/kWp	1,200	1,300	1,400	1,100	1,200	1,300
	In^{PV}	€	500	1,000	1,500	500	1,000	1,500
	M^{PV}	€/(a·kWp)	$2\,\% \cdot S^{PV}$					
	C^{Fit1}	ct/kWh	12.68	12.30	11.8	13.89	12.11	10.63
	C^{Fit2}	ct/kWh	12.33	11.96	11.47	13.11	11.78	10.56
	I^{BSSkWh}	€/kWh	450	600	750	400	500	600
	I^{BSSkW}	€/kW	250	300	350	200	250	300
	In^{BSS}	€	0	250	500	0	250	500
	M^{BSSkWh}	€/(a·kWh)	$1\,\% \cdot S^{BSSkWh}$					
	M^{BSSkW}	€/(a·kW)	$1\,\% \cdot S^{BSSkW}$					
	C^{E}	ct/kWh	28.0	33.0	40.0	28.0	33.0	40.0
	C^{Sc1}	ct/kWh	$19\,\% \cdot C^{E}$					
	C^{Sc2}	ct/kWh	40 %·6.0					
	Sub^{BSS}	%	0	19	30	0	13	25
Other	ERR	%	1.5	3.0	4.5	1.5	3.0	4.5
	$W^{[Npv,Self]}$	%	0 - 100					
	$\mathcal{T}$	-	1h: 1..8,760, 15 min: 1..35,040, 10 min: 1..52,560, 5 min: 1..105,120, 1 min: 1..525,600					

Table A.3: Input parameters for the different scenarios

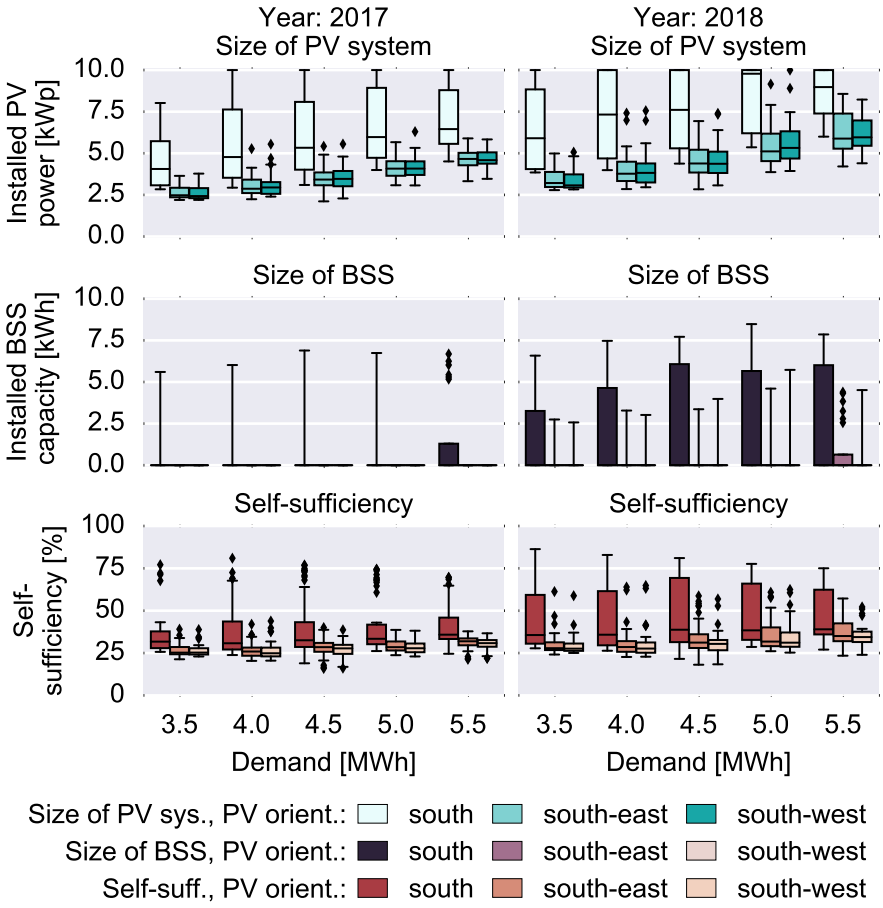

Figure A.4: Results for the reference scenario (according to yearly demand and orientation of PV system): size of PV system (top), size of BSS (middle) and self-sufficiency (bottom) for 2017 (left) and 2018 (right)

demand, which goes along with a higher margin of every self-supplied kWh, and an increased PV self-consumption, which decreases subsidizing PV network feed-in. For SEs and SWs, median PV sizes only range from 2.4 kWp to 4.7 kWp for the different load categories. While SEs and SWs reach higher percentages of PV self-consumption, ranging from 42.0 % to 45.6 % (compared to 34.3 % to 35.7 % for SOs), self-sufficiency levels only reach up to 32.0 %. Differences between SOs and SEs or SWs are a result of a better cost ratio of produced energy per installed kWp, leading to lower generation costs despite higher self-consumption ratios for SEs and SWs.

Compared to 2017, the median PV size rises from 5.3 kWp to 7.6 kWp for SOs, from 3.4 kWp to 4.5 kWp for SEs and SWs in 2018. The rise is accompanied by a moderate increase in self-sufficiency (37.7 % for SOs, 30.9 % for SEs and 30.3 % for SWs). While the FIT drops by 1.5 %, PV system costs per kWp decrease by 7.7 %. That results in an increase of PV size by 39.1 % to 45.5 % for SOs depending on the load category. Thus, declining system costs provide a good leverage for PV size as margins on PV self-supply slightly improve, but also decrease losses on PV feed-in.

While in 2017 only SOs at one location adopt BSSs (see upper whisker), the attractiveness of increasing self-sufficiency through a BSS rises in 2018. Here, up to 40 % of SOs HHs invest into a BSS with sizes around 6 kWh and increase their self-sufficiency to 60 %. When comparing BSS sizes for HHs that already would have invested into a BSS in 2017, driving forces behind BSS sizing become visible. Here, the median increase of BSS size only amounts to 14.9 % for larger yearly demand compared to up to 32.1 % for HHs with low yearly demand. For larger loads, the additional benefit from increasing BSS size becomes less attractive as sizing comes closer to the average serviceable demand during night time, where BSS discharging typically occurs. Furthermore, excess PV energy for BSS charging is limited as PV sizes reach the 10 kWp threshold.[2]

Less than 25 % of SEs and SWs HHs invest into BSSs. Here, the median lies around 3 kWh, which is significantly smaller compared to SOs. However, BSS impact on PV sizing is better distinguishable for these HHs. For location 1, HHs with a large demand that did not invest in a BSS in 2017 start adopting BSSs for SEs and SWs. For these HHs, optimal PV sizing increases by up to 47 % or 2 kWp compared to 2017. Thus, as a result of BSS investment, 1 kWp is additionally installed compared to HHs with similar PV system orientation and no BSS.

The analysis highlights that an investment into a PV BSS is currently not economically efficient for the majority of analyzed HHs for the given scenarios. However, for locations with a good solar resource and HHs with a high yearly demand, it might already be a valid option today and is likely to become even more attractive in the years ahead. Investing in just a PV system without a BSS is reasonable for all HHs, even for those with systems that face south-east or south-west at locations in Eastern or Western Germany. Realizable savings are one or low two-digit percentages compared to procuring electricity from the network for these locations. If investors become more risk-averse, such low savings can be a threat to the overall PV investment decision.

A.2.2 *Cost analysis for reference case study*

To develop a better understanding of the overall electricity supply costs, all cost and revenue streams are mapped with component related energy flows. Four cost categories are derived: network demand, direct PV load supply, indirect PV load supply through a BSS and PV network feed-in. While the attribution of operational costs or revenues and BSS investment costs are obvious, PV investment costs are distributed according to PV usage. For example, the percentage of direct PV load supply determines the percentage of PV investment costs attributed to costs related to direct PV load supply.

- Costs related to direct PV load supply:

2 As stated above, PV systems sized over 10 kWp are obliged to pay the EEG surcharge partially on their self-supply and receive a lower FIT for network feed-in (see 3.2.2).

$$
\begin{aligned}
CPVL_j &= \sum_{t\in\mathcal{T}} (e_{j,t}^{PVL} \cdot (E_{j,t}^{PV} \cdot s_j^{PV})^{-1}) \\
&\cdot \ ((I^{PV} + M^{PV} \cdot PF^{HH} - TE^{Dep}) \cdot s_j^{PV} + In^{PV} \cdot b_j^{PV}) \\
&+ \ ((C^{Sc1} + C^{Sc2} \cdot b_j^{SkWp}) \cdot PF^{HH} + TE^{Sc}) \sum_{t\in\mathcal{T}} (e_{j,t}^{PVL}) \qquad \text{(A.3)}
\end{aligned}
$$

- Costs related to indirect PV load supply through a BSS:

$$
\begin{aligned}
CBSSL_j &= \sum_{t\in\mathcal{T}} (e_{j,t}^{PVBSS} \cdot (E_{j,t}^{PV} \cdot s_j^{PV})^{-1}) \\
&\cdot \ ((I^{PV} + M^{PV} \cdot PF^{HH} - TE^{Dep}) \cdot s_j^{PV} + In^{PV} \cdot b_j^{PV}) \\
&+ \ (I^{BSSkWh} + M^{BSSkWh} \cdot PF^{HH}) \cdot s_j^{BSSkWh} \\
&+ \ (I^{BSSkW} + M^{BSSkW} \cdot PF^{HH}) \cdot s_j^{BSSkW} \\
&+ \ In^{BSS} \cdot b_j^{BSS} - (Sub^{BSS} - TE^{BSS}) \cdot r_j^{BSSInc} \\
&+ \ ((C^{Sc1} + C^{Sc2} \cdot b_j^{SkWp}) \cdot PF^{HH} + TE^{Sc}) \sum_{t\in\mathcal{T}} (e_{j,t}^{BSSL}) \qquad \text{(A.4)}
\end{aligned}
$$

- Costs related to PV network feed-in:

$$
\begin{aligned}
CPVN_j &= \sum_{t\in\mathcal{T}} ((e_{j,t}^{PVN} + e_{j,t}^{PVC}) \cdot (E_{j,t}^{PV} \cdot s_j^{PV})^{-1}) \\
&\cdot \ ((I^{PV} + M^{PV} \cdot PF^{HH} - TE^{Dep}) \cdot s_j^{PV} + In^{PV} \cdot b_j^{PV}) \\
&- \ ((C^{Fit1} - C^{Fit2} \cdot b_j^{SkWp}) \cdot PF^{HH} - TE^{Fit}) \sum_{t\in\mathcal{T}} e_{j,t}^{PVN} \qquad \text{(A.5)}
\end{aligned}
$$

- Costs related to network demand:

$$
CNL_j = C^E \cdot PF^{HH} \sum_{t\in\mathcal{T}} e_{j,t}^{NL} \qquad \text{(A.6)}
$$

For the reference case study, mean yearly revenue and cost streams are displayed categorized according to yearly demand as well as PV system orientation for locations 1 and 2 for both simulated years. Furthermore, yearly electricity supply costs without a PV BSS are displayed in Fig. A.5.

For location 1, the realized mean savings per load category vary from 13.9 % to 17.8 % for 2017 and from 23.8 % to 24.1 % for 2018 for SOs. As more BSS capacity is adopted, higher investment costs for BSSs are offset by an additional decrease of costs for network procurement, which is mainly a result of an increased indirect PV load supply through the BSS. Additionally, costs of PV feed-in are reduced through larger a BSS, as PV investment costs are attributed to self-supply costs with increasing self-consumption. SEs and SWs only realize savings varying from 3.8 % to 8.0 % for 2017 and from 5.8 % to 9.6 % for 2018 as self-supply is less attractive due to a lower energy production per installed kWp.

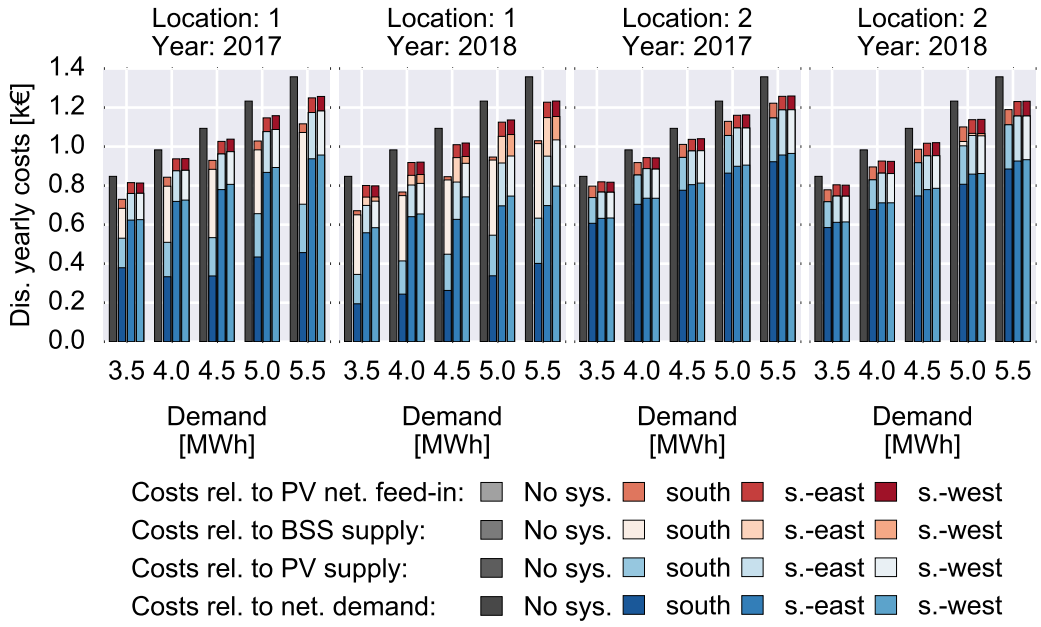

Figure A.5: Distribution of yearly mean system costs per HH (according to yearly HH demand and orientation of PV system) for location 1 and 2 and for year 2017 and year 2018.

For location 2, the realized mean savings per load category vary from 5.9 % to 10.0 % for 2017 and from 8.1 % to 12.4 % for 2018 for SOs. Additional savings between the two years are mainly realized through a larger amount of direct self-supply, which is a result of decreased PV system costs. SEs and SWs only realize savings varying from 3.3 % to 7.4 % for 2017 and from 5.1 % to 9.4 % for 2018. Compared to location 1, the changes are not as significant due to the lack of BSS adoption. Additionally, these small savings indicate that future PV systems do not provide high returns and might not be an attractive option for risk-averse investors.

In summary, the analysis indicates that next to reduced payments for network consumption, a BSS installation also improves the cost-benefit-ratio of PV network feed-in, whereas the margin of BSS self-supply is often close to zero or even negative.

A.2.3 *Energy flow analysis for reference case study*

An in-depth understanding of optimal sizing decisions is derived by analyzing the seasonal distribution of the different energy flows for demand and PV energy. The energy flows are categorized and aggregated according to three different seasons: winter (Wi.), spring/fall (S/F) and summer (Su.). The categorization follows the season approach used for SLP (see A.3). To distinguish the effect of a PV and a BSS adoption, three different scenarios are displayed for SOs at location 1 for 2018 in A.6. Scenario 'Load only' assumes that no PV or PV BSS is installed. Scenario 'PV only' shows re-

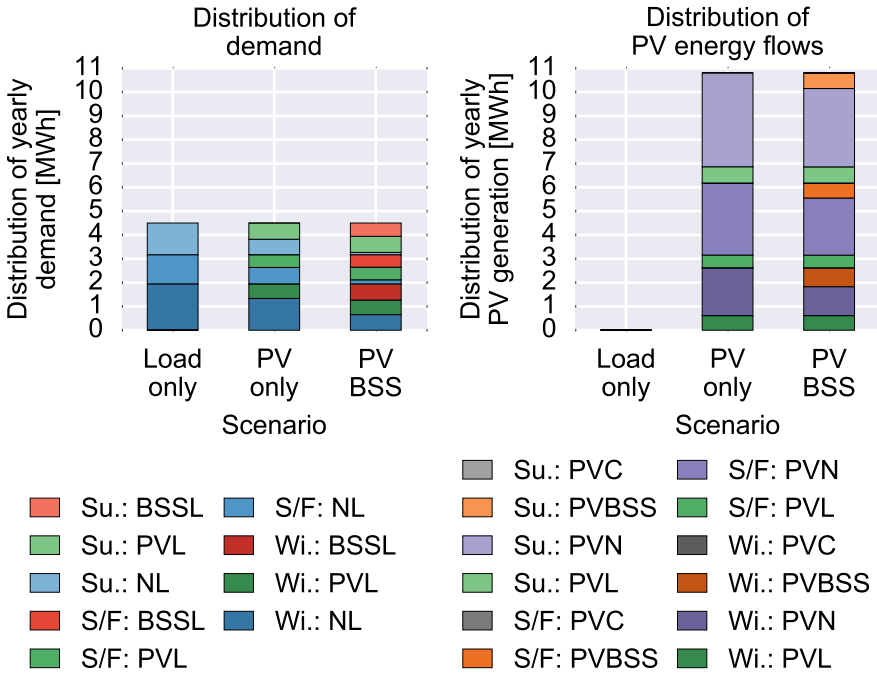

Figure A.6: Seasonal distribution of median energy flows for load supply (left) and PV energy usage (right) for different system configurations for south-facing systems for location 1 for year 2018.

sulting energy flows when only a PV system is installed. Scenario 'PV BSS' displays the previously discussed results.

43.2 % of the yearly demand occurs in winter, 27.2 % in spring and fall and 29.6 % in summer. As winter and summer have more days than spring and fall, a minor distortion is observed; the average demand is 13.9 kWh during a winter day, 12.0 kWh during a spring and fall day and 10.8 kWh during a summer day. When a PV system is installed, network demand drops to 29.6 % in winter, to 15.3 % in spring and fall and to 14.4 % in summer, implying that PV load supply decreases the average network demand by 31.4 % during a winter day, by 43.6 % during a spring and fall day and by 51.2 % during a summer day. Once a BSS is introduced, network demand further declines while direct PV load supply remains similar high. Average network demand decreases to 4.7 kWh during a winter day, 1.7 kWh during a spring and fall day and 0.8 kWh during a summer day.

When analyzing PV energy usage over the different seasons, certain aspects have to be highlighted. Even despite a BSS installation, PV feed-in remains the largest portion during each season, e.g. in winter an average of 8.7 kWh are still fed into the network, while only 4.4 kWh are consumed directly and 5.7 kWh indirectly. Comparing that to the average daily network demand of 4.7 kWh in winter, it becomes obvious that even BSSs cannot bridge longer low sun periods. Compared to winter with a seasonal PV self-consumption of 23.3 % for PV and 53.6 % for PV BSSs, spring and fall (15.0 %

for PV and 32.1 % for PV BSSs) as well as summer (14.7 % for PV and 28.7 % for PV BSSs) do not see such amounts of PV self-consumption. As less load is consumed and self-sufficiency is already at high levels during these seasons, the effectiveness of the BSS for increasing PV self-consumption also decreases. This highlights the second aspect that determines BSS sizing: the available average daily load. The following trade-off becomes visible: While it seems like there is a need for additional BSS capacity to store excess PV energy during the winter, lower demand and higher amounts of excess PV energy during the summer lead to limited need for larger BSS capacities. Thus, an additional installed kWh of BSS capacity needs to be refinanced with lower overall operation hours.

A.2.4 *Nominated sensitivity analysis*

The parameter variations used for the previous sensitivity analysis are based on a thorough literature review and create a realistic bandwidth for individual preferences and expectations. However, as each parameter is varied differently, percentage changes vary. For example, PV system costs vary by 8.3 % in 2018, while the ERR varies by 50 %. While such an analysis allows deriving conclusions with regard to network integration based on realistic assumptions, it does not properly address the elasticity of parameter changes with regard to other KPIs. To develop a better understanding for elasticities, an additional sensitivity analysis is performed. Here, parameters are equally varied in 10 % steps and additional KPIs are analyzed.[3]

- Self-sufficiency:

  Self-sufficiency or self-supply SP_j describes the amount of HH's demand being covered by self-supplied PV energy. In other words, it can also be expressed as the original demand minus the network procurement in relationship to the total demand:

$$SP_j = \frac{\sum_{t \in \mathcal{T}} (E^L_{j,t} - e^{NL}_{j,t}) \cdot 100}{\sum_{t \in \mathcal{T}} E^L_{j,t}} \tag{A.7}$$

- PV self-consumption:

  PV self-consumption SC_j describes the amount of locally generated PV energy for direct or indirect load supply:

$$SC_j = \frac{\sum_{t \in \mathcal{T}} (e^{PVL}_{j,t} + e^{PVBSS}_{j,t}) \cdot 100}{\sum_{t \in \mathcal{T}} (e^{PVL}_{j,t} + e^{PVBSS}_{j,t} + e^{PVN}_{j,t} + e^{PVC}_{j,t})} \tag{A.8}$$

- Yearly electricity costs:

3 Parts of this chapter are presented in [25].

Yearly electricity costs CL_j are the sum of all cost and revenue streams that are presented in the previous section or the value of the objective function dividend by the calculation period (here: 20 a):

$$\begin{aligned} CL_j &= z_j \cdot 20^{-1} \\ &= (cNL_j + cPVL_j + cBSSL_j + cPVN_j) \cdot 20^{-1} \end{aligned} \tag{A.9}$$

- Net present value:

  The NPV_j of the system is a function of the benefit z_j resulting from the investment in a PV BSS compared to the NPV of only procuring electricity from the network over the system's lifetime:

$$NPV_j = C^E \cdot PF^{HH} \sum_{t \in \mathcal{T}} E^L_{j,t} - z_j \tag{A.10}$$

Fig. A.7 displays the change in median KPIs for SOs for 2018 for location 2. HHs at this location are especially interesting, since the median BSS capacity for the ref. case is still zero and the median PV system size has not reached the 10 kWp threshold.

For the min. and max. scenarios in the previous analysis, the ERR has the highest absolute impact on PV sizes followed by PV system costs. A different picture appears with nominated changes. A change by -10 % in PV system costs results in a median PV size of 10 kWp, increasing by 85.6 %. BSSs are only slowly adopted and the BSS median remains at zero. Median PV self-consumption drops to 22.3 % from 29.6 %, while self-sufficiency increases from 31.1 % to 40.6 %. Lower PV costs result in lower overall electricity costs, which drop by 5.5 %. When the PV price drops by 20 %, the median PV size remains at 10 kWp because of additional self-consumption taxes and a lower FIT above 10 kWp. The median BSS jumps to 4.7 kWh and 65 % of the HHs adopt a BSS. That allows increasing PV self-consumption to 29.1 % and self-sufficiency to 56.7 %. Yearly costs drop by an additional 6.9 %-points, indicating the leverage BSSs provide once generation costs become cheap enough. An additional PV price drop barely leads to an increase in BSS size (only plus 0.2 kWh). Electricity costs drop by an additional 6.9 %-points. Higher PV costs lead to a median decrease of 30 % in PV size for a 10 % price surge. The effect slightly declines with further increasing costs; PV sizes drop by an additional 17 %-points and 11 %-points to 2.2 kWp. Yet, the increase in yearly costs is moderate with 3 % to 7 %. This highlights the upside potential of larger PV sizes, once prices drop.

The highest impact on overall supply costs is seen for a change in expected electricity prices. The trade-off of increasing self-supply becomes visible once more. While PV sizes as well as BSS sizes steadily increase with a higher electricity price, e.g. plus 54.1 % in PV size and to 5.1 kWh in BSS capacity (with all HHs being equipped with a BSS), electricity costs also rise by 6.9 %. An increase by 20 % results in an additional increase of 16.6 % for PV sizes and of 21.6 % for BSS capacities, indicating a shift from

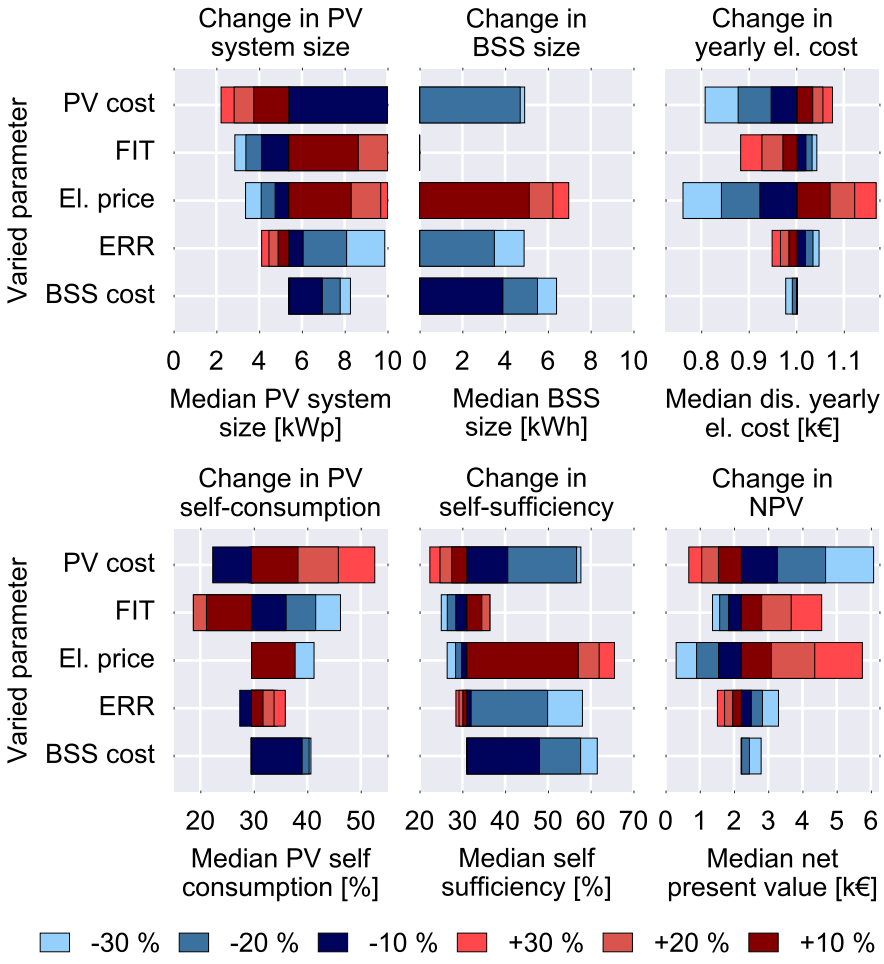

Figure A.7: PV system size (top, left), BSS size (top, middle), yearly for electricity cost (top, right,), PV self-consumption (bottom, left), self-sufficiency (bottom, center) and net present value (bottom, right) for south-facing systems for 2018 for location 2 for nominated parameter changes.

additional generation to storing. The cost increase is limited to additional 5.2 %-points. That is a result of a significantly increasing margin on indirect self-supply via a BSS. Overall, it is favorable for a HH if electricity prices drop. A decrease by 10 % results in 8.6 % lower supply costs, PV sizes decrease by 11.9 % and self-supply costs rise with fixed costs being distributed over a lower self-supply.

PV sizes can significantly vary depending on the assumptions and highly depend on the margin of every self-supplied kWh. With decreasing system costs or increasing revenues from self-supply, oversizing PV systems and subsidizing PV feed-in becomes attractive. BSSs mitigate potential losses on PV feed-in or are used for hedging against higher supply costs. Yet, the vulnerability of the business case increases when PV sizes depend less on PV feed-in as certain drivers of larger PV sizes and BSS adoption actually result in higher overall supply costs.

A.2.5 *Analysis of self-sufficiency modeling*

Nearly every second residential PV system was installed together with a BSS in 2016 [7]. However, presented simulation results for 2017 (here: ref. case) show that it is only economically attractive to invest in a BSS for approx. 20 % of the simulated HHs with SOs (only with the investment incentive program) and 0 % of the simulated HHs with SEs and SWs. Taking into account that BSS prices were higher in 2015 and 2016 and that only half of the HHs applied for the investment bonus, the results show that a strict economic focus does not sufficiently reflect the current reality. An additional trigger is the desire to increase self-sufficiency. It could also impact PV network integration as it might result in larger PV systems. The developed model includes such a preference either via an additional constraint or through weights in the objective function. To evaluate the interactions between self-sufficiency, system sizes and PV network integration, min. self-supply and weights are varied; corresponding results are displayed in Fig. A.8.[4] Furthermore, it is analyzed how the investment incentive program influences the adoption of BSSs and the limitation of the peak PV feed-in.

With weights, even a small adjustment towards a higher preference for self-sufficiency leads to an increase in installed BSSs. While the ref. case only leads to a BSS penetration of 20 % of HHs for SOs, a weight of 95 % increases the adoption rate to over 80 % with and to 35 % without the incentive. As BSS prices were higher in 2015 and 2016, a weight of 95 % seems to be sufficient to include the self-sufficiency component in the model. Self-sufficiency strongly impacts system sizing; the median PV size increases by 2.4 kWp and the median BSS capacity rises by 4.5 kWh compared the ref. case with incentive. Self-sufficiency nearly doubles from 33.0 % to 57.2 % in this case. A moderate rise in median peak PV feed-in with the incentive (from 3.6 kW to 3.9 kW) is observed. The median NPV is around 18.8 % or almost 500 € lower compared to the ref. case.

Lower NPV weights exemplary display how the additional self-sufficiency is achieved. Until the 10 kWp threshold is reached, the increases of PV and BSS sizes move at similar pace. Afterwards, the PV size remains at 10 kWp and only BSS capacity is added. Here, the 10 kWp threshold puts a strict economic limit on a higher preference for self-sufficiency. E.g. for a NPV weight of 80 % a median self-sufficiency of 72.4 % with the incentive is reached. Self-sufficiency gains come at a high price; the median NPV of this case is almost 70 % or 1,600 € lower compared to the ref. case.

Yet, this modeling strategy allows each HH to weigh additional costs against marginal increase in self-sufficiency. Especially for HHs with a low natural self-sufficiency, a flexibility is provided to choose reasonable sizes (with 75 % of all BSSs remaining under 10 kWh). The flexibility is a core difference to the approach using a self-sufficiency constraint.

4 For this case study, area constraints on PV and BSS size are lifted compared to the initial scenario (see Tab. A.3) to avoid running into limitations that influence the results.

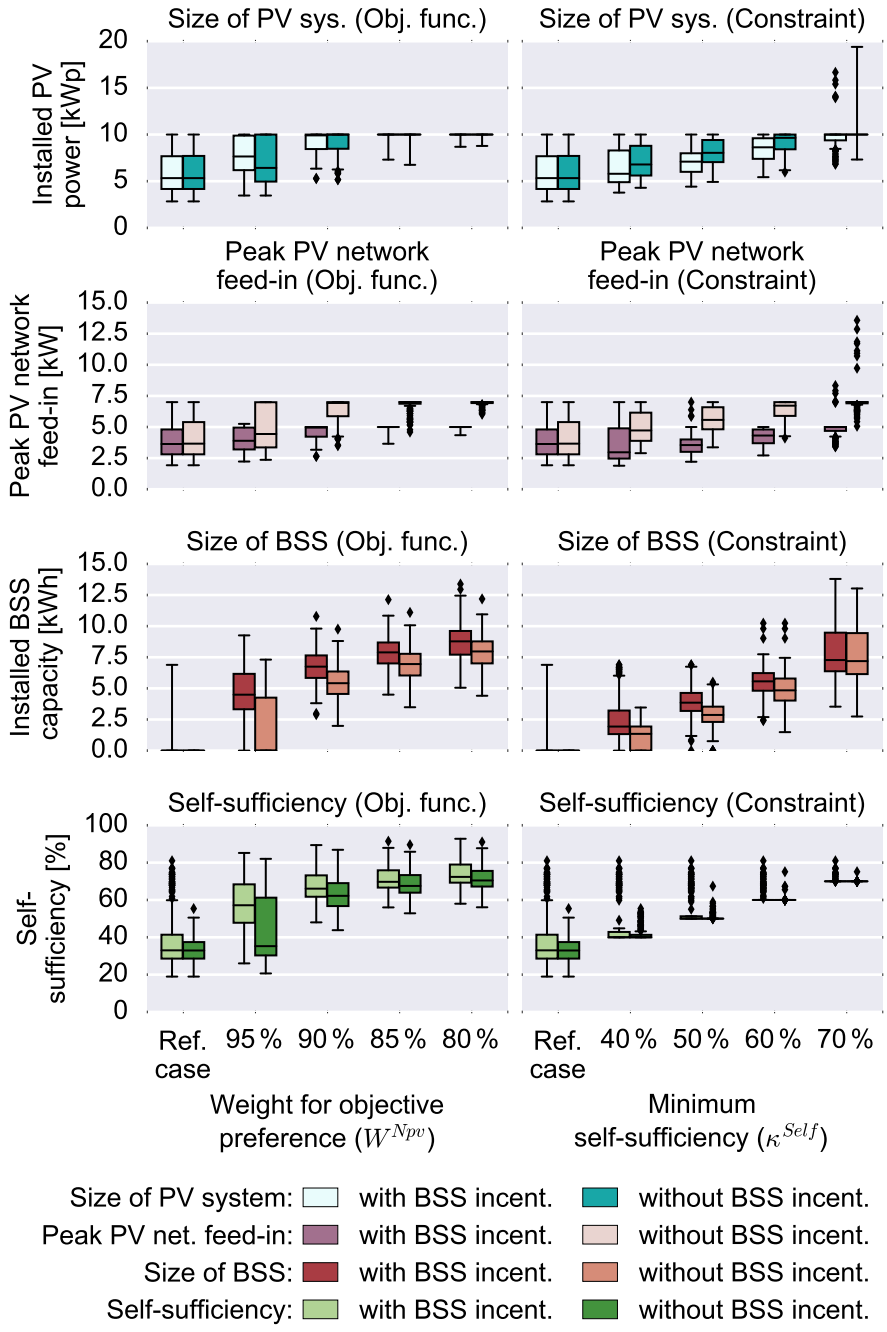

Figure A.8: Size of PV system (top), peak PV network feed-in (top-middle), size of BSS (bottom-middle) and self-sufficiency of PV BSS (bottom) for reference scenario in 2017 for south-facing PV systems for different modeling approaches: weights for cost vs. self-sufficiency preference in objective function (left) or minimum self-sufficiency constraint (right)

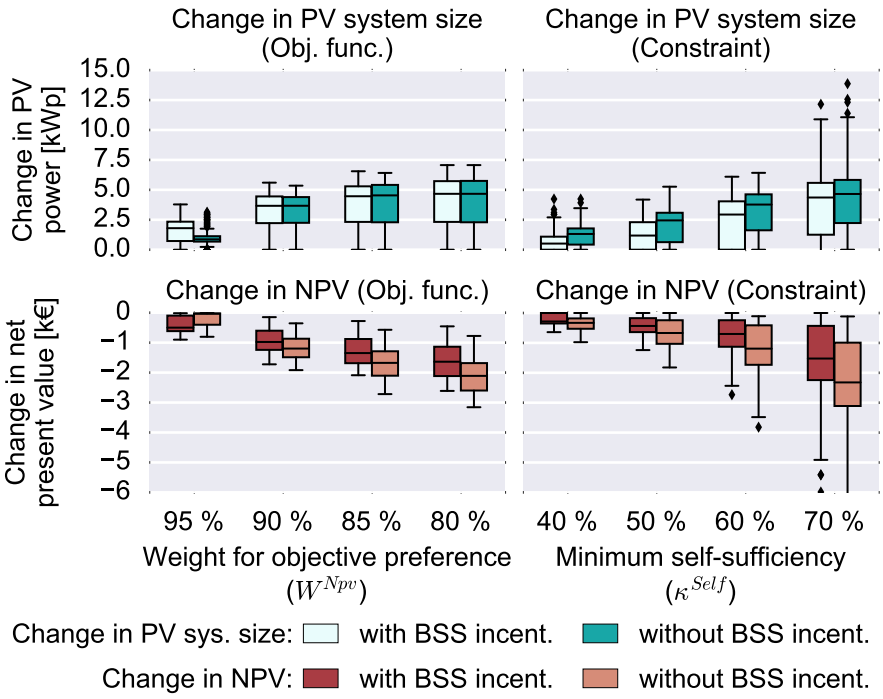

Figure A.9: Change in size of PV system (top) and change in net present value (NPV) (bottom) compared to reference case 2017 for south facing PV systems for weights for self-sufficiency preference in objective function (left) or minimum self-sufficiency constraint (right)

A min. required self-sufficiency of 40 % leads to a similar amount of installed BSSs, such as a NPV weight of 95 %. The median PV (BSS) size only increases by 0.5 kWp (1.9 kWh) with and by 1.5 kWp (1.3 kWh) without the incentive. In both cases the median self-sufficiency is exactly at the required min. of 40 %. The median NPV decreases only by 12.1 % or 283 € with the incentive, which is lower than for the NPV weight. When a higher min. self-sufficiency is required, e.g. 70 % (which is comparable to the NPV weights of 85 or 80 %), a disadvantage of this modeling approach becomes visible. Certain HHs are now required to surpass the 10 kWp threshold to hold the constraint. Then, the median BSS size (8.1 kWh) and the NPV decline (62 %) remain lower compared to the NPV weight of 80 %.

When analyzing changes in PV sizes and NPV (see Fig. A.9), additional aspects become visible. With the weighted objective function, the marginal system size decreases with a decreasing weight and the impact on the NPV becomes more significant. Yet, when comparing the NPV change between the modeling approaches, one can see the strength and the weakness of each approach. While the first approach allows for flexibility and leads to fewer outliers, it has a stronger impact on sizing for smaller weights compared to the constraint approach.

In summary, introducing a weighted objective function encourages larger PV and BSS sizes compared to a self-sufficiency constraint. While the min. cost approach in combination with a min. self-sufficiency constraint reduces

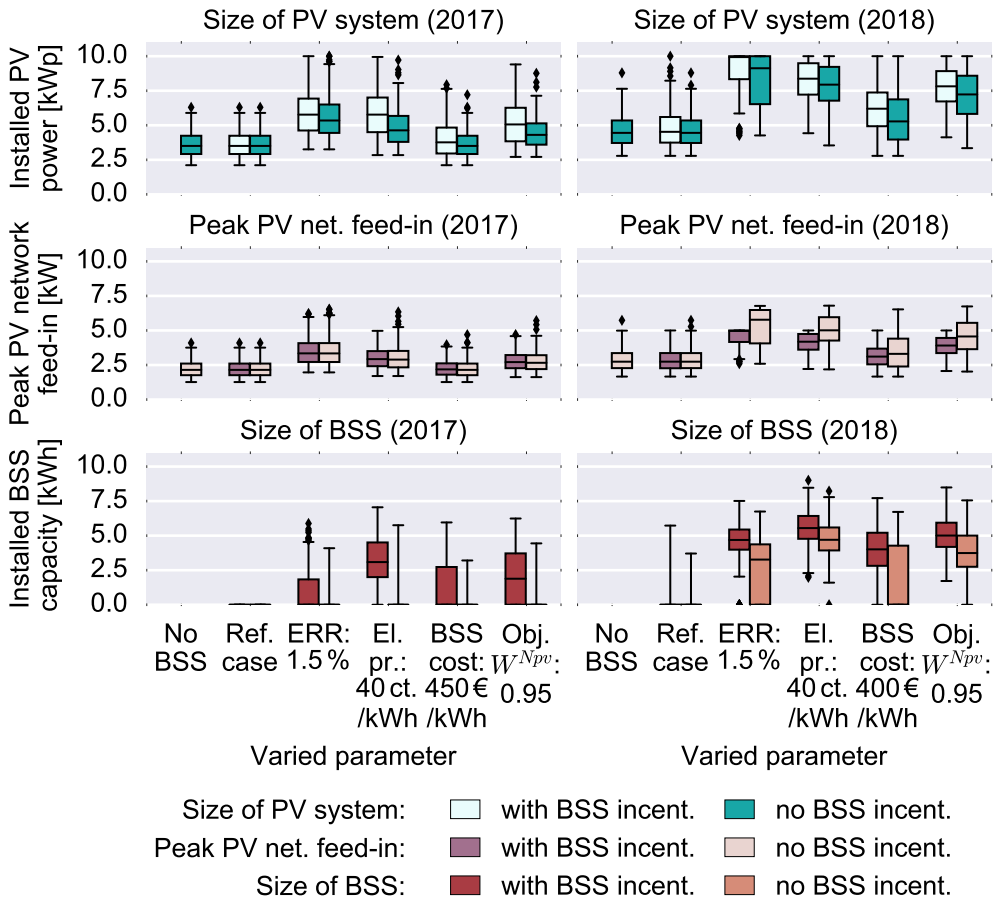

Figure A.10: Size of PV system (top), peak PV network feed-in (middle) and size of BSS (bottom) for selected case studies for 2017 (left) and 2018 (right) for south-east and south-west facing PV systems

NPV losses, it results in a lower sizing flexibility, which leads to highly oversized systems in certain cases. Some HHs need to surpass the 10 kWp threshold to fulfill the constraint, which is economically unfavorable.

A.2.6 *Additional analysis of peak impact of PV BSSs*

The peak impact analysis for SEs and SWs is displayed in Fig. A.10.

Compared to SOs, several aspects have to be highlighted. In 2017, the median BSS size only reaches values larger than zero in one case: expectation for high electricity prices together with the investment incentive. With the adoption of BSSs, the median installed PV size rises again and a slight increase in the median peak PV feed-in is observed. Nearly no difference is seen between peaks when comparing cases with and without the investment inventive in 2017. That changes in 2018. With the increasing economic attractiveness of BSSs, the incentive allows adopting larger PV sizes compared to the case without the incentive. While it also limits the increase in

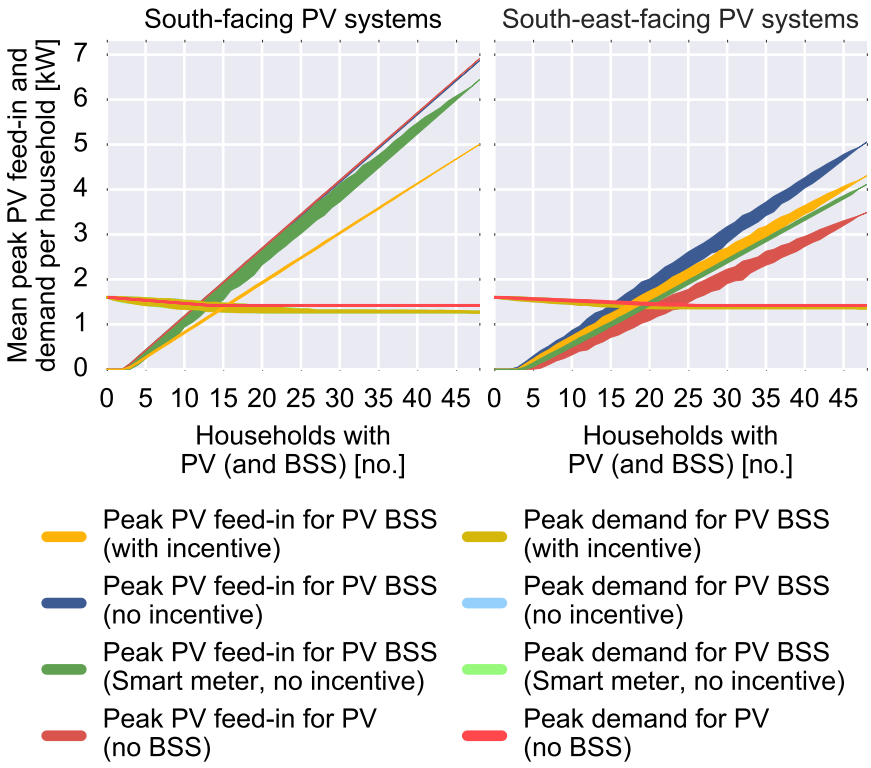

Figure A.11: Comparison of mean peak PV feed-in and peak demand per HH depending on the amount of HHs with a PV system for cases PV only, PV BSS with and without BSS investment incentive for high average electricity prices for south facing systems (left) and south east facing systems (right) for location 1 for 2018.

peak feed-in compared to the case without the incentive, it - just like for SOs - partially counteracts this limitation as system sizes increase as well.

A.2.7 *Analysis on aggregated peak feed-in and load of PV BSSs*

Fig. A.11 displays the results for the peak PV feed-in and demand peak per HH depending on the total number of HHs with a PV system and on different case studies for SOs and SEs for another location.

The results support the conclusion of the main section. For SOs, BSSs only allow for a higher PV penetration when a lower feed-in limit is imposed (as it is the case with the investment incentive program). For SEs, BSSs can act as an enabler to achieve larger sized PV systems with and without the incentive. Without the incentive, the peak feed-in surpasses peak demand for a lower HH number equipped with PV BSSs compared to the case 'no BSS'. Thus, the likelihood of network reinforcement rises. The incentive even further increases PV sizes and only slightly reduces the peak feed-in.

A.2.8 *Impact of time resolution*

While the presented analyses show how various parameters influence the sizing decision, one further source that might result in higher network peaks has been left out: the simulation time resolution. While previous analyses of the simulation time resolution have focused on energy losses due to PV curtailment [163] or self-consumption [28], the dynamics between system sizing and peak network feed-in have not been analyzed in-depth.

For the following analysis, a PV profile from Kassel, Germany, is chosen, since it is available at a higher time resolution.[5] Besides the ref. case for 2018, higher mean electricity prices and lower BSS costs are simulated with a 1 min, 5 min, 10 min, 15 min and 1 h time resolution and analyzed for all 48 HHs. Next to PV systems and BSS sizes as well as peak PV feed-in, energy losses due to PV curtailment are also displayed in Fig. A.12.

For the ref. case, no BSSs are installed (independent of the time resolution). The median PV size is 5.22 kWp for 1 min It slightly increases to 5.34 kWp for 5 and 10 min and then decreases to 5.26 kWp for 15 min and 5.22 kWp for 1 h; the peak PV feed-in varies accordingly. Thus, the 15 min simulation results provide a good estimate; the results are only 0.8 % larger than the results achieved with 1 min time step. The impact of the time resolution becomes clearer visible when comparing the change of PV curtailment losses. Losses steadily decrease with a lower time step (from 0.5 % with 1 min to 0.02 % with 1 h).

The interdependencies change once BSSs become economically viable options. The median PV size steadily increases with a lower simulation time step. E.g. for higher mean electricity prices (lower BSS prices) the median increases from 7.82 kWp (6.52 kWp) for 1 min over 8.16 kWp (6.74 kWp) for 15 min to 8.36 kWp (6.95 kWp) for 1 h. The median peak increases at a lower rate as a result of the 50 % curtailment limit. Median BSS sizes only marginally vary from 5.95 kWh to 5.93 kWh (5.17 kWh to 5.14 kWh) between 1 and 15 min. Curtailment losses slightly increase with a lower curtailment limit compared to the ref. case. BSS operation helps keeping median energy losses resulting from PV curtailment under 1 %, even with a 1 min time step.

A 15 min time step provides a good estimate for accurate sizing and peak results. Yet, a slight overestimation of PV sizes and peak is possible once BSSs are economically attractive. Size and peak variations lie within an acceptable margin of error (3-4 % for peak PV feed-in). BSS capacities are minimally underestimated. The general conclusions drawn above remain viable and are merely influenced by the simulation time step.

5 The DC-measured PV profile is adapted to lower time resolution as described in [163].

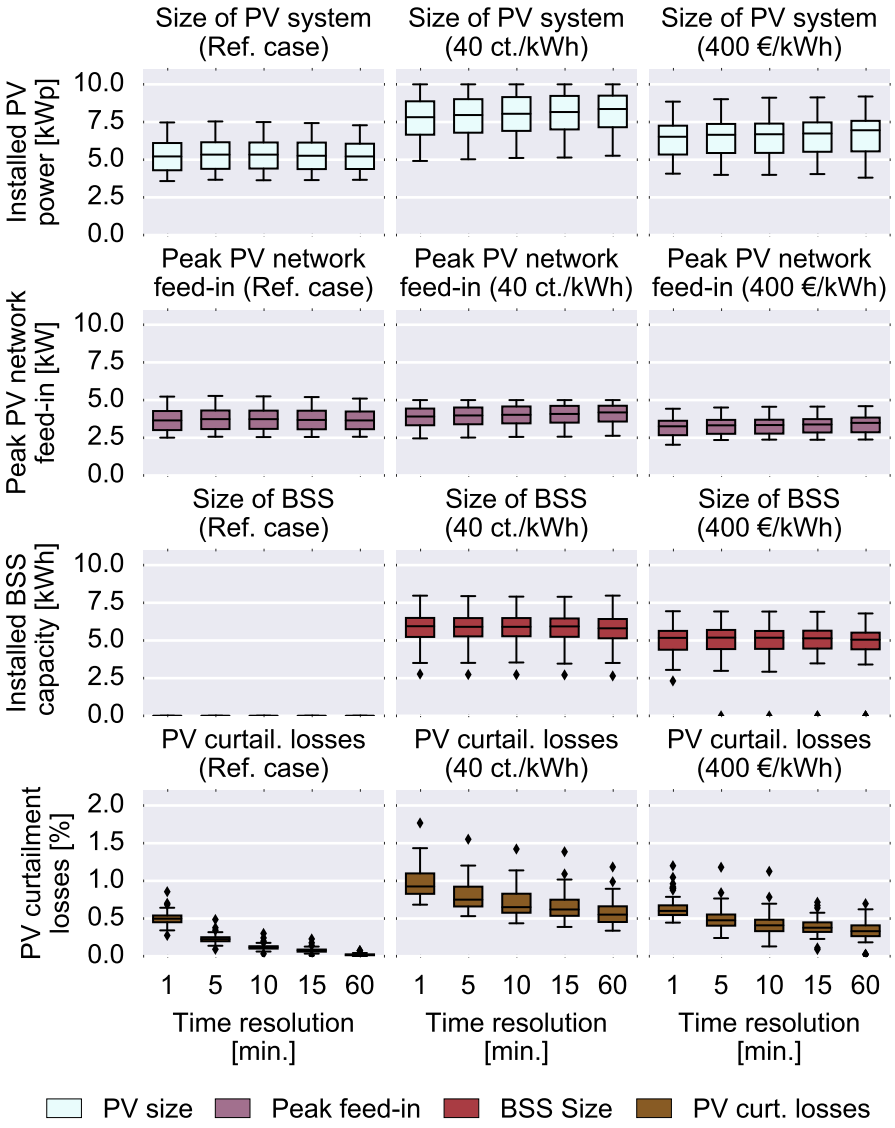

Figure A.12: Size of PV system (top), Peak PV network feed-in (top-middle), size of BSS (bottom-middle) and PV curtailment losses due to fixed feed-in limit (bottom) for selected case studies (reference scenario (left), high average electricity price (middle) or low BSS cost per kWh (right)) in 2018 for Kassel, Germany for different simulation time resolutions

A.3 *Standard load profiles*

A.3.1 *Key performance indicators for standard load profiles*

SLPs are used for forecasting energy demand in 15 min. time steps, procurement and billing processes for customers with a yearly demand of less than 100 MWh (see §12 StromNZV). Such SLPs can be constructed analytically or synthetically. An analytical procedure is based on deriving SLPs by subtracting all power-measured profiles and generation profiles from the overall residual profile for one specific area. The residual profile allows calculating an average profile for all energy-only customers. Depending on the knowledge about customer specifics in one network area, a dis-aggregation using time-based weights of the residual profile into customer-specific profiles is possible. The synthetic method derives a customer group's SLP based on previously measured data of representative customers. Characteristic daily profiles are derived for weekdays, Saturdays and Sundays for three seasons (winter, summer and an interim period for spring and fall) [165]. Nine reference days are used to derive a yearly profile by appending one day after another according to season and day type for the chosen year. Afterwards, a seasonal correction is applied to account for daily consumption differences. As characteristic days are nominated to a yearly consumption of 1 MWh, the individual profile needs to be adjusted to its yearly consumption by performing a corresponding multiplication [166].

For this work, an analysis of the impact of PV BSS operation on SLPs is of high interest. Next to load SLPs, standard PV feed-in profiles are required. Two different approaches are currently used by DNOs and utilities to derive such profiles. Monthly nominated feed-in profiles are published by some DNOs [167]. Such profiles usually suffer from high forecast errors as they are composed of historical data. The second method relies on reference measurement at certain PV systems within one TNO area. DNOs can then retrieve daily profiles from their TNO [168]. While it used to be sufficient to map a generation profile with SLPs to determine a typical residual profile for one network area, self-consumption and BSS operation impact the aggregated profile. To account for self-supply induced changes to load and PV profiles, case-study specific SLPs are derived by individually aggregating network consumption E_t^{NLagg} and PV network feed-in E_t^{PVNagg} over all HHs for each time step and nominating the aggregated profiles according to the total number of HHs with a PV BSS:

$$\forall t \in T: \quad E_t^{NLagg} = \quad J^{-1} \cdot \sum_{j \in \mathcal{J}} e_{j,t}^{NL} \tag{A.11}$$

$$\forall t \in T: \quad E_t^{PVNagg} = \quad -J^{-1} \cdot \sum_{j \in \mathcal{J}} e_{j,t}^{PVN} \tag{A.12}$$

Season	Dates
Winter	01/11 - 20/03
Interim	21/03 - 14/06
	15/09 - 31/10
Summer	15/06 - 14/09

Table A.4: Dates for classification of SLP seasons

Following the logic of the synthetic method, the aggregated profiles are categorized according to day types and seasons (see Tab. A.4 for the used date keys for the different seasons).

As the profiles are based on 15 min.-yearly data sets for individual HHs, a reverse application of the season correction would be necessary to adjust the daily energy demand. This step is skipped in this analysis and a statistical analysis is displayed using a box plot presentation as shown below. Such a representation allows indicating and evaluating the full bandwidth of load and PV induced variations. Especially the latter might significantly vary over the course of season and day type.

A.3.2 *Case study for impact of PV BSSs on standard load profiles*

The impact of the BSS adoption is not only important for PV network integration, but also for market integration as the load behavior of self-supplying HHs changes. The influence of PV systems on the residual demand is easily determinable: PV generation can be subtracted when it happens. Once a BSS is introduced, its operation influences both PV and load profile depending on the operational strategy. The overall PV market integration is impacted: Stored PV energy is not available for the market, but shifted to hours when not enough local energy is produced. To include the effect of different BSS operation strategies, not only the perfect forecast based BSS operation is displayed, but also a simple rule-based strategy is implemented that is currently used in most installed PV BSSs. It charges excess PV energy until the max. SOC is reached and discharges whenever demand is not met by direct PV supply (for details see [4]). For this strategy, the same PV and BSS sizes are used, which are determined through the optimization. A scenario is chosen where PV sizes with and without BSSs are the same for all HHs (high electricity prices and SOs at location 1). As HHs are usually billed according to SLPs and utilities purchase energy accordingly, the BSS impact is shown for one day type (here, weekday) and two different season (here: winter and summer) in Fig. A.13.

When analyzing the impact of BSS operation on the network demand two things have to be highlighted. No difference between the optimized and rule-based strategy is noticeable, neither for day type nor for season. This is fairly obvious during sun shine hours as direct PV load supply is model endogenous in both strategies. For BSS discharging, both strategies

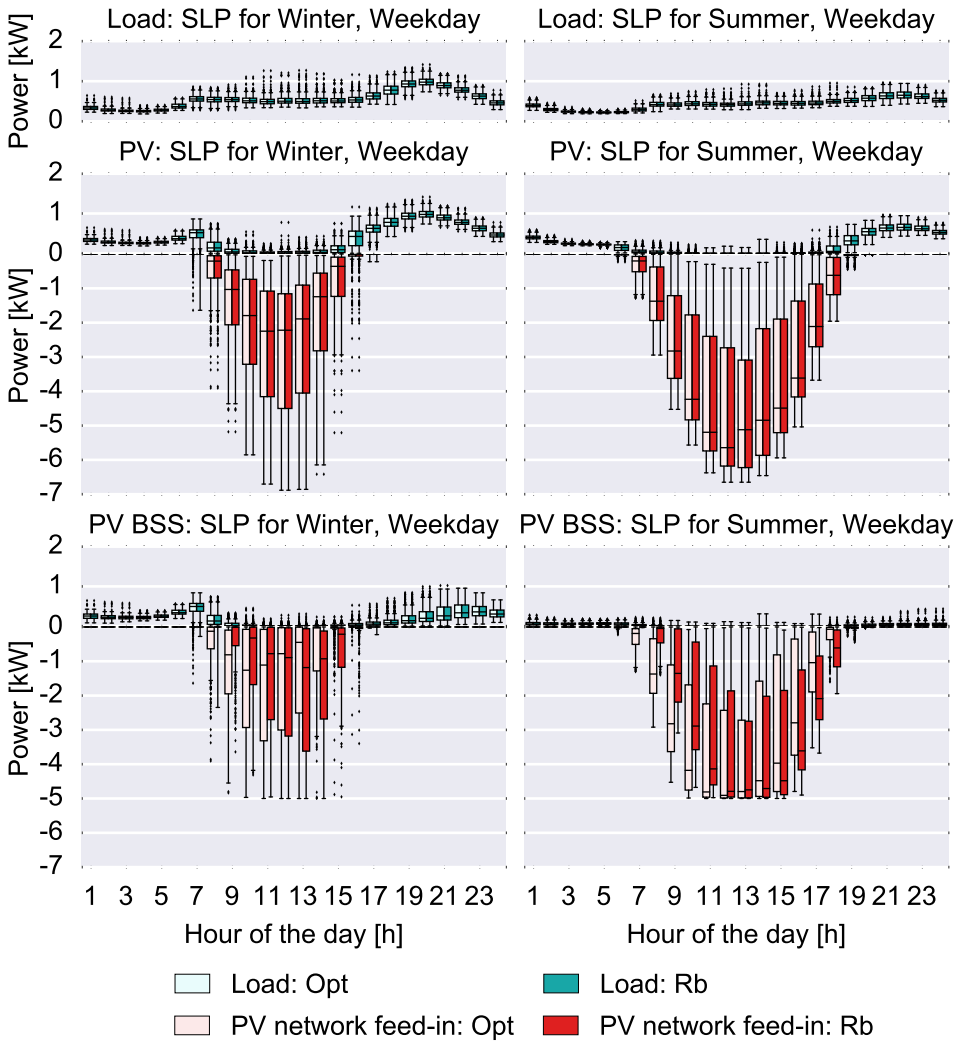

Figure A.13: Standard load profiles for load (top), PV (middle) and PV BSS (bottom, case: high electricity prices) for a winter weekday (left) and a summer weekday (right) for two BSS operation strategies (optimized (Opt) and rule-based (Rb)) for south-facing PV systems at location 1 for 2018

work similar since even the optimized strategy favors discharging as soon as there is demand to be covered to avoid self-discharging losses.

Compared to the load case, PV operation only impacts the demand profile during sun shine hours. Depending on the season, mid-day demand is completely reduced to zero and the HH profile turns into a feed-in profile. With a BSS, differences between seasons emerge more clearly. During summer, even evening hours see a median demand reduction of up to 95 %. During winter weekdays, the reduction is not quite as high as sun availability is lower and demand is higher. The median load is reduced by 33 % during evening hours, but only by 7 % in the early morning hours.

Differences in BSS operation become visible when comparing the PV network feed-in profile. Here, the optimized strategy operates based on a perfect forecast and schedules BSS charging to avoid PV curtailment and un-

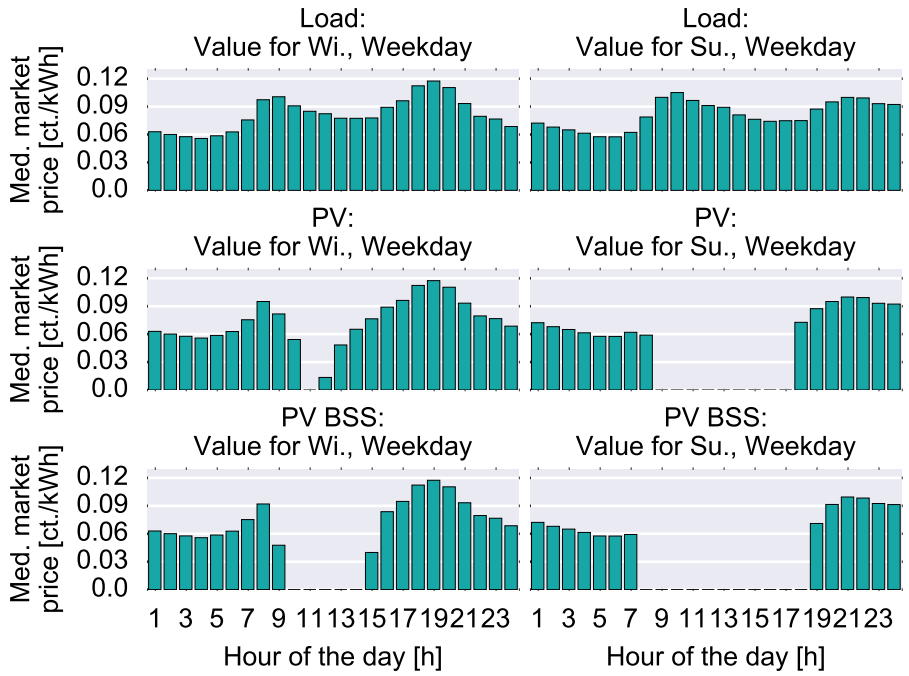

Figure A.14: Median value of consumed electricity for load (top), PV (middle) and PV BSS (bottom, case: high electricity prices) for a standardized winter weekday (left) and a standardized summer weekday (right) for south-facing PV systems at location 1 for 2018 (using EPEX spot market prices from 2015)

necessary self-discharging losses. Compared to the rule-based operation, less BSS charging is seen before mid-day and more charging happens during the afternoon hours. E.g. for summer weekdays a difference of 0-15 % (or up to 0.7 kW) is observed for the opt. strategy and 15-97 % (or up to 1.5 kW) for the rule-based strategy in the hours 6 to 12. The difference flips around in the hours 12 to 19 when the opt. strategy leads to a feed-in reduction of 7-90 % (or up to 1.0 kW) and the rule-based strategy only lowers the feed-in by up to 7 % (or up to 0.3 kW). The trend is similar during the winter days, but feed-in reductions occur during a shorter time window and less excess PV energy is available.

The feed-in and demand reduction have an impact on the overall electricity market, once significant amounts of PV BSSs are reached. Based on past spot market values, an analysis is performed to determine whether the current non-price driven operation of PV systems and PV BSSs would impact the HH's procurement cost. The hourly spot market prices of 2015 are used to determine the hourly median cost of electricity consumption and hourly median feed-in value for the standardized day type following the logic of the SLP. Fig. A.14 shows the median spot market value of each consumed kWh depending on day type and season for the load case, the PV case and the PV BSS case.

With PV and PV BSS, network demand is especially avoided in hours with mid-range prices. Here, the impact of the overall PV generation on the

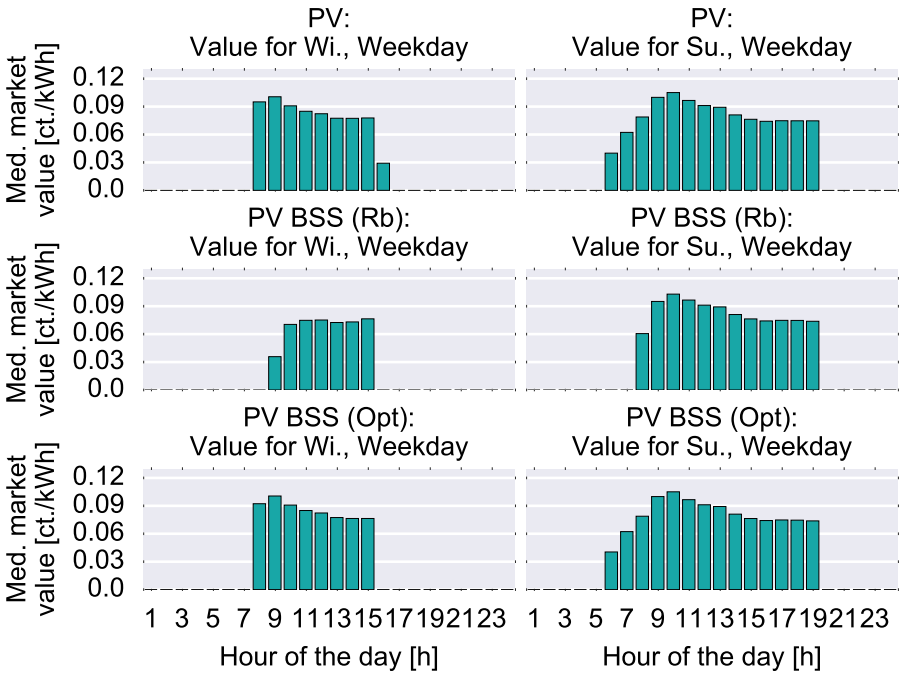

Figure A.15: Median market value of PV network feed-in for PV (top), PV BSS with rule-based operation (Rb) (middle, case: high electricity prices) and PV BSS with optimized operation operation (Opt) (bottom, case: high electricity prices) for a standardized winter weekday (left) and a standardized summer weekday (right) for south-facing PV systems at location 1 for 2018 (using EPEX spot market prices from 2015)

spot market value is already noticeable as mid-day peak prices are nearly not seen anymore. While the demand is significantly lower compared to the load case in the evening hours, the analysis also shows that BSSs are currently not operated according to price differences; the median price for the remaining demand is still as high as for the load case. However, a significant number of PV BSSs would likely lead to a decline of spot market prices in the evening hours, especially during summer.

While median costs of demand in hours of consumption do not significantly change in this ex-post analysis, the median market value of PV feed-in already sees a difference depending on the BSS operation strategy, as Fig. A.15 shows. Here, the median market value of PV feed-in depending on the scenario (PV, PV BSS with rule-based and optimized operation) and a typical day for summer and winter following the SLP logic are displayed.

The main difference between rule-based and optimized control strategy becomes visible. A rule-based strategy leads to early morning charging of excess PV energy, thus no energy is fed into the network and these hours see less PV energy. With an optimized control strategy, the charging happens later during the day. This results in a higher achievable market price during winter days.

B

Appendix for Part II

This appendix provides additional information on the presented bilevel approach.

B.1 *Optimization problems constrained by other optimization problems*

MPPDC, mathematical programs with primal and dual constraints, are a form of optimization problems constrained by other optimizations problems. Such problems can generally be described as follows [95].

$$\begin{aligned}
&Minimize_{\{x\}\cup\{x^1,...,x^n\}\cup\{\mu^1,...,\mu^n\}\cup\{\theta^1,...,\theta^n\}} \\
&\qquad f(x, x^1, ..., x^n, \mu^1, ..., \mu^n, \theta^1, ..., \theta^n) && \text{(B.1)} \\
&\qquad\qquad s.t. \\
&h(x, x^1, ..., x^n, \mu^1, ..., \mu^n, \theta^1, ..., \theta^n) = 0 && \text{(B.2)} \\
&g(x, x^1, ..., x^n, \mu^1, ..., \mu^n, \theta^1, ..., \theta^n) \leq 0 && \text{(B.3)} \\
&\begin{cases} Minimize_{x^1} & f^1(x, x^1, ..., x^n) \\ s.t & \\ h^1(x, x^1, ..., x^n) = 0 & (\mu^1) \\ g^1(x, x^1, ..., x^n) \leq 0 & (\theta^1) \end{cases} && \text{(B.4)} \\
&\qquad\qquad \vdots \\
&\begin{cases} Minimize_{x^n} & f^n(x, x^1, ..., x^n) \\ s.t & \\ h^n(x, x^1, ..., x^n) = 0 & (\mu^n) \\ g^n(x, x^1, ..., x^n) \leq 0 & (\theta^n) \end{cases} && \text{(B.5)}
\end{aligned}$$

Eq. B.1 describes the UL objective function, Eq. B.2 its equality constraints and Eq. B.3 its inequality constraints. Eq. B.4 and B.5 are LL problems that constraint the UL's problem. x is the vector containing the UL's decision variables, $x^1...x^n$ are the LLs' decision variables. $\mu^1...\mu^n$ are equality dual variables and $\theta^1...\theta^n$ are inequality dual variables. One important aspect here is that while each LL problem has a specific set of decision variables, e.g. x^1, its objective function, e.g. f^1, and its constraints, e.g. g^1 and h^1, depend on all primal variables (UL and other LL). The UL problem additionally depends on all LL dual variables next to the primal variables. Such a structure makes the problems interrelated and a reformulation possible.

Similar inter-dependencies can also be observed in Nash equilibrium problems [95, 98].

If the UL problem is constraint by linear programming problems, it can be displayed as follows:

$$\begin{aligned}
&Minimize_{\{x\}\cup\{x^1,\ldots,x^n\}\cup\{\lambda^1,\ldots,\lambda^n\}\cup\{\theta^1,\ldots,\theta^n\}} \\
&f(x,x^1,\ldots,x^n,\mu^1,\ldots,\mu^n,\theta^1,\ldots,\theta^n) && \text{(B.6)}\\
&s.t. \\
&h(x,x^1,\ldots,x^n,\mu^1,\ldots,\mu^n,\theta^1,\ldots,\theta^n)=0 && \text{(B.7)}\\
&g(x,x^1,\ldots,x^n,\mu^1,\ldots,\mu^n,\theta^1,\ldots,\theta^n)\leq 0 && \text{(B.8)}\\
&\begin{cases} Minimize_{x^1} & c^1x^1 \\ s.t & \\ a^1x^1-b^1=0 & (\mu^1) \\ d^1x^1-e^1\leq 0 & (\theta^1) \end{cases} && \text{(B.9)}\\
&\vdots \\
&\begin{cases} Minimize_{x^n} & c^nx^n \\ s.t & \\ a^nx^n-b^n=0 & (\mu^n) \\ d^nx^n-e^n\leq 0 & (\theta^n) \end{cases} && \text{(B.10)}
\end{aligned}$$

Such a representation allows replacing LL problems with their primal and dual constraints and ensuring optimality through a strong duality theorem equality:

$$\begin{aligned}
&\mathit{Minimize}_{\{x\}\cup\{x^1,\dots,x^n\}\cup\{\lambda^1,\dots,\lambda^n\}\cup\{\theta^1,\dots,\theta^n\}} \\
&f(x,x^1,\dots,x^n,\mu^1,\dots,\mu^n,\theta^1,\dots,\theta^n) && \text{(B.11)}\\
&s.t. \\
&h(x,x^1,\dots,x^n,\mu^1,\dots,\mu^n,\theta^1,\dots,\theta^n)=0 && \text{(B.12)}\\
&g(x,x^1,\dots,x^n,\mu^1,\dots,\mu^n,\theta^1,\dots,\theta^n)\le 0 && \text{(B.13)}
\end{aligned}$$

$$\begin{cases}
a^1x^1-b^1=0 & (\mu^1)\\
d^1x^1-e^1\le 0 & (\theta^1)\\
c^1+a^1\mu^1+d^1\theta^1=0 & \\
\mu^1,\theta^1\ge 0 & \\
c^1x^1=b^1\mu^1+e^1\theta^1 &
\end{cases} \qquad \text{(B.14)}$$

$$\vdots$$

$$\begin{cases}
a^nx^n-b^n=0 & (\mu^n)\\
d^nx^n-e^n\le 0 & (\theta^n)\\
c^n+a^n\mu^n+d^n\theta^n=0 & \\
\mu^n,\theta^n\ge 0 & \\
c^nx^n=b^n\mu^n+e^n\theta^n &
\end{cases} \qquad \text{(B.15)}$$

Primal constraints of LL remain unchanged compared to the standard formulation. Dual constraints are derived by using the Lagrangian function (see 6.4) and additionally introducing inequalities ensuring that dual variables are greater than zero. The strong duality theorem equality is derived, as outlined in 6.4.

B.2 *Primal constraints*

The following primal constraints describe the entire LL problem. All non-indexed equations are displayed in 6.3.2.

$$\forall j\in\mathcal{J}^{PV},t\colon h^1 \quad = e^{NL}_{j,t}+e^{PVL}_{j,t}+e^{BSSL}_{j,t}-E^{L}_{j,t} \quad = 0 : \mu^{h^1}_{j,t}$$

$$\forall j\in\mathcal{J}^{PV},t\colon h^2 \quad = e^{PVN}_{j,t}+e^{PVL}_{j,t}+e^{PVBSS}_{j,t}+e^{PVC}_{j,t}-E^{PV}_{j,t}\cdot s^{PV}_{j} \quad = 0 : \mu^{h^2}_{j,t}$$

$$\begin{aligned}
\forall j\in\mathcal{J}^{PV},t\colon h^3 \quad &= soc_{j,t}-\eta^{BSSSd}\cdot soc_{j,t-1}-\eta^{BSSCh}\\
&\cdot e^{PVBSS}_{j,t}+(\eta^{BSSDis})^{-1}\cdot e^{BSSL}_{j,t} \qquad = 0 : \mu^{h^3}_{j,t}
\end{aligned}$$

$$\forall j \in \mathcal{J}^{PV} : g^1 = s_j^{PV} - S^{PV} \leq 0 : \theta_j^{g^1}$$

$$\forall j \in \mathcal{J}^{PV} : g^2 = s_j^{BSSkWh} - S^{BSSkWh} \leq 0 : \theta_j^{g^2} \tag{B.16}$$

$$\forall j \in \mathcal{J}^{PV} : g^3 = s_j^{BSSkW} - S^{BSSkW} \leq 0 : \theta_j^{g^3} \tag{B.17}$$

$$\forall j \in \mathcal{J}^{PV}, t : g^4 = e_{j,t}^{PVN} - S^{PV} \cdot E_{j,t}^{PV} \leq 0 : \theta_{j,t}^{g^4}$$

$$\forall j \in \mathcal{J}^{PV}, t : g^5 = e_{j,t}^{PVL} - S^{PV} \cdot E_{j,t}^{PV} \leq 0 : \theta_j^{g^5} \tag{B.18}$$

$$\forall j \in \mathcal{J}^{PV}, t : g^6 = e_{j,t}^{PVBSS} - S^{PV} \cdot E_{j,t}^{PV} \leq 0 : \theta_j^{g^6} \tag{B.19}$$

$$\forall j \in \mathcal{J}^{PV}, t : g^7 = e_{j,t}^{PVC} - S^{PV} \cdot E_{j,t}^{PV} \leq 0 : \theta_j^{g^7} \tag{B.20}$$

$$\forall j \in \mathcal{J}^{PV}, t : g^8 = e_{j,t}^{NL} - E_{j,t}^{L} \leq 0 : \theta_{j,t}^{g^8}$$

$$\forall j \in \mathcal{J}^{PV}, t : g^9 = e_{j,t}^{BSSL} - E_{j,t}^{L} \leq 0 : \theta_j^{g^9} \tag{B.21}$$

$$\forall j \in \mathcal{J}^{PV}, t : g^{10} = e_{j,t}^{PVL} - E_{j,t}^{L} \leq 0 : \theta_j^{g^{10}} \tag{B.22}$$

$$\forall j \in \mathcal{J}^{PV}, t : g^{11} = e_{j,t}^{PVN} - \kappa^{PVLim} \cdot \tau \cdot s_j^{PV} \leq 0 : \theta_{j,t}^{g^{11}}$$

$$\forall j \in \mathcal{J}^{PV}, t : g^{12} = e_{j,t}^{NL} + e_{j,t}^{PVN} - \tau \cdot p_j^{NL} \leq 0 : \theta_{j,t}^{g^{12}}$$

$$\forall j \in \mathcal{J}^{PV}, t : g^{13} = e_{j,t}^{PVBSS} - \tau \cdot s_j^{BSSkW} \leq 0 : \theta_{j,t}^{g^{13}}$$

$$\forall j \in \mathcal{J}^{PV}, t : g^{14} = e_{j,t}^{BSSL} - \tau \cdot s_j^{BSSkW} \leq 0 : \theta_j^{g^{14}} \tag{B.23}$$

$$\forall j \in \mathcal{J}^{PV}, t : g^{15} = soc_{j,t} - \kappa^{BSSUc} \cdot s_j^{BSSkWh} \leq 0 : \theta_{j,t}^{g^{15}}$$

As all decision variables of the LL problem are greater or equal to zero, additional constraints and relating dual variables are displayed below.

$$\forall j \in \mathcal{J}^{PV} : g^{16} = 0 - s_j^{PV} \leq 0 : \theta_j^{g^{16}} \tag{B.24}$$

$$\forall j \in \mathcal{J}^{PV} : g^{17} = 0 - s_j^{BSSkWh} \leq 0 : \theta_j^{g^{17}} \tag{B.25}$$

$$\forall j \in \mathcal{J}^{PV} : g^{18} = 0 - s_j^{BSSkW} \leq 0 : \theta_j^{g^{18}} \tag{B.26}$$

$$\forall j \in \mathcal{J}^{PV}, t : g^{19} = 0 - e_{j,t}^{PVN} \leq 0 : \theta_{j,t}^{g^{19}} \tag{B.27}$$

$$\forall j \in \mathcal{J}^{PV}, t : g^{20} = 0 - e_{j,t}^{PVL} \leq 0 : \theta_{j,t}^{g^{20}} \tag{B.28}$$

$$\forall j \in \mathcal{J}^{PV}, t : g^{21} = 0 - e_{j,t}^{PVBSS} \leq 0 : \theta_{j,t}^{g^{21}} \tag{B.29}$$

Dual variable $\theta_{j,t}^{g^{22}}$ is only necessary when a fixed curtailment limit is implemented, as $e_{j,t}^{PVC}$ is then a decision variable of the LL problem.

$$\forall j \in \mathcal{J}^{PV}, t\colon g^{22} = 0 - e_{j,t}^{PVC} \leq 0 : \theta_{j,t}^{g^{22}} \tag{B.30}$$

$$\forall j \in \mathcal{J}^{PV}, t\colon g^{23} = 0 - e_{j,t}^{NL} \leq 0 : \theta_{j,t}^{g^{23}} \tag{B.31}$$

$$\forall j \in \mathcal{J}^{PV}, t\colon g^{24} = 0 - e_{j,t}^{BSSL} \leq 0 : \theta_{j,t}^{g^{24}} \tag{B.32}$$

$$\forall j \in \mathcal{J}^{PV}\colon g^{25} = 0 - p_{j}^{NL} \leq 0 : \theta_{j}^{g^{25}} \tag{B.33}$$

$$\forall j \in \mathcal{J}^{PV}, t\colon g^{26} = 0 - soc_{j,t} \leq 0 : \theta_{j,t}^{g^{26}} \tag{B.34}$$

B.3 *Dual constraints*

Dual constraints are derived by partially differentiating the Lagrangian function for all decision variables of the LL problems (see Eq. 6.18).

$$\begin{aligned} \forall j \in \mathcal{J}^{PV}\colon \nabla_{s_j^{PV}} \mathcal{L} \quad &= \\ (I^{PV} + M^{PV} \cdot PF^{HH} - TE^{Dep} \cdot PF^{HH}) - \sum(\mu_{j,t}^{h^2} \cdot E_{j,t}^{PV}) & \\ + \theta_j^{g^1} - \sum_{t \in \mathcal{T}} (\theta_{j,t}^{g^{11}} \cdot \kappa^{PVLim}) - \theta_j^{g^{16}} \quad &= \quad 0 \end{aligned} \tag{B.35}$$

$$\begin{aligned} \forall j \in \mathcal{J}^{PV}\colon \nabla_{s_j^{BSSkWh}} \mathcal{L} \quad &= \\ (I^{BSSkWh} + M^{BSSkWh} \cdot PF^{HH}) & \\ + \theta_j^{g^2} - \sum_{t \in \mathcal{T}} (\theta_{j,t}^{g^{15}} \cdot \kappa^{BSSUc}) - \theta_j^{g^{17}} \quad &= \quad 0 \end{aligned} \tag{B.36}$$

$$\begin{aligned} \forall j \in \mathcal{J}^{PV}\colon \nabla_{s_j^{BSSkW}} \mathcal{L} \quad &= \\ (I^{BSSkW} + M^{BSSkW} \cdot PF^{HH}) + \theta_j^{g^3} & \\ - \sum_{t \in \mathcal{T}} (\theta_{j,t}^{g^{13}} \cdot \tau) - \sum_{t \in \mathcal{T}} (\theta_{j,t}^{g^{14}} \cdot \tau) - \theta_j^{g^{18}} \quad &= \quad 0 \end{aligned} \tag{B.37}$$

$$\begin{aligned} \forall j \in \mathcal{J}^{PV}, t\colon \nabla_{e_{j,t}^{PVN}} \mathcal{L} \quad &= \\ (TE^{Fit} - C^{Fit1}) \cdot PF^{HH} + \mu_{j,t}^{h^2} + \theta_{j,t}^{g^4} + \theta_{j,t}^{g^{11}} + \theta_{j,t}^{g^{12}} - \theta_{j,t}^{g^{19}} \quad &= \quad 0 \end{aligned} \tag{B.38}$$

$$\forall j \in \mathcal{J}^{PV}, t: \nabla_{e_{j,t}^{PVL}} \mathcal{L} =$$
$$(C^{Sc} + TE^{Sc}) \cdot PF^{HH} + \mu_{j,t}^{h^1} + \mu_{j,t}^{h^2} + \theta_{j,t}^{g^5} + \theta_{j,t}^{g^{10}} - \theta_{j,t}^{g^{20}} = 0 \quad \text{(B.39)}$$

$$\forall j \in \mathcal{J}^{PV}, t: \nabla_{e_{j,t}^{PVBSS}} \mathcal{L} =$$
$$\mu_{j,t}^{h^2} - \mu_{j,t}^{h^3} \cdot \eta^{BSSCh} + \theta_{j,t}^{g^6} + \theta_{j,t}^{g^{13}} - \theta_{j,t}^{g^{21}} = 0 \quad \text{(B.40)}$$

As mentioned above, if a fixed feed-in limit is imposed, $e_{j,t}^{PVC}$ is a decision variable of each LL problem. Thus, $\mathcal{L}$ needs to be differentiated accordingly as follows:

$$\forall j \in \mathcal{J}^{PV}, t: \nabla_{e_{j,t}^{PVC}} \mathcal{L} =$$
$$(TE^{Cur} - C^{Cur}) \cdot PF^{HH} + \mu_{j,t}^{h^2} + \theta_{j,t}^{g^7} - \theta_{j,t}^{g^{22}} = 0 \quad \text{(B.41)}$$

$$\forall j \in \mathcal{J}^{PV}, t: \nabla_{e_{j,t}^{NL}} \mathcal{L} =$$
$$(C^{En} + C^{eN,org} + c^{eN}) \cdot PF^{HH} + \mu_{j,t}^{h^1} + \theta_{j,t}^{g^8} + \theta_{j,t}^{g^{12}} - \theta_{j,t}^{g^{23}} = 0 \quad \text{(B.42)}$$

$$\forall j \in \mathcal{J}^{PV}, t: \nabla_{e_{j,t}^{BSSL}} \mathcal{L} =$$
$$(C^{Sc} + TE^{Sc}) \cdot PF^{HH} + \mu_{j,t}^{h^1} + \mu_{j,t}^{h^3} \cdot (\eta^{BSS,dis})^{-1}$$
$$+\theta_{j,t}^{g^9} + \theta_{j,t}^{g^{14}} - \theta_{j,t}^{g^{24}} = 0 \quad \text{(B.43)}$$

$$\forall j \in \mathcal{J}^{PV}: \nabla_{p_j^{NL}} \mathcal{L} =$$
$$(C^{pN,org} + c^{pN}) \cdot PF^{HH} - \sum_{t \in \mathcal{T}} (\theta_{j,t}^{g^{12}} \cdot \tau) - \theta_j^{g^{25}} = 0 \quad \text{(B.44)}$$

$$\forall j \in \mathcal{J}^{PV}, t \setminus T: \nabla_{soc_{j,t}} \mathcal{L} =$$
$$\mu_{j,t}^{h^3} - \mu_{j,t+1}^{h^3} \cdot \eta^{BSSSd} + \theta_{j,t}^{g^{15}} - \theta_{j,t}^{g^{26}} = 0 \quad \text{(B.45)}$$

B.4 *Parameters for the case studies*

The following table summarizes the parameters used in the case studies. Here, only changed parameters compared to the previous part are indicated.

As power-based NCs are not common for HH customers in Germany, C^{pNorg} are derived by assuming that for the case without PV BSSs, the same revenue as for energy-based NCs needs to be collected. The total

Parameter		Unit	Value
Tariffs	C^{En}	ct/kWh	26.40
	C^{eNorg}	ct/kWh	6.60
	C^{pNorg}	€/kW	44.63
	C^{Fit1}&C^{Cur}	ct/kWh	10.50
	C^{Sc}	ct/kWh	$16\,\% \cdot (C^{En} + C^{eNorg} + c^{eN})$
DNO	$C^{NR}_{r=1}$	€	11,000
	$P^{NR}_{r=1}$	kVA	250
PV BSS	S^{PV}	kWp	10.0
	I^{PV}	€/kWp	1,300
	I^{BSSkWh}	€/kWh	500
	I^{BSSkW}	€/kW	250
Other	A^{DNO}	a	40
	A^{HH}	a	20
	ERR^{DNO}	%	9.0
	ERR^{HH}	%	3.0
	$\mathcal{T}$	-	1..35,040

Table B.1: Input parameters for case studies

amount of NCs is divided by the sum of the individual load peaks for all profiles. Furthermore, present value factors PF^l for all future cash flows are calculated using the expected rate of return ERR^l and the asset life A^l as follows:

$$\forall \in [^{DNO}_{,}{}^{HH}] : PF^l = \frac{(1 + ERR^l)^{A^l} - 1}{(1 + ERR^l)^{A^l} \cdot ERR^l} \tag{B.46}$$

C

Appendix for Part III

C.1 *Additional key performance indicators*

C.1.1 *KPIs for component-specific costs*

Some previously presented KPIs (see section A.2.2) need to be adjusted to incorporate heat related costs. Additional heat related KPIs are introduced as well.

- Costs related to direct PV heat pump operation:

$$\begin{aligned} CPVHP_j &= \sum_{t\in\mathcal{T}}(e_{j,t}^{PVHP}\cdot(E_{j,t}^{PV}\cdot s_j^{PV})^{-1}) \\ &\cdot \quad ((I^{PV}+M^{PV}\cdot PF^{HH}-TE^{Dep})\cdot s_j^{PV}+In^{PV}\cdot b_j^{PV}) \\ &+ \quad ((C^{Sch1}+C^{Sch2}\cdot b_j^{SkWp})\cdot PF^{HH} \\ &+ \quad TE^{Sch})\sum_{t\in\mathcal{T}} e_{j,t}^{PVHP} \end{aligned} \tag{C.1}$$

- Costs related to indirect load supply through a BSS:

$$\begin{aligned} CBSS_j &= \sum_{t\in\mathcal{T}}(e_{j,t}^{PVBSS}\cdot(E_{j,t}^{PV}\cdot s_j^{PV})^{-1}) \\ &\cdot \quad ((I^{PV}+M^{PV}\cdot PF^{HH}-TE^{Dep})\cdot s_j^{PV}+In^{PV}\cdot b_j^{PV}) \\ &+ \quad (I^{BSSkWh}+M^{BSSkWh}\cdot PF^{HH})\cdot s_j^{BSSkWh} \\ &+ \quad (I^{BSSkW}+M^{BSSkW}\cdot PF^{HH})\cdot s_j^{BSSkW}+In^{BSS}\cdot b_j^{BSS} \\ &+ \quad ((C^{Sc1}+C^{Sc2}\cdot b_j^{SkWp})\cdot PF^{HH}+TE^{Sc})\sum_{t\in\mathcal{T}} e_{j,t}^{BSSL} \\ &+ \quad ((C^{Sch1}+C^{Sch2}\cdot b_j^{SkWp})\cdot PF^{HH} \\ &+ \quad TE^{Sch})\sum_{t\in\mathcal{T}}(e_{j,t}^{BSSHP}+e_{j,t}^{BSSEH}) \end{aligned} \tag{C.2}$$

- Costs related to PV network feed-in:

$$\begin{aligned} CPVN_j &= \sum_{t\in\mathcal{T}}((e_{j,t}^{PVN}+e_{j,t}^{PVC})\cdot(E_{j,t}^{PV}\cdot s_j^{PV})^{-1}) \\ &\cdot \quad ((I^{PV}+M^{PV}\cdot PF^{HH}-TE^{Dep})\cdot s_j^{PV}+In^{PV}\cdot b_j^{PV}) \\ &- \quad ((C^{Fit1}-C^{Fit2}\cdot b_j^{SkWp})\cdot PF^{HH} \\ &- \quad TE^{Fit})\sum_{t\in\mathcal{T}} e_{j,t}^{PVN} \end{aligned} \tag{C.3}$$

- Costs related to network demand for heat pump operation:

$$CNHP_j = C^{Eh} \cdot PF^{NL} \sum_{t \in \mathcal{T}} e_{j,t}^{NHP} \tag{C.4}$$

- Costs related to network demand for electrical heater operation:

$$CNEH_j = C^{Eh} \cdot PF^{NL} \sum_{t \in \mathcal{T}} e_{j,t}^{NEH} \tag{C.5}$$

- Costs related to natural gas demand for condensing boiler operation:

$$CCB_j = C^{Ng} \cdot PF^{Ng} \sum_{t \in \mathcal{T}} q_{j,t}^{CB} \tag{C.6}$$

C.2 *Additional case studies*

C.2.1 *Sensitivity analysis for future PV systems*

To assess the robustness of the ref. case and to account for the uncertainty inherent to the ref. data set, simulations are repeated with varied parameters. The results for the sensitivity analysis are presented in Fig. C.1. The results are ordered by first presenting results for the two parameters that impact the overall supply cost most significantly. Afterwards, first cost-revenue and then technical parameter variations for thermal components are displayed. Additional BSS related parameters are varied for scenario 'PV+HP+BSS' and are displayed at the bottom of the corresponding subplots. The same order is kept for the result presentation of PV system sizes, PV self-consumption and electrical self-sufficiency.

Several highlights can be pointed out for scenario 'PV+HP'. While the development of mean electricity prices over the next 20 years has the biggest impact on PV system sizing, the overall heat demand has the biggest impact on the overall supply cost. Compared to the ref. case, the median PV system size increases (decreases) from 3.9 kWp to 4.8 kWp for higher electricity prices and only to 4.3 kWp for more heat demand (2.9 kWp for lower prices and 3.5 kWp for less heat demand). A change in heat demand has nearly no impact on PV self-consumption as PV system sizes are adjusted accordingly. The change in electricity prices goes along with change in PV self-consumption (self-sufficiency) to 53.6 % (21.5 %) for high prices and 70.3 % (17.2 %) for low prices compared to 62.0 % (19.2 %) of the ref. scenario. By making self-supply more attractive, a higher electricity price also leads to higher PV feed-in and the heat pump is only able to absorb a bit of the additionally generated PV energy. The price for electricity used for heating impacts KPIs similarly to a change in overall electricity rate.

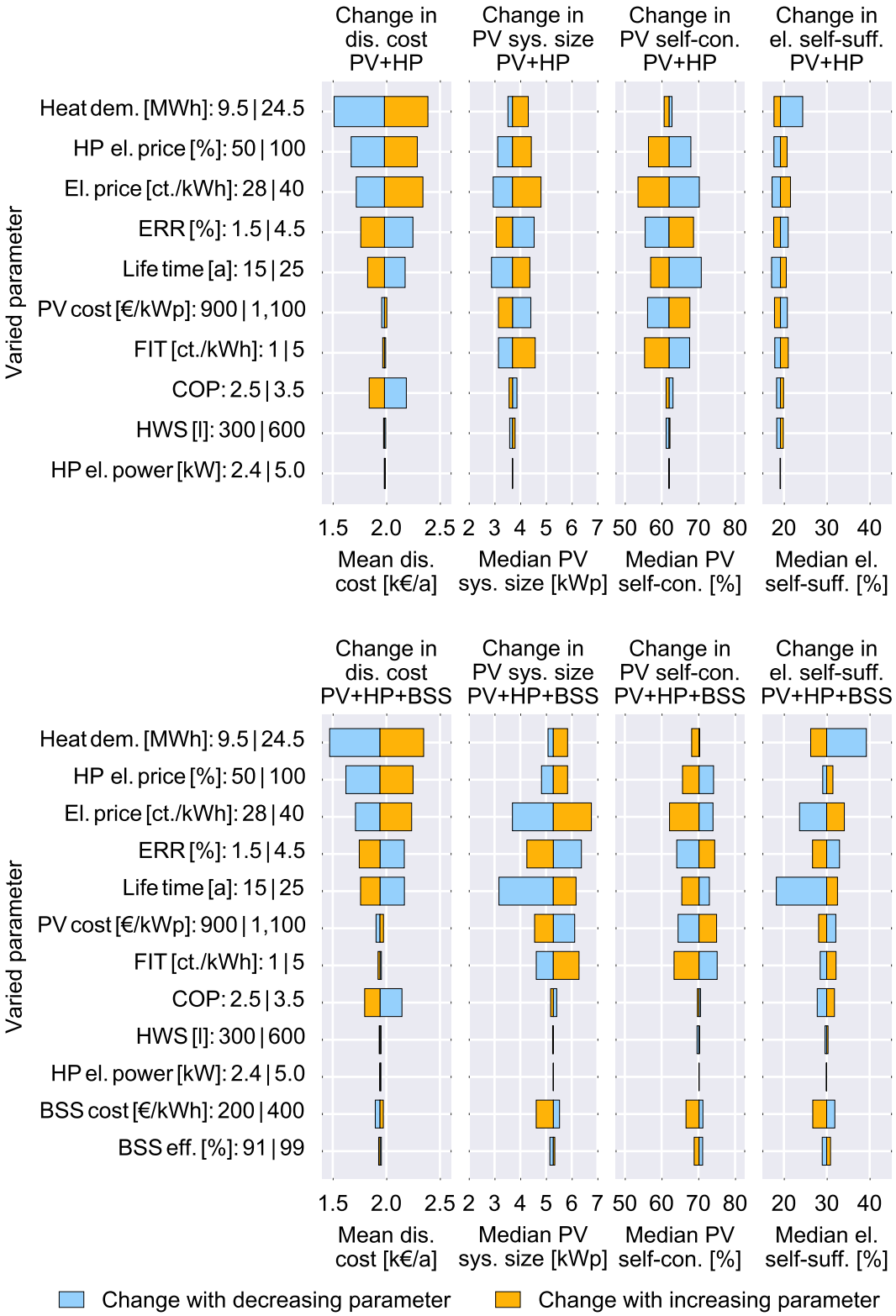

Figure C.1: Sensitivity analysis for median overall energy supply cost (left), for median PV sizes (left-middle), for median PV self-consumption (middle-right) and for median el. self-sufficiency (right) for scenarios 'PV+HP' (top) and 'PV+HP+BSS' (bottom)

A higher reimbursement of PV feed-in leads to a slightly lower increase in PV system size to 4.6 kWp, which goes along with a decline in PV self-consumption to 55.0 % and a marginal increase in self-sufficiency to 23.0 %. The overall supply costs only minimally improve, indicating that the economic benefit from additional self-supply can barely compensate the losses resulting from network feed-in despite the increased FIT. While different ERR result in similar sizes, lower PV system prices only lead to an increase of 0.9 kWp and higher PV system prices to a drop of 0.7 kWp. The results underline the importance of the value of self-consumption. Even with higher system prices PV self-consumption is still attractive.

Technical parameters of thermal components have a lower impact on sizing of power-heat systems than parameters that influence the value of self-generating or storing electricity, such as system costs or electricity prices. A better efficiency or a smaller HWS lead to a slight decrease in PV system size by 0.1 to 0.2 kWp. However, technical efficiency heavily impacts overall supply costs as a higher or lower COP can result in ± 10 % of cost variations while barely influencing system sizes.

Size sensitivity remains low for changes in thermal components when a BSS is introduced. Yet, the impact of changes in cost and revenue parameters is amplified in scenario 'PV+HP+BSS'. The median PV system size for ref. scenario lies at 5.3 kWp or 1.6 kWp above the case without BSSs. PV self-consumption and self-sufficiency increase to 70.2 % and 30.0 % as a BSS with a capacity of 6.4 kWh is introduced. A variation of the mean electricity price still results in the most significant change in PV system size (by 1.5 kWp to 6.8 kWp for high prices), which goes along with minor increase in BSS capacity to 7.9 kWh. The marginal value added in optimal BSS size reaches a limit. Even with a higher value of self-consumption, temporal and seasonal differences between PV generation and demand cannot fully be bridged with larger BSSs and the self-sufficiency only increases to 34.1 %. However, BSSs help reducing the decline of PV self-consumption with larger PV system sizes. It only drops to 62.1 %, which is still above PV self-consumption in scenario 'PV+HP'. Low electricity prices further underline the importance of the value of self-consumption. As refinancing conditions for BSSs become less attractive with lower prices, additional excess generation of PV energy is reduced and PV system sizes and BSS capacities drop to 3.7 kWp and 3.6 kWh. While self-sufficiency decreases to 23.7 %, PV self-consumption remains above 70.0 % as the decline in BSS capacity is compensated by a decrease in PV system size.

A change in ERR, FIT or PV system costs result also in slightly larger or smaller PV system sizes compared to the previous scenario as the leverage of BSSs on PV system sizes becomes more or less attractive. A clear differentiation between the different drivers of PV system sizes is possible when evaluating the change in overall supply costs. Higher electricity prices or a lower ERR lead to an increase of PV system size that is accompanied by larger BSS capacities. Here, additional PV generation primary aims at increasing self-supply as the overall supply cost rise. A higher FIT or lower

PV costs lead to a similar increase in sizes like lower ERR, but do not go along with a significant change in BSS capacity. Again, the attractiveness of PV feed-in rises and subsidies for feed-in slightly decrease, but a minimal reduction of overall supply costs is seen.

Changes of thermal parameters have a similar low impact on PV system sizes like in scenario 'PV+HP'. A lower or a higher yearly thermal demand leads to a slightly lower change in PV system size than when no BSS available, indicating a good complementarity between BSSs and heat pumps, but limited direct coupling potential. While BSS sizes see nearly no changes depending on heat demand, a BSS already increases PV system size and can partially compensate the need for a larger sized PV system as a result of higher heat demand. Similar effects are seen when electricity for heating purposes is priced differently as in the ref. scenario.

BSS efficiency does not have an impact on PV system sizing. That underlines that heat pump operation and BSS have limited coupling potential as even the possibility of close to loss-free BSS operation does not result in significant BSS discharging for heat pump operation. Higher BSS prices have a significant impact on the attractiveness of over-sizing PV systems; system sizes decrease by 0.7 kWp and 2.3 kWh compared to the ref. case. Lower BSS prices only have a small impact on the PV system size (+0.2 kWp and +2.0 kWh). That supports the conclusion that PV and BSS sizes are more determined by the load shifting potential and the overnight load than lower BSS prices (compare to section A.2.4).

Overall, demand and cost related parameters have a higher impact than technology parameters on PV system sizes. PV system sizes react more significantly to changes in electrical parameters than in thermal parameters. Seasonal differences in heat demand and PV generation drive PV heat pump operation. Here, BSS operation provides sufficient short-term, but not mid-to-long-term flexibility for load shifting. Using HWSs for mid-to-long-term storage is also not an attractive alternative. The sensitivity analysis shows a good complementarity between heat pumps and BSSs, but limited coupling potential for direct BSS heat pump operation.

C.2.2 *Impact of different heat profiles*

To evaluate the impact of different modeling approaches for thermal demand, an additional analysis is conducted that compares profiles generated based on the VDI approach and profiles with a variation of thermal demand of $\pm$ 10 % per time step to previous results. Fig. C.2 shows PV system sizes, PV self-consumption and self-sufficiency for the different modeling approaches for thermal demand.

The allowed $\pm$ 10 %-load variation only has a minor impact on PV system sizes, PV self-consumption and self-sufficiency for both IWES and VDI profiles. For both scenarios, median PV system sizes can slightly increase by 0.1 kWp for IWES and by 0.2 kWp for VDI profiles. The increase goes

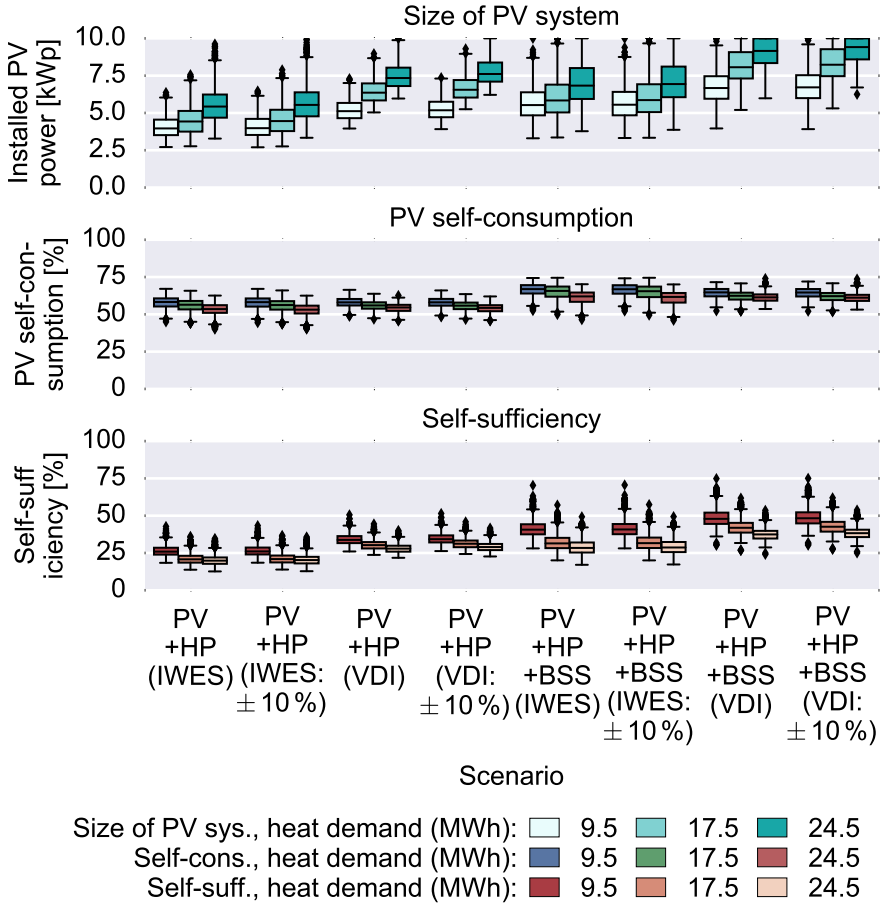

Figure C.2: PV system size (top), PV self-consumption (middle) and electric self-sufficiency for different thermal profiles and modeling approaches depending on the yearly thermal demand (with full electricity price for heat) for south-facing PV systems at location 1

along with minimal rise in median self-sufficiency by 0.2 to 0.6 %-points and a similar high decrease of PV self-consumption as larger systems allow covering more load but also result in a higher PV feed-in. As it is possible to shift thermal energy to PV producing hours, over-sizing of PV systems becomes a bit more attractive. However, it can be concluded that the HWS provides a sufficient option to decouple heat production from heat demand on a daily basis. More intraday flexibility does not significantly impact sizing and operation; seasonal differences in heat demand cannot be bridged.

Using a completely different modeling approach, such as the VDI approach, can lead to a significant change in results. For scenario 'PV+HP', median PV system sizes ranging from 4.0 to 5.4 kWp are observed with the IWES profiles and no variation, while the VDI profiles lead to median PV system sizes of 5.1 to 6.4 kWp depending on the yearly thermal demand. Thus, system sizes increase by approx. 1 kWp. The increase goes along with a rise in median self-supply from 19.9 to 25.9 % for IWES profiles to 27.9 to 33.8 for VDI profiles. PV self-consumption on the other hand

remains at similar high levels with 53.5 to 58.3 % for IWES profiles and 54.6 to 58.0 % for VDI profiles. The higher amount of self-supply can be explained through a higher overlap of PV generation and heat demand as heat demand is more evenly distributed over the entire year for the VDI profiles. For scenario 'PV+HP+BSS', the increase in PV system sizes in even higher. Median PV system sizes lie between 5.5 and 6.8 kWp for IWES profiles and increase to 6.7 to 9.2 kWp for VDI profiles. Here, an increase of 1.2 to 1.4 kWp is seen. Self-sufficiency rises from 28.4 to 40.6 % for IWES profiles to 37.5 to 41.9 % for VDI profiles. PV self-consumption remains again at similar levels for both types of profiles.

Differences in sizing and self-supply are a result of the different heat demand pattern as Fig. C.3 points out. It displays the fulfillment of heat and electricity demand as well as the usage of PV energy for scenario 'PV+HP+BSS' for the IWES and the VDI profile depending on the season. Seasons are defined according to the metric used to classify seasons for SLPs (see Tab. A.4).

The following differences between IWES and VDI profiles can be highlighted. The winter months comprise 79 % of the yearly heat demand with IWES profiles and only 64 % of the yearly heat demand with VDI profiles. This difference is compensated by a higher heat demand during spring and fall (25 %) as well as summer (11 %) with VDI profiles, while these periods only account for 17 % and 4 % with the IWES profiles. This general shift from heat demand from winter to spring, summer and fall when using VDI generated profiles allows for a higher amount of heat pump operation using PV energy and results in larger sized PV systems. Compared to the additional analyzed parameters, the impact of thermal demand modeling is comparable to the impact that a different overall thermal demand has. Cost related parameters tend to have a more significant impact.

C.2.3 *Energy flows analysis*

The sizing analysis points towards a good complementarity of heat pumps and BSSs in combination with PV systems. BSS sizes merely change depending on a variation of heat demand or heat related parameters, which suggests that BSSs are barely used to operate heat pumps, but mainly for standard load shifting. An explanation might be that seasonal differences in heat demand and excess PV energy provide a natural limit. Additionally, different pricing of standard and heat related electricity might impact operation as well. An energy flow analysis is conducted to confirm these hypotheses. Demand related energy flows are categorized and accumulated according to the seasons (based on dates used for SLPs (see section A.3)). To evaluate how BSS and heat pump influence PV usage and to avoid location induced effects due to varying heat demand or as a result of different PV system orientation, only one location and one PV system orientation is displayed in Fig. C.4.

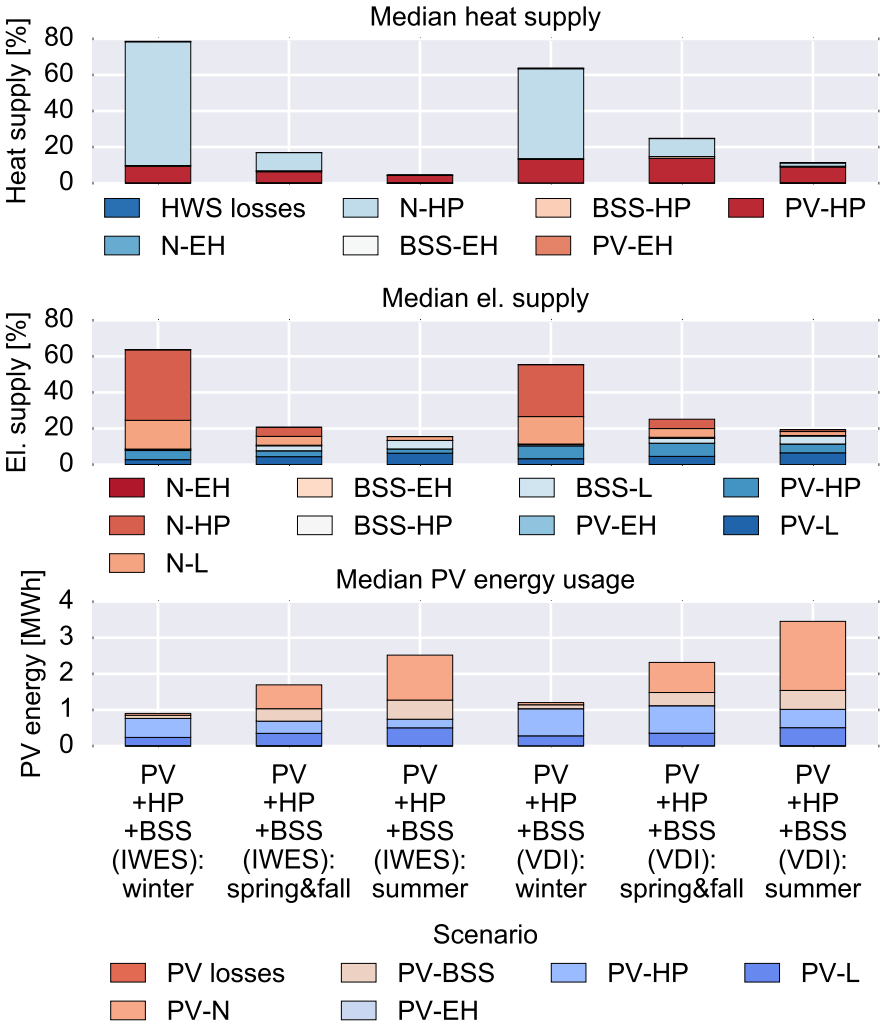

Figure C.3: Median distribution of energy flows to fulfill heat (top) and electric demand (middle) as well as usage of PV energy (bottom) for 'PV+HP+BSS' for IWES and VDI profile (yearly heat demand of 17.5 MWh) depending on the season

The distribution of energy flows according to seasons confirms the hypothesis that PV heat pump coupling is largely limited as a result of differences in heat demand and PV generation. While 79 % of the overall heat demand occurs in winter, only 18 % of PV energy is available then, imposing a natural limit despite the possibility of oversizing the PV system. Here, PV systems are in median 2.7 kWp larger when a heat pump installed with and without a BSS for the ref. case compared to the electricity only case. As a result more direct and indirect PV supply is possible, covering an additional 7 %-points of the standard load. The majority of additionally available PV energy is used for heating purposes. For the ref. case, approx. 14 % of the heat load in winter are served using PV energy without a BSS. With a BSS, it sinks to 11 %, indicating a slight competition between heat pump and BSS over excess PV energy. Differences are a result of the value of PV self-supply for standard demand and electricity for heating. As the latter

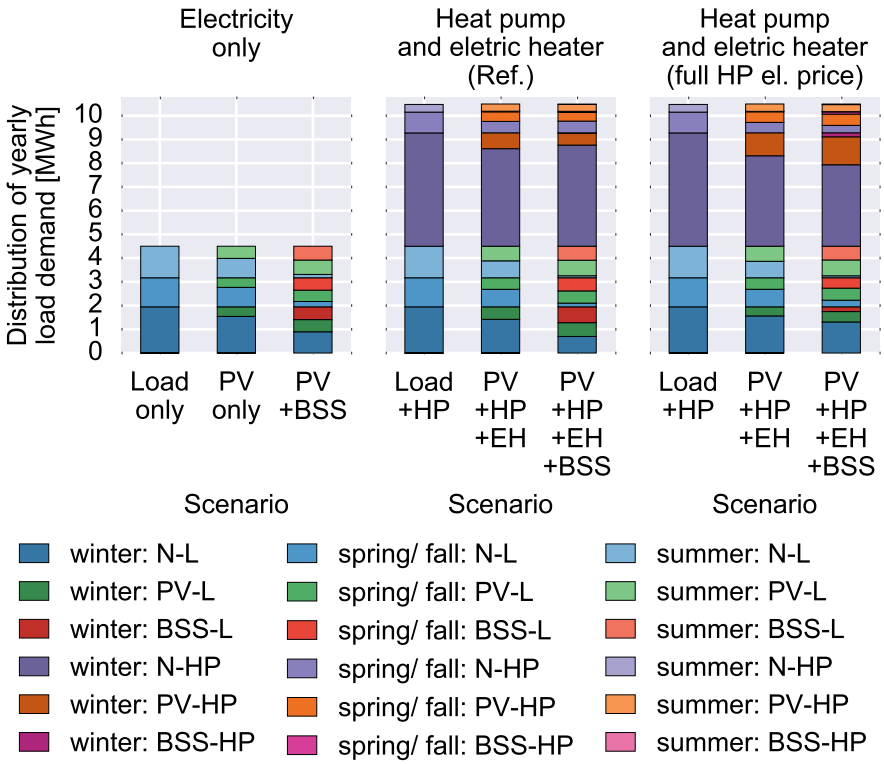

Figure C.4: Median distribution of energy flows according to different seasons for 'Electricity only' (left), 'Heat pump and electric heater (Reference case)' and 'Heat pump and electric heater (full electricity price for heat)' for south-facing PV systems at location 1

is purchased at a discount, it is more attractive to use self-generated PV energy for standard load supply. When a BSS is available as a second flexibility option, it is more attractive to operate a BSS for load shifting rather than to shift heat pump operation to mid-day hours at the cost of inefficiencies from HWS losses. The price difference also causes that BSS driven heat pump operation is rarely seen.

An equal electricity price for heating takes away the differentiation in self-consumption value, but also increases the overall energy supply costs. While the installed median BSS capacity is nearly equal to the case without heating and the ref. case, median PV system sizes increase to 6.3 kWp without and to 8.9 kWp with a BSS. As overall supply costs increase, a larger self-supply capability is desirable. For the case without BSS, direct PV load supply sinks to additional 2 %-points compared to 'Electricity only' despite higher amounts of excess PV energy, which is now used for heating purposes; PV heat supply increases to 29 % compared to 23 % for the ref. case. With a BSS, direct and indirect self-supply for standard load even decrease by 9 %-points compared to 'Electricity only'. Especially during winter time, heat pump operation is traded for less indirect load supply via BSS. It is more efficient to use excess PV energy for heating during certain days than using BSSs for load shifting, indicating that potential heat related losses

		Scenario (peak charges)					
		PV+HP			PV+HP+BSS		
		Full mod.	Mod. 100 %	Mod. 33 %	Full mod.	Mod. 100 %	Mod. 33 %
PV system size	kWp	4.4	4.1	4.5	5.8	5.2	5.9
BSS size	kWh	-	-	-	6.4	7.0	6.3
El. self-sufficiency	%	23.8	26.0	24.4	35.2	34.0	35.1
Th. self-sufficiency	%	17.9	10.7	17.8	22.3	15.9	19.6
PV self-consumption	%	52.8	68.4	53.3	61.3	67.8	61.0
Change in peak demand	%	-	5.5	0.0	-36.3	-21.5	-31.2

Table C.1: Results for different modulation capabilities for median demand profile for location 4 for 'PV+HP' and 'PV+HP+BSS' with peak charges

can economically outperform BSS losses during certain times. However, a coupling potential between BSSs and heat pumps also becomes visible. In winter, PV energy is now used for 28 % of the winter heat demand. BSS driven heat pump operation contributes 4 %-points here. Even higher values are seen for other seasons, but overall only 5 % of heat pump operation is based on BSS discharging.

Overall seasonal differences in heat demand and need for load shifting foster the complementary of heat pumps and BSSs. While excess PV energy for heat pump operation is especially used in winter and transition days that still require some heat supply, excess PV energy can also be used for load shifting through BSSs during those days. However, BSSs are beneficial for excess PV energy during summer days when no heat demand is available and network supply can be significantly reduced. Yet, load shifting potential is also not limitless here as it is defined by the amount of energy consumed during the night. BSS operation provides a good alternative for load shifting. Compared to BSS operation, mid-to-long-term thermal storage possibilities do not seem an attractive alternative.

C.2.4 *Flexibility analysis with peak charges*

Table C.1 displays the results for an additional flexibility case study. The same input parameters are used as in section 10.3.3, except for the electricity price. Here, a peak-oriented NC is introduced while energy-based NC are slightly reduced as described in the input data section.

It becomes visible that again inflexible heat pump operation can lead to smaller sized PV systems. BSSs can only partially compensate the loss of flexibility with regard to thermal self-sufficiency. However, they enable at least a partial reduction in peak demand and thus support network integration of heat pumps.

Acronyms

ARegV	German Incentive Regulation Ordinance
BSS	battery storage system
CAGR	compound annual growth rate
CHP	combined heat and power system
COP	coefficient of performance
DER	distributed energy resources
DNO	distribution network operator
DOD	depth-of-discharge
EEG	German Renewable Energy Act
EnWG	German Energy Industry Act
ERR	expected rate of return
FIT	feed-in tariff
GW	gigawatt
GWp	gigawatt peak
HH	household
HWS	hot water storage system
KPI	key performance indicator
kW	kilowatt
kWh	kilowatt hour
kWp	kilowatt peak
LL	lower level
LV	low voltage
MPPDC	mathematical program with primal and dual constraints
MILP	mixed integer linear programming
MWh	megawatt hour

NC	network charge
NPV	net present value
PV	photovoltaic
RES	renewable energy resource
SO	south-facing PV system
SE	south-east-facing PV system
SW	south-west-facing PV system
SLP	standard load profile
UL	upper level
VAT	value added tax

Nomenclature

The following nomenclature is used:

Superscripts, and General Symbols

a, b, c, d, e	General constraint vectors
f, g, h	Objective function, inequality, and equality constraints
θ^g, μ^h	Dual variables for inequality and equality constraints
x	General variable vectors
$\nabla \mathcal{L}$	Gradient of the Lagrangian function

Indices and Sets

$be \in \mathcal{B}$	Set of binary variables for linearization of increase of energy-based NCs
$j \in \mathcal{J}$	Household in the considered household set
k	General index for context-specific set
$k^S \in \mathcal{K}$	Scenario in corresponding scenario set
l	Temperature index

$r \in \mathcal{R}$	Network reinforcement measure in corresponding set
$t \in \mathcal{T}$	Time step for yearly simulation
$t^D \in \mathcal{T}^{\mathcal{D}}$	Day in day set
$u \in \mathcal{U}$	State of heat pump operation in corresponding set
$\mathcal{J}^{PV}, \mathcal{J}^{Load}$	Sub-set of HHs with and without a PV or PV BSS
$\mathcal{T}^{\mathcal{S}}$	Sub-set of all time steps during one day
B	Total number of binary variables for discretization of increase of energy-based NCs
J^{PV}	Total number of HHs with PV or PV BSS
J^{Load}	Total number of HHs without PV or PV BSS
R	Total number of network reinforcement measures
T^D	Length of a day
T^Y	Final time step of simulated year
U	Total states for heat pump operation

UL Parameter

A^{DNO}	Lifetime of DNO assets [a]
C^{eNorg}	Original energy-based NCs [EUR/kWh]
C^{pNorg}	Original power-based NCs [EUR/kW]
C_r^{NR}	Cost for network reinforcement measure r [EUR]
ERR^{DNO}	Expected rate of return for DNO [%]
P_r^{Lim}	Network capacity limit related to network reinforcement measure r [kW]
P_r^{NR}	Additional network capacity related to network reinforcement measure r [kW]
PF^{DNO}	Present value factor for DNO
W^e	Weight for energy-based NCs [kWh]
W^p	Weight for power-based NCs [kW]

UL Decision Variables

z_{UL}	Upper level objective function
c^{eN}	Increase in energy-based NCs [EUR/kWh]
c^{pN}	Increase in power-based NCs [EUR/kW]
ce_b	Linearizion variable for product of increase of energy-based NCs and network demand [EUR]

cp_d	Linearizion variable for product of increase of power-based NCs and network demand [EUR]
n_r^{bi}	Binary variable related to network reinforcement measure r [kW]
p^{PV}	Max. feed-in peak [kW]

LL Parameter and KPIs

A^{HH}	Lifetime of PV BSS [a]
C^{Cur}	Reimbursement of curtailed PV energy [EUR/kWh]
C^{E}	Electricity price [EUR/kWh]
C^{Eh}	Electricity price for heating electricity [EUR/kWh]
C^{En}	Electricity price without NCs [EUR/kWh]
C^{Fit1}	Feed-in tariff for PV network feed-in below or equal to 10 kWp[EUR/kWh]
C^{Fit2}	Feed-in tariff for PV network feed-in above 10 kWp[EUR/kWh]
C^{HPs}	Start costs of heat pump [EUR]
C^{Ng}	Natural gas price [EUR/kWh]
C^{P}	Peak charge [EUR/kW]
C^{Sc1}	Taxes on self-consumption below or equal to 10 kWp [EUR/kWh]
C^{Sc2}	Taxes on self-consumption above 10 kWp [EUR/kWh]
C^{Sch1}	Taxes on self-consumption for heating below or equal to 10 kWp [EUR/kWh]
C^{Sch2}	Taxes on self-consumption for heating above 10 kWp [EUR/kWh]
C^{S1}	Costs related to first sizing threshold for smart rollout per HH j
C^{S2}	Costs related to second sizing threshold for smart rollout per HH j
COP^{CB}	COP for natural gas boiler
COP^{EH}	COP for electric heater
COP_t^{HP}	COP for heat pump during each time step t
$E_{j,t}^{L}$	Electricity demand for HH j during each time step t [kWh]
$E_{j,t}^{PV}$	Normalized PV production for HH j during each time step t [kWh]
$E_{i,t}^{Res}$	Residual peak profiles depending on the number of HHs with a PV system i

ERR	Expected rate of return for HHs [%]
I^{PV}	Investment costs for PV system [EUR/kWp]
I^{BSSkWh}	Investment costs for capacity of BSS [EUR/kWh]
I^{BSSkW}	Investment costs for inverter of BSS [EUR/kW]
In^{PV}	Installation costs for PV system [EUR]
In^{BSS}	Installation costs for BSS [EUR]
M^{PV}	Yearly maintenance and operation costs for PV system [EUR/kWp]
M^{BSSkWh}	Yearly maintenance and operation costs for capacity of BSS [EUR/kWh]
M^{BSSkW}	Yearly maintenance and operation costs for inverter of BSS [EUR/kW]
$P^{HP}_{j,u}$	Power limit of heat pump for operation mode u per HH j [kW]
P^{NL}_{t}	Peak demand per HH j [kW]
P^{PVN}_{t}	Peak PV feed-in per HH j [kW]
P^{NLagg}	Aggregated peak demand [EUR]
PF^{HH}	Present value factor for HHs
$Q^{DHW}_{j,t}$	Hot water for HH j during each time step t [kWh]
$Q^{SH}_{j,t}$	Space heating demand for HH j during each time step t [kWh]
S^{CB}	Max. size of condensing gas boiler [kW]
S^{EH}	Max. size of electric heater [kW]
S^{HP}_{t}	Max. size of heat pump during each time step t [kW]
S^{PV}	Max. size of PV system [kWp]
S^{BSSkWh}	Max. size of capacity of BSS system [kWh]
S^{BSSkW}	Max. size of inverter of BSS system [kW]
SC_j	PV self-consumption per HH j [%]
SF^{NL}	Load simultaneity factor
SP_j	Self-sufficiency per HH j [%]
Sub^{BSS}	Percentage of BSS investment subsidy [%]
TE^{Dep}	Tax depreciation for investment in PV system [EUR/kWp]
TE^{Cur}	Taxes on earnings based on reimbursement of curtailed PV power [EUR/kWh]
TE^{Fit}	Taxes on earnings based on self-consumption of PV power [EUR/kWh]
TE^{Sc}	Taxes on earnings based on PV feed-in [EUR/kWh]
TE^{BSS}	Taxes on BSS investment incentive [%]

W^{Npv}	Weight for economic perference
W^{Self}	Weight for self-sufficiency perference
η^{BSSCh}	Charging efficiency of BSS
η^{BSSDis}	Discharging efficiency of BSS
η^{BSSSd}	Self-discharging of BSS
η^{HWSCh}	Charging efficiency of HWS
η^{HWSDis}	Discharging efficiency of HWS
η^{HWSSd}	Self-discharging of HWS
κ^{BSSCyc}	Allowed BSS cycles
κ^{BSSUc}	Usable capacity of BSS
κ^{HPdown}	Minimum down time for heat pump operation
κ^{HPup}	Minimum up time for heat pump operation
κ^{IncLim}	Feed-in limit for PV feed-in with BSS investment incentive
κ^{PVLim}	Feed-in limit for PV feed-in
κ^{Qmin}	Allowed thermal demand reduction
κ^{Qmax}	Allowed thermal demand increase
τ	Adjusting simulation step to timesteps

LL Decision Variables

z_{LL}	Lower level objective function
b_j^{PV}	Binary variable for PV installation per HH j
b_j^{BSS}	Binary variable for BSS installation per HH j
b_j^{BSSInc}	Binary variable for BSS investment incentive per HH j
b_j^{SkWp}	Binary variable for sizing threshold for PV per HH j
b_j^{S1}	Binary variable for first sizing threshold for smart rollout per HH j
b_j^{S2}	Binary variable for second sizing threshold for smart rollout per HH j
$b_{j,t}^{BSSChdis}$	Binary variable to avoid simultaneous BSS charging and discharging per HH j and time step t
$b_{j,t,u}^{HP}$	Set of binary variables for heat pump operation per HH j and time step t
$e_{j,t}^{BSSEH}$	Electric heater operation through BSS discharging for HH j during each time step t [kWh]
$e_{j,t}^{BSSHP}$	Heat pump operation through BSS discharging for HH j during each time step t [kWh]

$e_{j,t}^{BSSL}$ Load supply by BSS discharging for HH j during each time step t [kWh]

$e_{j,t,u}^{EH}$ Electricity used by electric heater for HH j during each time step t [kWh]

$e_{j,t,u}^{HP}$ Electricity used by heat pump for HH j during each time step t and in operation mode u [kWh]

$e_{j,t}^{NEH}$ Load for eletric heater from network for HH j during each time step t [kWh]

$e_{j,t}^{NHP}$ Load for heat pump from network for HH j during each time step t [kWh]

$e_{j,t}^{NL}$ Standard demand from network for HH j during each time step t [kWh]

$e_{j,t}^{PVBSS}$ PV BSS charging for HH j during each time step t [kWh]

$e_{j,t}^{PVC}$ PV curtailment for HH j during each time step t [kWh]

$e_{j,t}^{PVEH}$ PV for eletric heater for HH j during each time step t [kWh]

$e_{j,t}^{PVHP}$ PV for heat pump operation for HH j during each time step t [kWh]

$e_{j,t}^{PVL}$ Direct PV consumption for HH j during each time step t [kWh]

$e_{j,t}^{PVN}$ PV network feed-in for HH j during each time step t [kWh]

eb_{j}^{ScLin} Linearizion variable for product of self-consumption and binary variable for sizing [kWh]

eb_{j}^{FitLin} Linearizion variable for product of PV network feed-in and binary variable for sizing [kWh]

$o_{j,t}^{HPdown}$ Shut down variable for heat pump operation for HH j during each time step t [kWh]

$o_{j,t}^{HPup}$ Start variable for heat pump operation for HH j during each time step t [kWh]

p_{j}^{NL} Max. demand from network for HH j [kW]

$q_{j,t}^{CB}$ Natural gas demand for HH j during each time step t [kWh]

$q_{j,t}^{EH}$ Thermal energy provided by electric heater for HH j during each time step t [kWh]

$q_{j,t}^{HP}$ Thermal energy provided by heat pump for HH j during each time step t [kWh]

$q_{j,t}^{HWSL}$ Thermal load supply by HWS for HH j during each time step t [kWh]

$qsoc_{j,t}$	State of charge of HWS for HH j during each time step t [kWh]
r_j^{BSSInc}	Eligible BSS investment incentive for HH j [EUR]
s_j^{PV}	Size of PV system for HH j [kWp]
s_j^{BSSkWh}	Size of capacity of BSS system for HH j [kWh]
s_j^{BSSkW}	Size of inverter of BSS system for HH j [kW]
$soc_{j,t}$	State of charge of BSS for HH j during each time step t [kWh]

List of Figures

List of Tables

Publications and students

The following publications have been published during the course of this thesis or are currently under review.

Peer Reviewed Journal Publications (Listed)

- J. von Appen, M. Braun. "Interdependencies between self-sufficiency preferences, techno-economic drivers for investment decisions and grid integration of residential PV storage systems." Submitted to Applied Energy, currently under review, May. 2018.
- J. von Appen, M. Braun. "Strategic decision making of distribution network operators and investors in residential photovoltaic battery storage systems." Submitted to Applied Energy, currently under review, May. 2018.
- J. von Appen, M. Braun. "Sizing and improved grid integration of residential PV systems with heat pumps and battery storage systems." Submitted to IEEE Transactions on Energy Conversion and IEEE Journal of Emerging and Selected Topics in Power Electronics, currently under review, Apr. 2018.
- J. von Appen, T. Stetz, M. Braun, and A. Schmiegel. "Local Voltage Control Strategies for PV Storage Systems in Distribution Grids." In: IEEE Transactions on Smart Grid 5.2 (2014), pp. 1002–1009.

Journal Publications (Listed)

- J. von Appen, N. Gerhardt, C. Pape, B. Lehde, and J. Schmiesing. "PV-Eigenstromverbrauch: Treiber oder Bremse des PV-Zubaus?" In: BWK - Das Energie-Fachmagazin 12.2016 (2016), 47ff.
- T. Stetz, J. von Appen, F. Niedermeyer, G. Scheibner, R. Sikora, M. Braun. "Twilight of the Grids: The Impact of Distributed Solar on Germany's Energy Transition." In: IEEE Power and Energy Magazine 13.2 (2015), pp. 50-61.
- J. von Appen, M. Braun, T. Stetz, K. Diwold, D. Geibel. "Time in the Sun: The Challenge of High PV Penetration in the German Electric Grid." In: IEEE Power and Energy Magazine 11.2 (2013), pp. 55-64.

Conference Publications

- J. von Appen. "Incentive design, sizing and grid integration of residential PV systems with heat pumps and battery storage systems." 15th International Conference on the European Energy Market (EEM), Lodz, Jun. 2018.
- S. Engel, D. Nestle, E. Dörre, J. von Appen. "sema – Erkenntnisse aus dem Betrieb eines social energy management system." 15. Symposium Energieinnovation, Graz, Feb. 2018.
- C. Wittwer, M. Moser, B. Rech, R. Schlatmann, R. Brendel, R. Niepelt, J. von Appen, J. Hauch, F. Sehnke. "Rolle(n) der Photovoltaik im Energiesystem." In: FVEE – Jahrestagung, Berlin, Nov. 2016.
- B. Idlbi, J. von Appen, T. Kneiske, and M. Braun. "Cost-Benefit Analysis of Battery Storage System for Voltage Compliance in Distribution Grids with High Distributed Generation." In: Energy Procedia 99 (2016), pp. 215 –228, 10th International Renewable Energy Storage Conference and Exhibition, Düsseldorf, Mar. 2016.
- J. von Appen, M. Braun. "Grid integration of market-oriented PV storage systems." In: Proc. International ETG Congress 2015, Bonn, Nov. 2015.
- J. von Appen, J. H. Braslavsky, J. K. Ward, and M. Braun. "Sizing and grid impact of PV battery systems." In: 2015 Symposium on Smart Electric Distribution Systems and Technologies (EDST) Vienna, Sep. 2015.
- J. von Appen, A. Hettrich, M. Braun. "Grid planning and operation with increasing amounts of PV storage systems." In: 9th International Renewable Energy Storage Conference and Exhibition, Düsseldorf, Mar. 2015.
- J. von Appen, B. Burgenmeister, M. Braun. "Optimale Dimensionierung von PV-Speicher-Systemen unter Unsicherheit." In: 30. Symposium Photovoltaische Solarenergie, Bad Staffelstein, Mar. 2015.
- F. Niedermeyer, J. von Appen, M. Braun, A. Schmiegel, N. Kreutzer, M. Rothert, and A. Reischl. "Innovative Performancetests für PV - Speichersystemen zur Erhöhung der Autarkie und des Eigenverbrauchs." In: 30. Symposium Photovoltaische Solarenergie, Bad Staffelstein, Mar. 2015.
- A. Kanwar, D. Hidalgo, J. von Appen, M. Braun. "A Comparative Study of Optimization- and Rule-Based Control for Microgrid Operation." In: IEEE Power and Energy Student Summit, Dortmund, Jan. 2015.

- A. Hauer, P. Schossig, A. Wörner, P. Schumacher, B. Groß, K. Grashof, J. von Appen, D. Hidalgo, S. Kranz. "Wärmespeicher: Rolle im Energiesystem der Zukunft." In: FVEE – Jahrestagung, Berlin, Nov. 2014.
- J. von Appen, T. Stetz, B. Idlbi, M. Braun. "Enabling high amounts of PV systems in low voltage grids using storage systems." In: 29th European PV Solar Energy Conference, Amsterdam, Sep. 2014.
- H. Barth, B. Idlbi, J. von Appen, M. Braun, "Spannungshaltung und Leistungsausgleich erneuerbarer Energieerzeugung mittels Speichern im Mittelspannungsnetz." In: 2014 NEIS – Konferenz für Nachhaltige Energieversorgung und Integration von Speichern, Hamburg, 2014.
- F. Niedermeyer, J. von Appen, A. Schmiegel, N. Kreutzer, A. Reischl, W. Scheuerle, M. Braun. "Allgemeine Performanceindikatoren für PV-Speichersysteme." In: 29. Symposium Photovoltaische Solarenergie, Bad Staffelstein, Mar. 2014.
- T. Stetz, J. Töbermann, M. Kraiczy, J. von Appen, M. Braun, J. Brantl, S. Schmidt, A. Schmiegel, D. Premm, S. Bröscher, A. Jung, „Zusatznutzen von PV-Wechselrichtern mit kombinierter Q(U)-P(U)-Regelung in der Niederspannung." In: 29. Symposium Photovoltaische Solarenergie, Bad Staffelstein, Mar. 2014.
- J. von Appen, J. Haack, M. Braun. "Erzeugung zeitlich hochaufgelöster Stromlastprofile für verschiedene Haushaltstypen." In: IEEE Power and Energy Student Summit, Stuttgart, Jan. 2014.
- J. von Appen, M. Braun. "Assessment of Grid Supporting PV Storage systems." In: 8th International Renewable Energy Storage Conference and Exhibition, Berlin, Nov. 2013.
- J. von Appen, H. Barth, M. Braun, D. Hidalgo, P. Hochloff, P. Schumacher, H. Fink, „Dezentrale Strom- und Wärmespeicherung im Smart Grid," in Proc. 2013 Jahrestagung FVEE.
- A. Schmiegel, J. von Appen, M. Braun. "Untersuchungen zum Einfluss von eigenverbrauchsoptimierenden Betriebsführungen für PV-Speichersysteme auf ein Verteilnetz." In: NEIS – Konferenz für Nachhaltige Energieversorgung und Integration von Speichern, Hamburg, 2013.
- J. von Appen, M. Braun, T. Kneiske. "Voltage Control using PV Storage Systems in distribution systems." In: 22nd International Conference and Exhibition on Electricity Distribution (CIRED 2013), Stockholm, Jun. 2013..
- J. von Appen, M. Braun, T. Kneiske, A. Schmiegel. "Einfluss von PV-Speichersystemen auf das Niederspannungsnetz Betriebsführungen

für PV-Systeme und PV-Speichersysteme." In: 28. Photovoltaisches Symposium, Bad Staffelstein, 2013.

- A. Schmiegel, Y. Bennasia, J. von Appen, M. Braun. "Impact of PV storage systems on low voltage grids." In: 7th International Renewable Energy Storage Conference and Exhibition, Berlin, Nov. 2012.

- J. Binder, A.U. Schmiegel, D. Magnor, N. Martin, C. Williams, H.D. Mohring, M. Danzer, A. Linhart, D.-U. Sauer, M. Landau, J. von Appen, M. Braun, H. Schuh, U. Thomas, J.-C. Marcel, C. Jehoulet. "Sol-ion PV Storage System: Field Trial Results and Implications on Battery Lifetime Expectancy." In: 7th International Renewable Energy Storage Conference and Exhibition, Berlin, Nov. 2012.

- M. Braun, J. von Appen, H. Barth, T. Degner, K. Diwold, D. Geibel, E. Kämpf, F. Marten, F. Niedermeyer, T. Stetz. "Neue Auslegung und Betriebsführung von Verteilnetzen in dezentralen Versorgungsstrukturen." In: 17. Kasseler Symposium Energie-Systemtechnik, Kassel, 2012.

- J. von Appen, A. Schmiegel, M. Braun. "Impact of PV storage systems on low voltage grids." In: 27th European PV Solar Energy Conference, Frankfurt, 2012.

- J. Binder, H.D. Mohring, M. Danzer, O. Schanz, A.U. Schmiegel, A. Linhart, M. Landau, J. von Appen, F. Niedermeyer, M. Braun, D. Magnor, D.-U. Sauer, H. Schuh, U. Thomas, N. Martin, J. Marcel, C. Jehoulet. "Sol-Ion PV Storage System: Field Trial Results, Spread of Operating Conditions and Performance Evaluation Based on Field Data." In: 27th European PV Solar Energy Conference, Frankfurt, 2012.

- J. von Appen, M. Braun, R. Estrella. "A Framework for Different Storage Use Cases in Distribution Systems." In: CIRED 2012 Workshop, Lisbon May 2012.

- J. von Appen, M. Braun, B. Zinßer, D. Stellbogen. "Leistungsbegrenzung bei PV-Anlagen." In: 27. Symposium Photovoltaische Solarenergie, Bad Staffelstein, 2012.

- J. Binder, H.-D. Mohring, M. Landau, J. von Appen, M. Braun, A. U. Schmiegel, J. Marcel, N. Martin, U. Thomas, W. Woyke, M. Garhamer, D. Magnor, D.-U. Sauer, C. Jehoulet, H. Schuh. "Erfahrungen bei der Installation und beim Betrieb von PV Speichersystemen: Feldtest des Sol-ion Systems in Süddeutschland, Guadeloupe und an Forschungsinstituten." In: 27. Symposium Photovoltaische Solarenergie, Bad Staffelstein, 2012.

- M. Braun, J. von Appen, W. Yan, E. Kämpf, T. Stetz, C. Ma. "Maßnahmen für eine verbesserte PV-Netzintegration / Measures for improved PV grid integration." In: 2011 Internationaler ETG-Kongress, Würzburg, Nov. 2011.
- T. Stetz, J. von Appen, M. Braun, G. Wirth. "Cost-optimal Inverter Sizing for Ancillary Services." In: 26th European PV Solar Energy Conference, Hamburg, Sep. 2011.
- W. Yan, M. Braun, J. von Appen, E. Kämpf, M. Kraiczy, C. Ma, T. Stetz, S. Schmidt. "Operation Strategies in Distribution Systems with High Level PV Penetration." In: 2011 ISES Solar World Congress, Kassel, Jul. 2011.

Supervised student theses

- V. Rauth. "Optimized Control for Lithium-Ion Battery Ageing in Microgrid." Master's thesis at University of Kassel, Apr. 2015.
- J. Schiel. "Test und Optimierung unterschiedlicher Betriebsführungsalgorithmen zur Einspeiseleistungsbegrenzung von PV-Speichersystemen." Master's thesis at University of Kassel, Mar. 2015
- J. Haack. "Bilevel-optimisation for grid supporting operation of PV-battery systems." Master's thesis at University of Kassel, Mar. 2015.
- A. Hettrich. "Grid Impact Analysis and Economic Assessment of Market Price-Driven Operation Strategies for Residential PV Storage Systems." Master's thesis at University of Kassel, Mar. 2015.
- J. B. Burgenmeister. "Investitionsentscheidungen in dezentrale Photovoltaik-Speichersysteme." Master's thesis at University of Kassel, Jan. 2015.
- M. Valov. "Technische und wirtschaftliche Bewertung verschiedener Betriebsführungsstrategien für PV-Batteriesysteme in Niederspannungsnetzen." Diploma thesis at University of Kassel, Dec. 2013.
- A. Hashemi. "Optimizing Location of Battery System in a Grid with High PV Injections Using Particle Swarm Optimization Algorithm." Master's thesis at BTU Cottbus, May 2013.
- A. Talaat. "Forecast-based operation strategies for distributed storage in distribution systems." Master's thesis at Mines ParisTech, Dec. 2012.
- D. Coronado. "Analysis of Grid-Tied PV-Battery Systems and their Effect on the Low Voltage Grid." Master's thesis at Mines ParisTech, Dec. 2012.

- J. Haack. “Auswirkungen verschiedener Haushaltslastprofile auf PV-Batterie-Systeme.” Bachelor’s thesis at FH Flensburg, Dec. 2012.

Bibliography

[1] A. McCrone, U. Moslener, F. d'Estais, and C. Grüning. *Global Trends in Renewable Energy Investment 2017*. 2017.

[2] Fraunhofer ISE. *Net installed electricity generation capacity in Germany*. Online: accessed 2017-11-04. 2017. URL: https://www.energy-charts.de/power_inst.htm?year=all&period=annual&type=power_inst.

[3] Bundesverband der Solarwirtschaft (BSW-Solar). *Statistische Zahlen der deutschen Solarstrombranche (Photovoltaik)*. 2017.

[4] J. von Appen, T. Stetz, M. Braun, and A. Schmiegel. "Local Voltage Control Strategies for PV Storage Systems in Distribution Grids." In: *IEEE Trans. on Smart Grid* 5.2 (2014), pp. 1002–1009.

[5] J. Weniger, T. Tjaden, and V. Quaschning. "Sizing of Residential PV Battery Systems." In: *Energy Procedia* 46 (2014). 8th International Renewable Energy Storage Conference and Exhibition, pp. 78 –87.

[6] T. Stetz, J. von Appen, F. Niedermeyer, G. Scheibner, R. Sikora, and M. Braun. "Twilight of the Grids: The Impact of Distributed Solar on Germany's Energy Transition." In: *IEEE Power and Energy Magazine* 13.2 (2015), pp. 50–61.

[7] J. Figgener, D. Haberschusz, K.-P. Kairies, O. Wessels, B. Tepe, M. Ebbert, R. Herzog, and D. U. Sauer. *Wissenschaftliches Mess- und Evaluierungsprogramm Solarstromspeicher 2.0 - Jahresbericht 2017*. 2017. URL: http://www.speichermonitoring.de.

[8] Bundesverband der Solarwirtschaft (BSW-Solar). *Entwicklung PV- u. Speichermarkt*. 2018.

[9] KfW. *Erneuerbare Energien - Speicher*. Online: accessed 2018-01-01. URL: https://www.kfw.de/Download-Center/F%C3%B6rderprogramme-(Inlandsf%C3%B6rderung)/PDF-Dokumente/6000002700_M_275_Speicher.pdf.

[10] M. Braun, K. Büdenbender, D. Magnor, and A. Jossen. "PV self-consumption in Germany: using lithium-ion storage to increase self-consumed PV energy." In: *24th European PV Solar Energy Conference*. 2009.

[11] J. von Appen, J. H. Braslavsky, J. K. Ward, and M. Braun. "Sizing and grid impact of PV battery systems." In: *2015 Symp. on Smart Electric Distribution Systems and Technologies (EDST)*. 2015, pp. 612–619.

[12] T. Stetz, K. Diwold, M. Kraiczy, D. Geibel, S. Schmidt, and M. Braun. "Techno-Economic Assessment of Voltage Control Strategies in Low Voltage Grids." In: *IEEE Trans. on Smart Grid* 5.4 (2014), pp. 2125–2132.

[13] J. Büchner, J. Katzfey, O. Flörcken, A. Moser, H. Schuster, S. Dierkes, T. van Leeuwen, L. Verheggen, M. van Amelsvoort, and M. Uslar. *Moderne Verteilernetze für Deutschland (Verteilernetzstudie)*. Report for the German Ministry of Economics and Energy (BMWi). 2014.

[14] Bundesnetzagentur. *Monitoring report 2016*. Online: accessed 2017-09-01. 2017. URL: https://www.bundesnetzagentur.de/SharedDocs/Downloads/EN/BNetzA/PressSection/ReportsPublications/2016/MonitoringReport_2016.pdf;jsessionid=B5E7474D62A33CA43421766EE588A39A?__blob=publicationFile&v=3.

[15] Rocky Mountain Institute. *The economics of grid defection: When and where distributed solar generation plus storage competes with traditional utility service*. 2014.

[16] J. Jargstorf, C. De Jonghe, and R. Belmans. "Assessing the reflectivity of residential grid tariffs for a user reaction through photovoltaics and battery storage." In: *Sustainable Energy, Grids and Networks* 1 (2015), pp. 85 –98.

[17] R. Khalilpour and A. Vassallo. "Leaving the grid: An ambition or a real choice?" In: *Energy Policy* 82 (2015), pp. 207 –221.

[18] A. Kantamneni, R. Winkler, L. Gauchia, and J. M. Pearce. "Emerging economic viability of grid defection in a northern climate using solar hybrid systems." In: *Energy Policy* 95 (2016), pp. 378 –389.

[19] N. Gerhardt et al. *Interaktion EE-Strom, Wärme und Verkehr*. Project report. 2015.

[20] D. Fischer and H. Madani. "On heat pumps in smart grids: A review." In: *Renewable and Sustainable Energy Reviews* 70 (2017), pp. 342 –357.

[21] J. von Appen, N. Gerhardt, C. Pape, B. Lehde, and J. Schmiesing. "PV-Eigenstromverbrauch: Treiber oder Bremse des PV-Zubaus?" In: *BWK - Das Energie-Fachmagazin* 12 - 2016 (2016), 47ff.

[22] J. von Appen, B. Burgenmeister, and M. Braun. "Optimale Dimensionierung von PV-Speicher-Systemen unter Unsicherheit." In: *30. Symposium Photovoltaische Solarenergie*. 2015.

[23] J. von Appen, A. Hettrich, and M. Braun. "Grid planning and operation with increasing amounts of PV storage systems." In: *9th International Renewable Energy Storage Conference and Exhibition*. 2015.

[24] J. von Appen and M. Braun. "Grid integration of market-oriented PV storage systems." In: *Proc. Int. ETG Congress 2015*. 2015, pp. 1–8.

[25] J. von Appen and M. Braun. "Interdependencies between self- sufficiency preferences, techno-economic drivers for investment decisions and grid integration of residential PV storage systems." In: *Applied Energy* (2018). Currently under review.

[26] A. Zucker and T. Hinchliffe. "Optimum sizing of PV-attached electricity storage according to power market signals – A case study for Germany and Italy." In: *Applied Energy* 127 (2014), pp. 141 –155.

[27] Jochen Linssen, Peter Stenzel, and Johannes Fleer. "Techno-economic analysis of photovoltaic battery systems and the influence of different consumer load profiles." In: *Applied Energy* 185 (2017). Clean, Efficient and Affordable Energy for a Sustainable Future, pp. 2019 –2025.

[28] T. Beck, H. Kondziella, G. Huard, and T. Bruckner. "Assessing the influence of the temporal resolution of electrical load and PV generation profiles on self-consumption and sizing of PV-battery systems." In: *Applied Energy* 173 (2016), pp. 331 –342.

[29] T. Kaschub, P. Jochem, and W. Fichtner. "Solar energy storage in German households: profitability, load changes and flexibility." In: *Energy Policy* 98 (2016), pp. 520 –532.

[30] Y. Ru, J. Kleissl, and S. Martinez. "Storage Size Determination for Grid-Connected Photovoltaic Systems." In: *IEEE Trans. on Sustainable Energy* 4.1 (2013), pp. 68–81.

[31] A. Yoza, A. Yona, T. Senjyu, and T. Funabashi. "Optimal capacity and expansion planning methodology of PV and battery in smart house." In: *Renewable Energy* 69 (2014), pp. 25 –33.

[32] A. Askarzadeh. "Developing a discrete harmony search algorithm for size optimization of wind–photovoltaic hybrid energy system." In: *Solar Energy* 98 (2013), pp. 190 –195.

[33] O. Ekren and B. Y. Ekren. "Size optimization of a PV/wind hybrid energy conversion system with battery storage using simulated annealing." In: *Applied Energy* 87.2 (2010), pp. 592 –598.

[34] A. A. Al-Shamma'a and K. E. Addoweesh. "Optimum sizing of hybrid PV/wind/battery/diesel system considering wind turbine parameters using Genetic Algorithm." In: *2012 IEEE International Conference on Power and Energy (PECon)*. 2012, pp. 121–126.

[35] A. Kaabeche, M. Belhamel, and R. Ibtiouen. "Sizing optimization of grid-independent hybrid photovoltaic/wind power generation system." In: *Energy* 36.2 (2011), pp. 1214 –1222.

[36] M. Bruch and M. Müller. "Calculation of the Cost-effectiveness of a PV Battery System." In: *Energy Procedia* 46 (2014), pp. 262 –270.

[37] J. Hoppmann, J. Volland, T. Schmidt, and V. Hoffmann. "The economic viability of battery storage for residential solar PV systems - A review and a simulation model." In: *Renewable and Sustainable Energy Reviews* 39 (2014), pp. 1101 –1118.

[38] A. U. Schmiegel and A. Kleine. "Optimized Operation Strategies for PV Storages Systems Yield Limitations, Optimized Battery Configuration and the Benefit of a Perfect Forecast." In: *Energy Procedia* 46 (2014), pp. 104 –113.

[39] G. Merei, J. Moshövel, D. Magnor, and D. U. Sauer. "Optimization of self-consumption and techno-economic analysis of PV battery systems in commercial applications." In: *Applied Energy* 168 (2016), pp. 171 –178.

[40] G. Mulder, D. Six, B. Claessens, T. Broes, N. Omar, and J. Van Mierlo. "The dimensioning of PV battery sys. depending on the incentive and selling price conditions." In: *Applied Energy* 111 (2013), pp. 1126 –1135.

[41] E. Ratnam, S. Weller, and C. Kellett. "Scheduling residential battery storage with solar PV: Assessing the benefits of net metering." In: *Applied Energy* 155 (2015), pp. 881 –891.

[42] Z. Ren, G. Grozev, and A. Higgins. "Modelling impact of PV battery systems on energy consumption and bill savings of Australian houses under alternative tariff structures." In: *Renewable Energy* 89 (2016), pp. 317 –330.

[43] A. Colmenar-Santos, S. Campíñez-Romero, C. Pérez-Molina, and M. Castro-Gil. "Profitability analysis of grid-connected photovoltaic facilities for household electricity self-sufficiency." In: *Energy Policy* 51 (2012). Renewable Energy in China, pp. 749 –764.

[44] M. Bortolini, M. Gamberi, and A. Graziani. "Technical and economic design of photovoltaic and battery energy storage system." In: *Energy Conversion and Management* 86 (2014), pp. 81 –92.

[45] G. Brusco, A. Burgio, D. Menniti, A. Pinnarelli, and N. Sorrentino. "The economic viability of a feed-in tariff scheme that solely rewards self-consumption to promote the use of integrated photovoltaic battery systems." In: *Applied Energy* 183 (2016), pp. 1075 –1085.

[46] F. M. Vieira, P. S. Moura, and A. T. de Almeida. "Energy storage system for self-consumption of photovoltaic energy in residential zero energy buildings." In: *Renewable Energy* 103 (2017), pp. 308 – 320.

[47] R. Luthander, J. Widén, J. Munkhammar, and D. Lingfors. "Self-consumption enhancement and peak shaving of residential photovoltaics using storage and curtailment." In: *Energy* 112 (2016), pp. 221 –231.

[48] G. de Oliveira e Silva and P. Hendrick. "Photovoltaic self-sufficiency of Belgian households using lithium-ion batteries, and its impact on the grid." In: *Applied Energy* 195 (2017), pp. 786 –799.

[49] T. Khatib, I. A. Ibrahim, and A. Mohamed. "A review on sizing methodologies of photovoltaic array and storage battery in a standalone photovoltaic system." In: *Energy Conversion and Management* 120 (2016), pp. 430 –448.

[50] R. Luthander, J. Widén, D. Nilsson, and J. Palm. "PV self- consumption in buildings: A review." In: *Applied Energy* 142 (2015), pp. 80 –94.

[51] R. Loulou and M. Labriet. "ETSAP-TIAM: the TIMES integrated assessment model Part I: Model structure." In: *Computational Management Science* 5.1 (2008), pp. 7–40.

[52] F. J. Rubio, A. S. Siddiqui, C. Marnay, and K. S. Hamachi. "CERTS Customer Adoption Model." In: (2011).

[53] M. Stadler, C. Marnay, A. S. Siddiqui, J. Lai, B. Coffey, and H. Aki. "Effect of Heat and Electricity Storage and Reliability on Microgrid Viability: A Study of Commercial Buildings in California and New York State." In: (2009).

[54] HOMER Energy. *HOMER Pro - Software For Designing Optimized Hybrid Microgrids*. Online: accessed 2017-04-20. URL: `http://www.homerenergy.com/HOMER_pro.html`.

[55] G. Mendes, C. Ioakimidis, and P. Ferrão. "On the planning and analysis of Integrated Community Energy Systems: A review and survey of available tools." In: *Renewable and Sustainable Energy Reviews* 15.9 (2011), pp. 4836 –4854.

[56] M. Fadaee and M.A.M. Radzi. "Multi-objective optimization of a stand-alone hybrid renewable energy system by using evolutionary algorithms: A review." In: *Renewable and Sustainable Energy Reviews* 16.5 (2012), pp. 3364 –3369.

[57] R. Luna-Rubio, M. Trejo-Perea, D. Vargas-Vázquez, and G.J. Ríos-Moreno. "Optimal sizing of renewable hybrids energy systems: A review of methodologies." In: *Solar Energy* 86.4 (2012). ISRES 2010, pp. 1077 –1088.

[58] S. Sinha and S. S. Chandel. "Review of recent trends in optimization techniques for solar photovoltaic–wind based hybrid energy systems." In: *Renewable and Sustainable Energy Reviews* 50 (2015), pp. 755 –769.

[59] C. Gamarra and J. M. Guerrero. "Computational optimization techniques applied to microgrids planning: A review." In: *Renewable and Sustainable Energy Reviews* 48 (2015), pp. 413 –424.

[60] Y. Riffonneau, S. Bacha, F. Barruel, and S. Ploix. "Optimal Power Flow Management for Grid Connected PV Systems With Batteries." In: *IEEE Trans. on Sustainable Energy* 2.3 (2011), pp. 309–320.

[61] M. J. E. Alam, K. M. Muttaqi, and D. Sutanto. "Mitigation of Rooftop Solar PV Impacts and Evening Peak Support by Managing Available Capacity of Distributed Energy Storage Systems." In: *IEEE Trans. on Power Systems* 28.4 (2013), pp. 3874–3884.

[62] J. Bergner, J. Weniger, T. Tjaden, and V. Quaschning. "Feed-in Power Limitation of Grid-Connected PV Bat. Systems with Autonomous Forecast-Based Operation Strategies." In: *29th European PV Solar Energy Conference*. 2014.

[63] F. Braam, R. Hollinger, M. Llerena Engesser, S. Muller, R. Kohrs, and C. Wittwer. "Peak shaving with photovoltaic-battery systems." In: *Innovative Smart Grid Technologies Conference Europe (ISGT-Europe), 2014 IEEE PES*. 2014, pp. 1–5.

[64] P. Harsha and M. Dahleh. "Optimal Management and Sizing of Energy Storage Under Dynamic Pricing for the Efficient Integration of RE." In: *IEEE Trans. on Power Systems* 30.3 (2015), pp. 1164–1181.

[65] J. Moshövel, K.-P. Kairies, D. Magnor, M. Leuthold, M. Bost, S. Gährs, E. Szczechowicz, M. Cramer, and D. U. Sauer. "Analysis of the maximal possible grid relief from PV-peak-power impacts by using storage systems for increased self-consumption." In: *Applied Energy* 137 (2015), pp. 567 –575.

[66] J. Müller, M. März, I. Mauser, and H. Schmeck. "Optimization of Operation and Control Strategies for Battery Energy Storage Systems by Evolutionary Algorithms." In: *Applications of Evolutionary Computation: 19th European Conference, EvoApplications 2016, Porto, Portugal, March 30 – April 1, 2016, Proceedings, Part I*. Ed. by G. Squillero and P. Burelli. Cham: Springer International Publishing, 2016, pp. 507–522.

[67] J. Tant, F. Geth, D. Six, P. Tant, and J. Driesen. "Multiobjective Battery Storage to Improve PV Integration in Residential Distribution Grids." In: *IEEE Trans. on Sustainable Energy* 4.1 (2013), pp. 182–191.

[68] C. Heinrich, P. Fortenbacher, A. Fuchs, and G. Andersson. "PV- integration strategies for low voltage networks." In: *2016 IEEE International Energy Conference (ENERGYCON)*. 2016, pp. 1–6.

[69] F. Marra, Guangya Yang, C. Traeholt, J. Ostergaard, and E. Larsen. "A Decentralized Storage Strategy for Residential Feeders With PV." In: *IEEE Trans. on Smart Grid* 5.2 (2014), pp. 974–981.

[70] E. L. Ratnam, S. R. Weller, and C. M. Kellett. "Central versus localized optimization-based approaches to power management in distribution networks with residential battery storage." In: *International Journal of Electrical Power and Energy Systems* 80 (2016), pp. 396 –406.

[71] D. Parra, S. A. Norman, G. S. Walker, and M. Gillott. "Optimum community energy storage for renewable energy and demand load management." In: *Applied Energy* 200 (2017), pp. 358 –369.

[72] Y. Yang, H. Li, A. Aichhorn, J. Zheng, and M. Greenleaf. "Sizing Strategy of Distributed Battery Storage System With High Penetration of PV for Voltage Regulation and Peak Load Shaving." In: *IEEE Trans. on Smart Grid* 5.2 (2014), pp. 982–991.

[73] B. Idlbi, J. von Appen, T. Kneiske, and M. Braun. "Cost-Benefit Analysis of Battery Storage System for Voltage Compliance in Distribution Grids with High Distributed Generation." In: *Energy Procedia* 99 (2016). 10th International Renewable Energy Storage Conference, IRES 2016, 15-17 March 2016, Düsseldorf, Germany, pp. 215 –228.

[74] M. Graebig, G. Erdmann, and S. Röder. "Assessment of residential battery systems (RBS): profitability, perceived value proposition, and potential business models." In: *37th IAEE International Conference, New York City*. 2014.

[75] W. Hart, C. Laird, J.-P. Watson, and D. Woodruff. "Pyomo: modeling and solving mathematical programs in Python." In: *Mathematical Programming Computation* 3.3 (2011), pp. 219–260.

[76] W. Hart, C. Laird, J.-P. Watson, and D. Woodruff. *Pyomo–optimization modeling in python*. Vol. 67. Springer Science & Business Media, 2012.

[77] Bayerisches Landesamt für Steuern. *Hilfe zu Photovoltaikanlagen*. Online: accessed 2018-01-01. URL: https://www.finanzamt.bayern.de/Informationen/download.php?url=Informationen/Steuerinfos/Weitere_Themen/Photovoltaikanlagen/Hilfe_fuer_Photovoltaikanlagen_2015-02.pdf.

[78] S. Buller. "Impedance-Based Simulation Models for Energy Storage Devices in Advanced Automotive Applications." PhD thesis. 2002.

[79] H.P. Williams. *Model Building in Mathematical Programming*. Wiley, 2013.

[80] T. Stetz, H. Wolf, A. Probst, S. Eilenberger, Y.-M. Saint Drenan, E. Kämpf, M. Braun, D. Schöllhorn, and S. Schmidt. "Stochastische Analyse von Smart-Meter Messdaten." In: *VDE-Kongress 2012*. 2012.

[81] T. Stetz. "Autonomous Voltage Control Strategies in Distribution Grids with Photovoltaic Systems." PhD thesis. 2013.

[82] Deutsche Energie-Agentur GmbH (dena). *dena - Verteilnetzstudie*. Tech. rep. 2012. URL: https://shop.dena.de/fileadmin/denashop/media/Downloads_Dateien/esd/9100_dena-Verteilnetzstudie_Abschlussbericht.pdf.

[83] J. von Appen, T. Stetz, B. Idlbi, and M. Braun. "Enabling high amounts of PV systems in low voltage grids using storage systems." In: *29th European PV Solar Energy Conference*. 2014.

[84] K.-P. Kairies, D. Haberschusz, J. van Ouwererk, J. Strebel, O. Wessels, D. Magnor, J. Badeda, and D. U. Sauer. *Wissenschaftliches Mess- und Evaluierungsprogramm Solarstromspeicher - Jahresbericht 2016*. 2016. URL: http://www.speichermonitoring.de.

[85] Bundesnetzagentur. *Netz- und Systemsicherheitsmaßnahmen Überblick zum vierten Quartal 2016 und der Gesamtjahresbetrachtung 2016*. Online: accessed 2017-09-01. 2017. URL: https://www.bundesnetzagentur.de/SharedDocs/Downloads/DE/Sachgebiete/Energie/Unternehmen_Institutionen/Versorgungssicherheit/System-_u_Netzsicherheit/Kurzinformationen_Q4_2016.pdf?__blob=publicationFile&v=4.

[86] J. Büchner, J. Katzfey, O. Flörcken, A. Moser, H. Schuster, S. Dierkes, T. van Leeuwen, L. Verheggen, M. van Amelsvoort, and M. Uslar. "Smart Grids in Germany: How much costs do distribution grids cause at planning time?" In: *2015 Symp. on Smart Electric Distribution Systems and Technologies (EDST)*. 2015, pp. 224–229.

[87] J. von Appen and M. Braun. "Strategic decision making of distribution network operators and investors in residential photovoltaic battery storage systems." In: *Applied Energy* (2018). Currently under review.

[88] H. Wang, N. Good, P. Mancarella, and K. Lintern. "PV-battery community energy systems: Economic, energy independence and network deferral analysis." In: *2017 14th International Conference on the European Energy Market (EEM)*. 2017, pp. 1–5.

[89] E. Hittinger and J. Siddiqui. "The challenging economics of {US} residential grid defection." In: *Utilities Policy* 45 (2017), pp. 27 –35.

[90] N. R. Darghouth, R. H. Wiser, G. Barbose, and A. D. Mills. "Net metering and market feedback loops: Exploring the impact of retail rate design on distributed {PV} deployment." In: *Applied Energy* 162 (2016), pp. 713 –722.

[91] N. D. Laws, B. P. Epps, S. O. Peterson, M. S. Laser, and G. Kamau Wanjiru. "On the utility death spiral and the impact of utility rate structures on the adoption of residential solar photovoltaics and energy storage." In: *Applied Energy* 185 (2017), pp. 627 –641.

[92] C. Cervilla, J. Villar, and F. A. Campos. "Bi-level optimization of electricity tariffs and PV distributed generation investments." In: *2015 12th International Conference on the Euro. Energy Market (EEM)*. 2015, pp. 1–5.

[93] T. Stetz, F. Marten, and M. Braun. "Improved Low Voltage Grid-Integration of Photovoltaic Systems in Germany." In: *IEEE Trans. on Sustainable Energy* 4.2 (2013), pp. 534–542.

[94] J. von Appen, M. Braun, T. Stetz, K. Diwold, and D. Geibel. "Time in the Sun: The Challenge of High PV Penetration in the German Electric Grid." In: *IEEE Power and Energy Magazine* 11.2 (2013), pp. 55–64.

[95] S. Gabriel, A. Conejo, J. Fuller, B. Hobbs, and C. Ruiz. *Complementarity Modeling in Energy Markets*. Springer, 2012.

[96] H. von Stackelberg. *Market Structure and Equilibrium*. Springer, 2011.

[97] D. S. Kirschen. "Demand-side view of electricity markets." In: *IEEE Trans. on Power Systems* 18.2 (2003), pp. 520–527.

[98] J. Nash. "Non-cooperative games." In: *The Annals of Mathematics* (1951), pp. 286–295.

[99] B. F. Hobbs, C. B. Metzler, and J. S. Pang. "Strategic gaming analysis for electric power systems: an MPEC approach." In: *IEEE Trans. on Power Systems* 15.2 (2000), pp. 638–645.

[100] S. Jin and S. M. Ryan. "A Tri-Level Model of Central. Transmission and Decentral. Generation Expansion Planning for an Electricity Market." In: *IEEE Trans. on Power Systems* 29.1 (2014), pp. 132–141.

[101] E. Nasrolahpour, S. J. Kazempour, H. Zareipour, and W. D. Rosehart. "Strategic Sizing of Energy Storage Facilities in Electricity Markets." In: *IEEE Trans. on Sustainable Energy* PP.99 (2016), pp. 1–1.

[102] S. M. Miri-Larimi, M. R. Haghifam, and E. Jalilzadeh. "Optimal sitting and sizing of renewable energy resources in distribution network with Bi-Level optimization." In: *CIRED 2012 Workshop*. 2012, pp. 1–4.

[103] Bundesnetzagentur. *EEG-Vergütungssätze für Photovoltaikanlagen*. Online: accessed 2017-01-01. 2017. URL: http://www.bnetza.de.

[104] S. N. Petrović and K. B. Karlsson. "Residential heat pumps in the future Danish energy system." In: *Energy* 114 (2016), pp. 787 –797.

[105] J. von Appen and M. Braun. "Sizing and improved grid integration of residential PV systems with heat pumps and battery storage systems." In: *IEEE Trans. on Energy Conversion* (2018). Currently under review.

[106] J. von Appen. "Incentive design, sizing and grid integration of residential PV systems with heat pumps and battery storage systems." In: *2018 15th International Conference on the European Energy Market (EEM)*. Accepted for publication. 2018.

[107] R. S. Kamel, A. S. Fung, and P. R.H. Dash. "Solar systems and their integration with heat pumps: A review." In: *Energy and Buildings* 87 (2015), pp. 395 –412.

[108] A. Modi, F. Bühler, J. G. Andreasen, and F. Haglind. "A review of solar energy based heat and power generation systems." In: *Renewable and Sustainable Energy Reviews* 67 (2017), pp. 1047 –1064.

[109] F. Ochs, G. Dermentzis, and W. Feist. "Minimization of the Residual Energy Demand of Multi-storey Passive Houses – Energetic and Economic Analysis of Solar Thermal and PV in Combination with a Heat Pump." In: *Energy Procedia* 48 (2014). Proceedings of the 2nd International Conference on Solar Heating and Cooling for Buildings and Industry (SHC 2013), pp. 1124 –1133.

[110] A. Franco and F. Fantozzi. "Experimental analysis of a self consumption strategy for residential building: The integration of PV system and geothermal heat pump." In: *Renewable Energy* 86 (2016), pp. 1075 –1085.

[111] P. Mancarella. "MES (multi-energy systems): An overview of concepts and evaluation models." In: *Energy* 65 (2014), pp. 1 –17.

[112] J. Allegrini, K. Orehounig, G. Mavromatidis, F. Ruesch, V. Dorer, and R. Evins. "A review of modelling approaches and tools for the simulation of district-scale energy systems." In: *Renewable and Sustainable Energy Reviews* 52 (2015), pp. 1391 –1404.

[113] S. Mashayekh, M. Stadler, G. Cardoso, and M. Heleno. "A mixed integer linear programming approach for optimal DER portfolio, sizing, and placement in multi-energy microgrids." In: *Applied Energy* 187 (2017), pp. 154 –168.

[114] A. Ashouri, S. S. Fux, M. J. Benz, and L. Guzzella. "Optimal design and operation of building services using mixed-integer linear programming techniques." In: *Energy* 59 (2013), pp. 365 –376.

[115] T. Capuder and P. Mancarella. "Techno-economic and environmental modelling and optimization of flexible distributed multi- generation options." In: *Energy* 71 (2014), pp. 516 –533.

[116] T. Falke and A. Schnettler. "Investment planning of residential energy supply systems using dual dynamic programming." In: *Sustainable Cities and Society* 23 (2016), pp. 16 –22.

[117] P. Balcombe, D. Rigby, and A. Azapagic. "Energy self-sufficiency, grid demand variability and consumer costs: Integrating solar PV, Stirling engine CHP and battery storage." In: *Applied Energy* 155 (2015), pp. 393 –408.

[118] D. Fischer, K. B. Lindberg, H. Madani, and C. Wittwer. "Impact of PV and variable prices on optimal system sizing for heat pumps and thermal storage." In: *Energy and Buildings* 128 (2016), pp. 723 –733.

[119] S. Zurmühlen, H. Wolisz, G. Angenendt, D. Magnor, R. Streblow, D. Müller, and D. U. Sauer. "Potential and Optimal Sizing of Combined Heat and Electrical Storage in Private Households." In: *Energy Procedia* 99 (2016). 10th International Renewable Energy Storage Conference, IRES 2016, 15-17 March 2016, Düsseldorf, Germany, pp. 174 –181.

[120] T. Beck, H. Kondziella, G. Huard, and T. Bruckner. "Optimal operation, configuration and sizing of generation and storage technologies for residential heat pump systems in the spotlight of self-consumption of photovoltaic electricity." In: *Applied Energy* 188 (2017), pp. 604 –619.

[121] B. S. Palmintier and M. D. Webster. "Impact of Operational Flexibility on Electricity Generation Planning With Renewable and Carbon Targets." In: *IEEE Trans. on Sustainable Energy* 7.2 (2016), pp. 672–684.

[122] C. Williams, J. Binder, and T. Kelm. "Demand side management through heat pumps, thermal storage and battery storage to increase local self-consumption and grid compatibility of PV systems." In: *2012 3rd IEEE PES Innovative Smart Grid Technologies Europe (ISGT Europe)*. 2012, pp. 1–6.

[123] J. Binder, C. Williams, and T. Kelm. "Increasing PV self-consumption, domestic energy autonomy and grid compatibility of PV systems using heat-pumps, thermal storage and battery storage." In: *Proceedings of the 27th European photovoltaic solar energy conference*. 2012, pp. 24–28.

[124] T. Tjaden, F. Schnorr, J. Weniger, J. Bergner, and V. Quaschning. "Einsatz von PV-Systemen mit Wärmepumpen und Batteriespeichern zur Erhöhung des Autarkiegrades in Einfamilienhaushalten." In: *30. Symposium Photovoltaische Solarenergie*. 2015.

[125] T. Tjaden, J. Weniger, J. Bergner, and V. Quaschning. "Beitrag von Solarspeichersystemen zur autarken Strom-und Wärmeversorgung von Gebäuden in Niederspannungsnetzen." In: *31. Symposium Photovoltaische Solarenergie*. 2016.

[126] B. Baeten, F. Rogiers, and L. Helsen. "Reduction of heat pump induced peak electricity use and required generation capacity through thermal energy storage and demand response." In: *Applied Energy* 195 (2017), pp. 184 –195.

[127] M. Brunner, K. Rudion, and S. Tenbohlen. "PV curtailment reduction with smart homes and heat pumps." In: *2016 IEEE International Energy Conference (ENERGYCON)*. 2016, pp. 1–6.

[128] A. L. M. Mufaris and J. Baba. "Scheduled Operation of Heat Pump Water Heater for Voltage Control in Distribution System with Large Penetration of PV Systems." In: *2013 IEEE Green Technologies Conference (GreenTech)*. 2013, pp. 85–92.

[129] K. Dallmer-Zerbe, D. Fischer, W. Biener, B. Wille-Haussmann, and C. Wittwer. "Droop controlled operation of heat pumps on clustered distribution grids with high PV penetration." In: *2016 IEEE International Energy Conference (ENERGYCON)*. 2016, pp. 1–6.

[130] M. C. Bozchalui, S. A. Hashmi, H. Hassen, C. A. Canizares, and K. Bhattacharya. "Optimal Operation of Residential Energy Hubs in Smart Grids." In: *IEEE Trans. on Smart Grid* 3.4 (2012), pp. 1755–1766.

[131] C. Protopapadaki and D. Saelens. "Heat pump and PV impact on residential low-voltage distribution grids as a function of building and district properties." In: *Applied Energy* 192 (2017), pp. 268 –281.

[132] Vaillant GmbH. *Planungsmodul Wärmepumpen 08/2015*. Aug. 2015.

[133] Fraunhofer ISE. *Current and Future Cost of Photovoltaics. Long-term Scenarios for Market Development, System Prices and LCOE of Utility-Scale PV Systems. Study on behalf of Agora Energiewende*. Online: accessed 2017-01-30. 2015. URL: https://www.agora-energiewende.de/fileadmin/Projekte/2014/Kosten-Photovoltaik-2050/Agora_Energiewende_Current_and_Future_Cost_of_PV_Feb2015_web.pdf.

[134] Bloomberg New Energy Finance. *New Energy Outlook 2017*. 2017.

[135] F. Creutzig, P. Agoston, J. Goldschmidt, G. Luderer, G. Nemet, and R. Pietzcker. "The underestimated potential of solar energy to mitigate climate change." In: *Nature Energy* (2017). Article number: 17140.

[136] VDI-Fachbereich Energiewandlung und -anwendung. *VDI4655: Reference load profiles of single-family and multi-family houses for the use of CHP systems*. Technical guideline. 2008.

[137] S. Drauz. *Synthesis of a heat and electrical load profile for single and multi-family houses used for subsequent performance tests of a multi-component energy system*. Master thesis. 2016.

[138] DIN V 4108-6:2003-06. *Thermal protection and energy economy in buildings - Part 6: Calculation of annual heat and energy use*. Technical guideline. 2003.

[139] T. Loga, B. Stein, N. Diefenbach, and R. Born. *Deutsche Wohngebäudetypologie: Beispielhafte Maßnahmen zur Verbesserung der Energieeffizienz von typischen Wohngebäuden*. Technical report. 2015. URL: http://www.building-typology.eu/downloads/public/docs/brochure/DE_TABULA_TypologyBrochure_IWU.pdf.

[140] Deutschen Wetterdienstes. *Climate Data Center*. Online: accessed 2017-04-15. URL: ftp://ftp-cdc.dwd.de/pub/CDC/observations_germany/climate/.

[141] U. Jordan and K. Vajen. *Realistic domestic hot-water profiles in different time scales*. Online: accessed 2017-02-10. 2001. URL: http://sel.me.wisc.edu/trnsys/trnlib/iea-shc-task26/iea-shc-task26-load-profiles-description-jordan.pdf.

[142] VDI-Verband deutscher Ingenieure. *VDI2067: Economic efficiency of building installations: calculation of energy requirements for heated and air-conditioned buildings*. Technical guideline. 1998.

[143] Bundesamt für Wirtschaft und Ausfuhrkontrolle. *Förderübersicht Wärmepumpe (Basis-, Innovations- und Zusatzförderung)*. Jan. 20, 2017. URL: http://www.bafa.de/SharedDocs/Downloads/DE/Energie/ee_waermepumpen_foerderuebersicht.pdf?__blob=publicationFile&v=4.

[144] Agora Energiewende. *Neue Preismodelle für Energie. Grundlagen einer Reform der Entgelte, Steuern, Abgaben und Umlagen auf Strom und fossile Energieträger*. Apr. 2017.

[145] L. Hirth. "The market value of variable renewables: The effect of solar wind power variability on their relative price." In: *Energy Economics* 38 (2013), pp. 218 –236.

[146] Oeko-Institute. *Projected EEG Costs up to 2035. A study commissioned by Agora Energiewende.* 2016.

[147] Agora Energiewende. *EEG Rechner*. v3_2_07.xlsm, accessed 2016-11-19. 2016. URL: https://www.agora-energiewende.de/en/topics/-agothem-/Produkt/produkt/130/Online+EEG-Rechner.

[148] ene't GmbH. *Endgültige Netzentgelte 2017 - Newsletter Netznutzung Strom, Ausgabe 101*. Online: accessed 2017-01-30. 2017. URL: https://www.enet.eu/newsletter/endgueltige-netzentgelte-2017-veraenderungen-zu-vorlaeufigen-veroeffentlichungen-nur-einseitig.

[149] Bundesverband der Energie- und Wasserwirtschaft. *BDEW-Strompreisanalyse*. 2016.

[150] A. Scheidler, L. Thurner, and M. Braun. "Automated Distribution System Planning for Large-Scale Network Integration Studies." In: *ArXiv e-prints* (Nov. 2017). arXiv: 1711.03331 [cs.CE].

[151] EuPD Research. *German PV ModulePriceMonitor*. 2013.

[152] M. Lohr. *Systempreise PV 2015*. 2016. URL: www.photovoltaikforum.com/download/file.php?id=54970.

[153] Bundesverband der Solarwirtschaft (BSW-Solar). *Solarstromspeicher-Preismonitor Deutschland*. 2015.

[154] Tesla Motors, Inc. *Powerwall*. Online: accessed 2017-02-07. 2017. URL: https://www.tesla.com/powerwall.

[155] Saft Industrial Battery Group. *Data sheet - Intensium Flex*. 2014.

[156] Verbraucherzentrale NRW. *Marktübersicht für Solarstromspeicher bis 12 kWh*. 2016.

[157] sonnen. *Technische Daten sonnenBatterie*. Online: accessed 2016-10-02. 2016. URL: http://www.sonnenbatterie.de.

[158] F. Niedermeyer, J. von Appen, M. Braun, A. Schmiegel, N. Kreutzer, M. Rothert, and A. Reischl. "Innovative Performancetests für PV - Speichersys. zur Erhöhung der Autarkie und des Eigenverbrauchs." In: *30. Symposium Photovoltaische Solarenergie*. 2015.

[159] Bundesministerium für Wirtschaft und Energie. *Bekanntmachung - Förderung von stationären und dezentralen Batteriespeichersystemen zur Nutzung in Verbindung mit Photovoltaikanlagen*. 2016.

[160] Deutsche Bundesbank. *Kurse und Renditen börsennotierter Bundeswertpapiere Februar 2017*. Online: accessed 2017-02-07. 2017. URL: https://www.bundesbank.de/Redaktion/DE/Downloads/Service/Bundeswertpapiere/Rendite/kurse_renditen_bundeswertpapiere_2017_02.pdf?__blob=publicationFile.

[161] HTW Berlin - University of Applied Sciences. *Repräsentative elekt. Lastprofile für Einfamilienh. in Deutschland auf 1-sek. Datenbasis*. Data set. 2015. URL: http://pvspeicher.htw-berlin.de.

[162] H. Schmidt and D. U. Sauer. "Wechselrichter- Wirkungsgrade." In: *Sonnenenergie* 4 (1996), pp. 43–47.

[163] J. von Appen, M. Braun, B. Zinßer, and D. Stellbogen. "Leistungsbegrenzung bei PV-Anlagen." In: *27. Symposium Photovoltaische Solarenergie*. 2012, pp. 47–52.

[164] SMA Solar Technology AG. *Wirkungsgrade und Derating - Sunny Boy Sunny Mini Central*. Data sheet. 2011.

[165] J. Berding, R. Bitterer, U. Bock, P. Müller, M. Pohlmann, G. Schimmel, and R. Weninger. *VDEW Materialien (M-02/2000): Lastprofilverfahren zur Belieferung und Abrechnung von Kleinkunden in Deutschland*. 2000.

[166] C. Fünfgeld and R. Tiedemann. *VDEW Materialien (M-05/2000): Anwendung der Repräentativen VDEW-Lastprofile step - by - step*. 2000.

[167] Stadtwerke Emmendingen. *EnBW-PV-Einsp. (EVo)*. Online: accessed 2016-01-15. 2012. URL: http://swe-emmendingen.de/wp-content/uploads/2012/09/lastprofile_photovoltaik_wasserkraft_kwkg_enbw_einspeiseprofile.xls.

[168] Transnet BW. *Erstellung und Übermittlung von PV- Referenzzeitreihen*. Online: accessed 2016-01-15. 2016. URL: https://www.transnetbw.de/downloads/strommarkt/weitere-dienstleistungen/dlpv-referenzverfahren.pdf?v2.

Colophon

This document was typeset using `classicthesis` style developed by André Miede. The style was inspired by Robert Bringhurst's seminal book on typography *"The Elements of Typographic Style"*. It is available for LaTeX and LyX at

`https://bitbucket.org/amiede/classicthesis/`

ISBN 978-3-7376-0554-0

The thriving business case of residential photovoltaic systems in combination with battery storage systems and other flexibility options, such as heat pumps, leads to additional questions for PV network integration and increases the complexity of planning processes for all involved stakeholders – especially for investors and distribution network operators.

In this thesis mixed integer linear and bilevel optimization models are developed for evaluating the interdependencies between these stakeholders and their strategic decision making. A case study-based approach allows assessing how different incentives impact sizing and operation of PV battery storage systems, their network integration and their complementarity towards other flexibility options for improved sector coupling.

The analysis of the case studies underlines the importance of using multi-stakeholder optimization models. Appropriate incentive setting and sector coupling decelerate emerging self-reinforcing processes between higher network charges, larger system sizes and inefficient PV network integration. Furthermore, curtailment limits and peak charges help activating a network-supporting operation of battery storage systems and other flexibilities.

kassel university press